# An experimental study of Electroluminescence in thin, evaporated films

by

G.A. Antcliffe B.Sc.

A Thesis submitted for
the Degree of Doctor of
Philosophy in the
Physics Department
University of Adelaide

November 1964

## PREFACE

This thesis contains no material which has been accepted for the award of any other degree or diploma in any University and to the best of the candidates knowledge and belief, the thesis contains no material previously published or written by any other person, except where due reference is made in the text of the thesis.

The research work to be described in this thesis was carried out in the Physics Department at the University of Adelaide during the period January 1961 to October 1964. The work was supervised by Dr. S.G. Tomlin.

The author wishes to thank Dr. S.G. Tomlin for making him aware of the electroluminescent effect in zinc sulphide and for patient and helpful supervision during this project.

It is a pleasure to acknowledge many particularly illuminating discussions with Mr. R. Lawrance of this department. Thanks are also due to Mr. B.C. Cavenett and Mr. D.G. McCoy for much discussion.

I would also like to thank Dr. J.V. Sanders of the C.S.I.R.O., Division of Tribophysics, Melbourne for making available a Siemens Emiskop I Electron Microscope.

The assistance given to the author by members of the Physics Department workshop, particularly by Mr. W. Jamieson, during the construction of equipment was invaluable.

My wife, Lesley patiently typed the first draft of this thesis from the often illegible original. The final copies were prepared by Miss. A. Shierlaw. The photographs used in this thesis were taken by Mr. G. Tomlinson and

Miss. A. Millbank. The figures and drawings were reproduced from tracings which were prepared from the originals by Miss. H. Barrow.

The author is grateful for financial assistance from the Commonwealth of Australia in the form of a Commonwealth Postgraduate award held from 1961-64 inclusive.

G.A. Antcliffe, B.Sc. (Hons.)

## SUMMARY

This thesis describes a comprehensive experimental investigation of the light emission produced in thin films by an applied voltage. This is the phenomenon of electroluminescence. The range of film thickness used was between 500 and 10,000Å. Most films used were therefore thinner than those used by other authors.

ZnS and ZnSe films, activated by manganese were prepared by evaporation onto a conducting glass substrate. No light emission was found unless the substrate temperature was greater than a critical value. The more usual diffusion methods of preparation require post-evaporation heat treatment whereas the method developed here gave electroluminescent films directly. The need for a high temperature substrate was interpreted as indicating that an anion excess must be removed from the film by re-evaporation from the substrate.

All films showed a component of the emission at 5860Å, which is characteristic radiation from the manganese ion. The way in which $Mn^{++}$ ions were incorporated in the film crystallites was investigated by electron spin resonance techniques.

Particular attention was paid to preparational techniques to ensure the optimum reproducibility in the experimental results. The most successful method of film preparation was found to be the evaporation of large crystals which were grown from the liquid phase. No light emission could be observed unless the film resistivity was reduced by

the addition of a donor (excess zinc). It was also necessary to provide a low conductivity layer between the film and the second electrode which was an evaporated metal film.

The influence of crystal structure on electroluminescence was studied by using X-ray and electron diffraction techniques. The films were found to be composed of cubic crystallites but a definite proportion of hexagonal structure was present. There was no structure change which could be correlated with the appearance of the light emission at theoretical substrate temperature. The size of the crystallites in the films varied between 150 and 1500Å, depending on preparation details. These changes were investigated by electron microscopy.

The latter sections of the thesis contain a number of results concerning the variation of the electroluminescent brightness with voltage, current, frequency and temperature. Light emission for both D.C. and A.C. voltage excitation is reported. It was possible to interpret most experiment results in terms of a model in which contributions to the brightness occur in the regions near the electrodes and in the volume of the film. The formulation of a complete model was not possible because of the lack of information concerning the electric field distribution between the electrodes. Nevertheless it seemed clear that a field controlled, rather than a minority injection, model was the appropriate one to describe light emission from evaporated films.

## CONTENTS

# 1. REVIEW OF ELECTROLUMINESCENCE

## 1.1 Experimental survey

The first report of light due solely to the application of an electric field to a solid (silicon carbide) was made by Lossev in 1923, Destriau (1936) was the first to observe the effect in zinc sulphide (ZnS) type materials. However, the first detailed explanation of the observed emission from ZnS excited by an electric field was proposed independently by Piper and Williams (1952) and Curie (1952).

Until 1961 experimental results from ZnS phosphors were interpreted in terms of this model, which supposed that free carriers were accelerated by the electric field to optical energies and were then able to excite luminescent centres by impact excitation. Visible (or Infra red) radiation was emitted when the centre recaptured an electron or an excited electron dropped back to a ground state.

Using results obtained from thin films of ZnS, Thornton (1961) suggested that the emission was the result of hole injection into the normally n-type ZnS. It is not immediately obvious whether earlier results could have been explained in terms of hole injection, but it is the opinion of this author that both mechanisms could well be operative simultaneously, together with other high field effects which, in principle may produce light emission.

Electroluminescence has been widely investigated in ZnS type phosphors. However, much information is contradictory, indicating the need for improved reproducibility in experimental studies. It is not possible to summarize

all previous results in this thesis, and therefore, only data of particular relevance to light emission from films will be considered. A more extensive review has been given by Henisch (1962).

Because of the very high electric fields which exist in thin films, this chapter includes also, a brief discussion of several high field effects which, in principle, can produce light emission.

(a) Thin films

Electroluminescent films of ZnS have generally been investigated by depositing the ZnS on a conducting glass substrate (usually tin oxide coated glass). The second electrode is usually of evaporated aluminium. A small voltage applied between these electrodes can give a high electric field in the ZnS film as the electrode spacing is of the order of 1 micron ($10^{-4}$cms).

Halsted and Koller (1954) found that for films made by a reaction between zinc and hydrogen sulphide ($H_2S$) at 550°, the brightness B of the electroluminescence was proportioned to $V^7$, where V was the applied voltage. This preparational technique was developed by Studer and Cusano (1955). The films were generally about 10 microns ($10^{-3}$cms) thick.

A diffusion method suggested by Feldman & O'Hara (1956)[7] was used by Thornton (1959). Impurity from an electroluminescent powder was diffused into an evaporated film of pure ZnS film at a temperature of 650-750°C. These films showed a brightness variation with voltage described by an equation of the

form $B = B_o \exp(-\frac{b}{V^{\frac{1}{2}}})$. Measurements of the resistive component of the A.C. current through these films led Thornton (1961) to suggest that the light emission from such films was due to minority carrier injection.

Diffusion of a film of metallic manganese evaporated over a pure ZnS film was successfully used by Vlasenko and Popkov (1960). These films showed a variation of average brightness B of the form $B = B_o \exp(\alpha E)$. However deviations from this equation occurred at both high and low voltage, and these authors implied that more significant deviations occurred if the film thickness was less than 2 microns. Electroluminescent films of manganese activated ZnS (to be written ZnS.Mn) have been prepared by a single evaporation onto a substrate which must be at a temperature greater than 250°C (Koller 1960). The properties of these films have not been studied.

Weiszburg (1961) has pointed out that many results of the brightness variation with voltage may be equally well described by several different equations, making careful experimentation necessary.

Most electroluminescent materials, previously studied contain two (or more) types of impurity ions. Most attention has been paid to ZnS containing copper usually, together with chlorine (written as ZnS:Cu,Cl). Double activation (i.e. two luminescent ions) is often used, for example ZnS:Mn,Cu,Cl. The emission from phosphors containing multiple activators is known to be affected by complex energy transfer processes

which occur under U.V. excitation. The mechanism involved in the transfer of energy from, for example copper to manganese in ZnS Cu.Mn has been explained by Dexter (1953) as a resonance transfer of energy through the lattice. This is in reasonable agreement with experiments, but Melamed (1958) has shown that this is not the only means of energy transfer. Possible modification of this process when excitation is due to an electric field is possible. However, this has not been considered theoretically.

According to Dexter (1953), resonance transfer can occur only over 40 to 100 lattice sites, and if this transfer process is important, some association of impurities may occur.

There is also a number of results which indicate close association of donor and acceptor sites in ZnS type materials. This is shown by the results of Prener and Williams (1956).

From the above considerations, a phosphor with a single impurity is to be preferred. However, there are relatively few reports of electroluminescence in phosphors of this type.

(b) Location of emission

While it is not possible to examine single crystallites on a film to determine the location of the emission, it is of obvious importance to know if light is generally emitted in the bulk of larger crystals or in localized spots.

Piper and Williams (1952) and other authors have observed light localized at the electrodes and in this case a correlation with electrode work function is often obtained. For emission localized near the cathode, an explanation using

a Schottky exhaustion barrier at the cathode is often used. Hole injection from the electrode would produce emission localized at the anode and extending into the bulk. This is not usually observed.

Henischand Marathe (1960) have suggested that electroluminescence could occur due to carrier accumulation, however no experimental support is available. This effect would also give localized emission at the anode.

Gillson and Darnell (1962) observed light emission at localized spots through crystals. Such localization is often observed. Because of the high refractive index of ZnS (2.42), internal reflections may occur and Frankl (1956) has reported that localized emission is replaced by a uniform glow when the crystal is immersed in a liquid of high refractive index. The data obtained by Gillson and Darnell showed detailed behaviour which can not be explained in this way. Localization may be due to the presence of stacking faults or boundaries between cubic and hexagonal ZnS as shown by many authors, for example Baum and Darnell (1962). These observations have led to Ballentyne (1960) and others to the conclusion that electroluminescence is a disorder phenomenon, the disorder being a necessary condition. These localized spots were considered by Thornton (1961, 1963) to be p-n junctions, although the structure of such functions has not been experimentally determined. The possibility of impurity segregation at dislocations (for example, Bullough (1960)) may be sufficient to form a p-type material in the normally n-type ZnS. The presence of copper sulphide in copper

activated ZnS has been postulated many times, recently by Marshall and Franks (1964). The presence of $Cu_2S$ seems relatively certain. The presence (or necessity) of a manganese compound in ZnS.Mn type phosphors has not been established.

The localized functions may also be formed between two ZnS regions of different conductivity, i.e. a $n\text{-}n^+$ junction (Oldham and Milnes 1963) although, the injecting properties of these functions are not as well known as that of p-n junction.

Emission throughout the crystal volume may in principle occur if electrons are accelerated to sufficient energies to excite an activator. This will require higher fields than are usually present when electroluminescence is observed in powder phosphors and large crystals. Thus the localized emission region is very often interpreted as a field enhancement region, in which high field effects, for example impact ionization may occur.

However, the fields attainable in thin films may be very high ($> 10^6$ volts/cm) and in this pre-breakdown region no localized field enhancement should be necessary. (A more detailed description of high field effects is given in the following chapter). However, it is not immediately obvious that the internal electric field is given by the applied external voltage divided by the film thickness. This is because of barriers at the electrodes (Henisch 1957) and space charge polarization in the film itself (Macdonald 1958).

There are few experimental results available of electroluminescence in ZnS crystals at pre-breakdown field strengths. However, emission in some CdS crystals required such high fields, (Boer and Kummel, 1952). Measurements could be made reversibly in this region and it was shown that only a small number of current carriers available for conduction took part in the luminescent process. Diemer (1954) observed complex emission patterns in the pre-breakdown region in CdS crystals, which he interpreted as due to non uniform space charge. It has been realized that interpretation of such effects is very difficult.

(c) Electrodes on electroluminescent films

Recently, Harper (1962) has shown that details of the light emission from ZnS.Cu films may be altered by a low conductivity layer between the metal electrode and the ZnS. In some cases (CdS crystals) the presence of this layer is necessary for the appearance of electroluminescence (Jaklevic et al 1963).

It has been reported that aluminium oxide ($Al_2O_3$) films between aluminium and cadmium oxide (transparent) electrodes shows light emission when a voltage is applied (Weslowski 1961). These cells gave stable light emission only for the aluminium positive, and brightness variations with current and voltage similar to those obtained from ZnS.Mn, Cl films reported by Cusano (1955).

This result introduced some doubt as to the location of electroluminescence in ZnS films with aluminium electrodes.

Fischer (1961) has summarized the properties of

junctions between various II-VI compounds. In particular, ZnTe on either ZnS or ZnSe should give a hole injecting contact. It may be possible to provide such hole injection in multiple layer films of these materials.

(d) Brightness waves

Electroluminescent films usually emit two unequal brightness peaks approximately in phase with the voltage maxima of a sinusoidal exciting voltage. Thick films (about 20$\mu$) show two equal peaks. Vlasenko and Popkov (1960) have observed two unequal brightness pulses from thinner films (about 1-4 microns). The relative intensity of these was a function of voltage and such behaviour is still unexplained. The unequal brightness peaks have been ascribed to the different properties of the electrodes used on either side of the ZnS. However, Hahn and Seeman (1957) have shown that for powder phosphors between two identical conducting glass electrodes, some asymmetry of the brightness waveform is observed.

(e) Frequency of excitation

In general, increasing frequency (in the audio range) at constant voltage increases the average brightness from an electroluminescent phosphor, as shown by the results of Thornton (1956). However, a saturation is often observed after the initial linear increase.

Halsted and Koller (1954) have suggested that the brightness versus frequency characteristic of films is influenced by at least two factors.

(a) The decay time of luminescent centre (manganese

1.4 millisec).

(b) The resistance of the transparent electrode becoming comparable with the dielectric impedance at higher frequency (especially important for thin films).

Smith (1955) has shown that excitation of single crystals by a constant voltage is possible. Thornton (1962) has demonstrated that thin films also show strong D.C. emission. In these cases the electrodes are in good contact with the crystals. Goldberg and Nickerson (1962) have found that the addition of manganese to a ZnS.Cu Cl film considerably increased the D.C. emission. The reason for this is not clear.

The necessity for an initial forming process before these films showed stable D.C. emission was shown by Goldberg and Nickerson. They observed high initial currents when a voltage was applied, and after 30 seconds light began to appear from the electrode edges. This extended into the whole electrode area. The current fell continuously during this time. This process occurred to some extent upon re-application of voltage after a period of time.

## 1.2 High electric field effects in solids

For films used in this investigation (500-5000Å), the applied voltages were sufficient to produce very high electric fields. In fact the upper limit for electroluminescent operation was imposed by excessive localized breakdown of the film. The voltage at which this occurred was usually only a factor of about 2 - 2.5 above the value at which light was first detected.

A more extensive review of possible high field

mechanisms capable of light production, has been given by Piper and Williams (1958) and Chynoweth (1960).

### 1.2.1 Hot electrons

At high electric field strength, free carriers retain a proportion of energy after each collision which is sufficient to establish a high energy electron distribution. This distribution is approximately Maxwell Boltzmann, and is described by a characteristic temperature $T_e > T$, the lattice temperature. The electrons are then referred to as hot electrons. The parameters which exactly describe such a distribution are not certain, however, Stratton (1957) has shown that electron-electron collisions are of particular importance.

This may impose a minimum electron density below which the concept of an electron temperature, $T_e$ is meaningless. This density seems to be approximately $10^{14} cm^{-3}$, (Fröhlich and Paranjape 1956) and therefore to excite luminescent centres by hot electrons, the conductivity may well need to be much higher than is usual with semi-insulators, such as ZnS.

Kovtonyuk (1963) has recently suggested a hot electron theory of the electroluminescent process which requires an appreciable (but undetermined) free electron density.

Hot electrons may excite a luminescent centre by collision excitation, or if the energy is sufficient a valence electron is excited giving an electron hole pair. The energy threshold for pair production must be at least

equal to the band gap of ZnS which is 3.7e.v. It is interesting to note that the number of ionizations/unit path length (in silicon), that is the number of pairs produced is experimentally proportional to $\exp\left[-\frac{b}{E}\right]$ for an electric field E, (Chynoweth 1960).

This relation has been observed many times for the variation of electroluminescent brightness with applied voltage (see for example Lehmann 1960).

The light emission has been related to the number of electrons in a hot distribution with energy greater than the required excitation energy. The results depend on the approach used to determine $T_e$ in terms of other measureable quantities.

Goffaux (1956) has obtained

$$B = B_o \exp(bE) \qquad \text{--- 1.1}$$

where B is the brightness, E the field and $B_o$ and b constants.

An alternative approach by Nagy (1956) showed that

$$B = B_o \exp\left[-\frac{b_1}{(1+b_2E)^2}\right] \qquad \text{--- 1.2}$$

where $B_o$, $b_1$ and $b_2$ are constants.

In general, the agreement between 1.1 or 1.2 and experimental results is not good.

It has been realized that substantial deviations from a Maxwell Boltzmann distribution occur in high fields, (Morgan 1957, 1958) and this would modify the above theories which assume a Boltzman distribution to make the mathematics

tractable.

Hot electron effects must occur at the fields generally used to excite electroluminescence. Therefore, the problem of conduction in high fields should be a basic problem in the theory of the light emission process. Even when the high field conductivity is known, two other mechanisms occur. Firstly, excitation (or ionization) of the luminescent centre and secondly recombination at the centre.

The final interpretation of the electroluminescent process must await a more extensive knowledge of all these processes. This is not available at the present time. It is therefore not surprising that models (such as described above) which assume rather simplified behaviour do not agree well with experimental results.

1.2.2 Impact ionization

Seitz (1949) has shown that the probability of ionization by impact in an electric field E is given by

$$p = \text{const. } \exp\left(-\frac{E_1}{E}\right) \qquad \text{--- 1.3}$$

where $E_1$ is a characteristic field.

It has been shown by Chuenkov (1960) and Wolff (1954) that this expression is valid at low fields (< some critical value) while, above this equation 1.3 should be replaced by

$$p = \text{const. } \exp\left(-\frac{E_2^2}{E^2}\right) \qquad \text{--- 1.4}$$

where $E_2$ is another characteristic field.

Equation 1.3 is appropriate at lower fields where

only the statistical electrons are accelerated to energies sufficient for excitation of centres. At higher fields where all the electrons gain energy from the field, the probability of impact ionization is given by 1.4. Piper and Williams (1958) quote a field strength of $10^5$ volts/cm for application of equation 1.3 and $10^6$ volts/cm for equation 1.4.

For the ZnS films investigated here, the field strength (assuming a uniform field distribution) was about $10^6$ volts/cm, making equation 1.4 relevant to the probability of impact excitation of centres.

It is theoretically possible to determine whether impact ionization occurs by analysis of the current-voltage relation. Several theoretical expressions for the current due to impact excitation are available, but comparison with experiment is difficult because other high field effects may obscure the impact excitation effect. As an example, it has been suggested that the sudden increase in current normally associated with the trap filled limit in space charge limited current flow is due to the onset of impact ionization, (Bube 1962).

The results of Cardon (1963) predict some noticeable effect on the current voltage relation, but observation would be difficult, particularly in an electroluminescent film with non ohmic electrodes.

### 1.2.3 Internal field emission

At fields approaching dielectric breakdown ($10^6$ - $10^7$ volts/cm), tunnelling of electrons between valence and conduction band may occur (Zener effect). Zener found that the transparency of the barrier was given by (Zener 1934)

$$f = \exp\left[-\frac{\text{constant } E_g}{E}\right] \qquad \text{--- 1.5}$$

where $E_g$ is the band gap and E the applied field. The original treatment was based on the free electron model and is therefore relevant to small band gaps. A modified form applicable to wide band gap materials e.g. (ZnS) shows that $E_g$ in the original equation should be replaced by $E_g^{\frac{3}{2}}$ (Franz 1952).

The threshold field for Zener emission has been estimated to lie between $3.10^6$ and $2.10^7$ volts/cm. The magnitude of the fields used to excite light emission in the ZnS.Mn films described in this thesis was often $3.10^6$ volts/cm, making the Zener effect a possible source of excitation.

Similar expressions to the above describe the probability of a transition from a localized level and the conduction band (Franz 1952). This requires a lower field than that necessary for Zener emission, and field release of donor electrons (i.e. tunnelling) has been postulated to account for experimental results (Georgobiani and Fok 1961).

A case of particular interest for tightly bound centres, such as manganese may be the probability of a transition between two localized levels of an impurity ion.

In general, the current observed when internal field controlled emission releases electrons to the conduction band is of the form

$$J = AE^n \exp\left(-\frac{b\,E_g^{\frac{3}{2}}}{E}\right) \qquad \text{--- 1.6}$$

where A and b are constants and n varies from 1 to 3 (Chynoweth 1960). Chynoweth gives an order of magnitude calculation for the current density when $E_g$ = 1 e.v., which shows that a change in E from 5 to $6.10^6$ volts/cm should result in an increase from 1 to 10 amps/$cm^2$.

For the reasons mentioned above, the identification of a particular field emission process from the current-voltage relation is very difficult.

### 1.2.4 Electric field configurations

In single crystals and phosphor powders, the average field strength is too low ($10^4$-$10^5$ volts/cm) to give any appreciable probability of excitation of luminescent centres by the field.

In general an exhaustion barrier of the Schottky type will exist at any metal semiconductor contact unless special precautions are taken (Henisch1957). The presence of this barrier layer allows the presence of a high field region in series with the bulk phosphor where the field strength is smaller. This allows the attainment of very high fields in the high impedance barrier region without the onset of avalanches leading to dielectric breakdown. This model of excitation of centres in such an exhaustion barrier where the electric field is proportional to the square root of the applied voltage has been developed by Piper and Williams (1955). Using a much simplified model of impaction ionization in an exhaustion barrier region they predict that the electroluminescent brightness B should be given by

$$B = B_o \left[ \exp - \frac{b}{\frac{1}{V^2}} \right] \qquad \text{--- 1.7}$$

where V is the barrier voltage and b and $B_o$ are constants.

However, the barrier voltage will not in general equal the external applied voltage, making direct comparison with experiment difficult. Nevertheless, a large number of experimental results (see for example Georgobiani and Fok, 1961) agree with equation 1.7 very well.

In such a barrier region, the value of the electric field may become sufficient to cause Zener emission. It has been shown that the Zener effect in a field of $3.10^6$ volts/cm can account for the number of quanta emitted from an electroluminescent phosphor (Georgobiani 1961). The average field in this case was $1.6\ 10^5$ volts/cm and the necessary $3.10^6$ volts/cm could occur in an exhaustion region.

Another effect, which will lead to deviations from the ideal barrier behaviour assumed above is the existence of non linear bulk effects (Diemer 1955), particularly polarization charge which may affect the time variation of the barrier profile when an A.C. voltage is applied.

When thin films are used, the width of any exhaustion region near the electrode may be comparable to the film thickness. In this case there is no distinct barrier region and the field distribution may be more uniform. In general however, the electric field will not be given by $\frac{V}{d}$ for a voltage V applied between electrodes d cms apart. While the field distribution is very difficult to determine in semi-insulating materials which show electroluminescence, the value of the field strength at every point is of obvious importance in the formulation of a model of the light emission

process.

The applied field may be enhanced by the action of a polarization field. If the decay time of the polarization charge accumulated at the electrodes is longer than the time in which the applied A.C. field reverses polarity, the internal field may be instantaneously enhanced by, at the most, a factor of two (Henisch1957).

The presence of polarization effects in semi-insulators with blocking electrodes (as used with electroluminescent materials) has been considered by Macdonald (for example, 1958). The potential distribution between the electrodes shows wide variations from a linear distribution. Rose (1955) has shown that the presence of injected space charge also modifies the internal field and has marked effects on the current, which is then space charge limited.

A p-n junction biased in the reverse direction will also provide a very high field which may extend over considerable distance (the junction width). The properties of such junctions are well known (Shockley 1949), and quantitative predictions may be made concerning junction behaviour, particularly in germanium and silicon. These calculations require knowledge of impurity gradients across the junction regions and of the bulk properties of the materials. The presence of such junctions is also reasonably easy to prove. The identification of p-n junctions in ZnS is not so straight forward and direct evidence of electroluminescence due to junctions in high resistance crystals is not available. However, the first grown junctions using ZnS and ZnSe have been

recently reported by Aven and Cusano (1964). Such work will lead to an increased understanding of the field distribution in such junctions.

A detailed study of the light emission resulting from reverse biased p-n junctions in germanium and silicon has been made (for a review see Chynoweth 1960). The light emission from relatively wide junctions ($\simeq$1000Å) has been ascribed to avalanche multiplication (associated with characteristic noise), while in narrower junctions of 400Å, Zener emission seems most likely. In the intermediate range both field emission and avalanching may occur simultaneously. The emission pattern appears to be characteristic of the excitation mechanism in these junctions; intense spots result from avalanche breakdown, while a more or less uniform glow is observed when field emission occurs.

An interesting process of field enhancement has been observed in germanium (Gunn 1956) and has been referred to as avalanche injection. When the field becomes sufficient to start impact ionization ($6.10^4$ volts/cm), the additional carriers accumulate near the anode. This space charge gives an increasing distortion of the internal field, because the electric field near the anode becomes larger than the average across the crystal. Ionization of valence electrons can occur in this thin avalanche region which then becomes a source of holes. These holes may diffuse into the low field bulk and be captured by (luminescent) centres.

### 1.3.5 Dielectric breakdown

As the upper limit to high electric field behaviour,

the applicability of the foregoing effects to dielectric breakdown will be outlined. A more extensive review has been given by Stratton (1961).

A necessary feature of the breakdown process is a rapid increase in the number of conduction electrons. The collective model of this process assumes that all electrons are at a temperature $T_e > T$, the lattice temperature. In the avalanche model, breakdown is initiated by cumulative release of bound electrons by impact ionization. Avalanche breakdown has been considered simply by Seitz (1949).

Breakdown may be also initiated by field release (tunnelling) of either bound electrons or valence electrons.

An upper limit to the breakdown field strength is obtained by requiring that all electrons gain more energy from the field than they lose to the lattice (Von Hippel 1935). A lower limit, which appears to be more realistic is predicted by imposing the condition that the rate of energy gain must exceed the loss only for electrons in some given energy range (Frohlich 1937).

The process of dielectric breakdown in CdS crystals has been found to occur by internal field emission from the valence to the conduction band (Williams 1961, 1962). However, Boer et al (1962) has shown that in thin films of CdS breakdown was due to release of electrons from impurity levels by impact ionization.

## 2. APPARATUS REQUIRED FOR THE INVESTIGATION

### 2.1 Vacuum system for evaporation of films

The essential requirement for this work was an evaporating plant working at pressures in the range $10^{-4}$ to $10^{-5}$mm of mercury ($10^{-4}$ - $10^{-5}$torr).

A conventional vacuum system using an Edwards $2\frac{1}{2}$" diffusion pump backed by a 50 litres/minute Genevac rotary pump was constructed (Figure 2.1), by the author.

In use, the system attained a pressure of $2.10^{-5}$ torr in one hour (using a liquid air trap) when the pumps were started from cold.

### 2.2 Evaporation equipment

To provide electrodes through the base plate of the system eight tapered holes were drilled through the plate. Glass cones were ground into these holes with fine carborundum powder so that finally they could be rotated, while the system was under vacuum without any fluctuation in the pressure. A metal-glass seal was joined to these cones providing electrodes through the base plate of the system as shown in Figure 2.2a.

This type of electrode was not suitable for the heavy currents used for the ZnS evaporation and more robust electrodes were made (Figure 2.2b). These were of mild steel sealed through the base plate with rubber rings.

A small molybdenum boat contained the ZnS and this boat was held between two heavy steel electrodes (Figure 2.3). One side of the heater was earthed through the base plate of the system.

FIG. 2.1 VACUUM SYSTEM

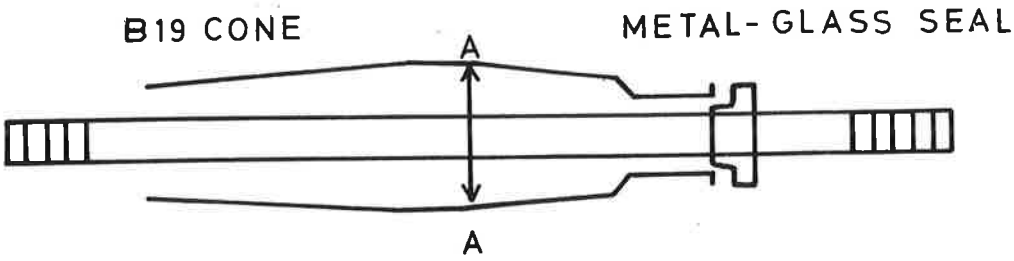


(A) GLASS ELECTRODE

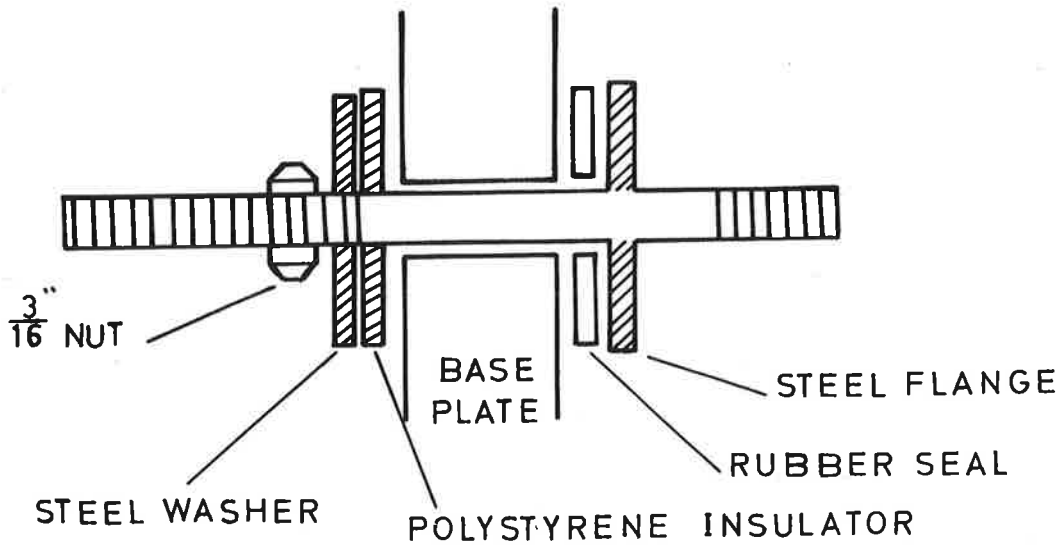


(B) HIGH CURRENT ELECTRODE

FIG. 2.2

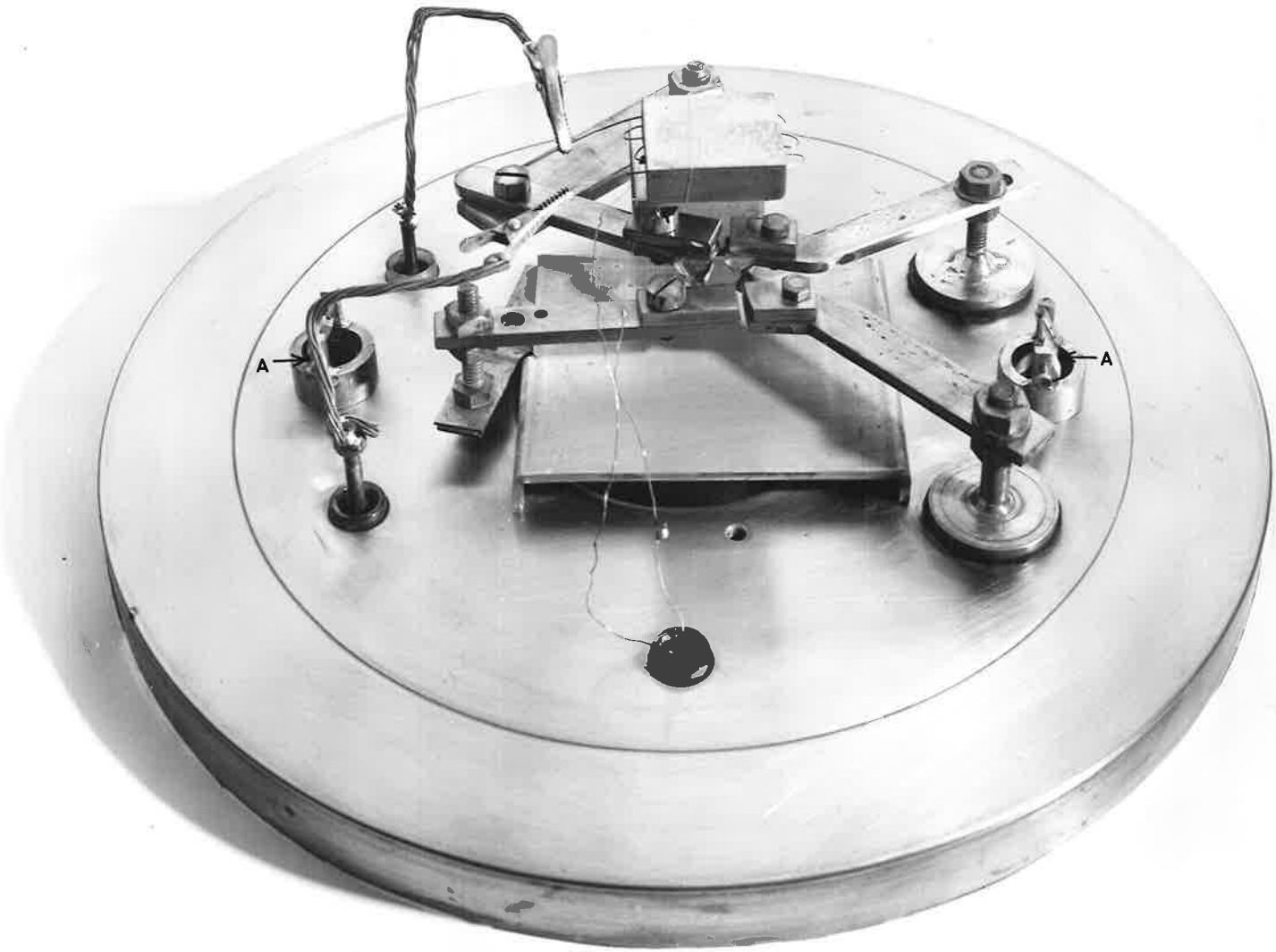


FIG. 2.3 BASE PLATE OF VACUUM SYSTEM.

Heavy current cable was used to connect these points to the secondary terminals of a 24V, 100A transformer. The primary voltage was controlled by a rotary auto transformer (Variac) and the current in the secondary circuit was monitored by a 0-100 amp meter.

Three methods of heating the substrate above room temperature were used.

(a) The initial form of heater is shown in Figure 2.4a. A quartz tube, 3" long was wound with a molybdenum strip. This was heated by an A.C. current from a transformer controlled by a Variac. A current of 35 amps at 7 volts maintained a temperature of approximately 375$^{o}$C. The quartz tube was supported by a steel rod held by two stainless steel supports screwed to the base plate. The substrate was held by a molybdenum clip on two stainless steel supports as shown. A stainless steel cover could be placed over the strip heater so that it was enclosed on three sides by stainless steel and by the substrate on the lower face.

Due to the size of the heater, the power required to obtain a substrate temperature of 400$^{o}$C was sufficient to cause localized heating of the glass bell jar during the time of a typical film evaporation.

The distance between the source and substrate was varied to obtain the maximum uniformity in the film. A distance of 7 cms was used in all the evaporations to be described in this thesis.

(b) A second substrate heater was used to overcome the problem of excessive heat dissipation, which was trouble-

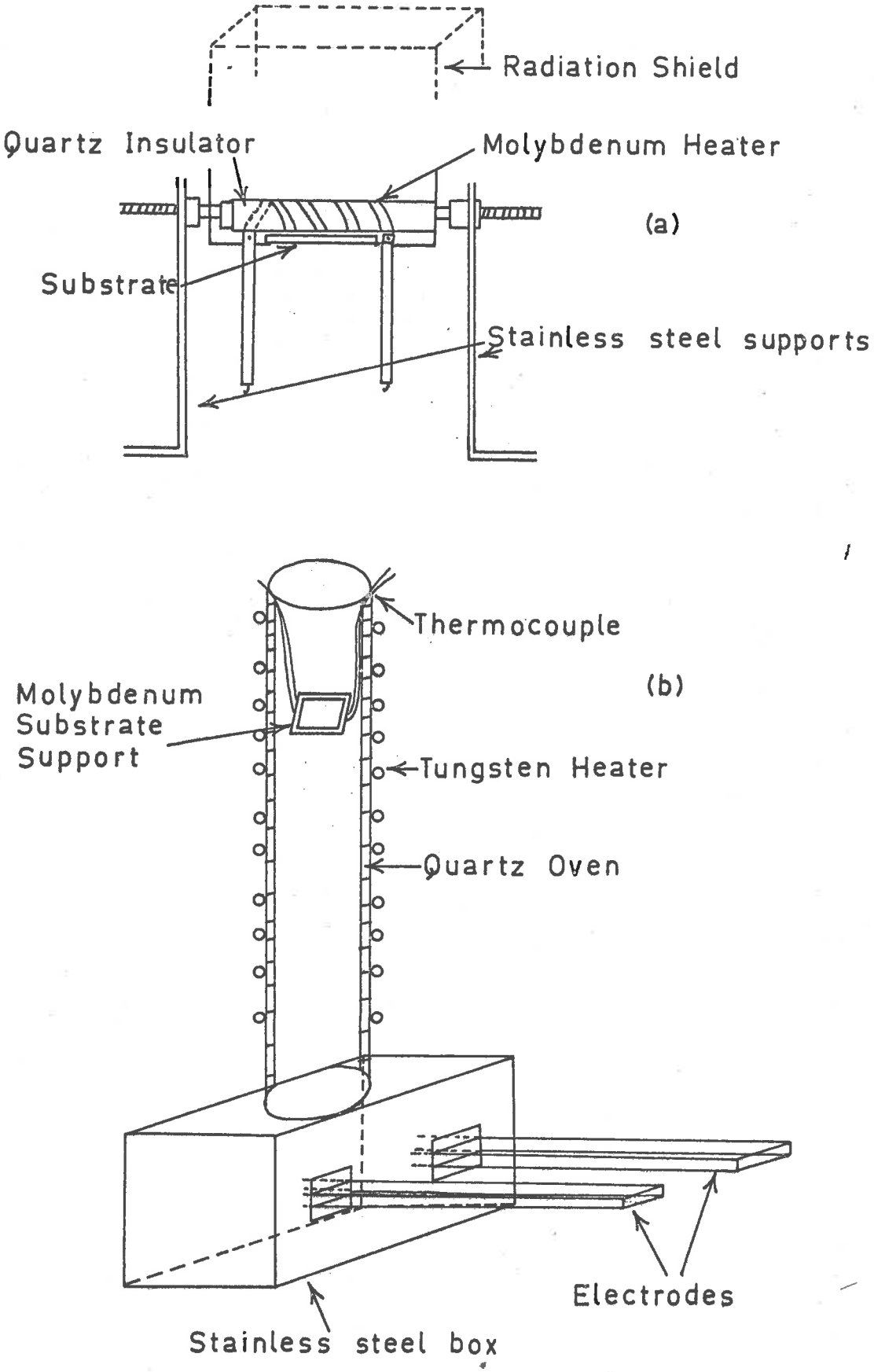


FIG. 2.4 SUBSTRATE HEATERS

some when the substrate was maintained at high temperatures ($> 400^{o}C$). A copper block (1" square by $\frac{1}{4}$") was milled to provide a recess in which the substrate was held by a molybdenum clip. Six holes were bored to take $\frac{1}{8}$" ceramic insulators through which 0.5mm tungsten wire was threaded.

The block was supported on four tapered ceramic insulators which were a close fit in holes drilled in the block and in supports attached to the base plate. This form of mounting was found to be rigid and to give good thermal insulation. Temperatures around $600^{o}C$ could be obtained with small power input (10 amps, 10 volts) without any marked rise in temperature of the bell jar. This heater is shown in Figure 2.3. One support has been removed to show the position of the evaporation boats.

(c) To vary the conditions under which a film was formed, the molybdenum boat was enclosed in a small stainless steel box, the electrodes entering through the two gaps in its wall. A $\frac{3}{4}$" circular hole in the box allowed the evaporating beam to enter a 1" quartz tube wound with tungsten wire in which the substrate was held by a small molybdenum stage supported by the oven wall. The substrate was held to this stage by two small tungsten wire clips. A thermocouple junction was held between the substrate and support (Figure 2.4b).

The upper open end was closed by a clear glass concave lens enabling the boat to be seen and the film thickness to be roughly gauged by the interference colour during the evaporation.

The oven was surrounded by a copper heat shield. Two small copper pipes were fitted to a glass cone assembly (as described earlier) to allow a flow of water to circulate around the copper heat shield, as it was expected the above oven would heat up the whole system. However, it was found that the copper heat shield effectively blocked all radiation from the bell jar walls without the need for water cooling at an oven temperature of 500$^{o}$C.

## 2.3 Film thickness monitor

The amount of sulphide deposited from a given weight of ZnS in the boat was dependent on the substrate temperature. This effect resulted in a dependence of the rate of film growth on this temperature. Therefore, evaporation of constant thickness films for a range of substrate temperatures required slight modifications to the amount of sulphide evaporated. One method of obtaining a given thickness film under varying conditions of substrate temperature was to continuously record the film thickness during the evaporation.

The light from a 100 watt mercury arc lamp was reflected into the bell jar through a glass cone in the base plate which had been fitted with a plane glass window (joined with Araldite to the glass extension of the cone). Two small aluminium mirrors (Figure 2.3A) were supported in the vacuum chamber just above these cones to reflect the light onto the substrate from which it was reflected and out through the base plate. A photomultiplier (1P21) with a narrow band interference filter to separate the

mercury green line at 5460Å was used to detect the light. (Filter centred at 5500Å supplied by Baird Atomic U.S.A.). The beam was focused on the photocathode by a lens held outside the bell jar under the entrance window and the mirrors were adjusted to give the maximum signal. The two mirrors were coated with several hundred angstroms of Silica to protect their surfaces.

The output from the photomultiplier was monitored by a D.C. Microammeter (Hewlett Packard 25A) and displayed on a chart recorder with 50mv full scale deflection. Figure 2.4.1 shows a typical recorder trace taken during an evaporation. As the film thickness increased from zero, the reflected light showed maxima and minima of intensity. Neglecting the unknown phase change occurring at the ZnS-$SnO_2$ interface, the maximum intensity occurred for value of the film thickness t, which satisfied the condition

$$2\mu t \cos\phi = (2p+1)\frac{\lambda}{4}$$

where $\phi$ is the angle of incidence (= 60°), p is an integer, $\mu$ is the refractive index of ZnS (= 2.36) and $\lambda$ is the wavelength of the incident radiation. Using these values t = 1750A at the first maximum. Using a multiple beam interference method the actual film thickness was only 1300Å. The discrepancy can be explained by the phase change occurring at the ZnS-$SnO_2$ interface.

However, because the device was only used as a convenient indication of the film growth process, no further attempt was made to account for the difference.

An added advantage from this display was that the

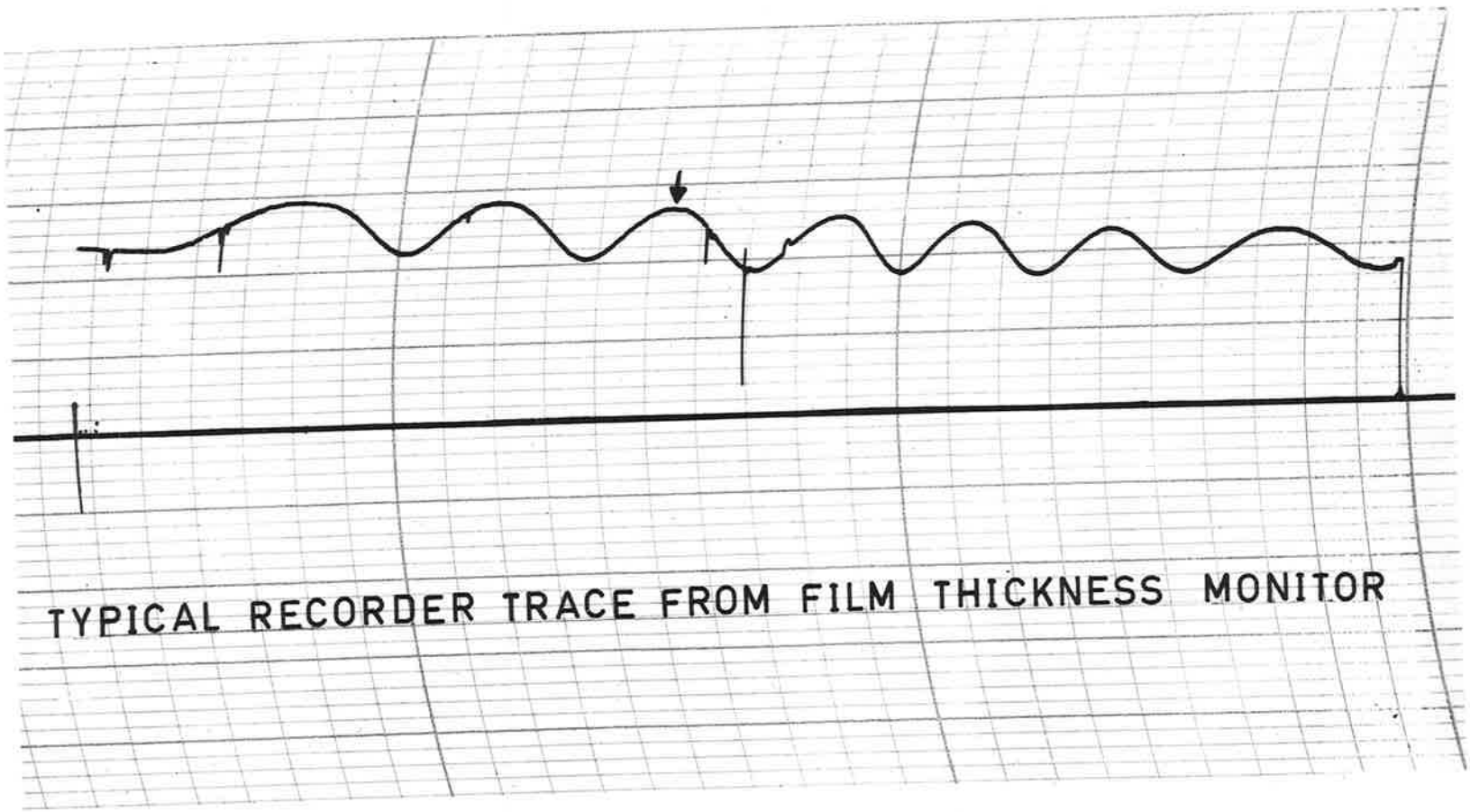


FIG. 2.4.1

rate of evaporation could be made more uniform during the film growth. With some practice the growth could be stopped to within ± 50A, by using a rotating shutter across the evaporant when the record trace reached any desired point. The accuracy of this monitor was found by measuring the films later by a multiple beam interferance technique (fringes of equal chromatic order). This technique has been adequately described by Tolansky (1960).

## 2.4 Crystal growing apparatus

Large single crystals (several grams) have been successfully grown by a method involving the melting of ZnS under pressure (Addamiano US patent 3022144). Pure hexagonal ZnS was obtained by controlled cooling of liquid ZnS (melting point 1830°C) in an argon atmosphere at a pressure of 150 p.s.i. (Addamiano and Aven 1960).

The basic requirement was a pressure vessel capable of withstanding pressure of this order and a furnace capable of 1830°C. The body of the bomb was machined from 8" diameter steel tubing with $\frac{7}{8}$" walls. The walls were machined to a mirror finish to facilitate cleaning. The body was coded by circulating water through copper cooling coils (Figure 2.5).

The bomb was purposely made more than adequate for the pressures expected during the sulphide growth so it could be used over a wider pressure range in the future. It was tested under hydrostatic pressure to 1200 p.s.i.

An electrode was machined and threaded from $\frac{1}{2}$"

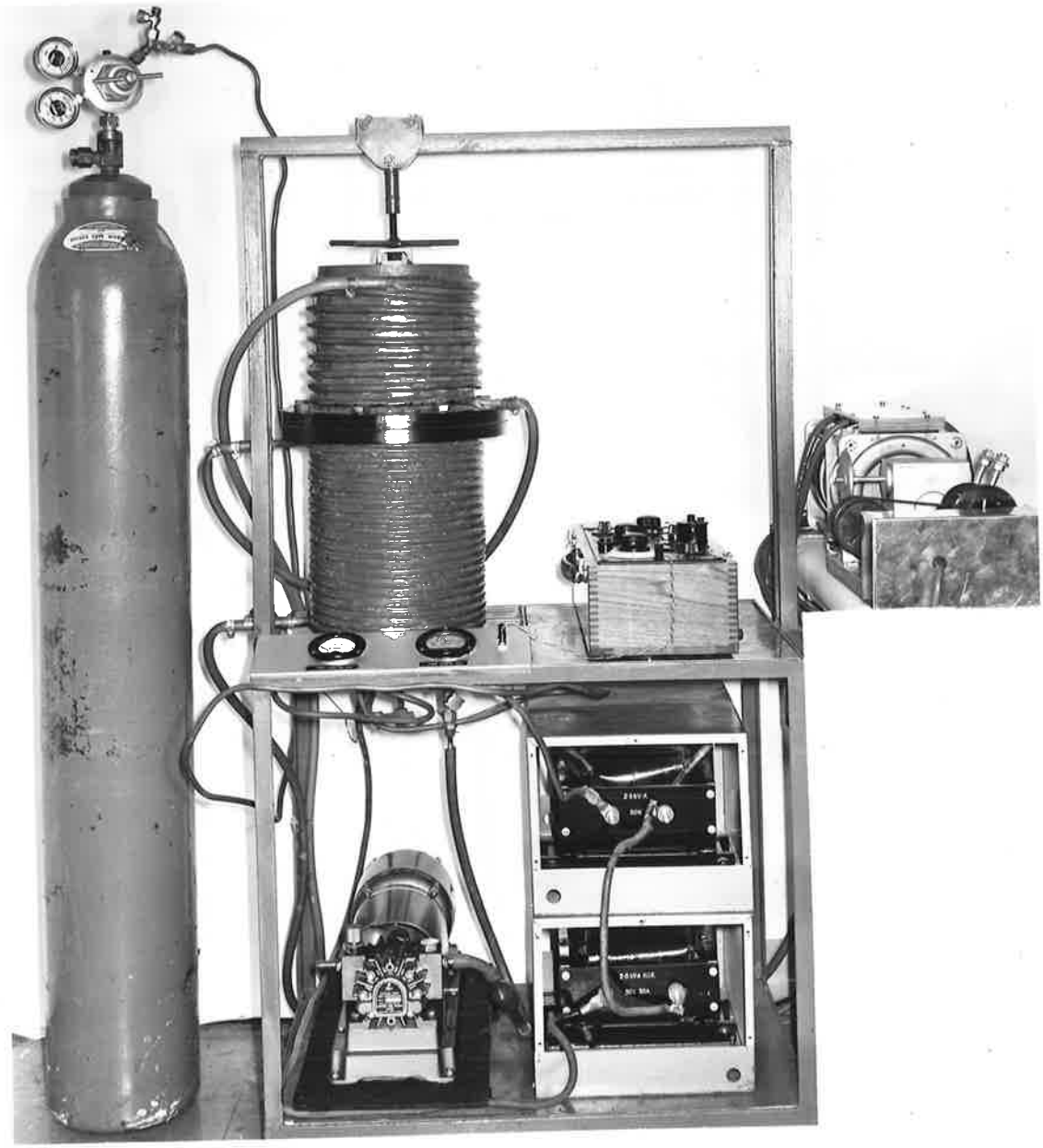

FIG. 2.5 CRYSTAL FURNACE

steel rod, (Figure 2.6). The electrode was mounted in the base of the bomb using two high pressure ceramic insulators (Hylumina, available from S. Smith, Sydney). Copper ring gaskets were used as seals. The base plate was also fitted with two insulated leads to enable a thermocouple to be used inside the bomb. Automobile spark plugs with the earth bar removed were found to be ideal for this purpose. Figure 2.8 also shows the actual heater element. This was machined from a solid carbon rod of 1" diameter. The centre section of a 6 inch length was reduced to $\frac{7}{8}$" diameter, and a screw thread (4 turns/inch) was cut to a depth of 0.013". One end of the heater was tapped to screw directly on to the heavy steel electrode, and the centre section was bored out leaving a high resistance carbon spiral (typical resistance 0.6 ohms). The crucible containing the ZnS was fitted into the heater as shown in Figure 2.7. Contact to the top of the element was made with a small carbon rod containing a recess of the same width as the top of the heating element. This was connected via a steel fitting to a welded contact on the bomb wall. When the heater was assembled the element was kept under slight compression to ensure good contact between the heater and the connecting carbon rod. The actual heater element was very robust and compression to a limited extent was possible without damage.

The heater was surrounded by two thin circular carbon heat shields supported by a carbon flange which was a tight fit around the solid lower part of the heating

FIG. 2.6 COMPONENTS OF CRYSTAL GROWING FURNACE.

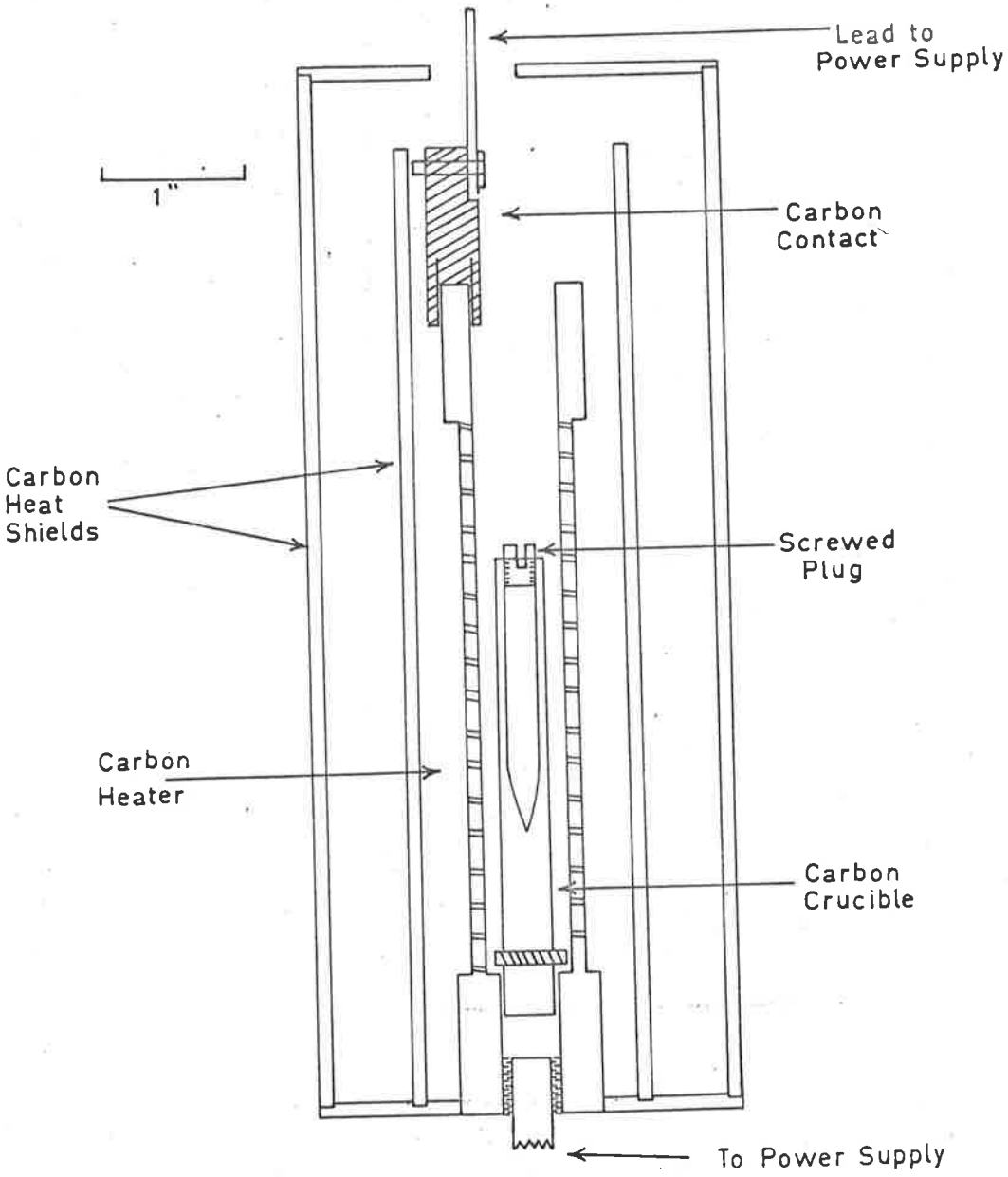


FIG. 2.7 CRYSTAL GROWING FURNACE

element. The outer shield was fitted with a top cover (Figure 2.7).

The actual crucible was a length of spectroscopically pure carbon rod with a $\frac{1}{4}$" tapered hole to take the ZnS powder. As the temperature gradient would be along the length of the crucible, the crystal would then begin to grow from a small nucleus at the bottom of the tapered hole. The crystal was removed after growth by removing the threaded end plug and tapping the crucible lightly, causing the crystal to drop out.

The bomb was supplied with argon or oxy free nitrogen directly from a gas cylinder through a regulator valve. The filling tube of 0.25" copper was sweated directly into the base plate of the bomb. A length of threaded brass tubing was soldered to a pressure tap sealed in the base plate to allow the air to be pumped out of the system before filling with inert gas. Power was obtained from two 50 volt 50 amp transformers in series. Their primaries were controlled by two coupled variacs. These were coupled to a variable speed gearbox-motor assembly allowing a range of cooling programs to be used (Figure 2.8).

Of utmost importance for the successful growth of crystals in this system was the particular point where the crystal began to grow, i.e. the temperature gradient over the region where the crystal was formed. Obviously the temperature at both ends of the heaters was low (perhaps several hundred degrees) while the centre of the heater was necessarily much higher. Because of the high

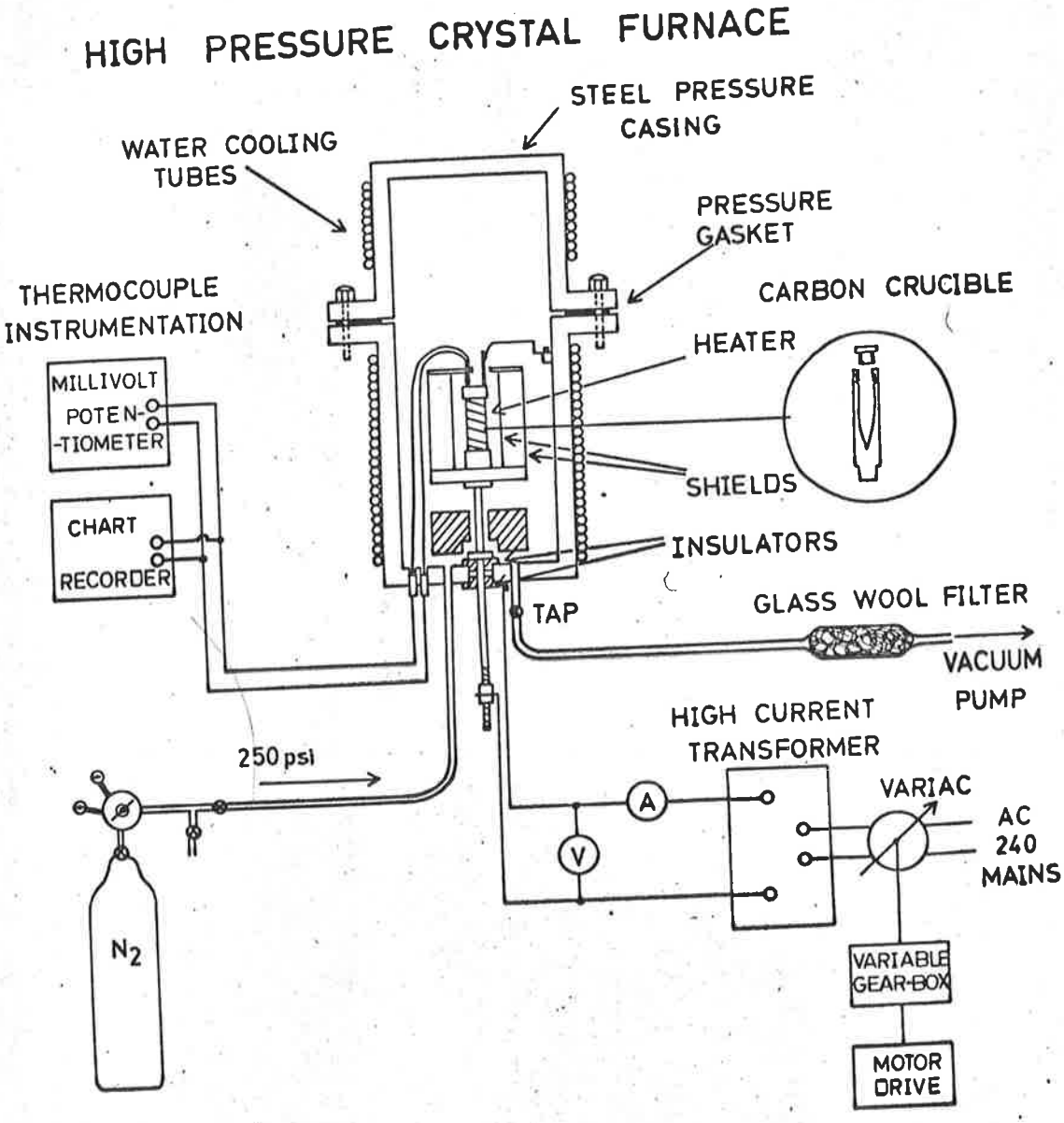
HIGH PRESSURE CRYSTAL FURNACE
STEEL PRESSURE CASING
WATER COOLING TUBES
PRESSURE GASKET
THERMOCOUPLE INSTRUMENTATION
CARBON CRUCIBLE
HEATER
MILLIVOLT POTEN--TIOMETER
CHART RECORDER
SHIELDS
INSULATORS
TAP
GLASS WOOL FILTER
VACUUM PUMP
HIGH CURRENT TRANSFORMER
250 psi
A
V
VARIAC
AC 240 MAINS
$N_2$
VARIABLE GEAR-BOX
MOTOR DRIVE

FIG. 2.8

temperature required to melt ZnS (1830°C), normal thermocouple methods were useless to determine the temperature gradient. High temperature thermocouples have been described by Davies (1960) but these were not available. Therefore the following procedure was used.

The bottom of the tapered crucible hole was made so that it was 0.25" below the centre of the heater element, when in position inside the heater. The pressure vessel was pumped out with a rotary pump and then flushed with dry oxygen-free nitrogen, care being taken to expel all traces of air from the filling pipes. This was repeated several times before the final filling to 200 p.s.i.

The power was raised slowly to 2, 2.5, 3 .... k.w. on successive runs. After each run, the power was reduced quickly to zero, and the ZnS inspected to determine whether the power had been sufficient to reach the melting point. This procedure gave the power required to just melt the sulphide at this particular position in the heater (3.5 k.w.). At this position (near the centre) any increase in the coding time over about 10 minutes resulted in the loss of nearly all the crystalline ZnS which had been formed, leaving only a small fraction or none at all. This loss coated the inside of the bomb heavily with sulphide. This effect occurred irrespective of pressure between 80 and 250 p.s.i.

The above procedure was repeated at intervals of 0.25" down the heater, each time finding the power required

to just melt the ZnS. The power increased to 4.8k.w. when the bottom of the growth region was $1\frac{5}{8}$" below the centre of the heater element. An improvement in the crystal formation was noticed as the growth point moved to regions of greater temperature gradient, even at rapid cooling rates. The final position used was $1\frac{1}{4}$" from the centre, requiring a power of 4.5k.w.

Measurements of the temperature gradient along the heater using a Platinum, Platinum-Rhodium thermocouple were made for a temperature of 1400°C. These showed that over a region between 1.25" and 1.0" from the centre of the heater (the length of the actual crystal) the temperature varied from 1350 to 1400°C. This gradient of 200°/inch may be modified slightly at 1830°C due to increased rate of heat loss.

Even at this optimum position loss of sulphide occurred during an extended cooling, although longer cooling times could be tolerated than near the centre of the heater. This suggested that the loss of sulphide was favoured by a small temperature gradient.

Evaporation at temperatures below the melting point occurred also. This was shown by a number of special cooling programs all of which were unsuccessful in reducing the loss to any great extent. For example, slow cooling through the melting point followed by a rapid cooling to the transition region ($< 1200$°C) and a slow cooling over this region indicated a loss dependent on cooling time, rather than the cooling rate at a particular

temperature. The amount of ZnS lost may be related to a reaction at the crucible walls. The walls were considerably affected after a crystal growth, indicating some attack by the sulphide. In fact, if the same crucible was used a number of times, the loss of ZnS increased.

Reasonable crystal formation occurred over a 60 minute cooling (linear rate) during which time, a loss in weight of 50-60% of the original charge occurred. The rather fast cooling rate usually produced a crystal boule, easily cleaved by tapping with a sharp edge to give about 3 large crystals. A 2.5 gram charge of sulphide was used to give a crystal boule of about 1 gram. The cleavage planes were vertical i.e. along the axis of the crucible, showing that the crystal growth had occurred from the bottom of the crucible. Some crystal boules showed obvious growth from the walls (usually resulting from a very fast cooling) and were polycrystalline.

The method described above was successfully used to grow large crystals of ZnSe and ZnTe.

These were easily grown from a position 1" below the centre of the heater using an input power of 3.3 and 2.7k.w. respectively. A negligible amount of the powder charge was lost and this allowed an extended cooling period of up to five hours. The crystal perfection was much greater in these crystals, because of the longer cooling time.

## 2.5 Detection of electroluminescent emission

The detector was a type 1P21 R.C.A. photomultiplier

encased in a light- tight housing fitted with a rotating shutter across the photocathode. The resistors supplying the dynode voltages (100K) were soldered directly between the valve pins, as was the anode load resistor (22K) from which the output of the photomultiplier was taken to a cathode ray oscilloscope. (Serviscope 10mv/cm maximum gain). A D.C. Microammeter (Hewlett Packard 25A) was used in the anode circuit to monitor the average value of the current through the last stage of the tube.

The D.C. voltage needed for this multiplier (1000 volts) was obtained from a bank of dry batteries in a shielded metal case. This method of supply minimized any 50c/s pick-up voltage which would appear across the load resistor and complicate the oscilloscope display.

Particular care was taken to keep the photomultiplier in darkness at all times and not to exceed the maximum specified anode current ($10^{-5}$ amps). A stable dark current (on the meter) of only $1.0 \times 10^{-9}$ amps was obtained by attention to these details. The output from the load resistor was amplified by a conventional two transistor A.C. amplifier with a gain of about 400. If the D.C. component of any A.C. light emission was required, a Philbrick USA 3D.C. amplifier with a gain of several hundred was used with a D.C. oscilloscope.

The linearity of the detector response with increasing light intensity was measured for several different wavelengths through the visible spectrum. This was done by setting the phototube 36" away from a small

point source of white light covered by appropriate interference filters. A large neutral density filter (density 0.3, thus giving a decrease in transmission of 50%) was cut into small squares and used to vary the intensity from the point source. Each additional filter reduced the intensity of 0.5 to within 1%. The density of the filter (0.30 ± 0.01) was determined by a Kodak Densitometer.

The measurements of anode current and the known decrease in light showed that over the range used, the light detected was proportional to the anode current of the photomultiplier (Figure 2.9). This allowed the values of the anode current to be used directly as a relative measure of the brightness falling on the photocathode.

The electroluminescent films were mounted in a light tight metal box which screwed directly to the photomultiplier housing. Pressure contacts were used on the film electrodes.

The value of the voltage at which light was just detectable will be often used in this thesis. If this voltage was to be compared for a number of films, the emitting area of the films was placed in a fixed position relative to the photocathode. This was necessary as the response over the cathode surface was not uniform. Spectra of the light were obtained by using a Schott wedge filter which was moved across a $\frac{1}{16}$" slit. The resolution was about 20Å. The filter was calibrated with a Hilger monochromator. Light near the absorption edge (3.7ev) and up to 4000Å was detected by an 1P28 photomultiplier and an 0X7 Chance Pilkington filter. The filter was transparent to light between

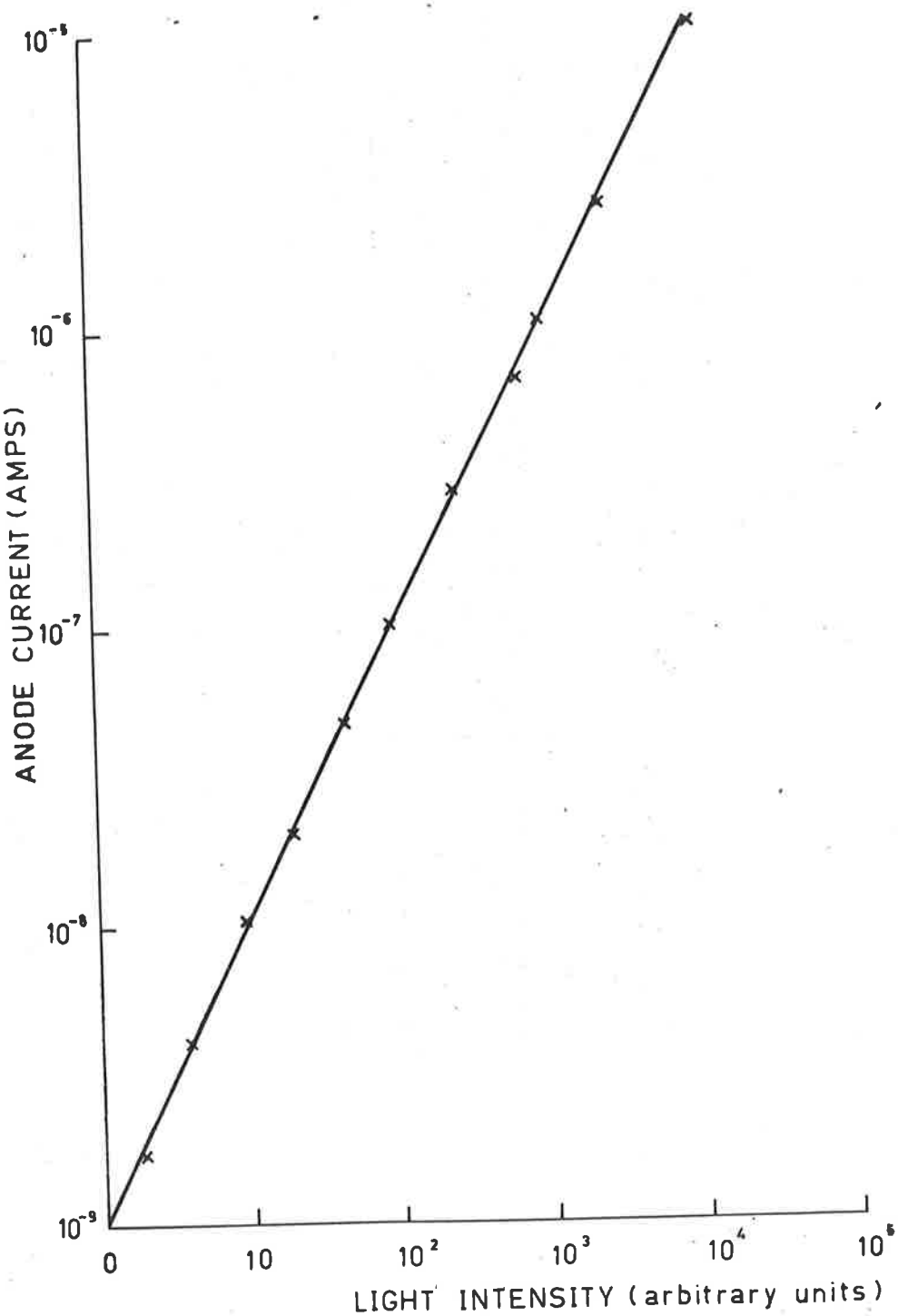


FIG. 2.9 LINEARITY OF PHOTOMULTIPLIER ANODE CURRENT WITH LIGHT INTENSITY.

2500 and 4000Å.

The photo-luminescent spectra of ZnS crystals were measured directly with a Hilger monochromator because of the increased light intensity available from crystals.

## 2.6 Low temperature apparatus

The basic form of this apparatus is shown in Figure 2.10. Glass construction was used and liquid air was used to cool a small copper block on which the film was mounted. Good thermal contact between the mounting face and the liquid air was obtained by making this face of thin copper plate soldered to a copper tube. The dimensions of the block were minimized to obtain the lowest temperatures. The lowest temperature was about - 185°C measured by a fine wire (0.01") chromel-alumel thermocouple. This was carefully calibrated at three points, liquid nitrogen, dry ice and freezing mercury for use below 20°C and, as described in the next section for use above 20°C. Temperatures above 20° were obtained by a nichrome heater in the copper block.

Two copper leads were used to apply the excitation voltage as shown. The dewar was operated at about $10^{-2}$ torr, sufficient to reduce the heat loss and prevent condensation on the window in the outer tubing. The whole dewar was mounted in a rigid metal assembly to which the photomultiplier was attached.

## 2.7 Measurement of substrate temperature

The original work of Koller (Koller 1960) showed

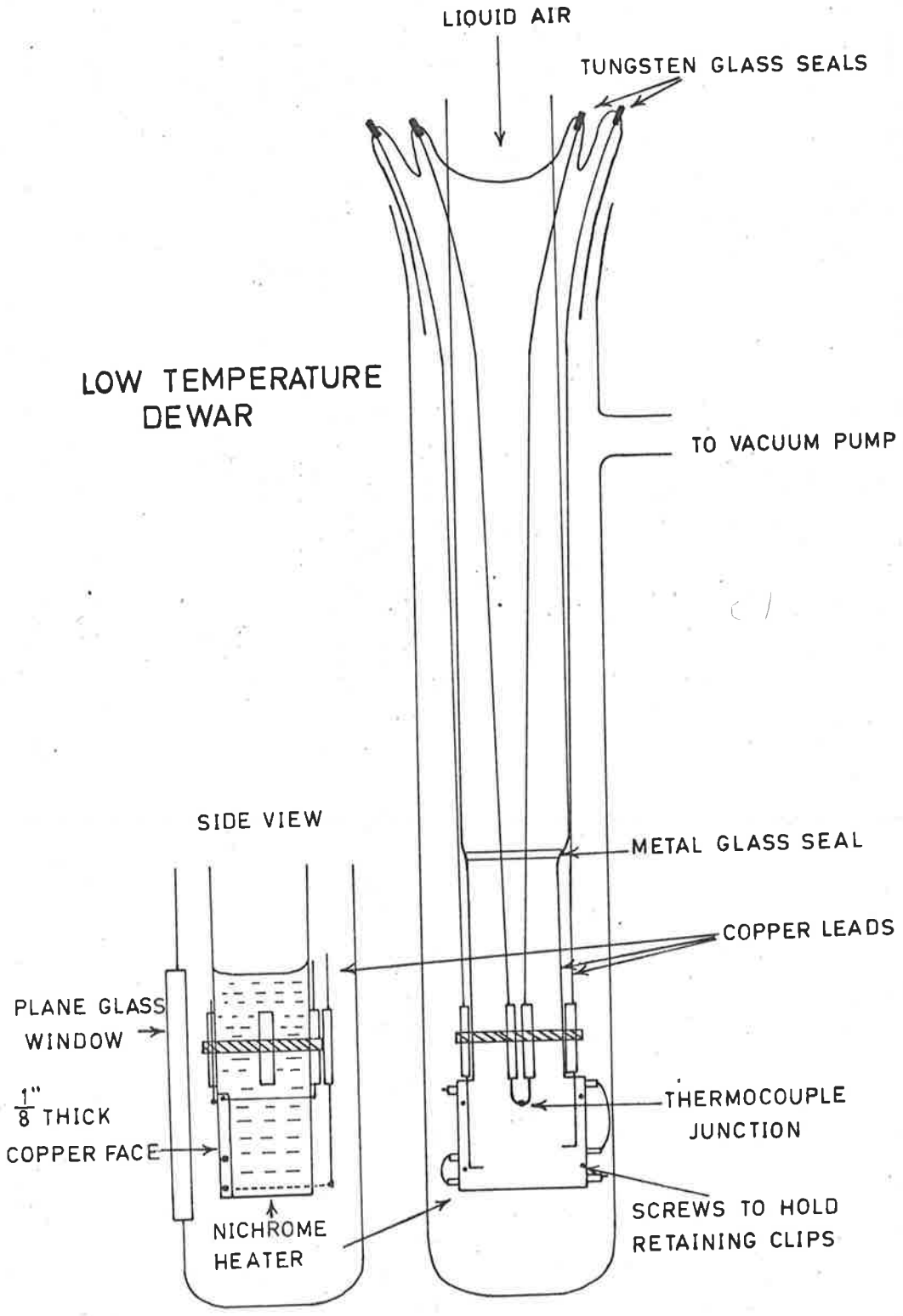
LIQUID AIR
TUNGSTEN GLASS SEALS
LOW TEMPERATURE
DEWAR
TO VACUUM PUMP
SIDE VIEW
METAL GLASS SEAL
COPPER LEADS
PLANE GLASS
WINDOW
1"
8 THICK
COPPER FACE
NICHROME
HEATER
THERMOCOUPLE
JUNCTION
SCREWS TO HOLD
RETAINING CLIPS

FIG. 2.10

that the minimum substrate temperature at which Electroluminescence appeared was 250°C. The temperature of the substrate (using the heater shown in Figure 2.4a) was measured by a chromel-alumel thermocouple. The wire was as thin as possible (38 gauge) to minimize heat loss by conduction. The two ends were twisted together for about 0.5cm and this length was held to the substrate surface by a thin (0.01") cover slip. The cover slip and $SnO_2$ glass substrate were held closely by two small molybdenum clips. The free ends of the thermocouple were soldered to two short tungsten leads, directly sealed through a glass electrode described earlier. The tungsten leads through the glass were reduced to a minimum length and the external leads were connected, with thicker chromel-alumel wire, which was terminated at a cold junction of melting ice (0°C). The output of the thermocouple was monitored by a Cambridge Portable Potentiometer with a reading accuracy of better than 0.01mv. The thermocouple was calibrated at three fixed points, ice (0°C), steam (100°C), and melting sulphur (444°C). From the voltage at these points the constants a, b and c in a polynomial $E = aT + bT^2 + cT^3$ were obtained. This allowed the output to be related to the temperature from a set of graphs which were prepared. It was considered that by using this method of temperature measurement, the 'hot' junction would be relatively free of any extraneous heat losses which would prevent

it from giving a true indication of the temperature of the substrate.

Recently the advantages of using thermocouple films for temperature measurement have been reported. Chromel-alumel films were evaporated to have a small overlap region so forming the film junction. Connection to the two films was made with chromel-alumel wire. Nickel-iron film junctions were also used with improved reproducibility between films (Morrison & Lachenmayer 1963).

It has been shown in this laboratory that errors of up to 50° in several hundred were liable to occur with this method of measuring temperature, unless careful annealing and calibration procedures were adopted (McCoy 1965).

The advantages of the films in this context was the intimate contact between the measuring junction and the surface which was being coated with ZnS. To check the accuracy of the temperatures measured by the previous method, a nickel-iron film junction was evaporated onto the normal conducting glass substrate. The metal films were then annealed at 550°C for 30 minutes under vacuum. The films were joined by silver paint to thin nickel and iron wires, leading through the base plate (via a glass cone as before) to a cold junction at 0°C. The chromel-alumel wire junction used previously was pressed, as described above, to the substrate close to the film junction, and the glass was positioned in the substrate heater. The voltage reading from both thermocouples was

tabulated for a number of temperatures between 100 and 450°C, obtained under the same conditions as used for a typical evaporation.

Over this range the film junction recorded a temperature of 22°C, higher than the thin wire junction. The linearity of the temperature difference showed that the error in the wire junction was due to bad thermal contact with the substrate, rather than heat loss by conduction through the wires. This effect was augmented by the method of radiation heating from above, because the heat transferred to the wire junction occurred by conduction through the glass substrate. A smaller amount of heat was radiated from the hot evaporating boat, but the main contribution at 50°C or above, was from the substrate heater itself.

As a result of this calibration, all previous values of substrate temperature taken with the chromel-alumel thermocouple were increased by 22°C.

## 2.8 Measurement of A.C. current through ZnS Mn films

A conventional power amplifier was constructed to supply a maximum of 250 volts for excitation of the electro-luminescent films. The output contained 0.5% first harmonic and negligible higher harmonic components.

The A.C. current was determined by use of a transformer ratio arm A.C. bridge using two Trimax audio coupling transformers. The film was connected in one arm of the bridge and the standard R-C network in the other

(Figure 2.11). Because of the high applied voltages (20-40 volts) which were required to give light emission, the linearity of the standard components over this voltage range was important. The film was replaced by a variable condenser with an air gap and a non-inductive resistance, and a balance obtained with the same value of R and C. The out of balance bridge current was detected by an amplifier (400X) and C.R.O. (maximum gain 10mv/cm). The bridge supply voltage was used on the X-plates of the C.R.O. to obtain a Lissajous figure, indicating the out of balance current through the common bridge arm. Perfect balance was indicated by a horizontal C.R.O. trace, and the presence of non-linearity in the components resulted in finite width in the figure at higher voltages (i.e. a flattened 'figure 8' pattern). Some non-linearity was present in the capicitance used in the reference arm of the bridge and so a film was measured, first using a bank of condensers with air dielectric, and then the standard. However, the values found in both cases were usually equal to the experimental accuracy of determining the balance point. If at any time the error became excessive ($\geq$ 10%), the results of this calibration were used as a correction factor on the measured values.

The Zns-Mn films showed non-linear characteristics and this made an exact balance with a simple R-C network impossible. Approximate balance gave a complicated pattern and introduced the problem of which particular condition represented a justifiable balance point.

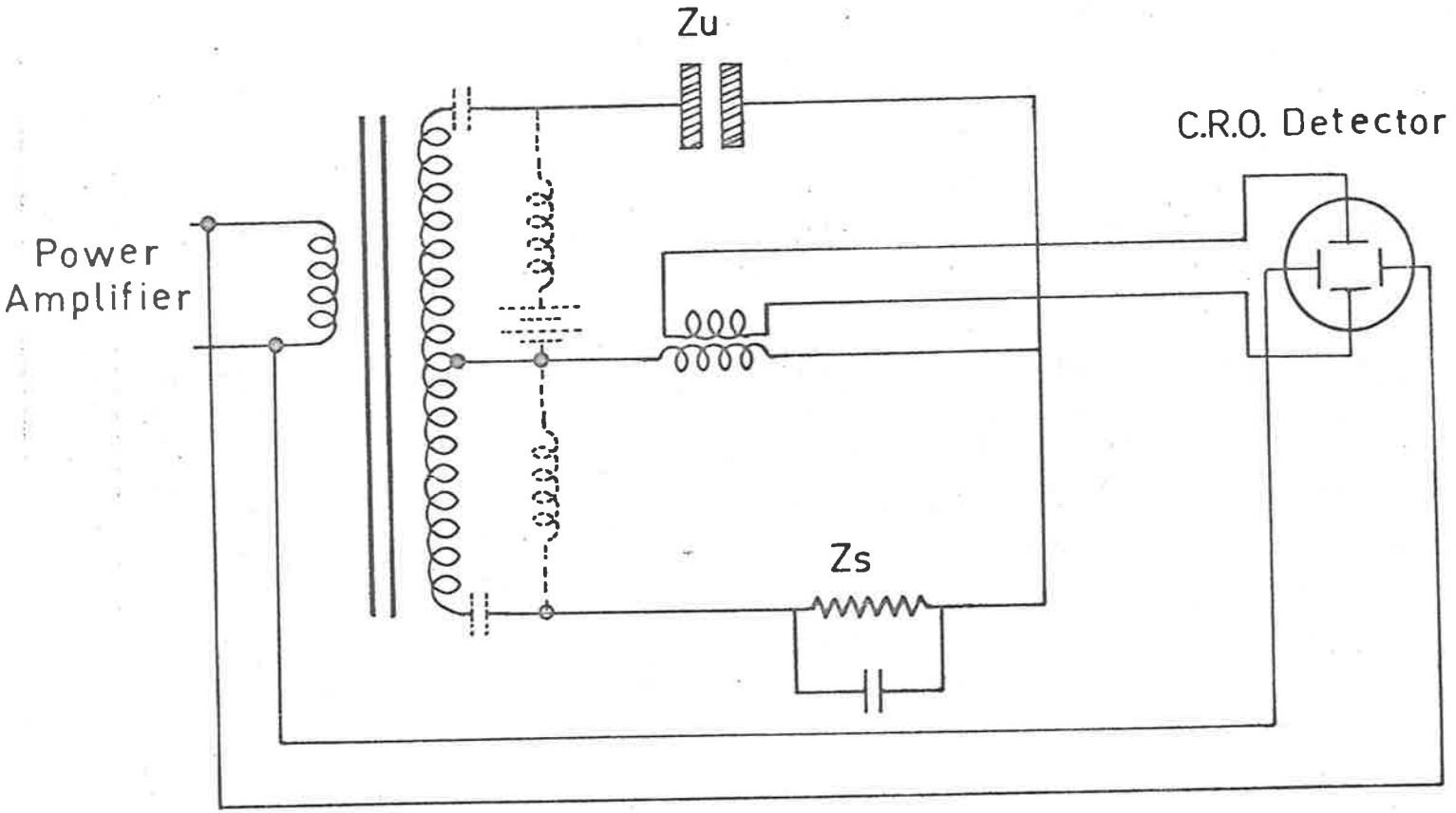


FIG. 2.11 A.C. BRIDGE

Thornton reported this uncertainty and took balance as the point of zero phase difference and zero slope at the origin, (Thornton 1961). This implied a balance at the zeros of the A.C. voltage, with a disregard for behaviour at other points in the voltage cycle. As emission occurred at voltage maxima, the value of the impedance at these points may be quite different from the value at the voltage zero.

Lehovic has suggested an oscillographic method for non linear elements, but to analyse the results it is necessary to assume that the impedance has the same value during the voltage increase and decrease, which is not a priori true for these films, (Lehovic 1949).

As it was impossible to match the film impedance through the voltage range exactly, it was necessary to find the impedance in terms of an equivalent R-C at each point of the voltage cycle. It was supposed that at balance for a given voltage, the C.R.O. trace at that voltage was horizontal and lying on the horizontal axis. For a linear device, this would imply balance at all voltages, but for the non-linear element this value of R and C was a function of the magnitude and direction of voltage. An exception occurred at the zeros of voltage, where it was usually possible to bring points 1 cycle apart into coincidence and maintain both approximately horizontal ($< 2^{o}$) on the C.R.O.

Balancing the bridge at about 20 points throughout the voltage cycle gave the variation of resistance and

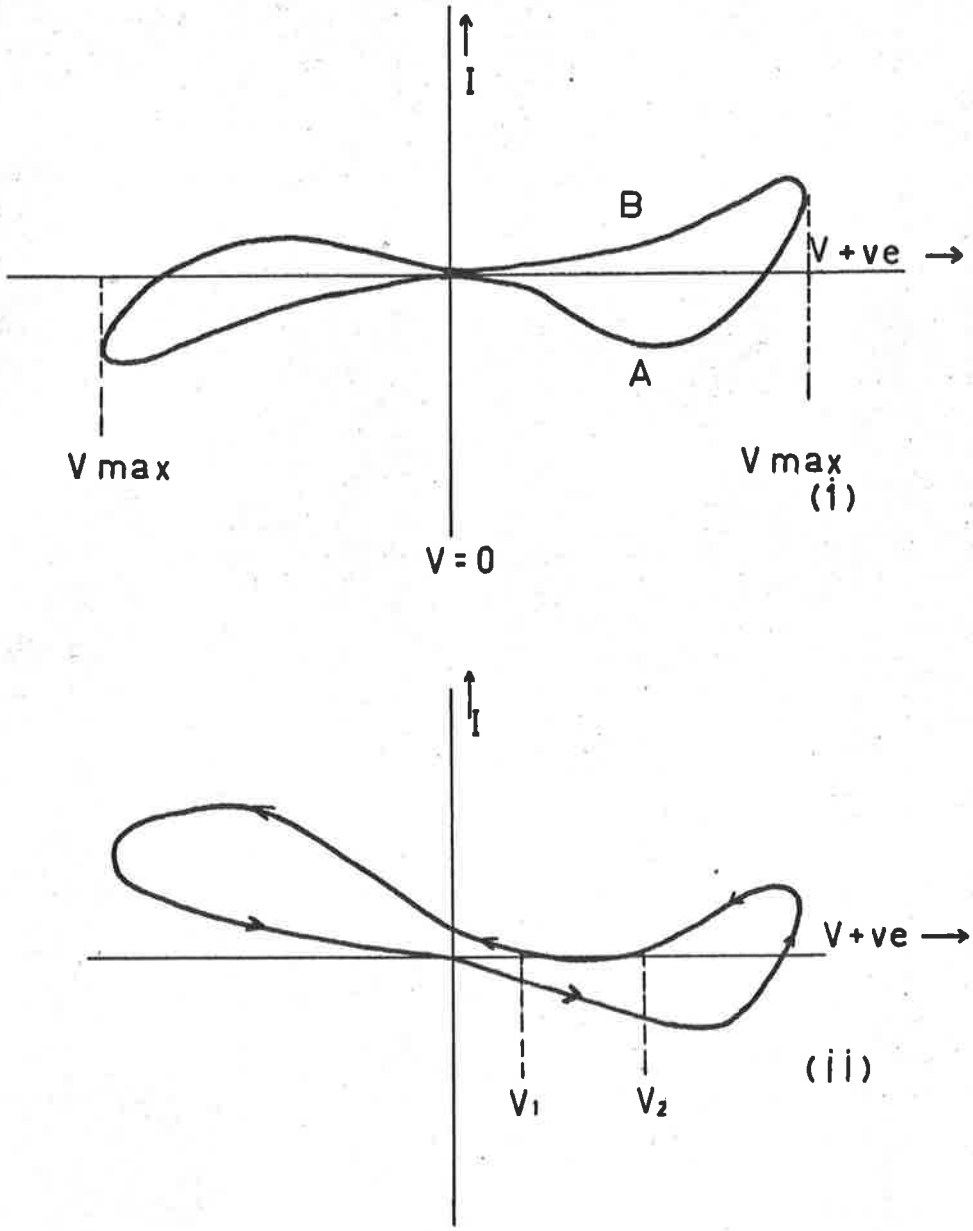


Balance at voltage $V_1$ to $V_2$ during voltage decrease.

FIG. 2.13 BALANCE CONDITION FOR A.C. BRIDGE.

capacitance through the voltage cycle. To determine which part of the balance figure corresponded to increasing voltage from zero (i.e. either curve A or B in Figure 2.13), a voltage, proportional to the light intensity from an electroluminescent film, was fed via the photo-multiplier to the bridge causing superposition of this pulse on the oscilloscope trace. The light pulse had a sharp rise followed by a slower decay, which enabled the identification of the voltage increase trace on the figure representing the out of balance bridge current.

The resistive component of the A.C. current was obtained at the mid point of the balance figure and at points corresponding to the two brightness pulses, over a range of voltage producing light emission. While the absolute values of the current were different (in general by about a factor of 1.5) the slope of the I-V characteristic was unchanged. This justified Thornton's results using the zero voltage balance point.

A balance at the mid point of the oscilloscope trace was used to obtain the results to be described later in this thesis.

# 3. PREPARATION OF CONDUCTING GLASS

## 3.1 Tinoxide films

Transparent conducting substrates are required to form one electrode of the condenser geometry used to study the emission from films. Two forms of conducting transparent films were used during this work. These were tin oxide ($SnO_2$ or a higher form) and cadmium oxide (CdO).

The $SnO_2$ films were deposited on 3" x 1" pyrex microscope slides by spraying them with a solution of equal parts of acetic acid, ethyl alcohol and stannic chloride. During the spray, the slides were maintained at a temperature of approximately 650°C, (Preston 1950).

A heavy stainless steel platform was made to slide through a $1\frac{1}{2}$" diameter tube furnace and the temperature of this was measured by a chromel-alumel thermocouple welded to the stage. Two glass slides could be mounted on this stage, which was then moved into the furnace until its temperature reached 650°C. It was then moved out and sprayed with the above mixture for about five seconds, during which the temperature fell by some 20°C. The slides were then returned to the furnace and the procedure repeated, until sufficiently low resistance films were obtained. The spray was obtained from a simple atomiser using compressed air to give more uniform results. An exhaust fan removed the large amount of gaseous products from this reaction. Three cycles of spraying were usually sufficient to produce films with resistance

of the order of 500 ohms measured over 1" by two point probes.

If a temperature in the neighbourhood of 700°C was used during spraying, the resulting film was of much lower resistance (100 ohms across 1"), but was covered with white specks which made the films unsuitable for use as electrodes. This was thought to be due to small flakes of metallic tin which would also account for the low resistance observed. If the temperature was too low the reaction was unable to proceed fully and the films were of much higher resistance (several thousand ohms). Heat treatment above 550°C was found to increase the resistance of the films made by this method.

The transmission of the best films was approximately 95% for visible light and they were of 250-500 ohms resistance. The optimum spraying temperature was 630-670°C.

During the course of this work some NESA conducting glass ($SnO_2$ coated glass) was obtained from the Pittsburg Glass Company U.S.A. The transmission properties of this were excellent approaching 100%, but the conducting layer was easily destroyed by heat treatment at 550°C. The films made in this Department were unaffected by this temperature and also by most acid treatment. However, both preparations of $SnO_2$ could be removed slowly by 40% HF, which appeared to attack the glass itself by piercing the $SnO_2$ in minute spots, possibly at microscopic defects.

It has been shown that deposition of $SnO_2$ films at

temperatures of 750°C produced films, which were almost unaffected by temperatures of 600-700°C after the film formation (Thornton 1962 private communication).

The results described above indicate that at these deposition temperatures, the transmission of the films decreases because of the supposed tin deposition. It is possible that these inhomogeneities are due to the random size of spray droplets causing localized reactions at higher temperatures. An alternative method (Gomer 1953) uses a reaction between vapour from $SnCl_2$ at 60°C and glass at a high temperature. This method would eliminate the microscopic droplets and may allow higher deposition temperatures without a drop in transmission.

The uniformity of the $SnO_2$ films was very good. A shadowed replica of a conducting film showed very small crystallites ($\simeq$100A) with no apparent preferred orientation.

## 3.2 Cadmium oxide films

The high temperature required for the preparation of $SnO_2$ films made them unsuitable for application to surfaces which would be affected by a high temperature, viz. 650°C. This was an important consideration when preparing ZnS.Mn films between two transparent electrodes, instead of one transparent and one metallic electrode.

Cadmium oxide (CdO) forms a transparent film of high conductivity when formed by cathodic sputtering in a controlled atmosphere (Holland 1960).

The sputtering chamber was a 6" glass bell jar

mounted on a steel base plate.

An aluminium stand was secured to the base plate and this supported the 1" square glass slides to be coated. A 2" diameter cathode of Cadmium (99% pure) was held 1.5cms above the slides by a glass cylinder. The cathode was machined to fit the top of the glass support and its surface was polished to reduce the possibility of an arc discharge initiating at irregularities in the cathode surface. The cathode-anode spacing was adjusted by packing with aluminium sheet under the glass slides. The lead from the cathode to the glass cone through the base plate was shielded by a glass cover, which was found necessary to confine the discharge to the region between the electrodes (Figure 3.1).

The power required for sputtering was obtained from a 1500 volt 20ma supply. The output was controlled by a rotary auto-transformer. The tendency to develop an arc discharge between the electrodes was reduced by connecting a large choke in series with the meter, which monitored the sputtering current. The pressure during sputtering was about $10^{-3}$torr. Higher pressures favoured the formation of an arc discharge between the electrodes. This tendency was favoured by a higher voltage ( 1500 volts).

The procedure used for sputtering was to apply about 1000 volts between the electrodes, with the pressure less than $10^{-4}$torr. The pressure was slowly increased by use of a leak valve until a glow discharge appeared. The voltage was then increased and the pressure adjusted until

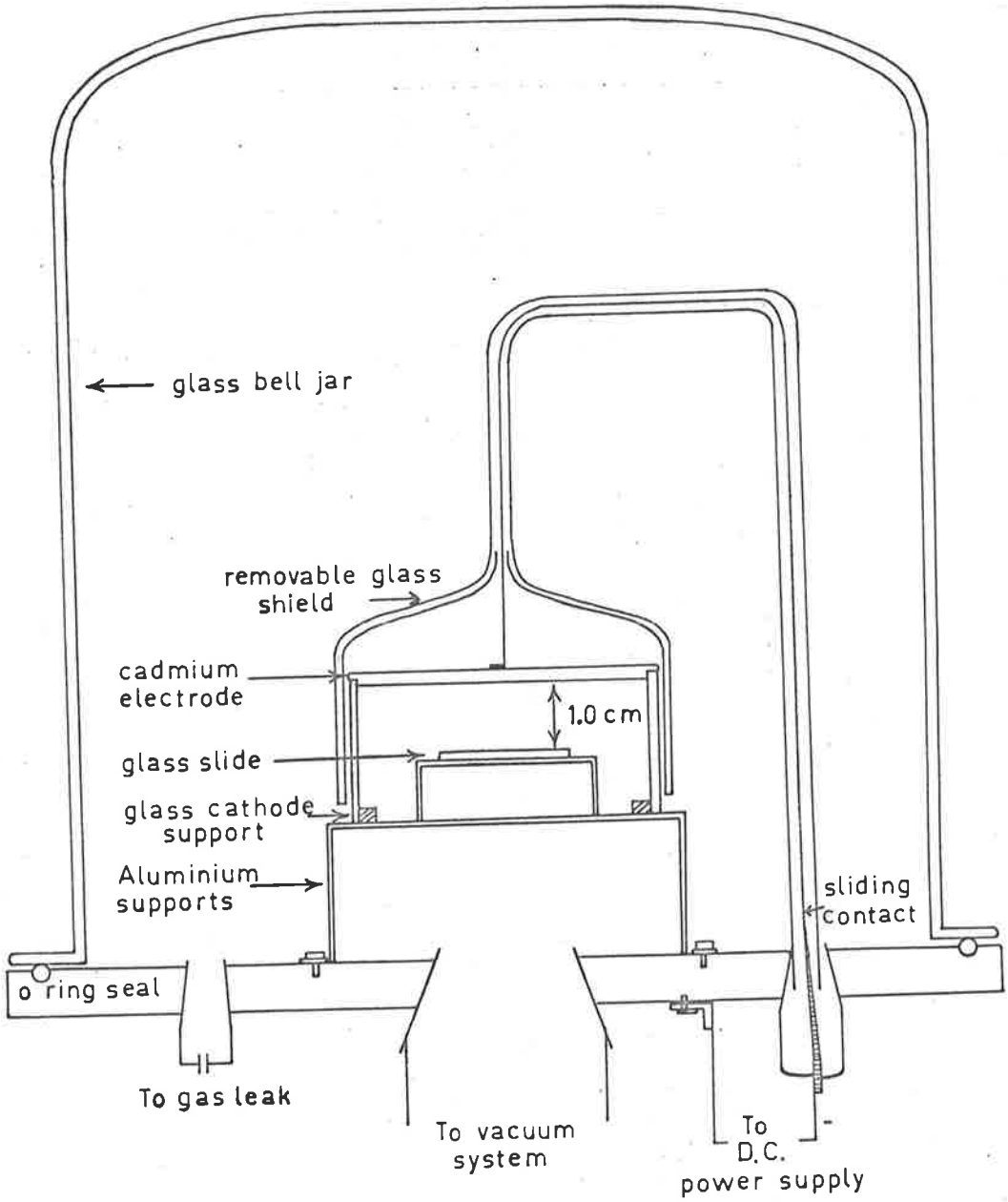


FIG. 3.1 SPUTTERING CHAMBER

the cathode dark space extended approximately 0.5cms from the cathode. The discharge current was varied between 8 and 10ma (0.4 to 0.5 amps/$cm^2$). An improvement in the stability of the glow discharge was noticed after prolonged operation. This effect has been reported before and explained by an ageing process at the cathode surface.

Holland has summarized the results which have been reported for CdO films (Holland 1960). The highest conductivity films were prepared by sputtering in an atmosphere of nitrogen and oxygen. This was consistent with the theory of conduction in these films which supposed an excess of cadmium atoms (Preston 1950).

Recent results also indicate conduction by donors resulting from excess cadmium (Lakshmanan 1963). This author observed a resistance of 22.4K ohms/square for a film sputtered in pure oxygen and a value as low as 88 ohms/square, using a 98% Argon 2% oxygen mixture.

The results obtained here agree with this conduction mechanism. Films with resistance of approximately 500 ohms (between two probes 1" apart) were obtained, using a leak from a cylinder of dry nitrogen. The thickness of the films was not measured, but they showed a strong yellow transmission indicating that the thickness was at least $\lambda/2$ optical thickness. The deposition time for these films was about five minutes. To minimize the temperature rise during this time, the sputtering could be carried out over five intervals of one minute each, allowing time to cool between each deposition.

The resistance of the films may be further decreased by heating in air or in vacuum at 350° for 30 minutes or longer. Reductions of up to five times in the resistance were obtained.

A number of films were prepared using different gas atmospheres. However, by variation of sputtering current and cathode dark space dimensions, it was not possible to reduce the resistance below several thousand ohms and maintain a film with good transmission properties.

The transparent conducting films finally used had a resistance of several hundred ohms with a transmission of approximately 85%, making them ideal for use as transparent electrodes.

## 3.3 Substrate preparation

$SnO_2$ coated glass was highly resistant to acid attack. Therefore to clean the substrates, in preparation for the ZnS film, they were immersed in hot chromic acid. They were then washed in distilled water and finally cleaned by ionic bombardment.

However, because deposition was usually made onto high temperature substrates, this cleaning procedure was not always required. Identical adhesion to the substrate was obtained by cleaning in acetone when the substrate was baked, before evaporating the sulphide.

CdO films were easily destroyed and therefore were usually used directly after they were made to ensure uncontaminated surfaces.

## 4. PREPARATION OF ZnS.Mn FILMS WHICH SHOW ELECTROLUMINESCENCE IN A REPRODUCIBLE FORM

The methods of film preparation described in the literature generally require either high temperature growth of ZnS or high temperature impurity diffusion. Both these techniques give little opportunity to vary the conditions which produce an electroluminescent film. However the method of a single evaporation reported by Koller (1960) offers improved possibilities. For films prepared by this method, the details of the light emission observed from the films may be directly related to the conditions during the film evaporation.

The properties of evaporated semiconducting films in general, are extremely sensitive to the conditions during an evaporation (Davey et al, 1963 on Germanium films). However, when diffusion methods are used, the temperature required for the diffusion is sufficient to destroy any properties of the film which may have been related to the conditions during the actual evaporation.

Koller (1960) found that a single evaporation would produce an electroluminescent film only if manganese was used as the activator. Other activators required post evaporation firing of the activated ZnS film.

Therefore interest was concentrated on ZnS.Mn films. This particular system was thought to possess several additional advantages, mainly because of the single activator. This would eliminate complex energy transfer processes between multiple activators. It is well known that the

transition responsible for the characteristic manganese emission at 5860Å occurs between two localized levels of the manganese ion in the ZnS lattice (Klick 1955). The ground state of the $Mn^{++}$ ion in ZnS lies sufficiently far below the valence band edge so that ionization of an electron into the ZnS conduction band is not thought possible (Piper and Williams 1958). These considerations show that only excitation of the manganese centres will occur, rather than ionization. Therefore, changes in free carrier density in the conduction band will not effect the rate at which an excited centre will emit radiation. This may simplify the interpretation of experimental results.

It is shown in the following sections that, when used in low concentration (about 0.01%), manganese must be present with a second impurity ion to produce an electroluminescent film. However, it will also be shown that an electroluminescent film containing only manganese is possible, and differences between these two techniques will be discussed in a later chapter in terms of energy transfer processes.

Koller also found that a substrate temperature, greater than 250°C was necessary if an electroluminescent film of ZnS.Mn was to be evaporated. This temperature was redetermined, and found to be 290 ± 5°C for ZnS.Mn films evaporated from ZnS.Mn powder phosphors (see Section 4.2b). This critical temperature was also determined for ZnSe films activated by manganese (see following sections).

The values for critical temperature could not be given to an accuracy better than 10°C, because the change in the intensity of the electroluminescence was not sufficiently rapid. The electroluminescent brightness decreased as the substrate temperature decreased through the critical temperature. This therefore increased the voltage at which light was just detectable. As the substrate temperature decreased further, the breakdown voltage for the film was reached before stable emission was observed.

The variation of the voltage at which light could be just detected, hereafter called the 'threshold voltage', with substrate temperature for ZnS.Mn (0.01%) films is shown in Figure 4.1. It should be noted that this threshold is a threshold of the light detecting system rather than a threshold for a process in the electroluminescent film.

## 4.1 Preparation of electroluminescent films by diffusion

To obtain a comparison between electroluminescent films prepared by evaporation and by diffusion techniques, some ZnS.Mn films were prepared by a modified diffusion method. A film of manganese metal was deposited on an evaporated film of pure ZnS without admitting air to the vacuum system between the two evaporations. The manganese contained only trace impurities (several parts/million). The metal was diffused into the sulphide for three hours at a temperature of 550°C (Vlasenko and Popkov 1960). An aluminium electrode was then evaporated on the film to form the second electrode. This was done in a vacuum system operating at $5.10^{-5}$ torr. The aluminium was usually about 5000A thick. Similar electrodes were used on all electroluminescent films described

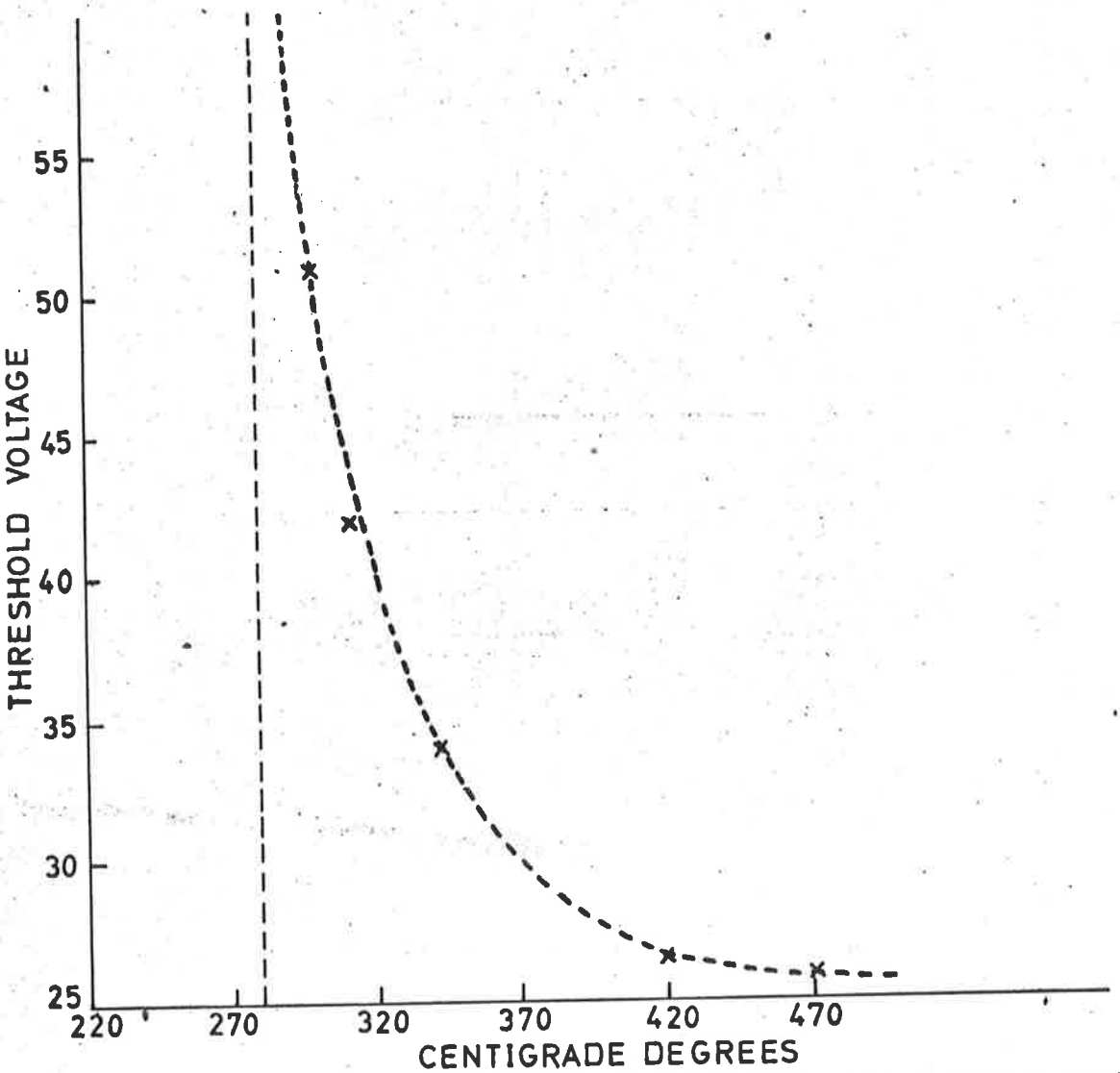


FIG. 4.1 VARIATION OF ELECTROLUMINESCENT THRESHOLD VOLTAGE WITH SUBSTRATE TEMPERATURE DURING EVAPORATION FOR ZnS.Mn(0.01%) FILMS. FILM THICKNESS 1300 ± 100 Å.

in this thesis unless stated to the contrary.

The diffused film was electroluminescent showing the characteristic radiation of the manganese ion. The thickness of the manganese layer, relative to the sulphide thickness was such that the proportion of manganese to ZnS was about 1 in 500. As all the manganese apparently diffused into the ZnS, the concentration in the film was about 0.2%Mn. Preferential diffusion between crystallites may have reduced the concentration in the ZnS crystals.

The preparation of films by this method was critically dependent on the diffusion temperature. This dependence would make controlled variation of the properties of the activated film difficult. In fact the crystallite size was considerably modified by this diffusion so that the structure of the diffused ZnS.Mn film was not closely related to that of the pure sulphide film (see Chapter 5.1).

The preparation techniques described in the following sections gave films which were electroluminescent without any need for post evaporation heat treatment.

## 4.2 Preparation techniques for direct evaporation of electroluminescent films

### (a) Zinc sulphide and metallic manganese

Luminescent grade ZnS (99.99% supplied by Derby and Co. England) was used in this work. The powder showed a green-blue luminescence most likely due to free chloride and oxygen. Pure manganese metal (impurity several parts per million) was obtained from Johnson - Matthey, London.

Thin molybdenum foil (0.01") was used to form a small

evaporating boat. Several small chips of manganese were placed in the boat which was then filled with ZnS powder. The powder was pressed together to minimize loss during the evaporation.

The heating current through the boat was slowly increased until the ZnS began to evaporate. This temperature was approximately 950-1050$^{o}$C, measured by viewing the walls of the boat with an optical pyrometer. If the temperature of the (tin oxide coated glass) substrate was greater than 290$^{o}$C, the resulting films showed electroluminescence at an applied voltage of 20-30 volts. The emission seemed quite uniform and its wavelength (5850A) showed that manganese ions had been excited by the applied field. Some properties of the light emission from these films are discussed in a following chapter.

This method, although rather crude gave the first successful electroluminescent films, but was difficult to control because both the ZnS and Manganese necessarily evaporated at the same temperature. Thus there was no way of varying the activator concentration. Increasing the boat temperature to give a thicker film (> 1000A) resulted in films which did not show electroluminescence. This may have been due to excessive manganese evaporating at the higher temperature, or to some other change caused by the increased boat temperature. The sensitivity of film resistivity to small changes in the evaporating temperature has been reported (Davey 1963).

To obtain an electroluminescent film by this technique

the evaporation rate could not be varied from a value of about 100Å/minute.

The success of the method as regards the appearance of electroluminescence in the films was very dependent on the boat temperature and as a result many films were inactive, although the conditions were apparently the same as when successful films were made. This sensitivity was thought to result from the strong temperature dependence of the maganese evaporation rate.

Several attempts to determine the concentration of manganese in the films were made by weighing the manganese chips before and after evaporation of all the ZnS in the boat. Although the weighings were carried out to the nearest 10 micrograms, the results were not reproducible. However an indication that the films contained about $10^{-4}$ grams of manganese per gram of ZnS was obtained. The amount incorporated at each evaporation was likely to have been different from this average because of the large excess of manganese used (about one milligram).

Another disadvantage of this method was an uncertainty concerning the even doping of the film because of the different temperature threshold for evaporation of the two materials.

It was found that it was possible to slowly evaporate a ZnS film which contained no manganese because the boat temperature was not sufficiently high to evaporate the metal. As the boat temperature was slowly increased during the evaporation to maintain the same evaporation rate, the

above result introduced some doubt about the uniformity of the manganese incorporation.

To obtain a greater degree of control during the film preparation, pure ZnS and metallic manganese were evaporated from two independently heated boats. The boats were as close as possible to ensure that the two beams of ZnS and manganese were directed onto the substrate. The current through the manganese boat was monitored and adjusted until a film of given thickness (e.g. 100A) was deposited at a uniform rate in a given time (e.g. 2 minutes). This procedure was repeated exactly when the ZnS was being evaporated. After 2 minutes of both materials evaporating, a cover was moved over both boats to end the film formation. The concentration of manganese in the films was found from the known thickness of manganese deposited initially and the final thickness of the composite film.

It was difficult to obtain uniform films of manganese with thickness much less than 100Å. Therefore to obtain a concentration of even $10^{-2}$g/g, the final film needed to be one micron thick. To keep the thickness of the ZnS within reason the path of the evaporating manganese was interrupted by a rotating chopper. This was of 2" diameter aluminium with a 0.1" width slot cut out on the circumference. It was rotated from outside the bell jar wall by using magnetic coupling between 2 short bar magnets, one rotated by an electric motor outside the vacuum system. The rate of rotation was several hundred revolutions/minute, so that over a five minute period in which a 5000Å ZnS film was

deposited, the shutter was open about 2500 times. This ensured that manganese was deposited uniformly on the substrate as the ZnS crystals were formed, because the shutter was open every 2Å of film growth. However, no electroluminescence could be detected in films made by this method.

It was thought that this negative result may have been due to the manganese not being incorporated in the ZnS film. That this was not the case was shown by placing a small piece of film (on a cover slip) in the cavity of an E.S.R. spectrometer. A six line spectrum, superimposed in some cases on a broad line was observed which showed the presence of the $Mn^{++}$ ion at an approximate concentration of 0.1% (Schneider and England, 1951). This agreed with the amount supposed present from the details of the preparation.

The determination of the manganese content from the character of the E.S.R. spectrum was considered and will be described later in this chapter.

The failure of this method to produce successful films was not a fault in the particular technique, but rather the result of not fulfilling one condition which was necessary to give electroluminescent films. The importance of this condition was discovered at a later time and with the knowledge of its importance the above technique was then modified and used successfully. This necessary condition will be described in the next section.

4.2 (b) Evaporation of ZnS powders

Because of the lack of success with the above technique direct evaporation of an electroluminescent powder was considered. Methods for preparing luminescent phosphor powders are well known, and it was found that a luminescent phosphor could be made very easily by firing a mixture of pure ZnS with the impurity (0.01% Mn as $MnSO_4$) in a stream of dry oxygen-free nitrogen for 3 hours at 1100°C. The powder was cooled over several hours, washed in acetic acid to remove free ZnO and washed finally in distilled water. This was then evaporated from a molybdenum boat as before. (In the initial stages of this work an electroluminescent powder was kindly made available by D.H. Brown, Weapons Research Establishment, South Australia. This gave the same results as powders prepared in this Laboratory.)

It was found that if conditions were such that excess of zinc was evaporated with these activated powders, electroluminescent films could be produced. The emission was then centred at the characteristic manganese wavelength, and different evaporation rates (200Å/minute to 2000Å/min) were used successfully to deposit films of varying thickness. The presence of excess zinc during these evaporations was shown by the following observations.

The molybdenum boat was always initially degassed and cleaned by heating to 1300°C for 5-10 minutes. During this time the potassium, usually present in molybdenum, evaporated and so minimized the contamination from the boat during subsequent ZnS evaporations. The first evaporation

from a clean boat always produced a non electroluminescent film. A new charge of powder was placed in the boat and a second evaporation performed onto a new substrate. This was repeated until the films suddenly began to show light emission. Usually this occurred after 3-5 evaporations from the same boat. As long as the same boat was used, additional films were successful but if a new boat was used another series of 3-5 films had to be made before electroluminescence appeared.

The resistance of the films made from powder evaporation was measured at a D.C. voltage of 1 volt, using electrodes of constant area. It was generally found that non electroluminescent films showed relatively high resistance, $10^8$ ohms or more, (implying an approximate resistivity $\rho$, greater than $10^{\text{"}}$ ohm cm . Films which showed light emission were of much smaller resistance, $10^4$-$10^5$ ohms ($\rho = 5.10^7$-$5.10^8$ ohm cm ). This correlation was confirmed by making several series of films under identical conditions using the same boat. The first four or five films showed no electroluminescence and were high resistance, while the next and subsequent films were low resistance and showed strong light emission.

Electroluminescence in films evaporated from ZnS powder contained in a clean degassed boat could not be produced by variation of evaporation rate, oxygen pressure in the vacuum system or the temperature of the substrate. While all of these quantities produced small variations in the resistance the observed changes were not as marked as

the decrease correlated with the appearance of light emission.

These results suggested that the cause of the low resistance films was related to the use of the same boat for several evaporations. The condition of the boat was therefore examined and it was found that as the number of evaporations from a given boat increased, there was a corresponding increase of a grey metallic coating over the inner walls of the boat. It was possible to scrape a small amount of this off and an analysis showed it to be zinc metal. There was a small amount of manganese metal present also.

Therefore, either the manganese content had been too small to give emission or the excess zinc caused by reduction of the ZnS on the crucible walls was necessary. The first possibility was not valid because even at a manganese concentration of 1.0% in the powder, the accumulation effect occurred. Later evidence showed that as little as $5.10^{-5}$ gm/gm of manganese was sufficient to give light emission.

The excess zinc in the boat would build up over the period of 3-5 evaporations and reach a sufficient level to provide appreciable zinc doping of subsequent films. This also explained the sudden fall of resistance as excess zinc in ZnS may act as a donor with energy levels 0.25 - 0.30e.v. below the conduction band of ZnS (Bube 1960 , Baba 1963).

From these results the evaporation of an electroluminescent film must be performed from a ZnS.Mn phosphor containing an excess of zinc. The way in which this excess

produced electroluminescence was not clear from these experiments, however the presence of a zinc excess was associated with a decrease in film resistivity.

With this information it was possible to deposit a film from an electroluminescent powder in a new boat immediately, by adding an excess of zinc metal to the powder before the evaporation. It was found necessary to use 1% of zinc. However, the actual mixing of the two was only mechanical and it was possible that the difference in evaporating temperatures affected the amount of zinc incorporated in the film. The mixture was preheated at 500$^{o}$C for 30 minutes and then raised steadily to the evaporating temperature of ZnS. No initial evaporation of zinc was detected on a moveable glass slide placed over the boat containing the ZnS.Mn - Zn mixture.

Using this technique there was still some doubt concerning the relation between the manganese concentration in the film and in the original powder because of the manganese deposit in the evaporating boat. This was also shown by evaporating powders with a high manganese content (1%). A green residue was left in the boat after evaporation which contained about 10% manganese (possibly MnO, melting point 1546$^{o}$C). This proved that it was difficult to incorporate a large concentration of activator in the films by this method.

4.2 (c) Evaporation of ZnS.Mn films from large crystals of ZnS

The most successful method of film preparation was

the evaporation of large single crystals. The reproducibility of films prepared in this way was excellent, and by evaporating the whole volume of a crystal the doping impurities were transferred to the film with a minimum loss by preferential evaporation. This was shown by the sensitivity of the films to small amounts (0.01%) of impurity added to the crystals during their preparation.

The usual preparation of ZnS crystals uses growth from the vapour phase (Frerichs 1947). A preliminary attempt was made to ascertain the suitability of crystals obtained in this way for the preparation of electroluminescent ZnS.Mn films.

The preparation method was conventional. Five grams of ZnS.Mn (0.01%) were heaped at the closed end of a quartz tube (1" diameter). The tube was then filled with dry $H_2S$ to a pressure of 10mm of mercury. The $H_2S$ was produced by a chemical reaction between calcium sulphide and a saturated solution of magnesium sulphate at $60^{\circ}C$.

The furnace tube was evacuated to $10^{-4}$torr before filling with $H_2S$ to a pressure monitored by a mercury manometer. The tube was then heated in a furnace for 62 hours at $1170^{\circ}C$. The ZnS sublimed from the high temperature end of the furnace tube and condensed to form needle shaped crystals on the cooler walls of the tube (Figure 4.2). The average size of the crystals was 0.5cm in length with a square cross section of 0.5mm on a side. The average weight of a crystal was 1.0 milligrams. The crystals showed a pale yellow colour indicating the presence of manganese.

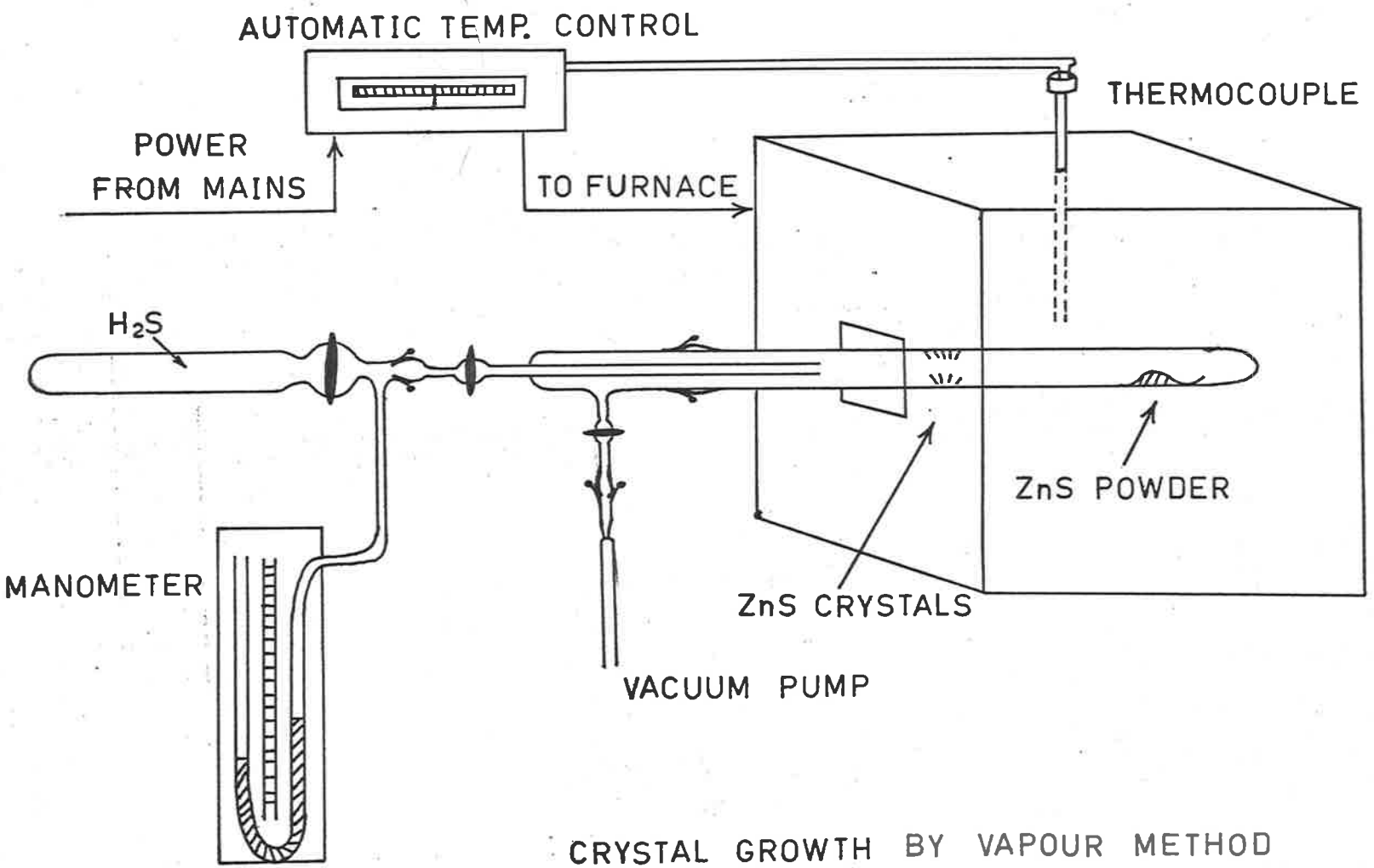


CRYSTAL GROWTH BY VAPOUR METHOD

FIG. 4.2

These crystals of ZnS.Mn, grown from the vapour phase without any zinc doping, did not produce electroluminescent films when evaporated. Negative results were also obtained with cubic ZnS.Mn crystals obtained from Semi-elements Inc. U.S.A.

X-ray analysis of the crystals grown in this laboratory showed the presence of a large concentration of stacking faults in a basic hexagonal structure, but no evidence for the cubic phase of ZnS. (The analysis was done by Dr. B.W. Matthews in this laboratory). This observation is similar to that made for ZnS crystals grown in vacuum (Piper 1952).

This variation of the vapour phase method produced very small crystals and required an excessive time for their growth. Although the formation of large crystals from the vapour phase is possible (Greene et al 1958), an alternative method involving melting ZnS under pressure was developed.

Pure ZnS and ZnSe powders (99.99% purity) were used to grow crystals from the liquid phase. ZnS melts under pressure (> 100 p.s.i.) at 1830$^{o}$C while ZnSe melts at 1515$^{o}$ at a similar pressure. The method of growth has been described (Chapter 2.4).

The crystals of ZnS grown by this technique were shown to be of mixed cubic and hexagonal structure by X-ray diffraction. An oscillation of 15$^{o}$ about the vertical axis of the crystals (i.e. the axis of the crucible during growth) gave a photograph showing spots corresponding to reflections from both crystal modifications of ZnS.

Many reflections appeared as rather diffuse spots indicating the presence in the crystal of regions of disorder (Henry et al, 1953).

The mixed crystal structure of the crystals was also evident from the electron spin resonance spectrum of manganese ($Mn^{++}$) in the crystals. Lines due to $Mn^{++}$ ions in sites of hexagonal symmetry were observed, together with lines identified as due to $Mn^{++}$ in cubic sites.

Further investigation of the crystal structure was not considered because the crystals were only a convenient source of ZnS for evaporation purposes.

In contrast to this mixed crystal structure, ZnSe formed pure cubic crystals. This was shown by X-ray diffraction (Cavenett 1964).

Figure 4.3 shows some crystals used in this work and others successfully grown in the apparatus described in Chapter 2. The ZnS cubic crystal was obtained from Semi-elements Inc. The colour of the ZnS.Mn vapour phase crystals was pale yellow (due to manganese), while the melt grown crystal showed a pale green body colour, together with a yellow colouration due to manganese.

Of particular importance was the incorporation of manganese in the crystals. At an added concentration of 0.01% in ZnS, the crystals showed a pale yellow luminescence (3650Å excitation) together with a faint green emission. The glow was uniform indicating uniform activation. The segregation of impurity at the top of the crystal observed by Addamiano was not noticed here, due to the rapid cooling


FIG. 4.3 GROUP II-VI CRYSTALS.

used. Sufficiently uniform doping (even at ZnS.Mn 1.0%) was obtained to ensure that each small part of the crystal used, contained the same proportion of impurity. However, if the cooling time was extended, segregation occurred at the top of the crystal boule as shown in Figure 4.3. Crystals of zinc selenide prepared by a rapid cooling (60 minutes) also showed no segregation.

Analysis by the X-ray fluorescence technique (Australian Mineral Development Laboratory, Adelaide) showed that all the manganese added to the ZnSe crystals had been incorporated in the crystals. However, the proportion in the ZnS was 2 - 2.5 times more than originally added. This was due to the loss of ZnS during crystal growth.

ZnSe.Mn crystals grown from the melt did not produce electroluminescent films when they were evaporated. This was observed for all substrate temperatures. However, if excess zinc (as the metal) was added to the powder which was used to grow the crystals, the evaporated films showed electroluminescence. The amount of zinc required was about 1%. However, 0.4% was insufficient to produce an electroluminescent film at any substrate temperature.

The critical substrate temperature for ZnSe.Mn (0.01%), Zn(1%) films was determined as 310 ± 5°C, using a nickel iron thermocouple. For ZnSe.Mn (0.01%) Zn (2.6%), this temperature was also found to be 310 ± 5°C.

In contrast to the results for ZnSe, ZnS.Mn crystals grown from the melt produced electroluminescent films without the excess zinc doping. The critical substrate

temperature was 290 ± 5°C, the same value as found for films deposited from activated powders.

The resistivity of electroluminescent films (both ZnS and ZnSe) was about $5.10^{9}$ ohm $cm^{-1}$, an order of magnitude higher than observed for ZnS.Mn, Zn films prepared from powders. This difference may have been a result of the unknown amount of excess zinc present when powders were evaporated. However, even when 1% of zinc was mixed with ZnS.Mn and evaporated from a clean boat, the film resistivity was lower than when crystals were used.

The variation of film resistivity with substrate temperature is shown in Figure 4.4. A similar variation was observed for ZnSe.Mn, Zn films.

Because electroluminescent films could be deposited from ZnS.Mn crystals without zinc doping, it was necessary to suppose that they contained this excess due to some reaction during crystal growth from the melt. This possibility is considered in the following section.

## 4.3 Excess zinc in ZnS.Mn crystals

Some properties of excess zinc in ZnS have been reported. The excess provides two donor electrons, one easily ionized (0.3e.v.) below the conduction band and the other responsible for a green luminescent transition between the ion and the conduction band of the ZnS, (Krŏger 1956).

It has been suggested (Addamiano 1963) that the ZnS in the carbon crucible used for the crystal growing may be reduced to zinc on the crucible walls. A similar reaction may occur for ZnSe in a carbon crucible, but evidently the

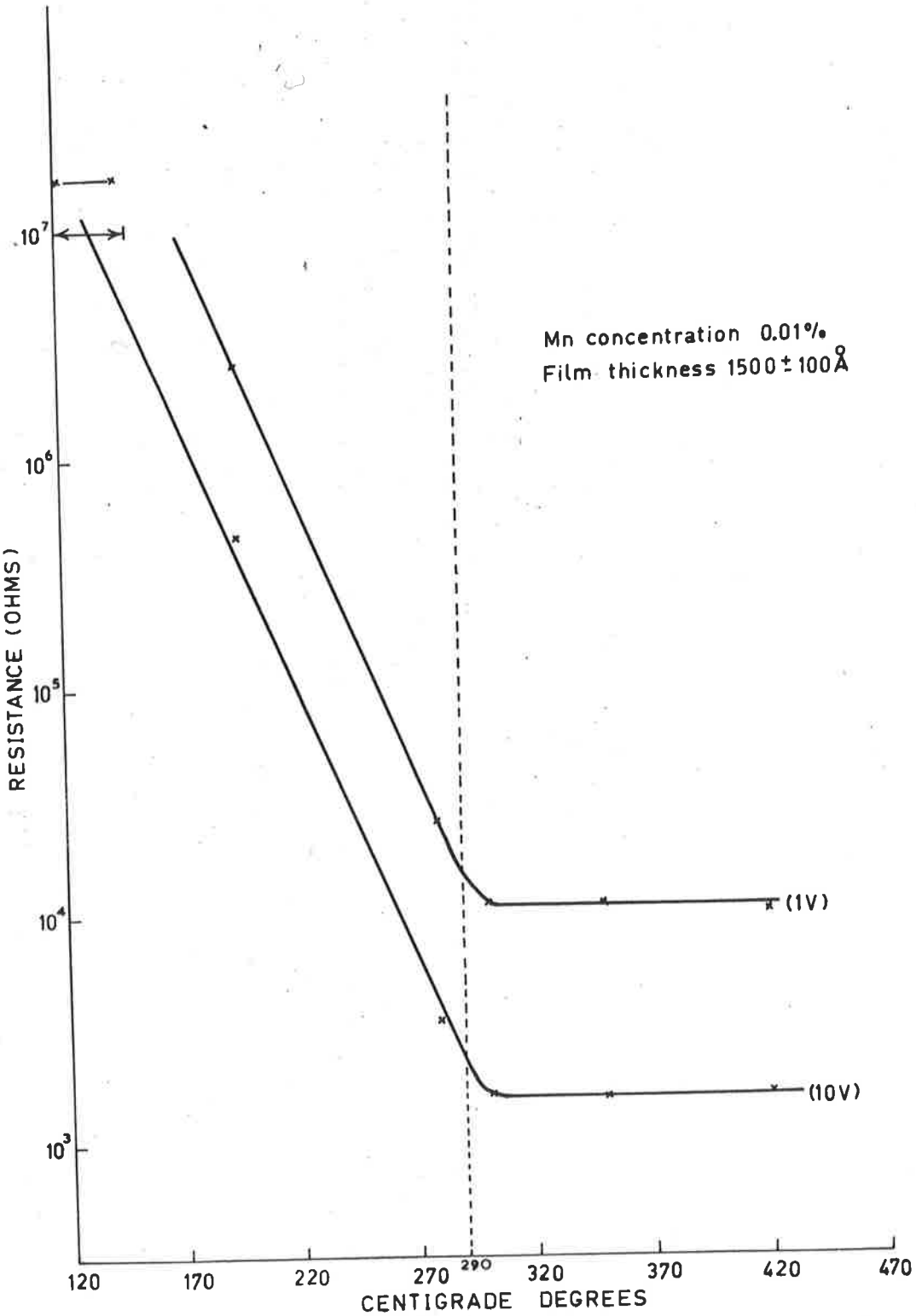


FIG 4.4 D.C. RESISTANCE OF ELECTROLUMINESCENT ZnS.Mn FILMS AS A FUNCTION OF SUBTRATE TEMPERATURE DURING EVAPORATION.

amount of zinc introduced is not sufficient to produce electroluminescence in films evaporated from the crystals.

Pure ZnS was sintered at 1600°C for several minutes in the bomb and then cooled quickly. A self supporting pellet of ZnS was obtained and this was broken across its length and the exposed section irradiated with 3650Å radiation. A strong green luminescent ring around the outside of the pellet was visible. This green area penetrated into the bulk about 1mm. The bulk showed a weaker blue-orange luminescence (Figure 4.5).

Analysis of the powder from the outside and the centre of the ZnS showed that the ZnS which had been in contact with the crucible walls contained about 1.0% more zinc than the bulk. This difference was a significant one in the opinion of the Analyst (Australian Mineral Development Limited, Adelaide). This supported the theory of excess zinc formed next to the crucible walls when ZnS crystals were grown from the liquid phase.

After the ZnS had been melted and cooled to form a crystal, the photoluminescent spectrum was modified. Figure 4.6 shows the spectrum from a pure ZnS crystal. The crystals showed a uniform pale green colour, and this was reflected in a strong emission peak at 5600Å when the crystals were excited by U.V. (3650Å) radiation. This was assumed to be due to the excess of zinc which on melting had been uniformly distributed in the crystal. Photoluminescence in ZnS due to excess zinc has been found at 5100Å by Smit and Kröger (1949). The difference in

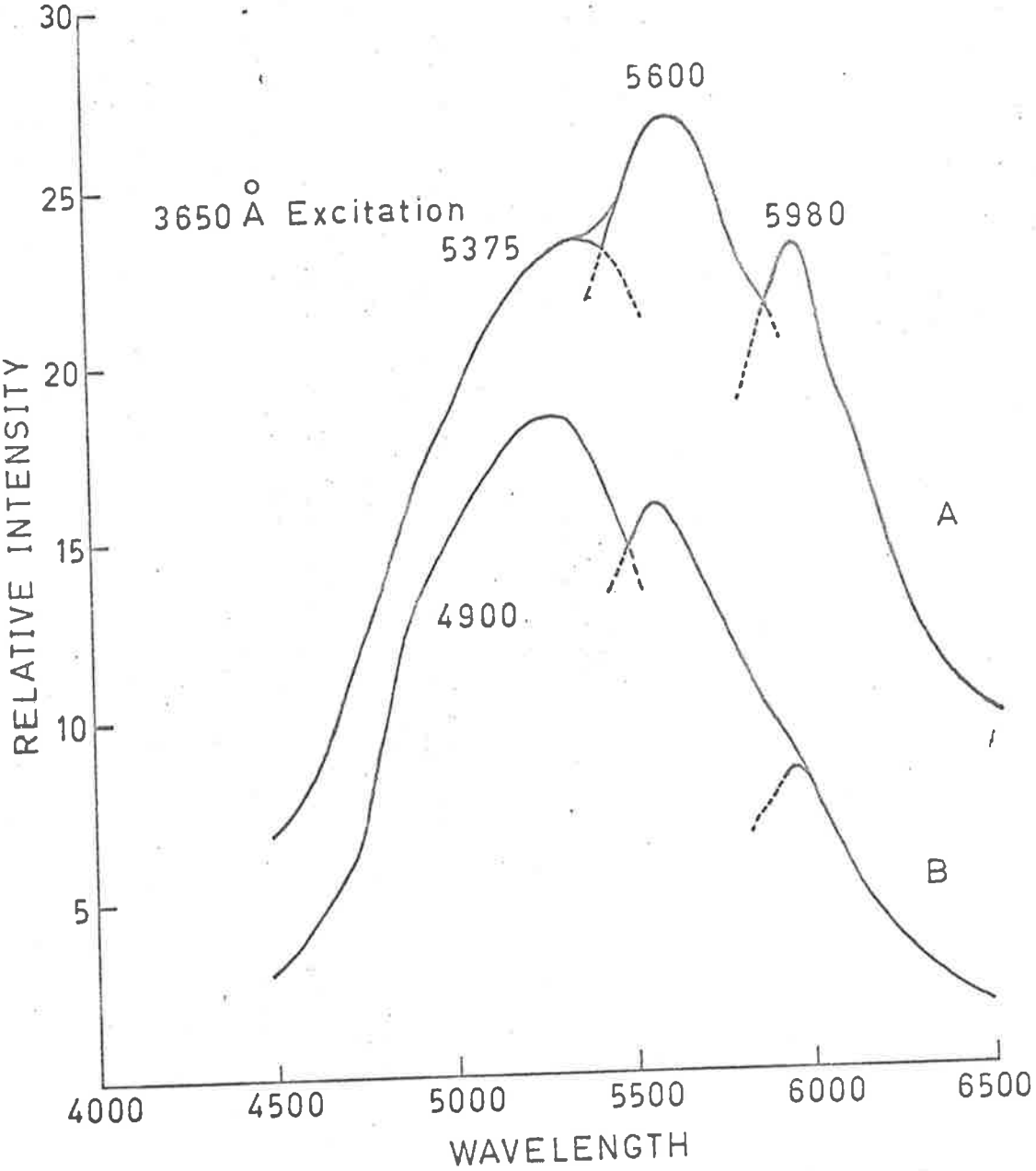


FIG 4.5 LUMINESCENT SPECTRA OF SINTERED ZnS IN CONTACT WITH CARBON CRUCIBLE (A) AND IN CENTRE OF MASS (B).

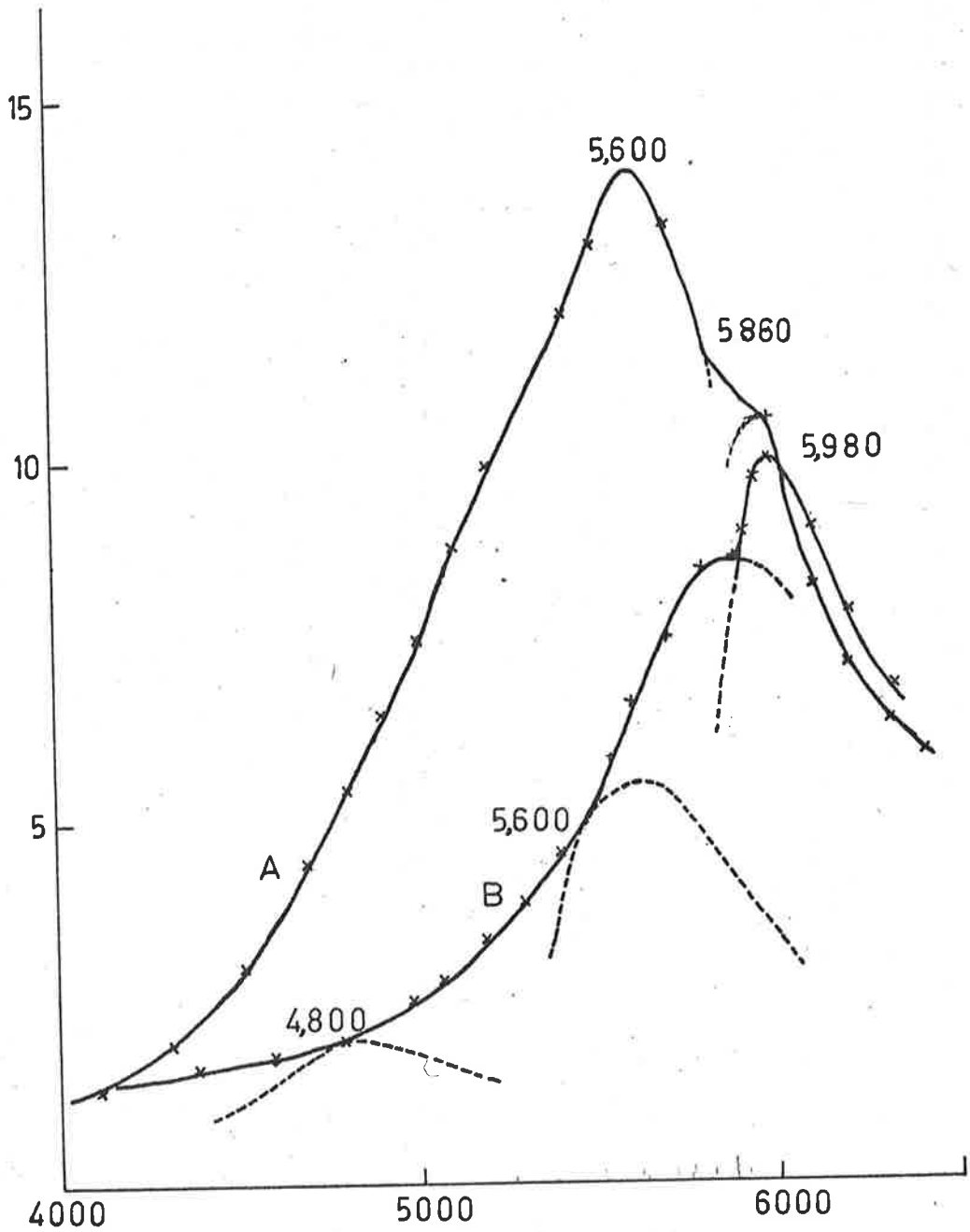


FIG 4.6 PHOTOLUMINESCENT SPECTRA OF A ZnS CRYSTAL (A) AND A ZnS Mn (0.01%) CRYSTAL (B). EXCITATION BY 3650 Å. RADIATION. CURVES CORRECTED FOR PHOTOMULTIPLIER RESPONSE.

wavelength may be attributed to other trace impurities in the ZnS used by these authors.

An additional emission band in the ZnS crystals was observed at 5900-5980Å. It was noted also that the emission bands at 5375 and 4900Å, observed from the sintered ZnS, were negligible.

Figure 4.6 also shows the spectrum of ZnS.Mn (0.01%). The manganese was added as $MnSO_4.H_2O$. The characteristic manganese emission at 5850Å was observed and the 5980Å peak enhanced. A new band at 4800Å was also observed. If the manganese was added as the metal only 5850 and 5600Å emission peaks were observed. Therefore the peaks at 5980Å and 4800Å were caused by the oxygen in the $MnSO_4.H_2O$. The presence of oxygen in the system ZnS-MnO shifts the manganese band at 5860Å to approximately 5900Å (Osiko 1962) and this may account for the band about 6000Å. The presence of oxygen in a nearest neighbour site of an excess zinc ion may be sufficient to explain the 4900Å band.

These results showed that ZnS.Mn crystals contained a zinc excess and that oxygen as well as manganese was present. The effect of the incorporated oxygen in the crystals on the electroluminescent properties of films was negligible, because similar results were obtained when ZnS.Mn and ZnS($MnSO_4$) crystals were used to deposit the films.

The emission band at 5600Å discussed above, was attributed to a zinc excess. However, it was shown that zinc alone would not produce luminescence in ZnSe crystals. This suggested that the ZnS.Zn luminescence was caused by

zinc associated with another impurity. Some information concerning this emission was obtained by an examination of the original pure ZnS used to grow the crystals.

This pure powder showed some emission when excited by 3650Å radiation. The spectrum contained three peaks at 5250, 5400 and 5600Å with a smaller band centred at 4800Å. The emission must be due to either impurities or to a defect centre. The powder was washed in acetic acid to remove traces of zinc oxide (which may also give green luminescence in this range), however, the spectrum was unchanged.

Analysis of the powder showed that it contained 5-7 parts per million of copper (the most likely cause of luminescence in the wavelength range observed). Copper centres gave rise to emission bands at 5230 and 4450Å (in hexagonal ZnS) and at 5350 and 4600Å (in cubic ZnS) (Curie 1960).

Three observations oppose an explanation in terms of copper impurity.

(a) The luminescence was destroyed by heating in hydrogen sulphide for 3 hours at 400°C, (b) there were no emission bands corresponding to the 5250 and 5400Å emission from the ZnS powder in the ZnS crystals, and (c) no definite emission bands were observed at 4450 or 4600Å (characteristic copper emission).

Heating in hydrogen sulphide is the conventional technique for removing traces of chlorine and oxygen which are usually present in commercial ZnS powder. Result (a) above, therefore suggested the presence of a defect luminescent centre due to excess zinc. The various emission

peaks of the pure powder would then be due to an excess zinc ion with nearest neighbours of $Cl^-$ or $O^{--}$. The 4800Å peak was due to oxygen as demonstrated above. The presence of the excess zinc in pure ZnS powder may explain why zinc is deposited in the molybdenum boat used for powder evaporations. However, an unknown proportion of decomposition in the boat may also explain the deposition of zinc (see Chapter 4.5).

It has been shown that ZnS.Mn crystals grown from the liquid phase contain chlorine (as $Cl^-$) and oxygen (as $O^{--}$). It may then be argued, that the lower film resistivity observed when these crystals are evaporated to form electroluminescent films, is a result of $Cl^-$ which is an electron donor, rather than of the zinc excess. The observation that evaporation of ZnS.Mn powder (containing $Cl^-$) did not produce an electroluminescent film showed that $Cl^-$ was not sufficient for the light emission effect to occur. However, the addition of zinc to the powder produced strong electroluminescence.

Addition of 1% of a donor ($Al^{+++}$) to ZnSe.Mn (0.01%) did not produce an electroluminescent film. The total added aluminium was incorporated in the crystal as evidenced by analysis. The incorporation of a substitutional donor ion (e.g. Cl or $Al^{+++}$) in ZnSe (or ZnS) usually does not result in the expected decrease of resistance because of the auto-compensation mechanism which is assumed to occur in the II - VI compounds (see for example Fischer 1961). This process automatically results in the formation

of one anion vacancy for the addition of two donors, thus capturing the donor electrons. However, the final result (the localization of two electrons at a sulphur vacancy) should be the same for both $Cl^-$, $Al^{+++}$ and excess zinc. The observation that, only zinc causes electroluminescence and a decrease in resistance in films, may be due to the limited solubility in ZnS of ions with different charge states ($Cl^-$ or $Al^{+++}$) to the lattice ions. This is in accord with the results described in the following section, where excess of the $Mn^{++}$ ion is shown to give the same effects as excess of the $Zn^{++}$ ion.

Alternatively, doubly charged ions may be incorporated at interstitial positions and therefore would not be associated with the formation of sulphur vacancies. This double donor should be more readily ionized than an electron localized at a vacancy.

It has been reported above that ZnSe.Mn Zn crystals did not luminesce when excited by radiation in the absorption band of manganese. Also, a ZnS.Mn crystal grown from the melt using ZnS powder treated with $H_2S$, as described earlier, showed no photoluminescence. Curie (1964) has suggested that the 5860Å manganese emission can only be obtained when the manganese ion is associated with a defect in the lattice, e.g. excess zinc or $Cl^-$. The two observations above do not agree with this model because, in both cases, the crystals contain excess zinc and show no luminescence. The results obtained here favour a model in which, the manganese emission is caused by a defect (excess zinc or

a sulphur vacancy) in association with either $Cl^-$ or $O^{--}$.

## 4.4 Evaporated films without excess zinc which show electroluminescence

It has been shown that an evaporated film of ZnS.Mn (0.01%) must be prepared from a zinc doped ZnS.Mn crystal (or powder) if the electroluminescent effect is to be observed in the film. The proportion of zinc in crystals is not accurately known, but is about 1.0%. These crystals and films are therefore more correctly ZnS.Mn Zn.

Electroluminescent films of ZnSe.Mn (0.01%) must be evaporated from ZnSe.Mn, Zn (1%) crystals. An excess of zinc of 0.4% is not sufficient to give an electroluminescent film.

Diffusion of metallic manganese into an evaporated film of pure ZnS will produce an electroluminescent film. No excess zinc in the ZnS film is required.

From these results, electroluminescent films prepared by evaporation require excess zinc, while for diffusion, no excess is required.

Films prepared by these two techniques may be similar in so far as a large excess of metal (either Mn or Zn) should be present. In the diffusion method, manganese will diffuse preferentially along intercrystallite boundaries and stacking faults (for example Bullough et al, 1960). In the evaporation of material containing 1% excess zinc, some zinc deposition in the film, in similar locations is likely. This reasoning suggested that an electroluminescent film may be directly evaporated by using a large excess of manganese

instead of excess zinc. All electroluminescent films prepared previously contained about 0.01% of manganese which was insufficient to produce emission without the zinc.

However, it has already been shown that an electroluminescent ZnS powder containing 1% manganese does not produce an electroluminescent film by evaporation.

However, a ZnSe.Mn (1%) crystal was used to prepare electroluminescent films directly on a high temperature substrate. The critical temperature was the same as for ZnSe.ZnMn (Mn 0.01%, Zn 1.0%), viz. 310°. The failure to produce an electroluminescent film from the ZnS.Mn (1%) powder appeared to be due to a reaction in the evaporating boat which prevented all the available manganese from evaporating with the ZnS (see page 57).

A decrease in resistivity for these ZnSe.Mn (1%) films was observed as the substrate temperature increased through the critical temperature. It was of particular importance, especially at the high (1%) manganese concentration used in these ZnSe films to determine whether, the concentration of manganese in the films was the same as that in the crystals used for evaporation. One technique which is ideal for such an investigation is electron spin resonance (E.S.R.). The $Mn^{++}$ ion gives rise to a well known spectrum consisting of six characteristic lines when the concentration of the ion is about 0.01%. As the concentration increases, these lines are broadened and become superimposed on a single broad line. This indicates increasing interaction between $Mn^{++}$ ions (Schneider and

England, 1951). Aven and Parodi (1960) have used these properties to study crystalline transformation in ZnS.Cu, while Garlick et al (1962) have used the E.S.R. spectrum to study manganese diffusion in strontium and calcium fluoride.

The films to be studied were evaporated onto thin (0.01") cover slips which were subsequently cut into two pieces, and put at the bottom of the cavity of a super-heterodyne E.S.R. spectrometer, described by Cavenett (1964). For comparison, a small amount from each crystal used in the film evaporation was crushed to a fine powder and glued to a similar glass cover slip. This was subsequently placed in the same position in the cavity as the evaporated film to obtain a comparison spectrum.

Figure 4.7 and 4.8 show this comparison between powders and films for four manganese concentrations in ZnS.Zn (1%), Mn films. The same features were observed from films of ZnSe.Mn without the 1% zinc excess.

Several conclusions may be made from a comparison of the signal obtained from the powdered crystal and the film evaporated from it.

(a) At $3 \times 10^{-4}$ gm/gm the two spectra were very similar, indicating that the concentration of manganese in the film was the same as in original crystal. The six main lines were of equal width superimposed on a broad line (just visible). The six well defined lines result from $Mn^{++}$ ions which are well spaced in the ZnS lattice, so no appreciable overlap of electron wave functions occurs between them. As the concentration of manganese increase, this overlap

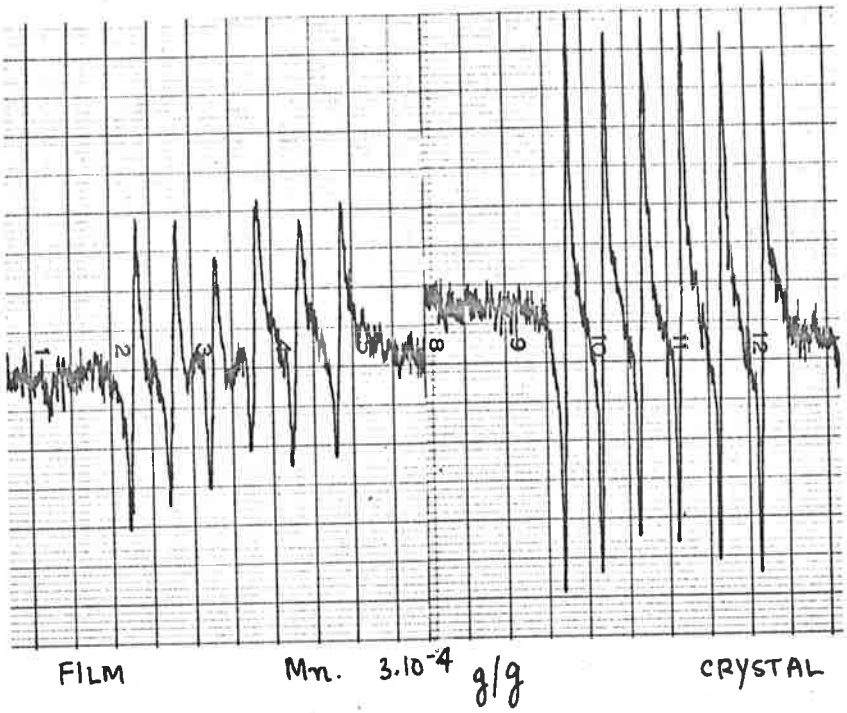


FIG 4.7 E.S.R. SPECTRA

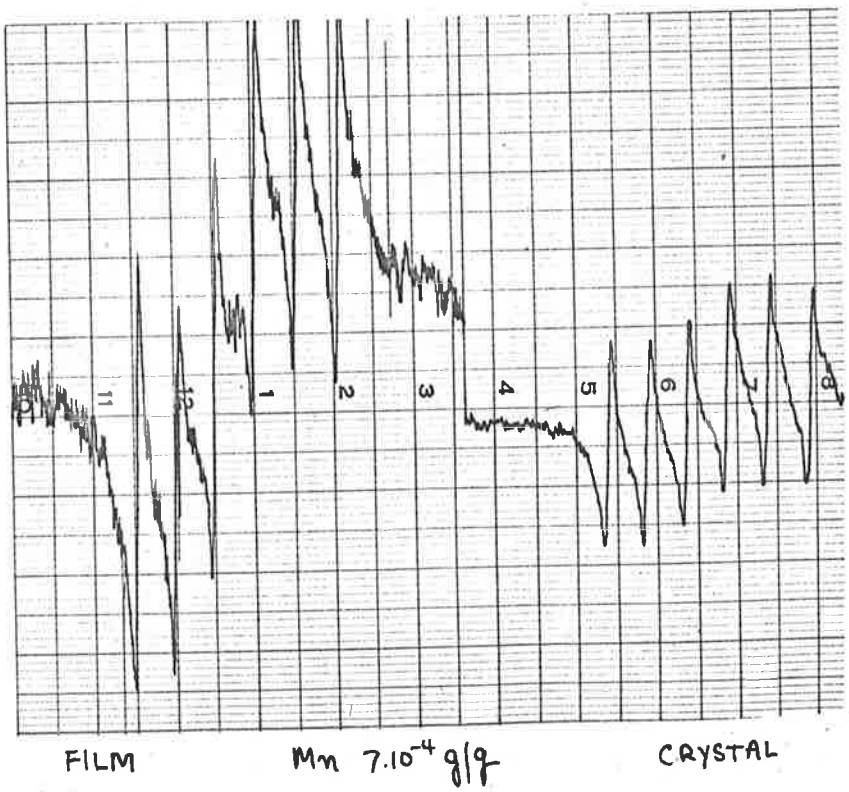

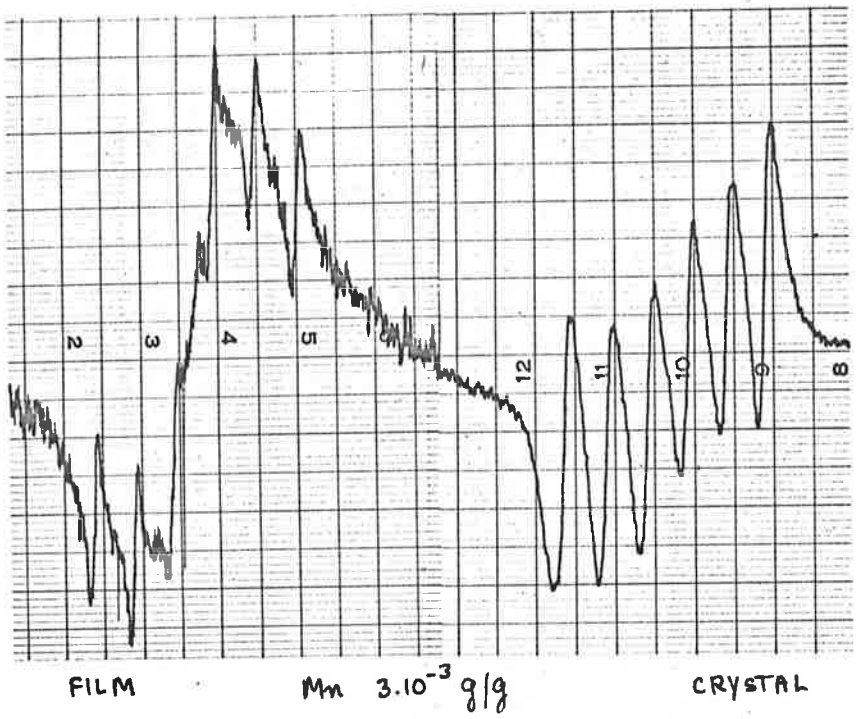


FIG 4·8 E.S.R. SPECTRA

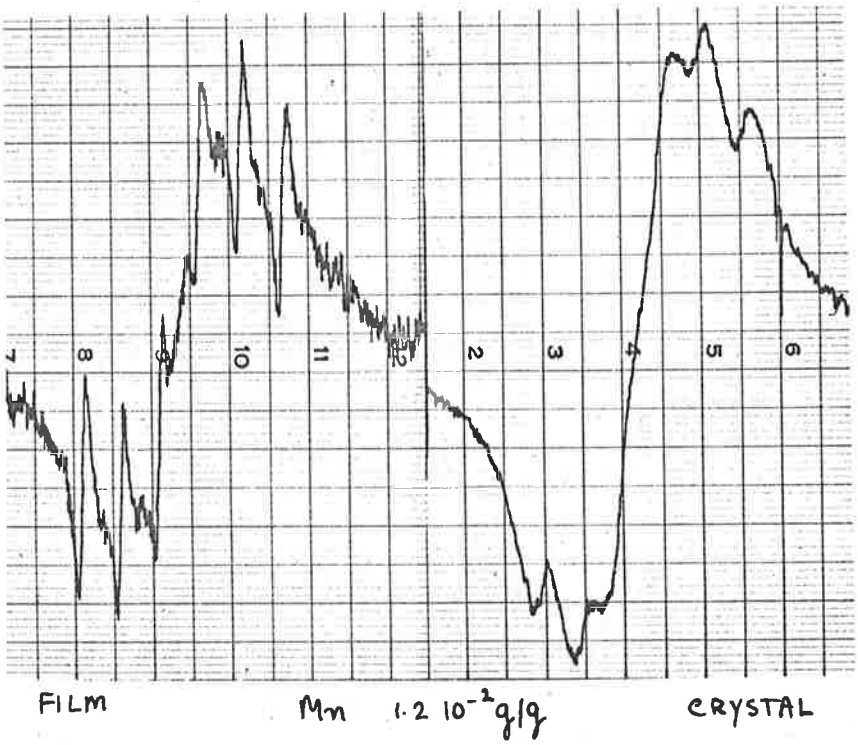

broadens the lines and eventually only one broad line is obtained at about 1%. This trend is shown in Figure 4.7b for ZnS.Mn crystal powders.

Therefore, sharp line spectra showed isolated $Mn^{++}$ ions while the appearance of a single broad line indicated the decreased distance between the ions resulting in increased overlap. At this concentration, overlap was visible in approximate agreement with the results of Schneider and England.

(b) At $7 \times 10^{-4}$ gm/gm, the details of the spectra were very similar. Line width was the same while the broad line had also increased as expected, showing again all the impurity in the crystal had been incorporated in the film.

(c) At $3 \times 10^{-3}$ gm/gm there was an obvious difference. The crystal showed an increased line width and an increasing amplitude in the broad line. However, the film showed narrower lines superimposed on a stronger broad line. This indicated that the concentration of manganese in the crystals was approximately the same as at $7 \times 10^{-4}$ gm/gm and that the additional manganese had clustered together in localized regions where the concentration was 1-10%.

(d) This tendency to aggregate was very clearly seen in the results from crystals containing $1.2 \times 10^{-2}$ gm/gm. The six line spectrum had nearly disappeared in the main broad line from the crystal, but from the film the lines were still sharp and well defined although, slightly broadened from the $3 \times 10^{-3}$ gm/gm spectra.

These results showed that the amount of manganese in

evaporated films was approximately the same as in the crystals used for evaporation although, the details of the incorporation were different. At a concentration $\leq 10^{-3}$gm/gm, most of the manganese ions were dissolved in the ZnS crystallites, while some were associated to provide overlap of the electronic wave functions. Above this concentration, there was a strong tendency to form aggregates, while the amount of $Mn^{++}$ in the ZnS crystallites increased much more slowly up to $1.2 \times 10^{-2}$gm/gm total manganese.

It should be noted that metallic manganese was found to give no E.S.R. signal and so such deposits would not be observed. However, the approximate agreement obtained between the powder and film spectra suggested no large metal deposit.

Spin resonance spectra were also used to study changes in the films as the substrate temperature increased through the critical temperature. Films were prepared onto substrates at 280°C and 325°C (i.e. below and above the electroluminescent threshold), and examined in the spectrometer. The spectra were identical, indicating that there was no change in the way in which the manganese was incorporated in the film at the critical temperature. The shape of the spectra were similar to those for ZnS.Mn Zn at high manganese content (Figure 4.8). This result showed that the same number of metal ions were deposited in regions of high concentration above and below the critical temperature. This shows that the decrease in film resistance about this temperature is not caused by these regions of high density.

## 4.5 Discussion of critical substrate temperature

In order to discuss the problem of excess zinc (or manganese) and of a critical substrate temperature ($T_c$), both of which are necessary in the preparation of an electroluminescent film, it is convenient to summarize here a number of results relevant to these problems.

(a) ZnS.Mn (0.01%) with no added zinc, when evaporated gives a high resistance film at all substrate temperatures. If ZnS.Mn Zn (about 1%) is evaporated, the film resistance is still high if the substrate temperature ($T$) is less than $T_c$. If $T > T_c$ the film becomes low resistance and electroluminescence is observed. This is also observed for ZnSe films.

(b) If 1% of manganese is used instead of 1% zinc in a ZnSe crystal, the resulting film is electroluminescent. For ZnSe Mn (0.01%), Zn(1%) and ZnSe.Mn (1%) films, the value of $T_c$ is the same, viz 310°C. There is no detectable change in the amount of manganese in the films if the substrate temperature is above or below $T_c$. It is assumed that this result will also be true for films containing 1% zinc.

(c) The value of the critical temperature is the same for ZnSe.Mn, Zn films evaporated from crystals containing about 0.6 to 2.6% of zinc. Although the concentration of zinc in ZnS.Mn films is not accurately known (because of the reaction during crystal growth), the value of the critical temperature appears to be insensitive to the amount of zinc present. Therefore, it seems valid to compare the observed critical temperatures for ZnS.Mn (0.01% Zn and ZnSe.Mn (0.01%) Zn(1%) films.

In addition to these results, the importance of re-evaporation from the substrate surface during film growth should be considered. This may be an important factor in determining the film resistivity because excess of the cation (zinc) forms electron donors, while excess of the anion (sulphur or selenium) forms electron acceptors.

A complete discussion of this aspect of film preparation is difficult because very little information on the mechanism of re-evaporation from a high temperature substrate is available. There may also be some doubt about the amount of dissociation in the evaporating boat. For ZnS (and CdSe) some authors suggest complete decomposition (Goldfinger and Jeunehomme, 1959) while others (for CdS) suggest only partial dissociation (Lawrance 1965). However, it may be reasonable to suppose that there exists on the substrate ZnS (or ZnSe), together with sulphur (or selenium) and zinc. The rate of re-evaporation will be a function of the vapour pressure of these elements, as well as a number of other factors such as the accommodation coefficient on the surface (Langmuir 1961 and Danforth 1963). Additional complication may arise because in the event of dissociation ZnS gives $S_2$ while ZnSe produces mainly $Se_6$ (Goldfinger and Jeunehomme 1959).

For deposition on low temperature substrates, a high resistance film is formed because the amount of excess sulphur incorporated in the crystallites is sufficient to localize all donor electrons. As the substrate temperature is increased, the sulphur re-evaporates more rapidly than

the zinc. Therefore, at (and above) a certain temperature the film will contain more zinc (donors) than sulphur (acceptors), and the resistance decreases. However, because no large decrease in resistance occurs (at least below 500°C) it is necessary to postulate the presence of additional acceptors. These are possibly due to surface states, and are present in sufficient number to accept all available (donor) electrons. Excess of zinc must be added to reduce the resistance. It is apparently not possible to dope the crystallites with sufficient zinc to outweigh the acceptor density below the critical temperature, because no amount of zinc doping will change this temperature (result (c) above).

If ZnSe.Mn Zn of identical composition is evaporated onto the same temperature substrate, the loss of selenium will not be so great because of the lower vapour pressure. This reasoning suggests that the critical substrate temperature will be higher for the selenide, i.e. a higher temperature is required to evaporate the selenium. This temperature difference is observed.

If a high concentration of manganese is used in place of zinc, the manganese will act as a donor provided the $Mn^{++}$ ion is incorporated with an anion vacancy in a similar way to the zinc excess. Therefore, the above discussion also explains how excess manganese can produce an electroluminescent film.

Re-evaporation of the cation excess (zinc) was not likely to effect the appearance of electroluminescence because the same critical temperature was observed for

ZnSe.Mn (1%) and ZnSe.Mn Zn (1%). However, if excess zinc is present re-evaporation will occur, and the possible influence of this must be considered in the interpretation of any results from films prepared at different substrate temperatures (Chapter 7.3.2).

# 5. STRUCTURE OF EVAPORATED ZnS FILMS

The structure of both electroluminescent and non electroluminescent films was investigated by X-ray diffraction, electron diffraction and electron microscopy. These observations will now be described.

## 5.1 Structure of ZnS.Mn films by X-ray diffraction

The structure of electroluminescent films of ZnS.Mn, evaporated from electroluminescent powders and from ZnS.Mn crystals was investigated by X-ray diffraction techniques using a Unicam 3cm cylindrical diffraction camera.

The films were evaporated onto glass cover slips (0.01" thick) and from these, strips of about 3mm in width were used. These were mounted in the X-ray beam at glancing incidence, and an oscillation of $15^{o}$ from this position was used to obtain the powder photographs. A control photograph of the glass slides was taken and, a more or less uniform blackening of the photographic film, together with a diffuse ring close to the position of the undeviated X-ray beam was observed. This ring was not near the positions where rings due to ZnS were observed. Conducting glass substrates were not used because the $SnO_2$ produced a strong diffraction pattern.

For films of thickness of about 2000A, an exposure time of two hours was sufficient to record three clearly defined lines. Figure 5.1a shows a photograph from a thicker film (approximately 10 microns) evaporated

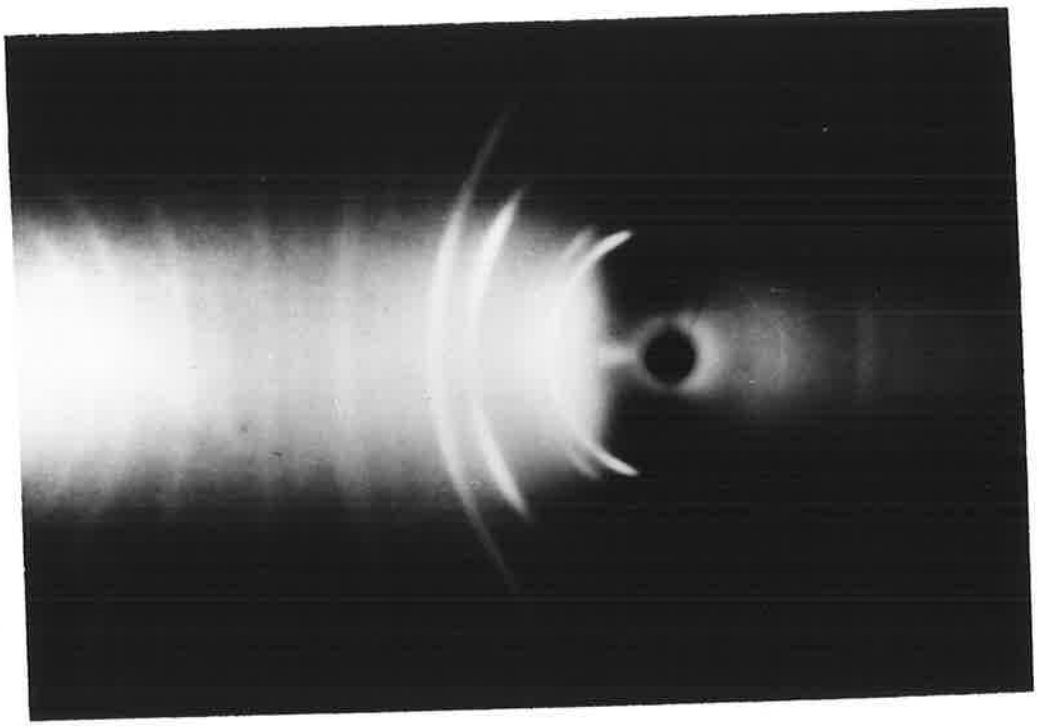

FIG.5.1(a) X-RAY DIFFRACTION PATTERN FROM ZnS.Mn.Zn FILM.

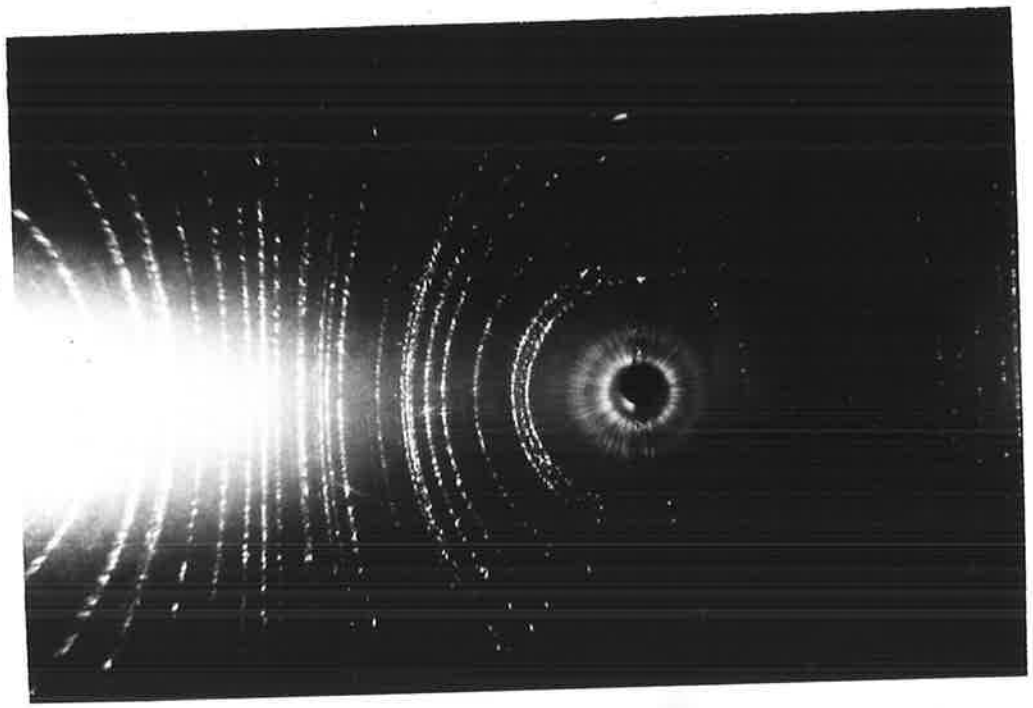

FIG.5.1(b) X-RAY DIFFRACTION PATTERN FROM ZnS.Mn.Zn POWDER.

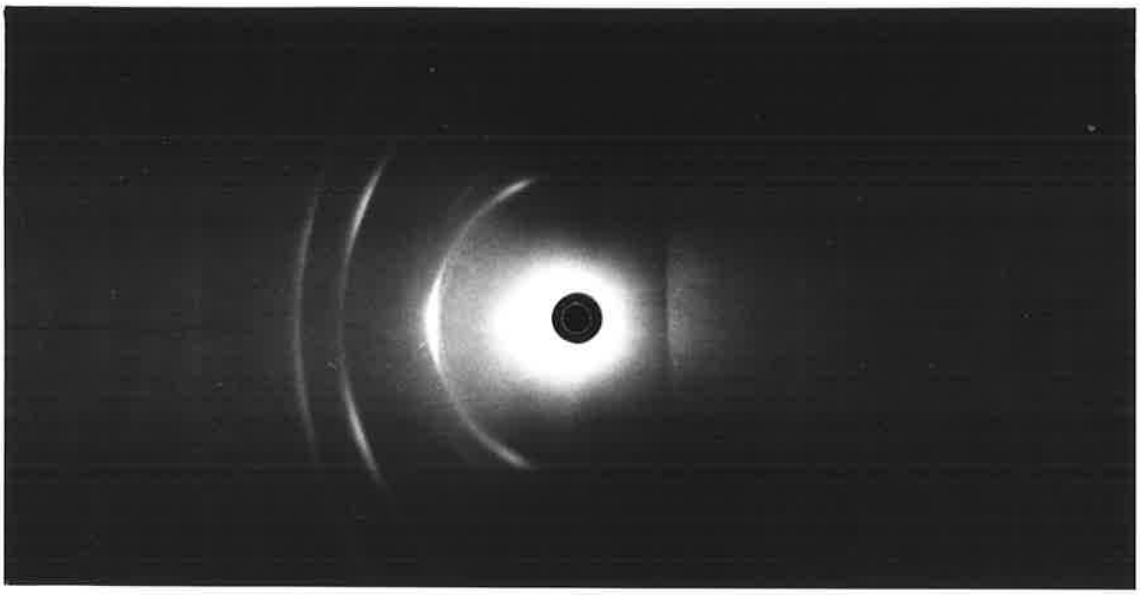

FIG. 5.2 ARCING IN POWDER RINGS FROM ZnS.Mn,Zn FILM.

at a faster rate. The background density has risen due to incoherent scattering from the film, which contains smaller crystallites, but nine diffuse lines may be identified. To obtain this number of powder rings from a film with larger crystallites and therefore decreased width of the rings, the evaporation time was prohibitively long. The correlation between evaporation rate and crystallite size in these films will be established later.

This method of obtaining the diffraction pattern gave only one half of the powder pattern because of the absorption of the thin glass substrate. Therefore, the centre of the diffraction pattern was uncertain. To display the whole ring pattern, a film was stripped from its substrate by a technique used in Electron Microscopy. The films could not be removed from the glass onto a water surface by the usual techniques. A 5% solution of hydrofluoric acid was used successfully, followed immediately by several washings in double distilled water. A thin (1mm diameter) rod was formed from tragacantha in water and the floating film was caught around this post which, after drying, was mounted in the X-ray camera. The photographs from films mounted in this way gave values of ring diameters and therefore improved accuracy in indexing the lines was possible.

Table 5.1 shows the line positions measured to the nearest 0.2mm from a number of photographs. Copper $K_\alpha$ radiation ($\lambda = 1.54$Å) filtered by nickel foil was used. The lattice spacings used in the calculation of $\sin^2\theta_{hkl}$

were for hexagonal ZnS, a = 3.82Å, c = 6.26Å while the parameter of cubic ZnS was 5.41Å. (Swanson and Fuyat, 1953).

The theoretical values of $Sin^2\theta_{hkl}$ are given for both the cubic and hexagonal form where hkl are the Miller indices of the reflecting plane and $\theta$ is the angle of diffraction.

$$Sin^2\theta_{hkl} = \frac{\lambda^2}{4a^2}(h^2+k^2+l^2) \quad \text{for cubic lattices.}$$

a = side of unit cell.

$$Sin^2\theta_{hkl} = \frac{\lambda^2}{3a^2}(h^2+hk+k^2) + \frac{\lambda^2}{4c^2}l^2 \quad \text{for hexagonal lattice.}$$

a = side of unit cell in basal plane.

c = side of unit cell along the c axis perpendicular to the basal plane.

For films about 1000Å in thickness, only the strong (111), (220) and (311) reflections were observed.

Because of the diffuse nature of many of the lines which were indexed, the agreement between the experimental values and the theoretical values for cubic ZnS was taken as sufficient to show that the films were composed of cubic crystallites. Additional confirmation was obtained by noting that all the allowed cubic reflections for ZnS were observed, with the exception of those from the (420) and (440) planes. According to Swanson and Fuyat, these are the two weakest lines in the powder pattern.

A parameter $\Delta_{cubic}$ was defined which showed the deviation of experimental and theoretical line positions (Table 5.1, column 5).

## TABLE 5.1

Observed line positions in diffraction photographs of ZnS.Mn electroluminescent films

| x cms | Experimental $\sin^2\theta_{hkl}$ | Theoretical $\sin^2\theta'_{hkl}$ (cubic) | Theoretical $\sin^2\theta'_{hkl}$ (hex.) | $\Delta_{cubic} = \frac{\sin^2\theta'_{hkl} - \sin^2\theta_{hkl}}{\sin^2\theta'_{hkl}}$ |
|---|---|---|---|---|
| 1.41 | 0.0542 | - | $0.0544_{100}$ | - |
| 1.50 | 0.0611 | $0.0608_{111}$ | $0.0604_{002}$ | - 0.005 |
| 1.72 | 0.0800 | $0.0810_{200}$ | * | + 0.012 |
| 2.50 | 0.164 | $0.162_{220}$ | $0.162_{110}$ | - 0.012 |
| 2.95 | 0.223 | $0.223_{311}$ | $0.223_{112}$ | 0.000 |
| 3.10 | 0.244 | $0.243_{222}$ | $0.242_{004}$ | - 0.004 |
| 3.60 | 0.319 | $0.324_{400}$ | * | + 0.015 |
| 4.05 | 0.391 | $0.385_{331}$ | $0.396_{211}$ | - 0.015 |
| 4.65 | 0.490 | $0.486_{422}$ | $0.490_{300}$ | - 0.008 |
| 5.05 | 0.556 | $0.547_{511}$ | $0.550_{302}$ | - 0.011 |
| 6.05 | 0.716 | $0.709_{531}$ | $0.705_{116}$ | - 0.010 |
| 6.70 | 0.807 | $0.810_{620}$ | * | + 0.004 |
| 7.20 | 0.869 | $0.871_{533}$ | Not observed | + 0.003 |

With the exception of a ring at r = 1.41 (clearly seen in Figure 5.2) the observed rings agree well with the positions of the allowed reflections from cubic ZnS. The mark * shows that there is no reflection from a hexagonal plane near the experimental value. The ring at r = 1.41 corresponds to the strong (100) hexagonal reflection and this indicates that while the film is made up of cubic ZnS crystallites, there is a small proportion of hexagonal ZnS present.

There was some intensity concentration (arcing) observed in the first strong powder ring (x = 1.50). This occurred around an axis on the photographic film, defined by the intersection of a horizontal plane containing the X-ray beam and the plane of the film. However, a photograph taken from a film with no glass substrate did not show this concentration. A similar concentration effect often occurs in photographs taken by reflection electron diffraction (Thomson and Cochrane 1939).

The sensitivity of the diffraction technique in detection of another chemical compound was not expected to be sufficient to show traces of, for example, MnS, MnO or ZnO. However, it may be noted that no additional lines were observed.

Figure 5.1b shows a powder photograph from an electroluminescent ZnS.Mn powder used in evaporation of some films. The powder was mixed with tragacantha and water, and a rod (1mm diameter) was used on the X-ray camera to give a powder photograph. An oscillation of $15^{o}$ was used to increase the continuity in the ring pattern.

In contrast to powder patterns from electroluminescent films, both cubic and hexagonal rings were found. This confirmed that the film structure was not identical to that of the powder used for evaporation. The intensity of both cubic and hexagonal rings was approximately the same in these photographs.

TABLE 5.2

Powder photograph of ZnS.Mn powder

| x(cms) | Experimental | Theoretical (cubic) | Theoretical (hex) |
|---|---|---|---|
| | $\sin^2\theta_{hkl}$ | $\sin^2\theta'_{hkl}$ | $\sin^2\theta'_{hkl}$ |
| 1.41 | 0.0542 | * | $0.0544_{100}$ |
| 1.50 | 0.0611 | $0.0608_{111}$ | |
| 1.59 | 0.0689 | * | $0.0692_{101}$ |
| 2.07 | 0.115 | * | $0.115_{102}$ |
| 2.50 | 0.164 | $0.162_{220}$ | $0.162_{110}$ |
| 2.71 | 0.190(5) | * | $0.190_{103}$ |
| 2.89 | 0.214(5) | * | $0.218_{200}$ |
| 2.95 | 0.223 | $0.223_{311}$ | $0.223_{112}$ |
| 3.00 | 0.230 | * | $0.233_{112}$ |
| 3.09 | 0.242 | $0.243_{222}$ | $0.242_{004}$ |
| 3.31 | 0.275 | * | $0.278_{202}$ |
| 3.60 | 0.319 | $0.324_{400}$ | * |
| 3.82 | 0.353(5) | * | $0.354_{203}$ |
| 4.00 | 0.382 | $0.385_{331}$ | $0.396_{211}$ |
| 4.10 | 0.399 | * | $0.405_{213}$ |

The rings were indexed using values of a = 3.82, c = 6.28Å for hexagonal ZnS. It has been shown that using these values, indexing of reflections from larger ZnS crystals is not possible (Czyzak et al, 1962). A value of c = 9.39Å was required, and this was interpreted in terms of stacking faults between cubic and hexagonal forms of ZnS. No evidence for this larger spacing along the c axis was found in the ZnS powder used here.

An important characteristic of a number of X-ray diffraction patterns of ZnS.Mn films was a pronounced non uniformity in intensity, around the powder rings (Figure 5.2). It is well known that a preferred orientation of the crystallites in a specimen will modify the appearance of the normal powder pattern. The intensity distribution in any given ring will be concentrated about particular angular positions, from which the orientation of the crystallites may be found.

A series of 30 films was made, using different substrate temperatures and a range of film thickness in an attempt to correlate this orientation effect with other film properties, particularly the appearance of electroluminescence.

Pure ZnS films produced identical patterns to films evaporated from electroluminescent ZnS.Mn powder when evaporated onto substrates at temperatures between 50° and 350°C. These films were not electroluminescent because new evaporation boats were used (Chapter 4.2). The diffraction patterns from these films showed

pronounced arcing of the rings. However, if the conditions were such that an electroluminescent film was made, the corresponding diffraction pattern showed a much more uniform intensity distribution, although a slight degree of orientation was still visible. Simultaneous deposition onto conducting glass and a glass cover slip provided films which, when removed from the glass with HF showed that the preferred array was characteristic of the non-electroluminescent film and not of the substrate.

The preferred direction may be found by noting the position of maximum intensity in the powder pattern. The presence of a strong concentration on the axis of the film for the (111) and (222) reflections indicated that these planes in the crystallites are orientated parallel to the surface of the substrate. This direction was confirmed by noting that the intensity of the (220) and (311) diffraction rings was concentrated about positions $35^{o}$ and $30^{o}$ from the axis of the photograph respectively. From the geometry of the cubic lattice, the angular separation of the (111) and (220) planes is $35^{o}$ and that of the (111) and (311) planes is $30^{o}$.

From these results the orientation of the crystallites is destroyed by the presence of the excess zinc necessary to produce electroluminescent films. The growth of a film containing crystals with their (111) planes parallel to a substrate will be dependent on the formation of the first layer of $Zn^{++} - S^{--}$ molecules on the substrate. The presence of the zinc excess may result in aggregates

of zinc ions which impede the growth of large ZnS crystals. Such aggregation has been shown to occur by E.S.R. (Chapter 4). As a result, the influence of the substrate surface which defines the preferred direction is minimized.

No change in the diffraction pattern was observed as the film thickness increased, however, only the strong reflection from the (111) plane was observed from the thinner films. This was due to the small amount of diffracting material available from very thin films ($< 1000\text{Å}$). The (111) reflection was the only one obtainable from films deposited on substrates between $20^{\circ}$ and $200^{\circ}C$, irrespective of their thickness. The small crystallite size in these films can explain this result. From these observations, it may be inferred that the crystallite size in these films increased with increasing substrate temperature. (This is confirmed in more detail in Chapter 5.4).

In some diffraction photographs of electroluminescent films, the presence of distinct spots in the diffuse powder rings was observed. These spots must originate from crystals much larger than the average, so there appeared to be regions of abnormal crystal growth on the substrate. Alternatively, they may result from larger crystallites thrown onto the substrate from the evaporating powder.

The large excess of zinc present may influence the crystal growth on the substrate. While this proportion does not prevent crystal formation in ZnS grown from the

melt, the conditions on the substrate are entirely different. Segregation of zinc may occur and initiate new crystallites rather than form a larger single crystallite. The large crystals mentioned above may be those which have not been affected by the excess. Alternatively, they may result from the fulfillment of a number of other conditions favourable to crystal growth which may occur at localized spots on the substrate.

As described in Chapter 4.1, diffusion of manganese into a film of pure ZnS resulted in an electroluminescent film of ZnS.Mn. The original pure ZnS film was cut into two pieces, one of which was coated with manganese. Both films were heat treated. The diffraction pattern of the pure ZnS was unchanged before and after the heat treatment. However, the ZnS now containing diffused manganese showed very sharp powder rings and no orientation effects.

Evidently the diffusion process had caused appreciable crystal growth in the film, making the crystallites larger than observed for evaporated films. Such recrystallization has been observed by heating copper and cadmium sulphide at 600°C (Gilles and Van Cakenberghe 1958).

Table 6.3 shows the indexing of the powder rings. The same cubic lines as before are observed with the exception of a line giving a value of $Sin^2\theta_{hkl} = 0.112$. This value agreed with that from the forbidden (211) cubic reflection ($Sin^2\theta'_{211} = 0.112$). Forbidden reflections, e.g. (102) have been observed from electroluminescent powders (Peters et al 1963). No diffraction rings could be explained by the presence of metallic manganese

**TABLE 5.3**

Observed line positions from diffraction pattern of ZnS.Mn after diffusion

| x | $\sin^2\theta_{hkl}$ | $\sin\theta_{hkl}$ (cubic) | $\Delta = \frac{\sin^2\theta'_{hkl} - \sin^2\theta_{hkl}}{\sin^2\theta'_{hkl}}$ |
|---|---|---|---|
| 1.50 | 0.0611 | $0.0608_{111}$ | - 0.005 |
| 1.72 | 0.0800 | $0.0810_{200}$ | 0.012 |
| 2.05 | 0.112 | $0.112_{211}$ | 0.000 |
| 2.50 | 0.164 | $0.162_{220}$ | - 0.012 |
| 2.95 | 0.223 | $0.223_{311}$ | 0.000 |
| 3.10 | 0.244 | $0.243_{222}$ | - 0.004 |

in the films after heat treatment.

It is possible from the X-ray diffraction pattern to obtain an estimate of the linear dimensions of the crystals producing the pattern. For large crystals ($10^{-1}$mm) single spots indicate the Bragg reflections. As the size decreases, many more (hkl) planes are present with different orientation, which produce many spots which draw together to give the usual powder pattern. If the crystal size is $> 10^{-4}$cms the powder rings are made up of resolvable spots (Henry Lipson and Wooster 1953), and in this case, an estimate of the size may be made from the 'spotiness' of the rings. If the crystals are smaller and more numerous, the spots draw together, finally giving a continuous ring.

Therefore the size of the particles making up the

electroluminescent powder, giving the photograph in Figure 5.1b as roughly $10^{-4}$ - $10^{-3}$cms while those in a film are considerably less than this, making the above method of no use.

The width of the lines now gives the information concerning particle size, but any calculations using this method are difficult and unreliable, giving only an order of magnitude result. While line broadening occurs from an array of small crystallites, additional broadening may be caused by imperfections in the crystals. The ZnS.Mn crystallites could be reasonably expected to contain some regions of disorder because of the temperature at which they were formed (the substrate temperature).

Because of these factors, the particle size was obtained directly from Electron micrographs which will be described in Chapter 5.4.

The results described in this section have shown that an electroluminescent film is composed of cubic crystallites and contains no detectable hexagonal structure. To produce an electroluminescent film, the excess zinc required destroys the preferred orientation of the crystallites in the film. This direction is with the (111) crystal plane parallel to the substrate surface.

## 5.2 Reflection electron diffraction

This technique is particularly useful to investigate the surface of specimens because, at the glancing incidence used, the penetration of the electron beam is only about $5.10^{-6}$cms.

A modified Metropolitan Vickers reflection camera using 50k.v. electrons was used. The films were deposited on glass cover slides or conducting glass, and there was no obvious difference in the diffraction patterns. The film was set at glancing incidence to the electron beam (about $1^{o}$). A typical diffraction pattern is shown in Figure 5.3a. The most striking feature of the patterns was the strong intensity concentration in the powder rings, indicating strong orientation.

The lines were indexed by using a magnesium oxide standard pattern and all allowed lines from cubic ZnS were found. However, because of the diffuse nature of the pattern, the accuracy was not particularly good. The preferred direction was that of the (111) crystal plane parallel to the substrate surface, which was the same as found previously.

One obvious difference between X-ray and electron diffraction technique is the depth of penetration of each beam. While it is more certain that the X-ray radiation was diffracted from the total bulk of the film, the depth of penetration for electrons is not much more than several hundred angstrom units. If the beam penetrates larger crystals, the electrons have a large probability of inelastic collision which results in excessive line broadening and diffuse background level on the photographic plate (Thomson and Cochrane 1939). If these projections are of width 500Å or less they will contribute to the diffraction pattern. This is one reason why the width of

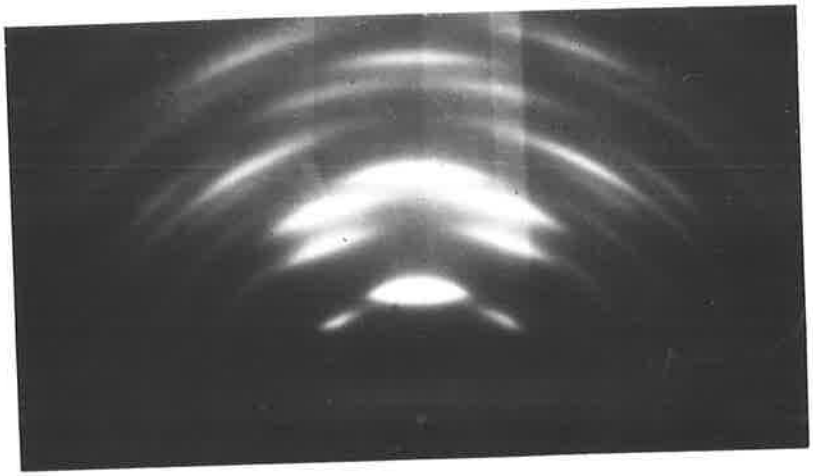

(a)
T = 320°, 100 A/min.

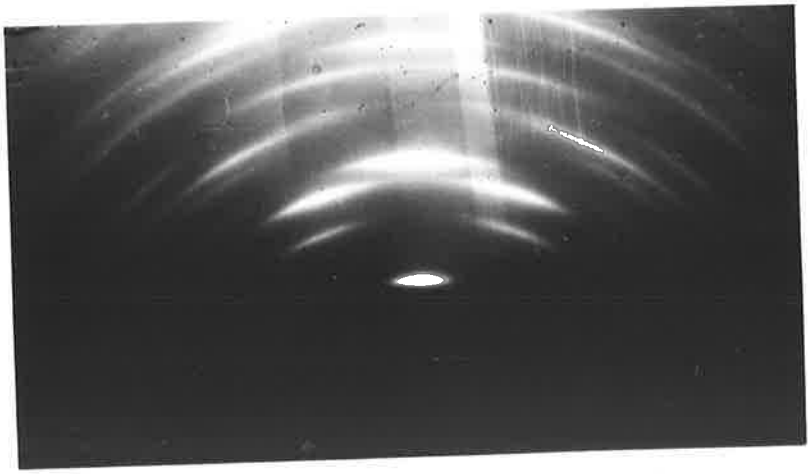

(b)
T = 400°, 100 A/min.

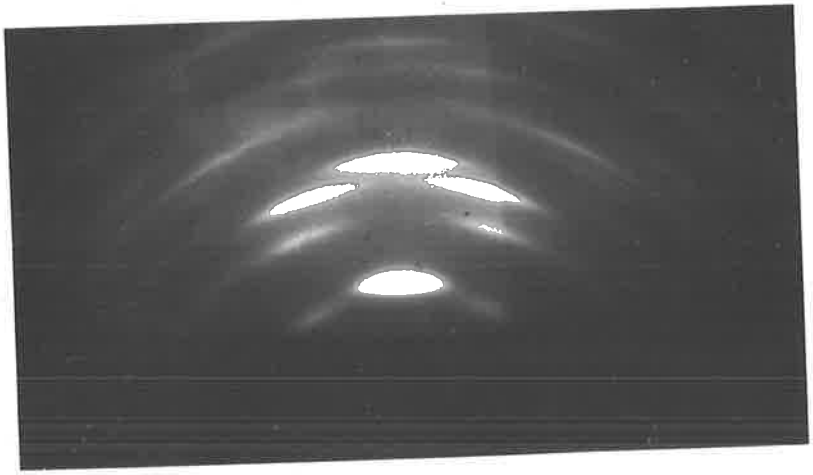

(c)
T = 320°, 200 A/min.

FIG. 5.3 ELECTRON REFLECTION DIFFRACTION PATTERNS FROM ZnS.Mn.Zn FILMS AS A FUNCTION OF SUBSTRATE TEMPERATURE (a & b) & EVAPORATION RATE (a & c).

these lines cannot be used to estimate the size of the crystals in the bulk of the film.

The strong orientation indicated by the diffraction patterns indicated that the surface of film contained a number of sharp projections, which are the corners of the cubic crystallites.

Because the strong orientation effect did not occur in X-ray powder photographs of electroluminescent films, the crystals causing the electron reflection diffraction pattern must form only a small fraction of the total number in the film.

The X-ray diffraction photographs showed that some crystallites were larger than average. These may occur because of favourable conditions on the substrate surface, i.e. they may have their (111) planes parallel to the substrate. Therefore, they would contribute to the reflection pattern.

Alternatively, the sharp edges may be due simply to the random nature of the crystallites making up the bulk of the film. In this case the number of crystals with the (111) plane in the plane of the substrate will be the same, on the average, as any other orientation. However, the electrons are only diffracted by the sharp edges which come exclusively from the crystals, which have their (111) planes approximately in the plane of the substrate.

Figure 5.3 shows that an increase in substrate temperature gives sharper rings,i.e. larger crystallites (a,b), while increased rate of evaporation appears to give smaller particles (a and c). A photograph from a film evaporated

onto a 150°C substrate showed a very faint pattern with a heavy background, which was interpreted as the result of a more uniform surface due to smaller crystallites. From these photographs, the effect of increased substrate temperature from 300°C was to increase the crystallite size in the film. Crystal growth appeared to be improved by a slow evaporation rate. However, these results are obtained by a surface investigation and therefore may not be representative of the bulk film.

No noticeable difference in the diffraction patterns was observed for films of pure ZnS or ZnS.Mn evaporated from powder or crystal form. These films were representative of electroluminescent and non active preparations and this indicated that the surface conditions of ZnS films was not critical for the appearance of the light emission.

## 5.3 Transmission electron diffraction

A Philips Electron Microscope (Model M100) was used as a diffraction camera. To obtain improved resolution of the ring pattern, a Siemens Electron Microscope was necessary (Emiskop I).

The photographs obtained by this technique contained additional information which allowed a more positive identification of crystal structure, and the confirmation of the presence of a hexagonal phase of ZnS in the films of ZnS.Mn.

Figure 5.4b shows a typical transmission pattern from an electroluminescent ZnS.Mn film evaporated from a

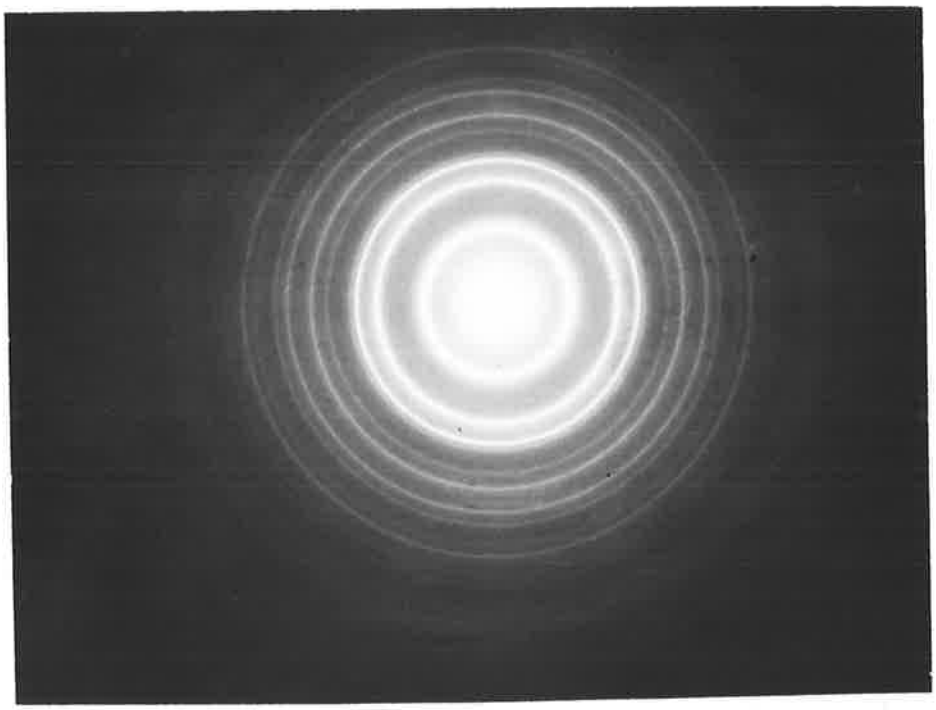

(a)

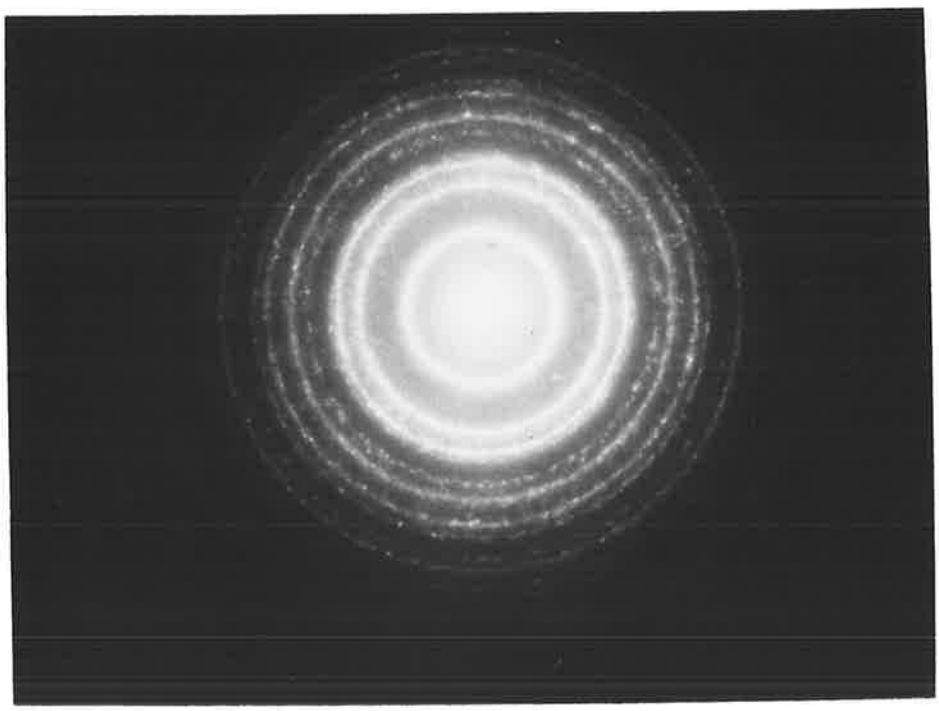

(b)

FIG. 5.4 ELECTRON DIFFRACTION PATTERNS FROM ZnS:Mn.Zn FILM.

powder. The films were removed from thin glass substrate by 5% HF as described in Chapter 5.1.

Improved accuracy was obtained by measurement of the ring diameter, and from the well defined lines from higher order reflections.

Table 5.4 shows results obtained by indexing a typical diffraction pattern. The ZnS.Mn film was moved during the exposure of the photographic plate so that the electron beam scanned over 1 square of the specimen grid. This gave improved continuity in the diffraction rings and ensured that the diffraction pattern was truly representative of the film structure (Figure 5.4a).

All allowed reflection were indexed for the cubic modification of ZnS.

The width of the first strong ring was sufficient to account for a number of rings. These were the (100), (002) and (101) reflections from hexagonal ZnS and the (111) reflection from cubic ZnS. This structure could be seen in other photographs with reduced exposure, where rings at r = 1.52 and 1.71 could be resolved in addition to the ring at r = 1.60.

The three most intense rings in the pattern from hexagonal ZnS according to five authors is shown below (Swanson and Fuyat 1953).

| Author | 1 | 2 | 3 |
|---|---|---|---|
| 1. | 110 | 112 | 302 |
| 2. | 110 | 112 | 002 |
| 3. | 110 | 103 | 100 |
| 4. | 100 | 101 | 103 |
| 5. | 100 | 002 | 101 |

**TABLE 5.4**

Indexing of diffraction pattern from 1000Å electroluminescent ZnS.Mn film. Camera constant = 5.00. I is the intensity of X-ray reflections observed by Swanson and Fuyat (1953).

| r | $d = \frac{5.00}{r}$ | d(cubic ZnS) | $I_C$ | d(hex.ZnS) | $I_H$ |
|---|---|---|---|---|---|
| 1.52 | 3.29 | * | | $3.28_{100}$ | 100 |
| 1.60 | 3.13 | $3.13_{111}$ | 100 | $3.13_{002}$ | 86 |
| 1.71 | 2.92 | * | | $2.92_{101}$ | 84 |
| 1.85 | 2.70 | $2.71_{200}$ | 10 | * | - |
| 2.60 | 1.92 | $1.91_{220}$ | 51 | $1.90_{110}$ | 74 |
| 3.06 | 1.63 | $1.63_{311}$ | 30 | $1.63_{112}$ | 10 |
| 3.18 | 1.57 | $1.56_{222}$ | 2 | $1.56_{004}$ | 2 |
| 3.70(5) | 1.35 | $1.35_{400}$ | 6 | * | - |
| 4.02 | 1.24 | $1.24_{331}$ | 9 | $1.23_{211}$ | 3 |
| 4.10 | 1.22 | $1.21_{420}$ | 2 | $1.21_{114}$ | 10 |
| 4.51 | 1.11 | $1.10_{422}$ | 9 | $1.10_{300}$ | 13 |
| 4.80 | 1.04 | $1.04_{511}$ | 5 | $1.04_{302}$ | 5 |
| 5.22 | 0.958 | $0.956_{440}$ | 3 | $0.955_{220}$ | 6 |

The (200) reflection is very weak (just detectable) although higher order reflections are easily resolved. This was true for the thin (about 1000Å) films of both ZnS and ZnSe examined by electron diffraction. Tilting the films through ± 20° in the diffraction camera showed only a very small degree of orientation for the crystallites. This suggested that the absence of the (200) reflection was not due to orientation effects but was a property of these very thin films.

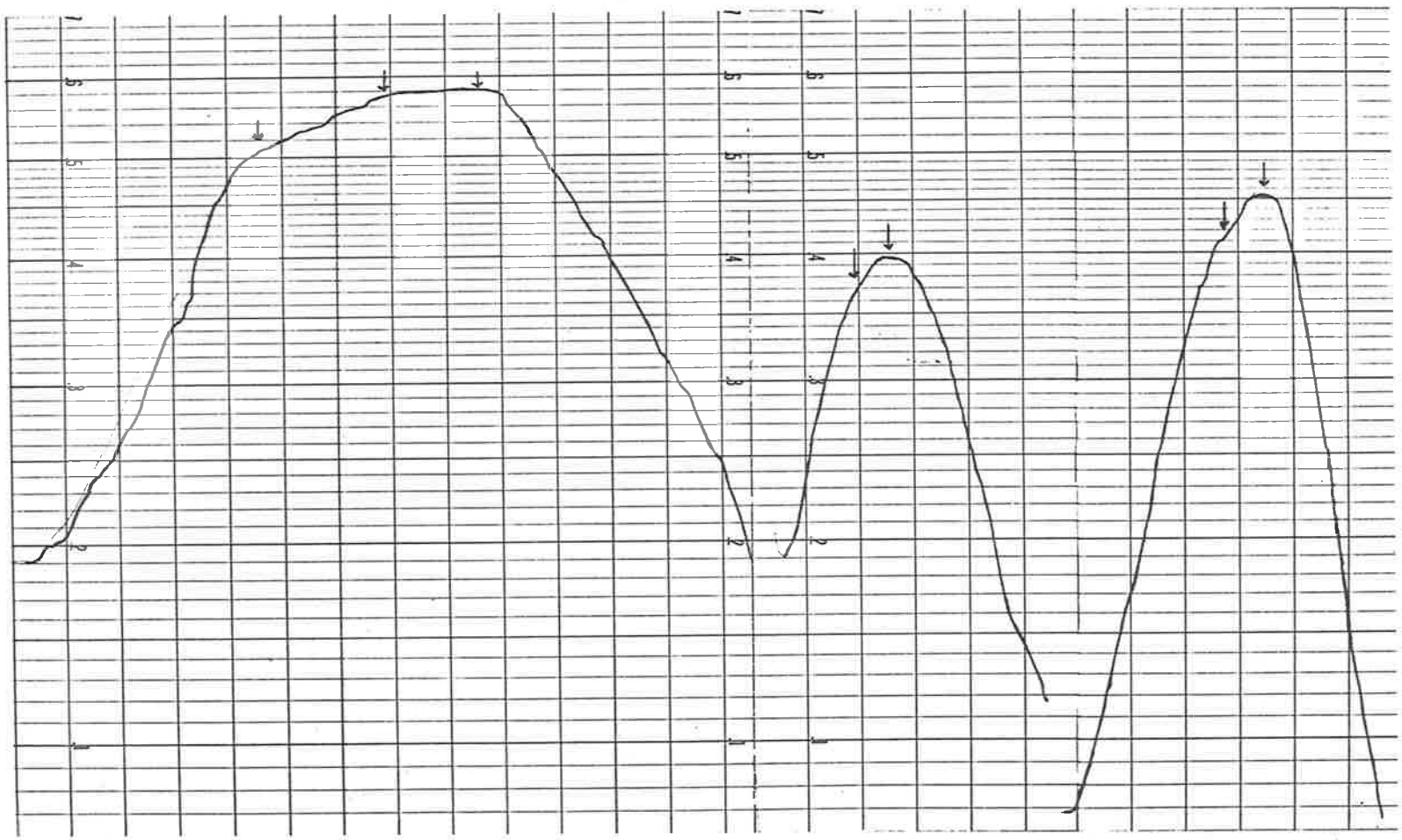

FIG. 5.5 DENSITOMETER TRACE OF THE THREE STRONGEST RINGS IN ELECTRON DIFFRACTION PATTERNS.

The strong hexagonal reflections (110) and (112) would give rings at r = 2.60 and 3.06 respectively. These r values are the same as expected from the cubic (220) and (311) reflections. The structure in these two rings was studied using a Jarrel Ash microdensitometer. Figure 5.5 shows a trace taken using a slit width of 6 microns, scanning the original plates at 1mm per minute. The first strong ring contained three components, while the second and third have two components.

The (302) reflection mentioned above should fall over the cubic (511) reflection pattern, but no double structure was found.

These results showed conclusively the presence of the hexagonal modification in these crystals, which was described by parameters a = 3.82, c = 6.26 (see discussion in Chapter 5.1).

It has been suggested many times that crystal imperfection is necessary for electroluminescence, and so it was of interest to compare the diffraction patterns from non electroluminescent and electroluminescent films. However the results showed clearly that there was little difference between them, the same line widths being observed in the pattern from each type of film.

This suggested that the presence of mixed crystal structure was not sufficient for the appearance of light emission from the films. However, it was impossible to decide from these results if disorder was necessary.

Diffraction patterns from ZnSe films were also obtained. The general line patterns indicated that the films

were predominantly cubic in structure as for ZnS films.

From the diffraction photographs of ZnSe, a densitometer trace was taken of the three strong cubic reflections, viz. reflections from the (111), (220) and (311) planes. While the two outer rings appeared to be due to single reflections (cf. ZnS), the first ring showed evidence for a multiple structure of three (or at least two) components. This is very similar to the ZnS films where the presence of hexagonal reflections accounted for the other lines. ZnSe forms pure cubic crystals and a hexagonal phase has not been reported. However the presence of a number of extra reflections from evaporated films of CdTe (generally pure cubic) have been explained in terms of a hexagonal phase (Semiletov 1962). Semiletov found a regular arrangement of the cubic and hexagonal forms, the relative orientation of the crystallites being described as the (001) hexagonal face parallel to the (111) cubic face and the [110] hexagonal direction parallel to the [110] cubic direction.

The presence of reflections due to hexagonal tellurium in films of CdTe has also been found, but generally at a lower substrate temperature than used by Semiletov (Glang et al 1963). The extra lines found for ZnSe cannot be explained by the presence of free zinc (hexagonal) or selenium. The number of non-cubic lines observed was not enough to allow the period of any hexagonal phase to be determined, and the only conclusion which could be made was that there was some small regular deviation from the cubic packing in the ZnSe crystallites.

A number of qualitative results were obtained from the diffraction patterns.

The effect of increasing substrate temperature on the crystallite size in ZnS.Mn films evaporated from large crystals was found on electron diffraction patterns for substrate temperatures of 200°, 330° and 500°C. The films were evaporated onto cover slips and their thickness was only about 200A. The same qualitative behaviour was shown by films of 1500A thickness. From the photographs several conclusions were made.

The width of the first strong ring, while sufficient to account for several reflections showed no visible structure for films evaporated onto 200°C substrates. Two distinct rings were easily seen from films deposited at 330, and at 500°C a ring of resolved spots was identified around the outer edge of the main pattern.

The second strong ring (normally due to the strong 220 cubic reflection) showed increasing evidence of two components (r = 2.61 and 2.65) as the substrate temperature increased. These r values correspond to d = 1.91(5) and 1.90, in better agreement with the 220 cubic reflection (d = 1.91) and the (110) hexagonal reflection (d = 1.90).

The crystal size obviously increased as the temperature of the substrate increased, gauged by the "spottiness" most clearly seen in the outer rings of the pattern, although the quantitative increase was difficult to assess.

The effect of increasing film thickness was also to increase the crystallite size in the films. Films were

evaporated from crystals of ZnS.Mn and therefore were representative of electroluminescent material. Again the "spottiness" of rings (particularly in the 222 diffraction ring) was taken as an indication of this crystal growth. A correlation between thickness and crystal size over an extended range of thickness was difficult because of increased absorbtion of the electron beam in the film. However, in a qualitative way, the crystal size increased as the thickness increased to 3000A. Therefore, the ultimate size of the crystallites in the films was dependent on the amount of ZnS available. This result is in disagreement with data from germanium films, where the crystallite size was independent of thickness between 1000 and 6000A (Davey 1963) implying that the crystal growth was limited by the substrate temperature.

A difference between patterns obtained from electroluminescent films evaporated from powders and from crystals was noticed. The size of crystallites was approximately doubled when powders were used. This increase was reflected in the resistance of films, which was approximately 50K ohms compared to 500K from crystal evaporations. This difference was thought to be due to the presence of nuclei on the substrate provided by larger particles thrown off during powder evaporations. These would not be present during a crystal evaporation because there were no crystallites in the evaporant, which could be thrown onto the substrate to act as nuclei.

The possibility of improved crystal growth on

substrates of conducting glass (polycrystalline $SnO_2$) was considered by evaporating two identical films on conducting glass and a pyrex cover slip at 450°C. There was an increase in crystal size by about a factor of two, when $SnO_2$ coated glass was used, seen more clearly in the higher order reflections of the pattern. In all other respects, the diffraction pattern did not depend on the substrate used.

The most important result obtained from the electron diffraction studies was demonstration of the presence of a hexagonal ZnS crystal modification in the ZnS.Mn films. This was not detected by X-ray diffraction because of the small volume of diffracting material available. No change in the crystal structure occurred at 290°C. Rings from both cubic and hexagonal ZnS were identified from photographs taken from non electroluminescent films.

An increase in crystal size was caused by an increase of substrate temperature as shown by changes in the "spottiness" of the powder rings. Crystal size also increased as the film thickness increased. Films evaporated onto polycrystalline tin oxide contained crystals of approximately twice the linear dimensions of crystals forming a film on a pyrex glass slide.

## 5.4 Particle size by electron microscopy

The first experiments were performed using carbon coated microscope grids. The ZnS.Mn was evaporated onto the carbon film and examined in the electron microscope

(Philips M100). In some cases the ZnS.Mn film was shadowed by evaporation of Palladium in a vacuum system operating at $5.10^{-5}$ torr.

The only conclusion possible from these specimens was that the crystallites were very small, the resolution of the instrument not being sufficient to show any detail.

The deposition onto a carbon substrate was an undesirable feature of this method, because of a possible change in the film structure on a $SnO_2$ glass substrate. While the diffraction patterns, described above, suggested only a change in crystallite size, other changes in the individual crystals may have occurred.

ZnS.Mn films on conducting glass were very difficult to remove using the standard techniques of electron microscopy, and so the replica technique was used. This has been adequately described by Cosslett (1951).

The ZnS.Mn films were covered with a 1% solution of collodion in amyl acetate. After drying, the collodion film was stripped from the ZnS by using the surface tension of distilled water.

There was a strong adhesion between the collodion and ZnS (implying a smooth surface for the ZnS) which made this stripping difficult. The floating off procedure was often initiated by breaking the surface of the replica with a fine needle point.

The floating replica was cut into small pieces (3mm diameter) and a microscope grid was placed on top of the film. When this was lifted out, the surface of the

replica which had been in contact with the ZnS was uppermost on the grid. The replicas were dried and shadowed as before.

From the photographs it was possible to distinguish areas which appeared to contain crystalline faces (Figure 5.6). It must be remembered that areas which are the high spots (and therefore coated with palladium) in Figure 5.6 were the depressions in the original ZnS film. The linear dimensions of areas which appeared to be crystallites was between 0.4 and 1.0 microns. In some areas smaller crystallites could be found ( $\approx$ 1000Å in size). This suggested that the film was made up of small crystallites ($\simeq$ 1000Å), and that several of these were associated in a region which then showed a plane area of larger dimensions in the replica. This explained the apparently larger crystallites. Alternatively, the film was made up of large micron size crystallites, and the small crystallites were merely graininess in the palladium shadowing.

There was no apparent difference between replicas taken from electroluminescent and non electroluminescent films.

Because of the uncertainty in the interpretation of the replica photographs, a number of ZnS.Mn films were directly observed in a Siemens Emiskop I microscope. The resolution of this instrument was between 10 and 15Å. This enabled the qualitative conclusions made from the earlier results to be confirmed in a semi-quantitative way and also gave some information of the structure of single crystallites.

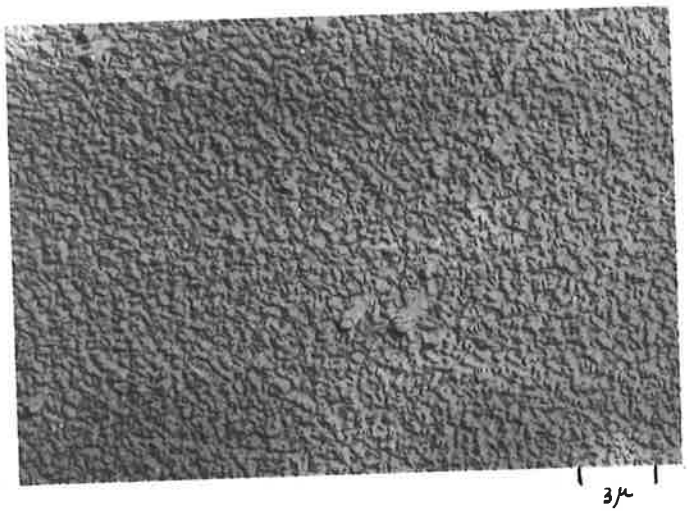


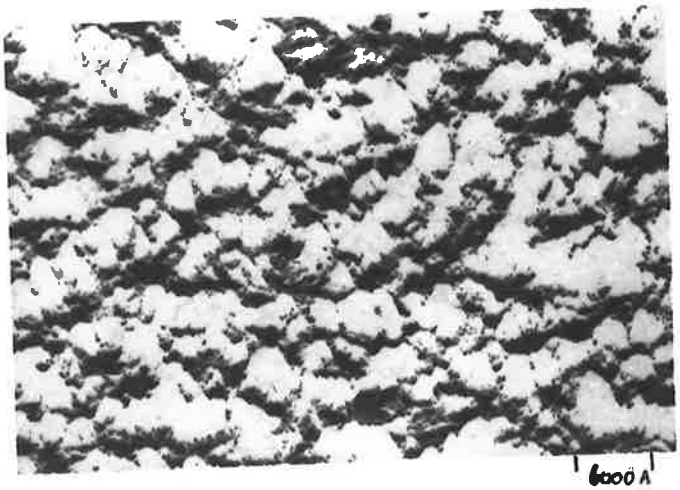


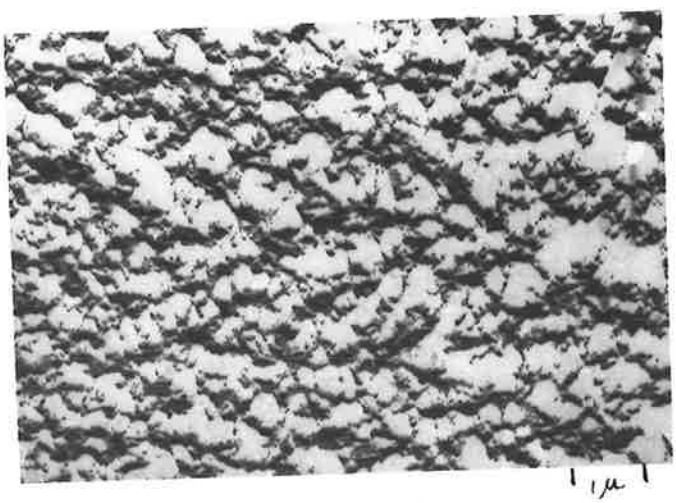


FIG. 5.6 REPLICAS OF ZnS.Mn.Zn FILMS.

Films were removed from both pyrex cover slides and conducting glass by the following technique.

A 5% solution of HF was used and a small piece of glass coated with ZnS film was placed on its surface. After several seconds the acid attacked the interface between glass and ZnS at the edges of the film. By lightly tapping the glass, it could be made to sink in the HF leaving small pieces of ZnS floating on the surface. These were immediately lifted out with fine platinum mesh and immersed in distilled water. This rinse was repeated 3 times to remove all traces of acid.

Immersion in the HF solution certainly would have etched the surface of the films. Differences due to etching were minimized by using the same time of acid treatment for all films. However, it was possible that films containing varying amounts of impurity (e.g. excess zinc) were attacked at a different rate.

Most of the results to be described in this section were taken from films evaporated from ZnS.Mn crystals. However, the conclusions reached were considered relevant to the electroluminescent effect in films, whether evaporated from powders or crystals.

The individual crystallites of ZnS in the films were resolved and in some cases this enabled the structure of the crystallites to be seen (Figure 5.7). This photograph was taken through a thin spot on a film evaporated from an activated ZnS powder. A general feature of the crystallites was that many were crossed with dark fringes. This

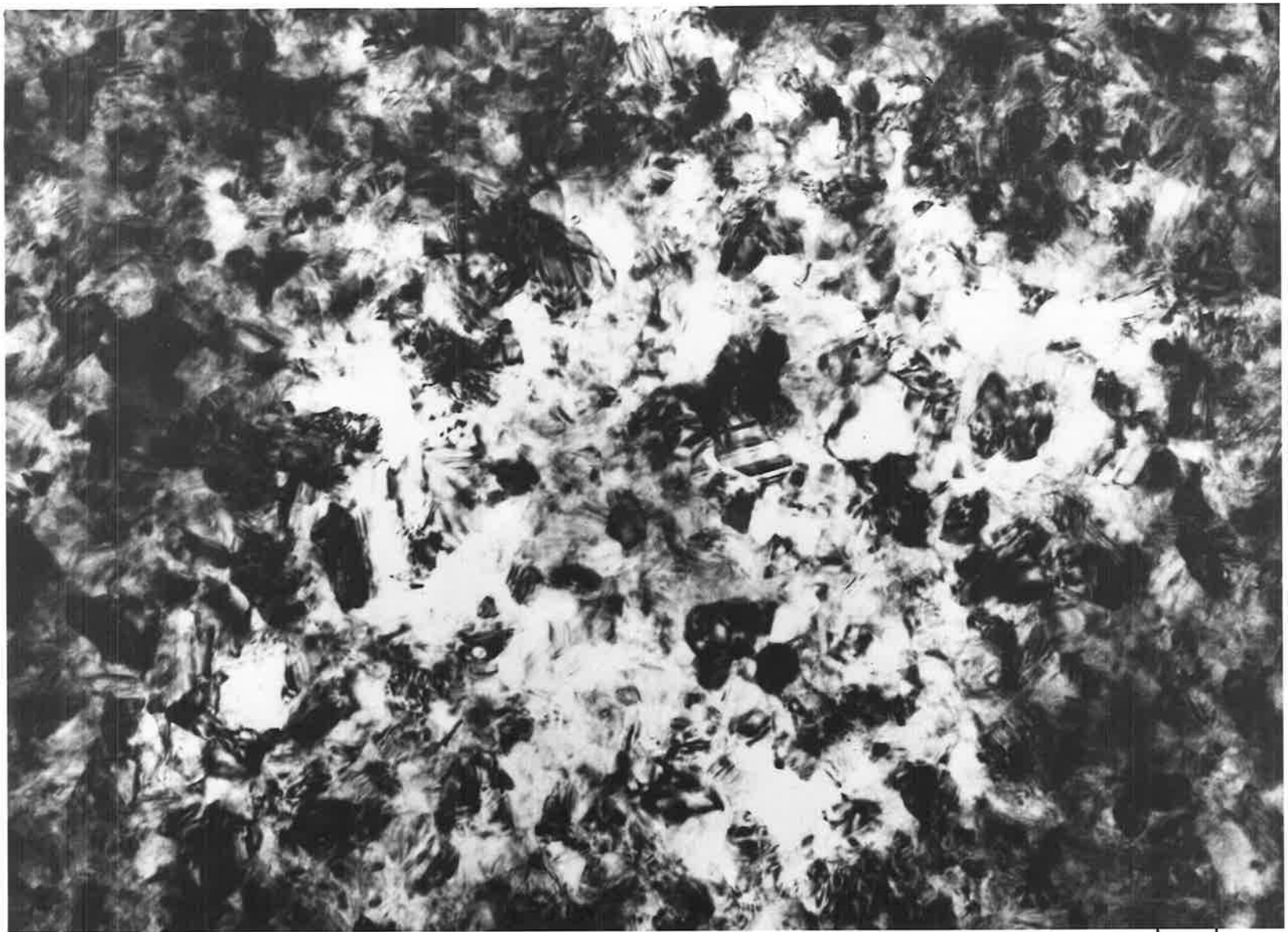


FIG. 5.7 ELECTRON MICROGRAPHS OF ZnS.Mn.Zn FILM. MAGNIFICATION 140,000 x.

effect is also seen clearly in a micrograph from thinner films (for example Figure 5.11).

Whelan and Hirsh (1957) have shown that it is possible to obtain (a) fringes of equal inclination observed in wedge shaped crystals and (b) Moiré fringe patterns due to overlap of two crystals of slightly different orientation. These latter are produced by interferance of electron waves after successive Bragg reflections in the composite crystals. Fringes observed at grain boundaries and stacking faults are the result of both effects - diffraction by two overlapping wedge crystals and the effect of overlap (as in Moiré patterns).

While interference effects could not be definitely neglected, the presence of two crystal modifications in the film (shown by electron diffraction) suggested that the fringes were formed at boundaries between the two crystal structures. Evidence of twin formation could be seen in Figure 5.7, and thus the fringes may also arise from thin twins. In some micrographs crystals were seen which were crossed by two sets of fine fringes at right angles to each other. In general some crystals contained not clear dark fringes, but many irregular dark spaces giving the crystallites a mottled appearance. There seemed to be a continuous range of crystallites from those containing one or two fringes, to crystals almost entirely black, although details could still be seen in the darker crystallites.

### 5.4.1 Factors affecting crystallite size

#### (a) Effect of substrate temperature

Figure 5.8 shows micrographs from three films (evaporated from crystals) deposited on substrates at 150°, 325° and 500°C. The substrates were pyrex glass and the films were about 400A thick. The crystal size variation was the same for films of 1300A, but the micrographs from the thinner film were of improved clarity.

At 150° the crystals were about 150A, and no structure was visible in individual crystals. Generally there were a number of black areas (crystals) which seemed to contain a large fault concentration. At 325°, the size had increased to about 200-250A and the crystals showed bands. The banding diminished at 500° and the crystallites were not as clearly resolved. This may be due to a tendency for crystals to grow together, thus reducing the number of boundaries. The size at 500° was about 250-300A.

These results suggested that a certain size crystallite was required before the film showed the electroluminescent effect. However, it was shown that the light emission effect was not dependent on the absolute size of the crystals. In films of the same thickness, but evaporated from powders, the crystallites were larger. The same increase in particle size about 290°C was observed.

There was some correlation between the film resistivity and the crystallite size from 100° to 500°C (Figure 5.9). These results were taken from a film evaporated from a crystal. However, the same change occurred when powders

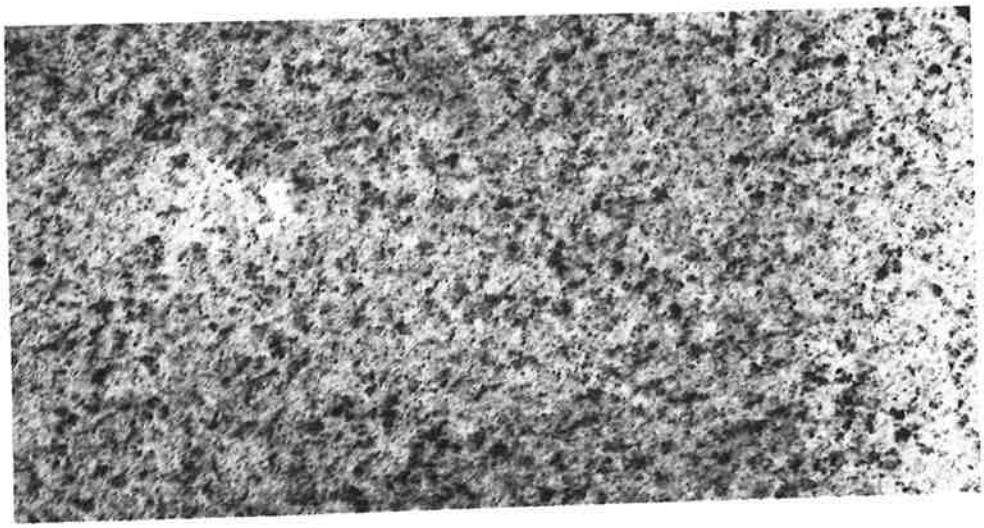

150°

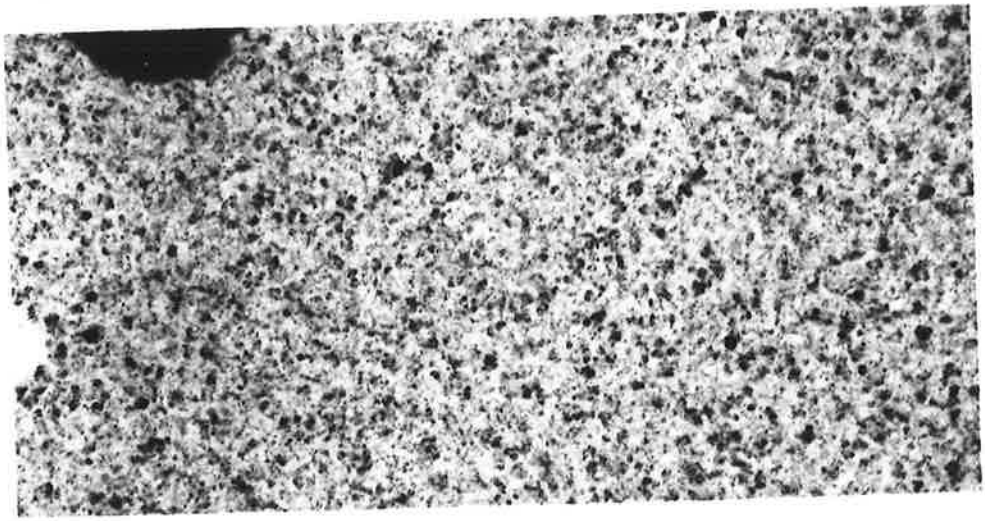

325°

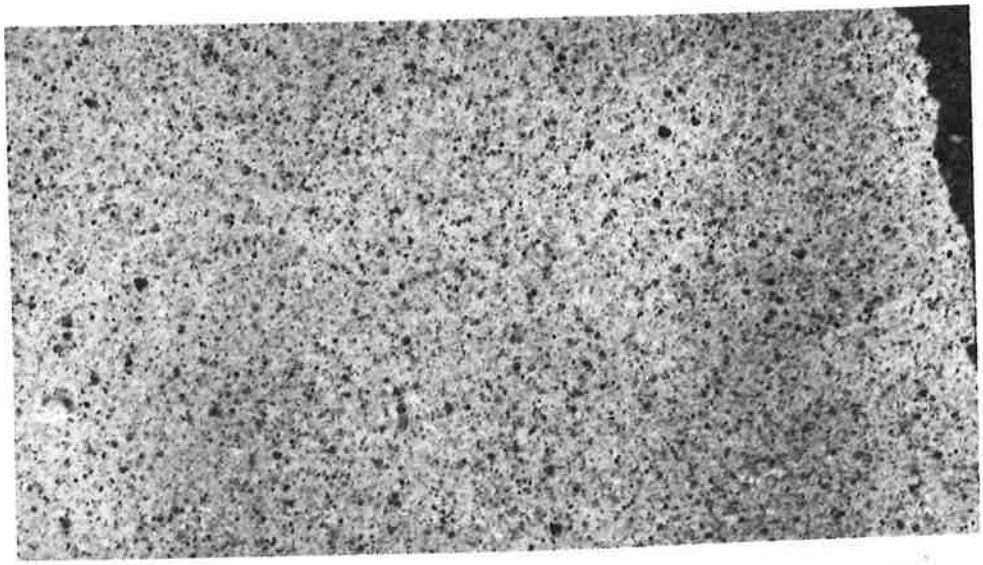

500°

FIG. 5. 8 MICROGRAPHS AT THREE SUBSTRATE TEMPERATURES. MAG. 120,000 x.

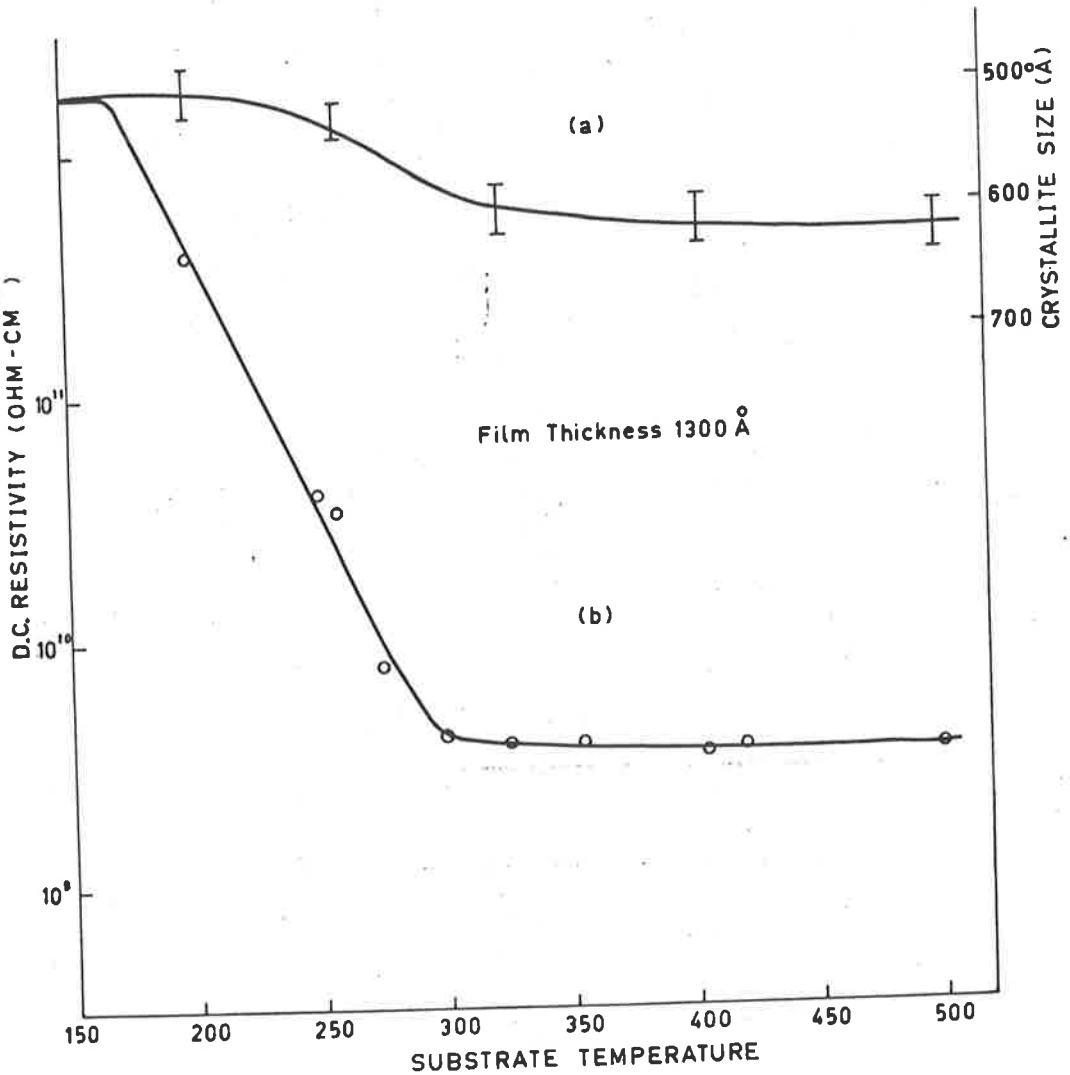


FIG. 5.9 VARIATION OF PARTICLE SIZE (a) AND RESISTIVITY (b) WITH SUBSTRATE TEMPERATURE FOR A ZnS.Mn FILM.

were used to prepare the films.

Therefore crystallite size was not critical for the production of an electroluminescent film. Because the same relative increase in conductivity occurred for films evaporated from powders and crystals, the electroluminescent effect appeared to be correlated with a change in the composition of the crystallites rather than in their size.

Micrographs from films on conducting glass substrates showed crystallites approximately twice the size of crystals obtained under the same conditions on a pyrex glass substrate. The crystallite size was 400-450Å at a substrate temperature of 500°C compared to 250-300Å on pyrex glass at this temperature. Otherwise the micrograph was identical to those obtained from films deposited on pyrex glass.

(b) Rate of evaporation

This was controlled by varying the temperature of the evaporating boat.

Films of 200Å thickness were deposited from crystals at the rate of 50, 100, 150, 200 and 400Å/min. The substrate was glass and the evaporation rate was determined from the thickness and time of evaporation.

The crystallite size was an increasing function of evaporation rate (Figure 5.12a). At 50Å/min crystals were not clearly resolved in the micrographs, indicating a tendency to grow together rather than form individual particles. The banding in the crystallites was not very strong. At faster rates (e.g. 200Å/min) the crystallites were resolved and an increase in banding was observed,

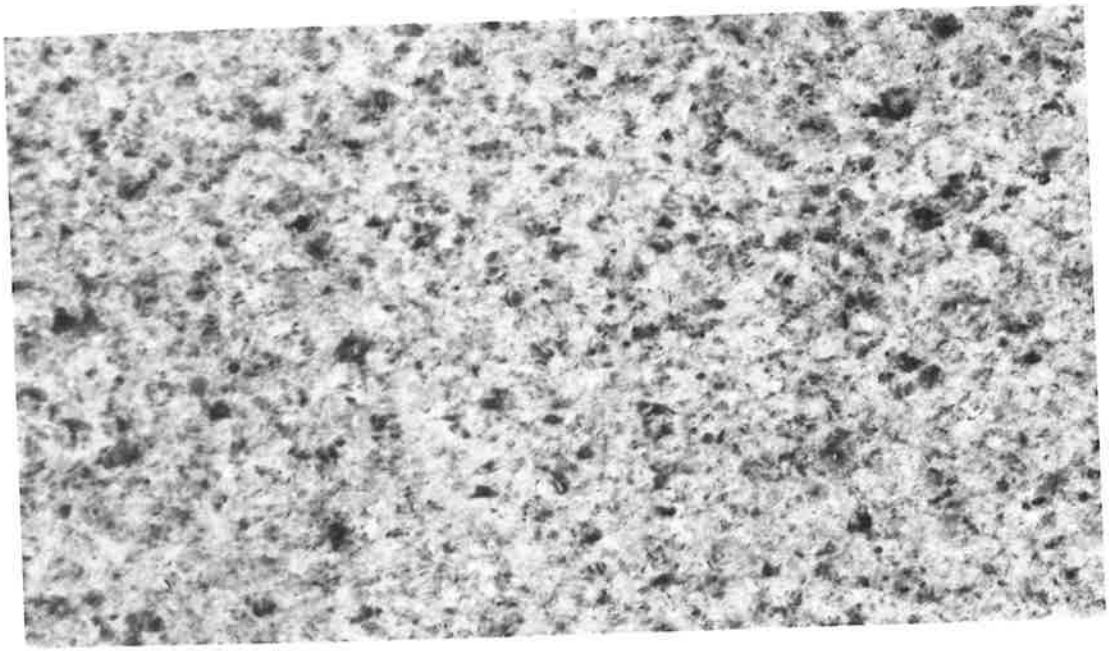

50 Å/MIN

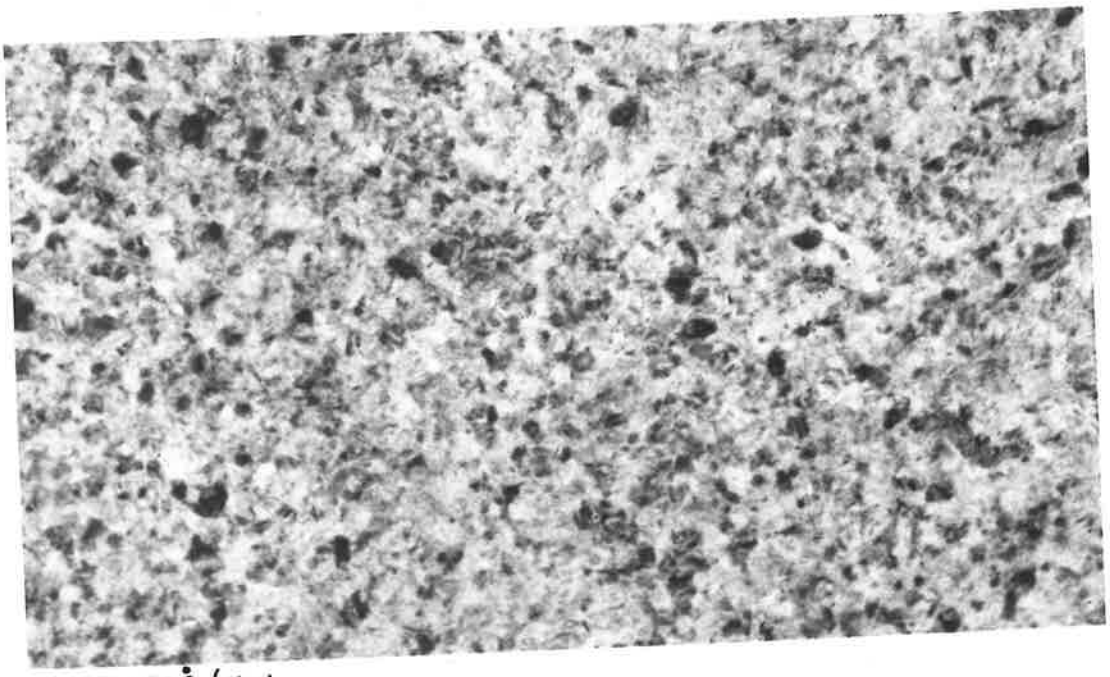

100 Å/MIN.

FIG. 5.10 MICROGRAPHS FROM ZnS. Mn.Zn FILMS DEPOSITED AT DIFFERENT RATES.

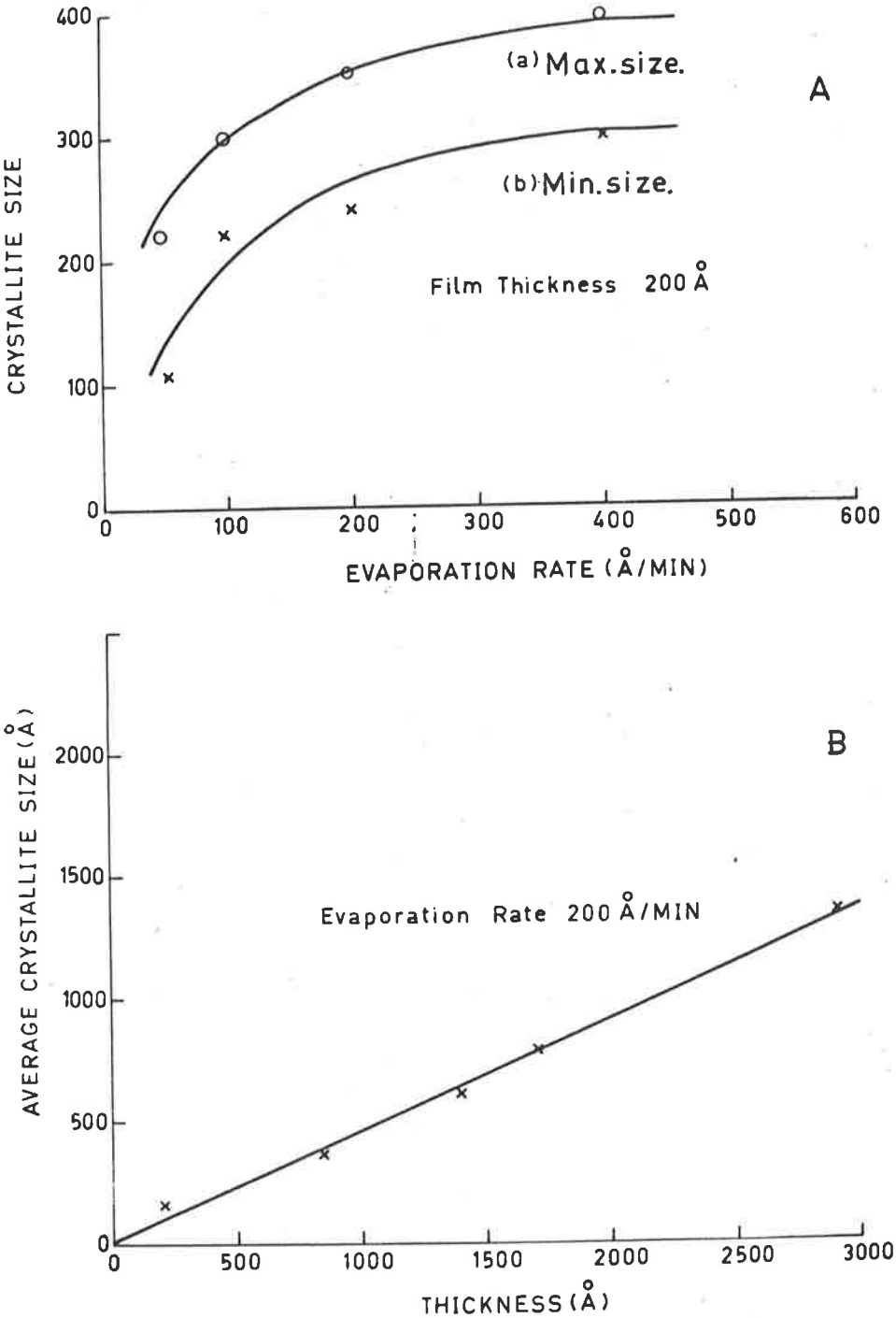


FIG.5.12 PARTICLE SIZE VARIATION IN A ZnS Mn FILM EVAPORATED FROM A ZnS Zn Mn CRYSTAL WITH EVAPORATION RATE (A) AND THICKNESS (B).

(Figure 5.10, 5.11).

(c) Film thickness

Because the electron beam was rapidly absorbed by films of increasing thickness, the thickest films giving useful micrographs was about 3000Å. Estimates of crystal size in these thicker films were made through thin spots in the film. The crystals observed in these thin spots were the same size as crystals which made up the thicker parts of the film. This conclusion was made by comparing the crystals in the thin region to those at the edges where the film was much thicker. If this was not true, then no measurement of the crystal size was taken, and other parts of the film (or other films) were investigated. A linear increase of crystal size with thickness was observed (Figure 5.12b). The linear dimensions of the crystallites were about one half the film thickness. It was not possible to determine the crystallite thickness and so make an estimate of the number of crystallites through the films.

(d) ZnSe films

ZnSe films were more easily removed from substrates than ZnS. Figure 5.13 shows micrographs from non-electroluminescent (a) and electroluminescent (b) films evaporated from ZnSe.Mn (0.01%) and ZnSe.Mn, Zn respectively. The substrate temperature was 350°C and the film thickness about 250Å. The crystallites are well resolved with linear dimensions about 180Å in each film, approximately the same

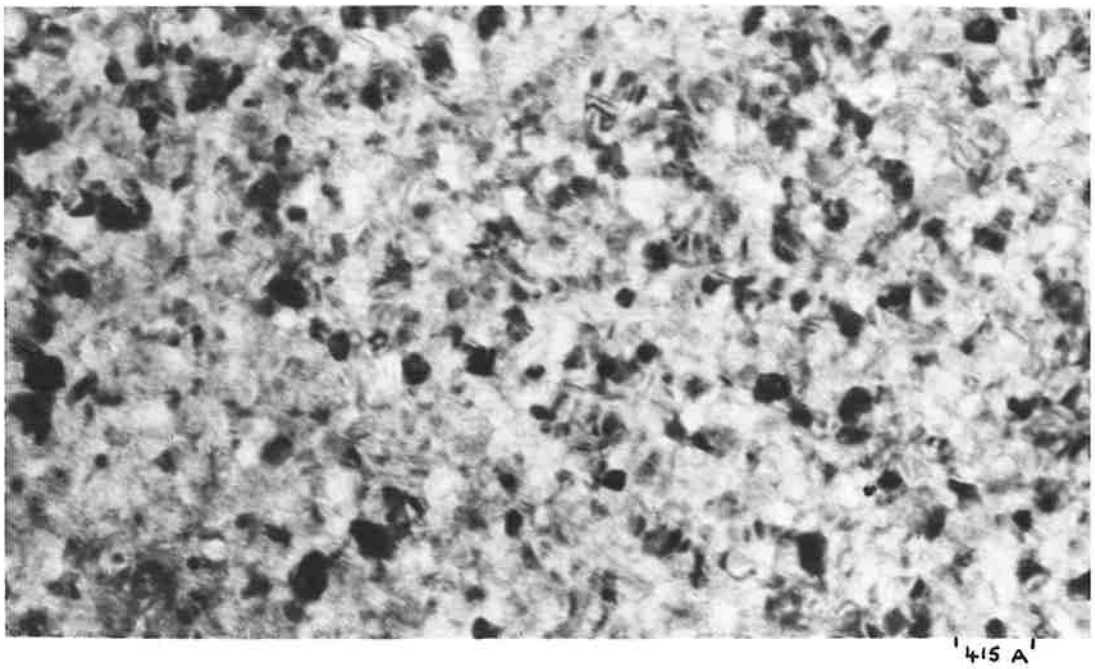


B

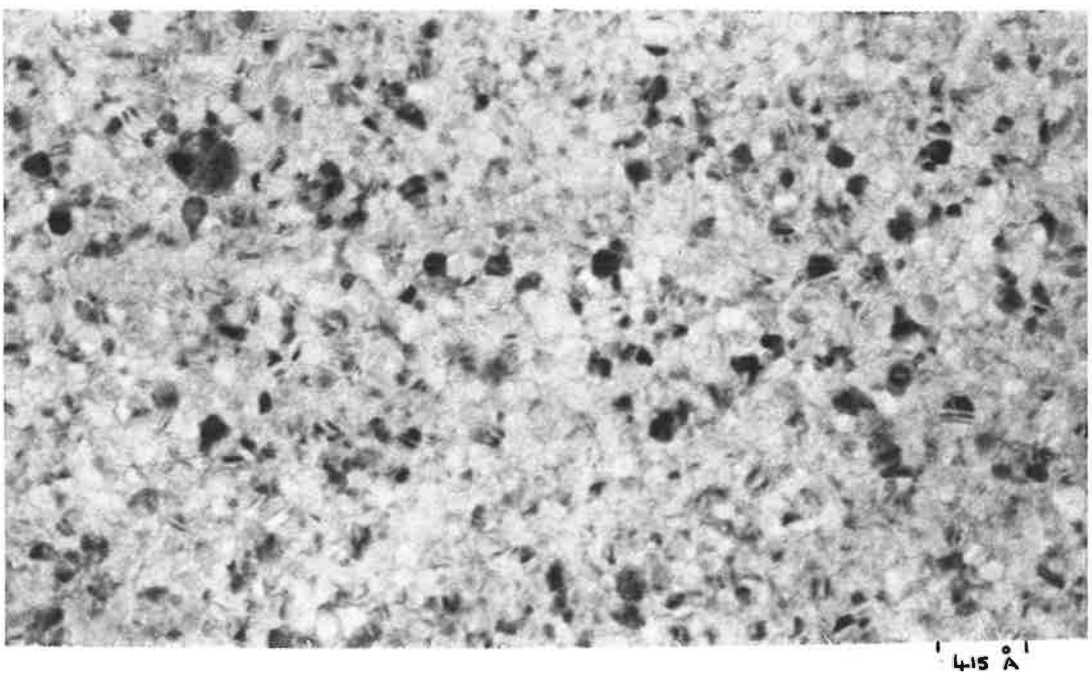


A

FIG. 5.13 MICROGRAPHS OF ELECTROLUMINESCENT FILM (A), NON ELECTROLUMINESCENT FILM (B).

as ZnS crystallites. The surface appeared to be covered with smaller crystallites (130Å) showing fringe patterns. The presence of these bands may be correlated with the abnormal width of the first strong ring observed in the diffraction patterns of these films.

There was no difference observed between electroluminescent and non electroluminescent films.

An increase in crystallite size, similar to that observed for ZnS films was observed about a substrate temperature of 310°C which was also the critical temperature for the appearance of electroluminescence.

## 5.5 Summary and discussion of results relating to the structure of evaporated films

Each result described in this chapter was obtained by investigation of a number of films to ensure that the conclusions made were representative of a particular condition in the films. The electron micrographs and diffraction patterns were likewise representative of large areas of the films. The presence of rings in the electron diffraction patterns which could be attributed to either cubic or hexagonal material were observed. The intensity of the observed lines due to reflections attributed to hexagonal ZnS was comparable to the intensity of the stronger lines from cubic ZnS. Evidence for the presence of the three strongest hexagonal reflections only was found. The mixed crystal structure was observed from electroluminescent and non electroluminescent films.

The absence of the (200) cubic reflection in the

electron diffraction patterns is difficult to explain. The absence of this ring introduced some doubt as to whether the films were composed of cubic or of hexagonal crystallites. The following results, obtained in this chapter suggest that the films contain cubic crystallites with some hexagonal modification.

(a) The (200) cubic reflection was observed in X-ray diffraction patterns for thick films.

(b) The (200) reflection was absent in electron diffraction patterns from thin films of ZnS and ZnSe (also of ZnTe). It is not likely that ZnSe (or ZnTe) films evaporated from crystals for which only a cubic phase is known will be predominately hexagonal.

(c) The observed rings in the electron diffraction photographs agree with all the allowed reflections from the f.c.c. lattice. However, when the lines are indexed according to the hexagonal lattice, a number of strong, higher order reflections which should be present are not observed.

(d) An observed ring, corresponding to the (400) cubic reflection does not fit any allowed reflections from hexagonal crystallites.

Because of these results, the structure of evaporated films of ZnS and ZnSe was assumed to be cubic with a small amount of an hexagonal modification.

The crystallite size in evaporated films was shown to vary between 150 and 1500Å, depending on the conditions of preparation. In general, smaller crystallites were obtained from the evaporation of large crystals than when

microcrystalline powders were used. The crystallite size was increased by increasing (a) the substrate temperature (b) the rate of evaporation and (c) the film thickness.

The absolute size of the crystallites (for a film of a given thickness) did not change the substrate temperature above which an electroluminescent film could be made. Therefore the appearance of electroluminescence could not be directly related to the change in crystallite size found at 290°C for ZnS and 310°C for ZnSe.

It has been shown in this chapter that diffusion of metallic manganese into pure ZnS increased the size of the crystallites and gave an electroluminescent film. These conditions are not necessarily related, and in fact, the above paragraph indicates that the increased size is not critical for the appearance of the electroluminescent effect. However, a similar effect caused by diffusion of the excess zinc present in films at the critical substrate temperature may occur. This would explain the increase of crystal size at this temperature. If the diffusion process was responsible for this change in crystal size, it would be expected that the critical substrate temperature (now the diffusion temperature) would be dependent on the metal used in the diffusion. This is not in accord with the experimental result that the critical temperature is unaltered when manganese is used (ZnSe.Mn (1%) Zn (1%)).

However, a satisfactory explanation may be given in terms of the process of sulphur (or selenium) re-evaporation

from the substrate. This process has been introduced in Chapter 4 (page 73). The evaporating material from the boat may consist of undissociated molecules (ZnS or ZnSe), together with zinc and sulphur (or selenium) atoms. The amount of dissociation is not certain, but may be complete according to the results of Goldfinger and Jeunehomme (1959), at least for ZnS and CdSe. If dissociation occurs in the evaporating boat, it is likely that more sulphur atoms will appear at the substrate surface than zinc atoms because of the difference in vapour pressure (Honig 1957).

It is now possible to envisage two processes during the formation of a film on the substrate surfaces. Consider ZnSe.Mn Zn (1%) as an example.

(a) ZnSe molecules evaporate from the boat together with a number of zinc and selenium atoms from partial dissociation of the ZnSe. On the substrate, inhomogeneous ZnSe crystals are formed containing regions of excess zinc and other regions of excess selenium. This results in both selenium and zinc vacancies in the ZnSe crystals. It is obvious that this is a non thermal equilibrium process. However, such formation may be likely because of the low substrate temperature with respect to the temperature used for evaporation. The defects are therefore frozen in.

(b) The second possibility is that molecules of ZnSe are formed from the zinc and selenium atoms on the surface. As a result, the film will contain an excess of one component (not both as in (a)). Therefore only selenium or zinc vacancies are present. This formation would be a thermal

equilibrium process, and must be the way in which a film is formed if the evaporation results in a completely dissociated compound.

Consider these two models of the film formation. According to (a), the film will contain excess zinc ions ($N_D$) and excess selenium ions ($N_A$). That is, $N_A + N_D$ lattice defects.

At low ($<< 310^{\circ}C$) substrate temperature, the film will contain more excess selenium ions than excess zinc because more selenium arrives on the substrate. The film resistivity is large because of donor electrons which are localized by (selenium) acceptors. As the substrate temperature increases, the selenium re-evaporates more rapidly than the zinc, until at some temperature, uncompensated donors due to excess zinc cause a fall in resistance. Increasing substrate temperature decreases the number of excess zinc and the number of excess selenium further.

This process predicts a high film resistance at low substrate temperature which decreases when the number of donors (uncompensated) is greater than zero. If the selenium is all removed at this temperature, the resistance shows a minimum, followed by an increase due to loss of excess zinc donors by re-evaporation. If the selenium is removed more slowly this minimum may be removed and the resistivity will then show a continuous decrease.

The second model of film formation, (b), predicts that the film will contain $N_A'$ defects at low substrate temperature due to excess selenium. As this temperature

increases the selenium excess is removed by re-evaporation until, at a certain temperature, ZnSe crystals with no defects are formed. Further increase in temperature gives a film with an increasing number of excess zinc defects (because the selenium is re-evaporating more rapidly than the zinc).

This process predicts that the film is high resistance at low temperature, excluding the possibility of p-type conduction. Increasing temperature reduces the selenium defects to zero and the film will remain high resistance. Selenium is lost more rapidly than zinc by evaporation above this temperature and the resistance falls. If the ZnSe has only been partly dissociated, and the loss of selenium by re-evaporation is sufficiently fast, a minimum in the resistance may occur. Above this temperature, only excess zinc remains and the resistivity increases. Similar smoothing out may be envisaged, as suggested above. However, if dissociation is complete in the evaporating boat, there are only zinc and selenium atoms on the substrate which then must form ZnSe crystals. In this case, increasing substrate temperature above that at which no excess is present will give a decreasing amount of selenium on the substrate (because of re-evaporation). The films contain therefore, an increasing amount of zinc excess in this temperature range. This mechanism predicts a continuous (and more rapid) decrease in resistance with increasing substrate temperature. No evidence has been obtained here for the formation of very low resistance films at high

temperatures (which would be expected in this case of total dissociation.

Both models predict a decrease in resistance with the possibility of a minimum in the resistance, if the dissociation of ZnSe during evaporation is not complete. The observed low voltage resistivity as a function of the substrate temperature is shown in Figure 5.9 (page 103). The variation may be interpreted equally well in terms of either of these models.

The important aspects of these models for the crystal size is the total number of defects which must be incorporated in the ZnSe crystallites. Model (a) predicts $N_A + N_D$ defects at low temperature, decreasing continuously as the substrate temperature increases.

Model (b) predicts $N_A'$ defects at low temperature decreasing to zero as all the selenium excess is removed. Above this temperature the number of defects (now due to excess zinc) increases.

It may not be unreasonable to assume that the ultimate crystal size is limited by the number of defects which must be dissolved in the lattice. Model (a) therefore suggests a continuous increase in crystal size (more rapid about some temperature if selenium is lost rapidly) while (b) predicts a maximum in crystal size followed by, either a decrease or an increase (depending on the rate of loss of selenium). These effects may average out to give a constant crystal size in this range. In fact, electron micrographs of these films would not detect a change of less than about

20%.

It can therefore be seen that in general, the expected variation of crystal size agrees reasonably well with the observed increase shown in Figure 5.9a.

While this does not definitely confirm the importance of re-evaporation, the above discussion shows that a re-evaporation process can explain the requirement for a critical substrate temperature and account for the increase of crystal size at this temperature. It should be noted that the same increase in crystal size was observed about the same temperatures (310 and 290$^{o}$C) for films of pure ZnSe (or ZnS), which were high resistance at all substrate temperatures. This shows clearly that the change in crystal size can not account for the observed changes in film resistance. However, the re-evaporation model can explain the observed variation of the film resistance.

# 6. GENERAL PROPERTIES OF EVAPORATED FILMS

## 6.1 Effect of evaporated metal electrodes on the electroluminescence of ZnS and ZnSe films

Harper (1962) has reported that light emission from electroluminescent films of ZnS may only be detected when, either an aluminium or a magnesium electrode is used. These films were prepared by the diffusion technique.

This result was verified for evaporated ZnS.Mn and ZnSe.Mn films, by depositing an aluminium electrode and an electrode of another metal side by side on the surface of an electroluminescent film. Metal electrodes of evaporated gold, silver, copper, zinc, indium and platinum were used. For all metals except aluminium, no electroluminescence was observed.

Closer examination of the non electroluminescent ZnS metal film combinations showed that they were of similar resistance to ZnS with an aluminium electrode for very small applied voltage (less than 1 volt). However, as the voltage (A.C.) was increased, there was a sudden (irreversible) drop in resistance to less than 500 ohms (the resistance of the transparent electrode. An explanation of this behaviour may be made by assuming that the ZnS (or ZnSe) film contained a number of regions considerably thinner than the average. In these regions the field strength would be sufficient to cause breakdown. This would result in localized heating and cause diffusion of some metal from the electrode, resulting in a permanent low resistance path through the film.

A similar change in resistivity was observed if metals (e.g. Ag or Au) were evaporated onto conducting glass which was subsequently covered by ZnS and an aluminium electrode. This result showed that pinholes formed through the sulphide film during evaporation (Haoskaylo and Feldman 1962) were not responsible for the rapid change in conductivity. If these pinholes had been subsequently filled by evaporated metal, a permanent short circuit would exist between the electrodes. This would not occur when these metals were deposited before the ZnS, and the composite film would be then high resistance which, however is contrary to the observed results.

An aluminium electrode therefore possessed some property which was essential to the electroluminescent process in evaporated films. This was shown to be the formation of an aluminium oxide ($Al_2O_3$) layer during the metal evaporation. The formation of such layers during an aluminium evaporation has been reported by Holland (1960). If the first products from an aluminium evaporation were prevented from reaching the ZnS film and only the latter metal formed the evaporated electrode, the film was low resistance and no electroluminescence was observed. This confirmed the importance of the initial evaporation products.

The initial 100Å (approximately) deposited during the aluminium evaporation at a pressure of 0.5 microns was compared by electron microscopy, with a deposit from the final stage of the evaporation. The final deposit was made up of closely packed cubic crystallites (presumably aluminium). An electron diffraction pattern confirmed the presence of

aluminium (for a centred cubic). However the initial deposit showed much smaller crystallites (500Å) scattered in what appeared to be an amorphous matrix. This was assumed to be $Al_2O_3$, which although hexagonal, may have appeared amorphous because of very small crystallites. However, the diffraction pattern only showed cubic aluminium to be present, although the rings were considerably broadened. Murbach and Wilman (1953) have pointed out the difficulty in identifying $Al_2O_3$ diffraction rings in the presence of even a small amount of crystalline aluminium.

It has already been mentioned (Chapter 1) that electroluminescence from $Al_2O_3$ layers has been observed, and that the properties of the emission were similar to some reported for electroluminescence of ZnS with an aluminium electrode. The light emission found in evaporated films did not occur solely in the $Al_2O_3$ layer for the following reasons.

(a) The light emission was characteristic of the manganese activator, and films not containing manganese (but with an aluminium electrode) were not electroluminescent.

(b) The light occurred for both polarities of the applied voltage, and was sensitive to impurities added to the sulphide (or selenide) film.

To demonstrate the importance of a barrier layer at the metal electrode - ZnS interface, an artificial layer of evaporated silica ($SiO_2$) was deposited on the sulphide film before the metal evaporation. If any of the metals, previously shown to give no light emission on ZnS films were evaporated on the silica, electroluminescence could be observed.

An approximate correlation between the work function of the metal electrode and the voltage at which light emission was just detectable was obtained. A high work function (platinum 5.3e.v.) resulted in a smaller threshold voltage. A more precise relationship could not be obtained because of the polycrystalline nature of the metal film. While the work function of polycrystalline ZnS is not well known, the improvement of light emission (shown by a decrease in voltage at which light is emitted) with increasing work function suggested that, an increase in barrier height between the metal and the artificial barrier improved the light emission process at constant applied voltage. Goodman (1963) has shown that the variation of the work function of an evaporated metal with respect to CdS (single crystals) suggests an increasing barrier at the interface, as the metal work function increases. The results showed that the electron affinity of CdS was 4e.v. The values for ZnS may not be very different.

These results showed that, as well as fulfilling certain conditions in the ZnS (or ZnSe) films which were described earlier, the metal electrode must be associated with a barrier layer before any light emission can be detected. The function of this barrier layer may simply be to prevent localized breakdown causing permanent low resistance paths through the film. However, it was thought that even if this was one result of the barrier layer, the low conductivity barrier may effect the light emission process in another way. This is discussed in the final chapter of this thesis.

## 6.2 Technique used to obtain reproducible measurements of the electroluminescent brightness

A number of techniques for the preparation of reproducible films of ZnS and ZnSe have been described. It was found that all electroluminescent films were subject to an effect which determined, at least in part, the characteristics of the emission. During the period after the first application of a voltage to an electroluminescent film, the emission was not constant, but showed a complicated variation with time. This was a result of what will be referred to as a 'forming' process, and indicated the need for some form of stabilization procedure before taking any measurements of the brightness.

During the initial application of an A.C. voltage to an electroluminescent film with a new aluminium electrode, a localized arcing could be observed over the metal electrode area. If the voltage was raised until light emission was detectable and then maintained at this value, the emission first increased slightly (about 5% for ZnS.Mn, Zn films) and then decreased below the original level over several minutes.

This initial increase was much more evident with ZnSe.Mn, Zn films where the light emission increased by up to a factor of two over the first ten minutes. This was followed by a slower decrease to a constant value, but still above the original brightness level at that voltage. If the voltage was removed and then re-applied after a period of time, an increase in brightness was again observed, although

of smaller magnitude.

The increase in light intensity during the initial operation of these films was not due to light emitted by the arcing effect between the electrodes. This was shown by the difference in this initial increase between ZnS and ZnSe films which both showed (visibly) a similar degree of arcing.

A similar forming was reported during D.C. electroluminescence of films, by Goldberg and Nickerson (1963). They observed that light emission first appeared at the edges of the electrode and gradually spread over the whole electrode area.

A similar change in the brightness was found for some ZnSe.Mn films deposited on substrates just above the critical temperature. Light emission from these films developed in the following way. As the voltage was increased, localized breakdown (arcing) appeared at some places around the electrode edge. This was then replaced by a stable emission in these regions. Increasing voltage then caused localized arcing in other areas which was replaced by steady light emission from these areas. This continued until the total electrode area was emitting uniformly. The light was characteristic of the manganese activator. The violent forming caused considerable electrode damage, but the final light emission was approximately uniform over the electrode area.

This destructive forming was not observed if the voltage was removed and re-applied after some time.

When this initial light variation was excessive (which it was for most films), the following procedure was used to stabilize the films. A voltage was applied to the film sufficient to excite a low level of light emission. Because of the forming process this brightness changed with time. The applied voltage was adjusted (an increase of voltage was usually required) until the brightness was the same as at the first application of the voltage. This was continued until the brightness was constant in time. The intensity of the emission was then increased by increasing the voltage and the above procedure repeated. This was continued until a brightness level, which would be the maximum for any subsequent measurements, was maintained at a constant value over a period of time during which the voltage was constant.

All experimental results described in this thesis were taken after a stabilization process of this type and were, as a result, reproducible.

If the electrode surface was examined microscopically after the film had been emitting light, it was seen to be covered with minute holes in the order of ten microns ($10^{-3}$cm) in diameter. These were smaller than the holes caused by arcing between the electrodes and they appeared to be regions where localized breakdown of the film had occurred.

Additional information on the initial operation of films was obtained from measurements of the resistive component of the A.C. current through the films during the

forming process.

The first increase of brightness at constant voltage was associated with a decrease in the current (at constant voltage) through the film. This could not be explained by a decrease in electrode area caused by initial arcing.

It has already been mentioned that this initial rise could also be observed if the voltage was removed and re-applied later. This can be explained by assuming that the effectiveness of the barrier layer is enhanced by the applied field due to some charge redistribution which will decay when the field is removed.

Goodman (1963) has also reported that barriers at an aluminium - CdS interface (CdS crystal) appear to form with time, and that these barriers reduce the current through the crystals. The pressure in the vacuum system used for evaporation of the aluminium was not given.

It was observed that if an artificial barrier layer was provided under a metal electrode by evaporating a film of silica onto the ZnS (ZnSe), the film required very little stabilization processing. This confirmed the suggested formation of a barrier layer during the forming process. Obviously, if this is provided by an artificial barrier layer, the forming is not so necessary for stable operation.

The decrease of brightness observed after this rise was associated with an increase in film resistance (and fall in capacity), but to maintain a constant brightness the resistive current was found to be constant. A fraction

of the resistance change was explicable by the electrode destruction caused by localized breakdown. The remainder was considered to be due to a build up of polarization charge which reduced the internal electric field. This accumulation, for A.C. voltage operation of films is discussed in the following section.

A number of experimental conditions increased the amount of forming (largely electrode destruction) and caused an excessive reduction of the light output from ZnS.Mn Zn films. Films containing low manganese (0.01%) concentration and evaporated onto substrates at high temperatures (about $350^{\circ}$) showed very little forming. The following conditions gave rise to excessive initial variation of the light output.

(a) Increasing zinc content above $1.10^{-3}$gm/gm added to ZnS.Mn Zn crystals used for the evaporation (Chapter 7.5.1).

(b) Increasing manganese above $1.10^{-3}$gm/gm added to the crystals used as an evaporant.

(c) Temperature of the substrate just above the critical substrate temperature for the appearance of electroluminescence (Chapter 7.5.2).

While such a complete investigation of the factors affecting the forming was not made for ZnSe films, an increase in forming for films deposited near the critical substrate temperature was confirmed.

It was difficult from the above observations, to correlate the forming with any particular property of the film. It seemed however, that an excess of an impurity

increased the electrode deterioration. This may be a result of deposition of $Mn^{++}$ and $Zn^{++}$ ions in sufficiently high concentrations to cause increased numbers of high conductivity paths through the film. This would lead to more extensive damage to the electrode and reduce the observed brightness. The results described in Chapter 4 (page 72 ) showed that regions of high concentration were always present. Therefore, some critical concentration was required to produce the increase in forming found at high added impurity concentration.

## 6.3 Space charge polarization in electroluminescent films

It has been recognized that a space charge type of polarization can occur in semi-insulators when a D.C. electric field is applied. Such polarization fields of more than $10^4$ volts/cm can exist for many days after the field is removed (Kallmann and Rosenburg 1955).

This space charge may be established by injecting electrons into a material at a greater rate than they are extracted from the other electrode. This condition is very probably fulfilled for a film with two non ohmic electrodes. Injected charge may be trapped in the bulk of the film (to be described in Chapter 6.4) and may also accumulate at the electrodes. A simplified band diagram for a ZnS.Mn Zn film between a tin oxide (n type semiconductor) electrode and an aluminium (with oxide layer) electrode, is shown in Figure 6.1a. The most important aspect of this diagram is that in the biased condition (Figure 6.1b) electrodes accumulate at the anode which is partly blocking. Electrons are injected through the thin insulating layer. The accumulated electrons

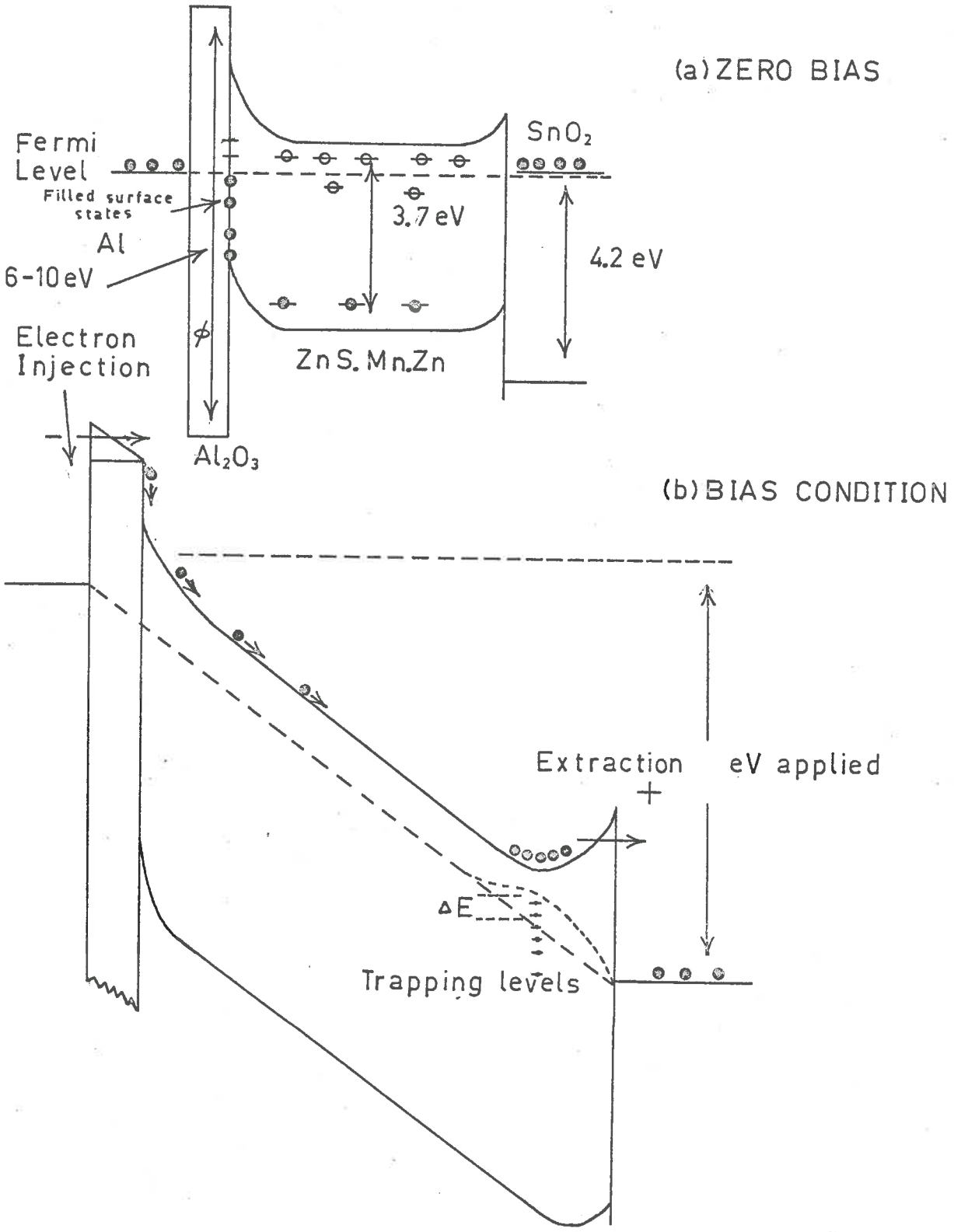


FIG. 6.1 SIMPLIFIED ENERGY BAND DIAGRAM FOR ZnS. Mn.Zn FILM.

raise the Fermi level in the region near the electrode as shown. If this rises above some trapping levels, previously empty, electrons are trapped. If the field is removed, the free electrons diffuse into the bulk rapidly and leak away. However, the trapped electrons are ejected more slowly as the Fermi level sinks to its original position.

If an A.C. voltage is applied to such a system and the time for one cycle is shorter than the release time for trapped electrons, charge will be permantly held at the electrodes. This reasoning also applies to electrons trapped in the bulk.

Injected charge may be trapped in the oxide layer supposed present between the metal electrode and ZnS film.

Because of the different nature of the electrodes, there will be some difference in the amount of charge trapped at each electrode. As a result the net field in the bulk of the film will be greater on one half cycle of an A.C. voltage than on the other. This may effect the brightness on alternate half cycles.

It should be mentioned here that electroluminescent films emit light in two pulses, approximately in phase with the voltage maxima of a sinusoidal A.C. voltage. In general, the intensity of these peaks is unequal.

If injected charge is accumulated in films in an asymmetric way, it should be possible to obtain a discharge current after the applied field is removed, by joining the electrodes through a sensitive D.C. meter.

A number of ZnS films were excited by an A.C. field

(300 c/s) sufficient to excite electroluminescence, and then short circuited through a meter. After a five minute excitation, a short circuit current of about $3.10^{-9}$ amps, decaying over about 5 seconds to $1.10^{-9}$ amps was observed. The decay was observed to continue for at least 30 minutes but at a slower rate (to $0.2\ 10^{-9}$ amps). The switching from excitation to short circuit conditions was done manually so that the characteristic decay time of the film (acting as a parallel plate condenser) was not observed. The resistance of the films was about $10^{5}$ ohms, the capacity about 0.004 farads giving a decay time constant $\tau = RC$ of $4.10^{-4}$ seconds. This was too rapid to explain the observed current.

As mentioned previously, this asymmetric charge should cause the net internal field to be different on the two half cycles of an A.C. voltage. This was investigated by using films of different thickness. Thin films (1500Å) showed a maximum brightness pulse when the metal electrode was positive, while thicker films (3000Å) showed a maximum when the metal was negative. This property of the films is discussed in a later chapter (page 193 ).

The same direction of the discharge current was observed from films of all thicknesses. This result indicates that the trapped charge did not produce sufficient electric field to influence the ratio of the brightness pulses on alternate half cycles. This of course assumes that the internal field determines the intensity of the brightness pulses, which seems to be a realistic assumption.

If a D.C. polarizing voltage was used, a discharge

current, usually larger than from an A.C. voltage of the same magnitude was obtained. The discharge current always appeared with the opposite polarity to the polarizing D.C. voltage. This showed that the discharge current was not due to diffusion of electrons from the bulk through the electrode with lowest barrier. If this were true, the polarity of the discharge current would be independent of the direction of the D.C. polarizing voltage. The results suggested that the direction of the discharge current was determined by the electrode at which electrons accumulated.

The observation of a current from each electrode (i.e. for both directions of the D.C. polarizing voltage) showed that in general, electrons could be trapped at each electrode. Therefore, for A.C. voltage operation, electrons can be trapped at each electrode while only the difference can be observed when the electrodes are joined.

While the asymmetry of the trapped charge was not sufficient to change the field distribution on alternate half cycles, the total charge may be sufficient to modify the average field strength in the bulk. Such a modification would account for part of the decrease in the electroluminescent brightness during initial operation of the films.

While it seems relatively certain that the internal field on alternate half cycles is not very different, the presence of a polarization field, which can follow the changes of an applied A.C. voltage (V) may cause the net internal field to be less than the value given by $\frac{V}{d}$, where d is the electrode spacing. Such a field would not be observed in

these experiments. The problem of the magnitude of the net field strength in the bulk of the film is discussed in Chapter 6.5 (page 136).

## 6.4 D.C. conduction in evaporated films

It is possible to obtain considerable information concerning the conduction processes from simple measurements of the current variation with applied voltage. For example, a linear plot of log I against $V^{\frac{1}{2}}$ indicates Schottky emission over a barrier (Mead 1962). Measurements of this type become more difficult to analyse as the field strength approaches the region of dielectric breakdown (Chynoweth 1960). The analysis may also be complicated by other factors, probably the most important being the nature of the electrical contacts to the material. Generally, experiments are performed using ohmic electrodes, or one ohmic and one blocking electrode. However, with two electrodes of unknown character (as for ZnS between aluminium and tin oxide) this approach is of limited use.

It was found that many values of current observed for a given voltage across the films used here were unsteady in time. This made definite conclusions concerning the shape of many curves impossible. This variation (in the form of both upward and downward fluctuations) is shown in the following figures as vertical lines, whose length reflects the uncertainty in the values of current. Time dependent behaviour (although not in the form of fluctuations) is often observed in semi-insulating materials with high trap densities. This effect has been described by Smith (1955) for CdS crystals.

For ZnS (and ZnSe) films on conducting glass and with aluminium electrodes, a small rectification was always observed. This was about 1.2:1 for the film used to obtain the data shown in Figure 6.2. For this particular film, the maximum emission peak occurred for the metal negative half cycle of the applied voltage. Maximum emission for this polarity of the applied voltage was a property of thick films (2500 - 10,000Å).

Thinner films ($<2500$Å) showed maximum emission for the metal positive. The direction of rectification was in the same direction for these films as for thicker films. This showed that the direction of rectification did not influence the intensity of the brightness pulses. It is possible that the measured current does not give a true indication of the current which may cause electroluminescent emission. Rose (1957) has pointed out that under certain conditions, for example in the space charge region of a p-n junction, the total current flow gives no indication of the current which may cause (impact) ionization. This is because the total measured current is the sum of a field current and a diffusion current and only the former gives rise to ionization (i.e. light emission).

An attempt to reduce the amount of rectification observed was made by preparing films between two supposedly identical electrodes. It was expected that the current-voltage curves for either polarity would then be identical.

No stable current flow was observed in a ZnS film between two aluminium electrodes. However, if the

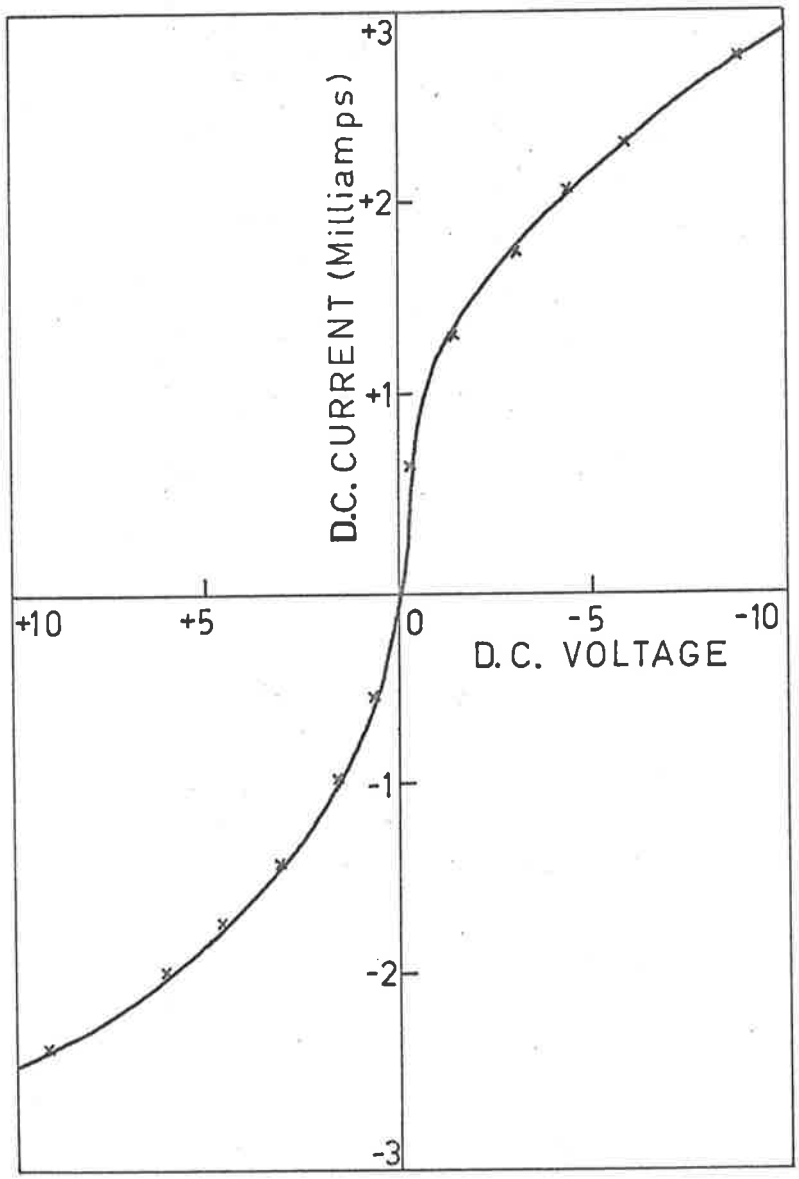


FIG. 6.2 CHARACTERISTIC D.C. RECTIFICATION CURVE FOR A ZnS FILM EVAPORATED FROM A PURE ZnS CRYSTAL. THE POLARITY SHOWN ON THE VOLTAGE AXIS CORRESPONDS TO THE POLARITY OF THE ALUMINIUM ELECTRODE.

aluminium was deposited on a glass slide and then oxidized (heat treatment at 300°C in vacuo for 30 minutes), deposition of the ZnS over this followed by another aluminium electrode gave a more stable current flow. It has already been shown that the aluminium electrode evaporated onto the ZnS was associated with an $Al_2O_3$ layer. Therefore, by oxidizing the surface of the initial electrode, the ZnS formed the centre layer of a (nearly) symmetric system.

For systems such as this with electrodes oxidized to different extents, large rectification was observed (ratios of 10 to 100:1). This emphasized the difficulty of preparing a film between two identical electrodes. In any case, results obtained from ZnS between aluminium and tin oxide should be more relevant to the electroluminescent process which occurred with these electrodes.

Figure 6.3 shows curves from a non electroluminescent (no added zinc) and an electroluminescent film deposited at about 350°C. Both films had been operated at high A.C. voltage (25 volts) previously, but the electrodes were not noticeably affected. Some current readings were unsteady and this is indicated by the vertical lines. Obviously, the electroluminescent film is lower resistance (at 3.5 volts $R = 7.10^3$ ohms compared to $7.10^7$ ohms). The current flow through the non electroluminescent film appeared to saturate at about 6 volts. However, for the electroluminescent film a marked increase in current occurred at about 3.5 volts. This may be due to a supply of electrons from impact ionization of donors from the excess zinc in this film. Similarly,

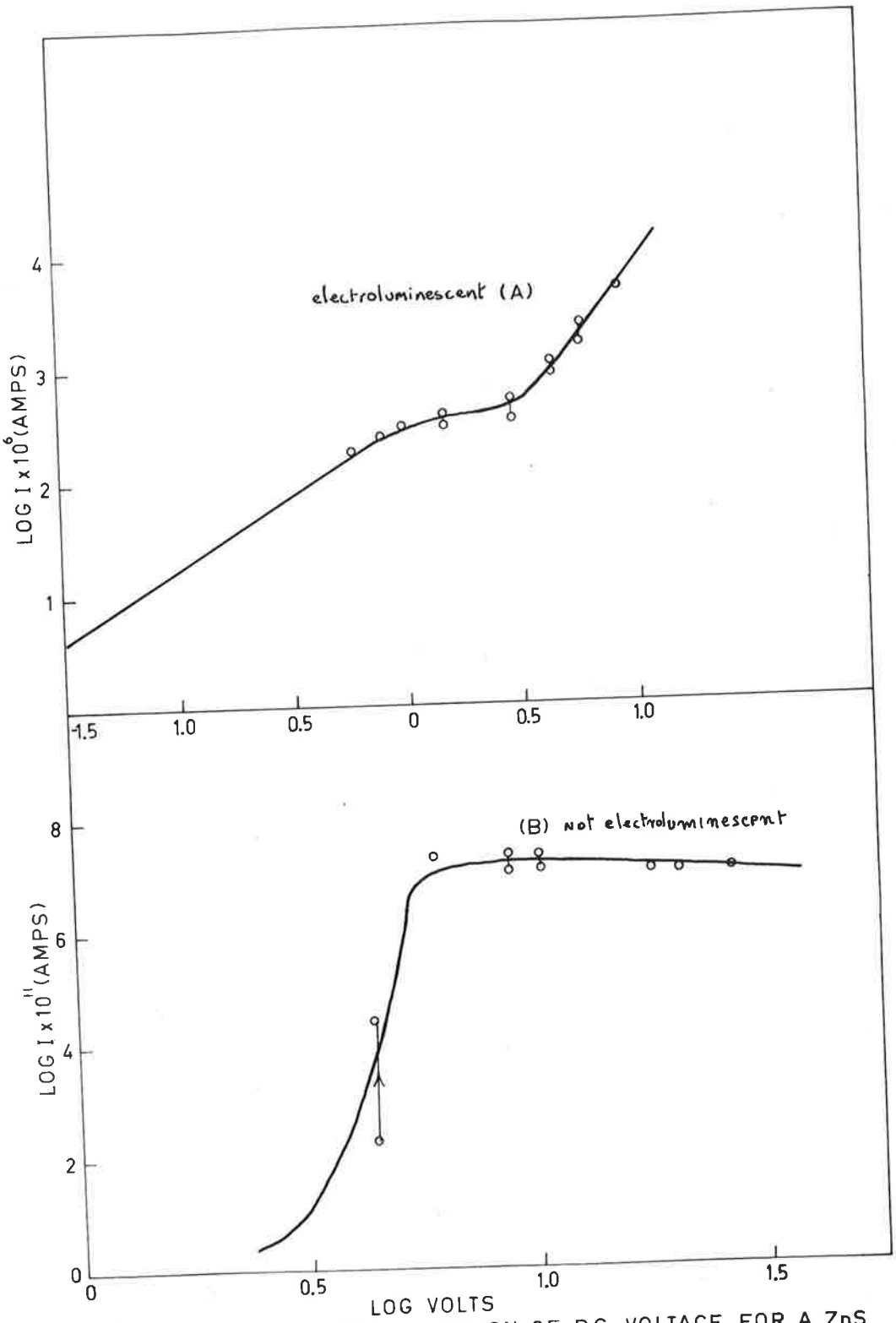


FIG 6.3 DC CURRENT AS A FUNCTION OF DC VOLTAGE FOR A ZnS FILM EVAPORATED FROM A CONTAMINATED BOAT(A) AND UNCONTAMINATED BOAT(B)

increases of current due to ionization of donors have been observed for germanium and silicon (Sohm 1961).

A large number of films were investigated and generally all films giving light emission gave a similar increase in the current flow at a particular voltage.

Figure 6.4 and 6.5 show data from three electroluminescent films and a non electroluminescent film (substrate temperature 280°), all containing excess zinc. All other conditions during preparation were identical. The aluminium electrodes were evaporated simultaneously and no voltages were applied before the curves in 6.4 and 6.5 were taken. It is clear from these figures, that the behaviour of such films (with an unused electrode) is complex. Similar effects were observed for both polarities of the applied voltage.

In general, the current at low voltage was small. The 300°C film showed a higher initial current which was considered to be caused by low resistance paths through the film, which were subsequently burnt away at higher voltage (by forming). These low current readings were unstable but at a certain voltage (about 3 volts) a more rapid increase of current occurred, which was followed at higher voltage by much steadier current readings. If the voltage steps were re-traced immediately, the current (steady values) decreased, but the magnitude was much greater than at the same voltage during the initial increase. If the voltage was increased again within a few minutes, the larger current flow was maintained as shown in Figure 6.5b. Similar hysteresis effects, although not so marked as observed here have been reported in current-voltage curves from beryllium oxide (Be 0) diodes by

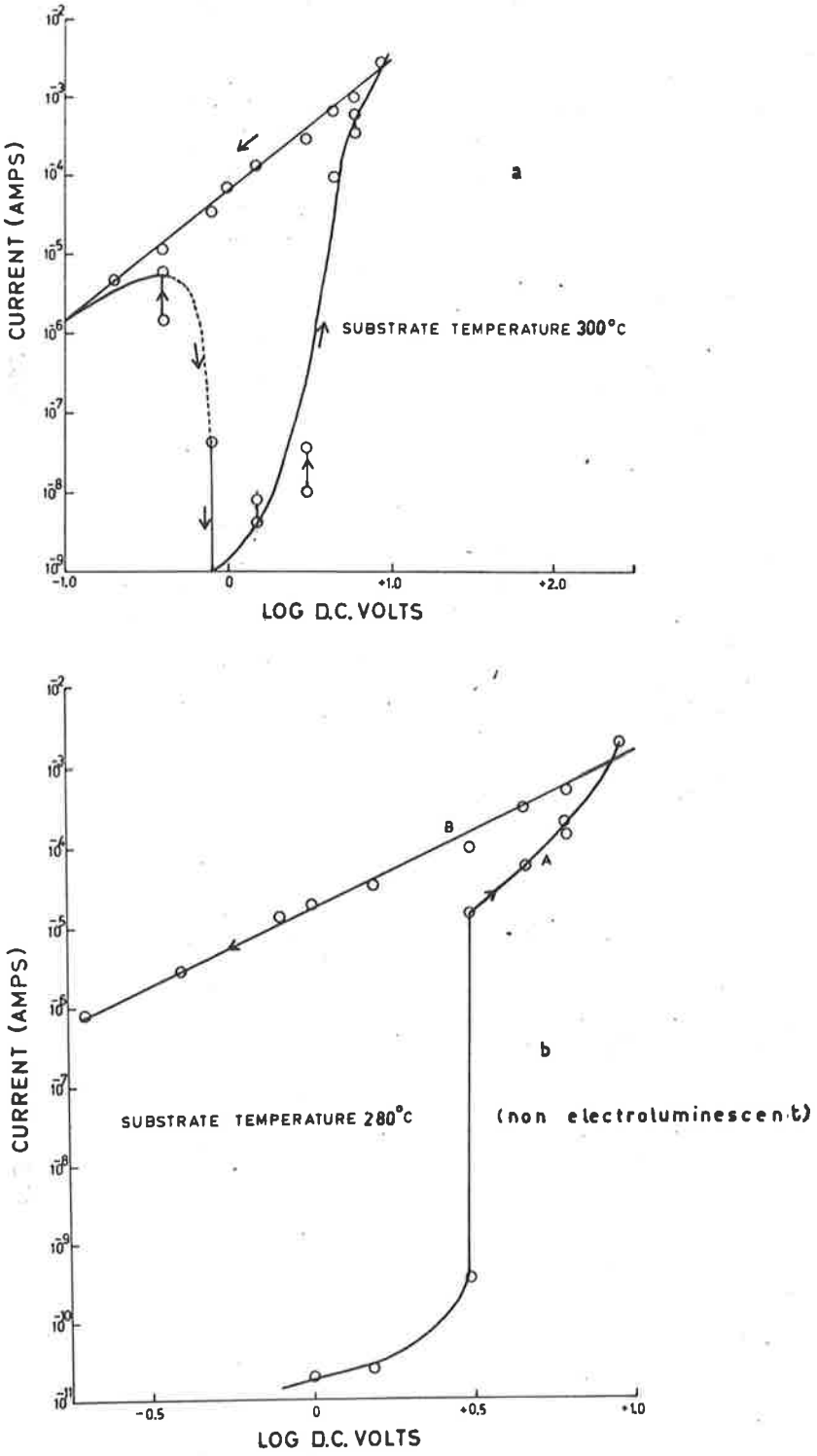


FIG. 6.4 D.C. CURRENT VOLTAGE CURVES FOR VARIOUS SUBSTRATE TEMPERATURES FOR A ZnS.Mn FILM. FILM THICKNESS 1300 ± 50 Å.

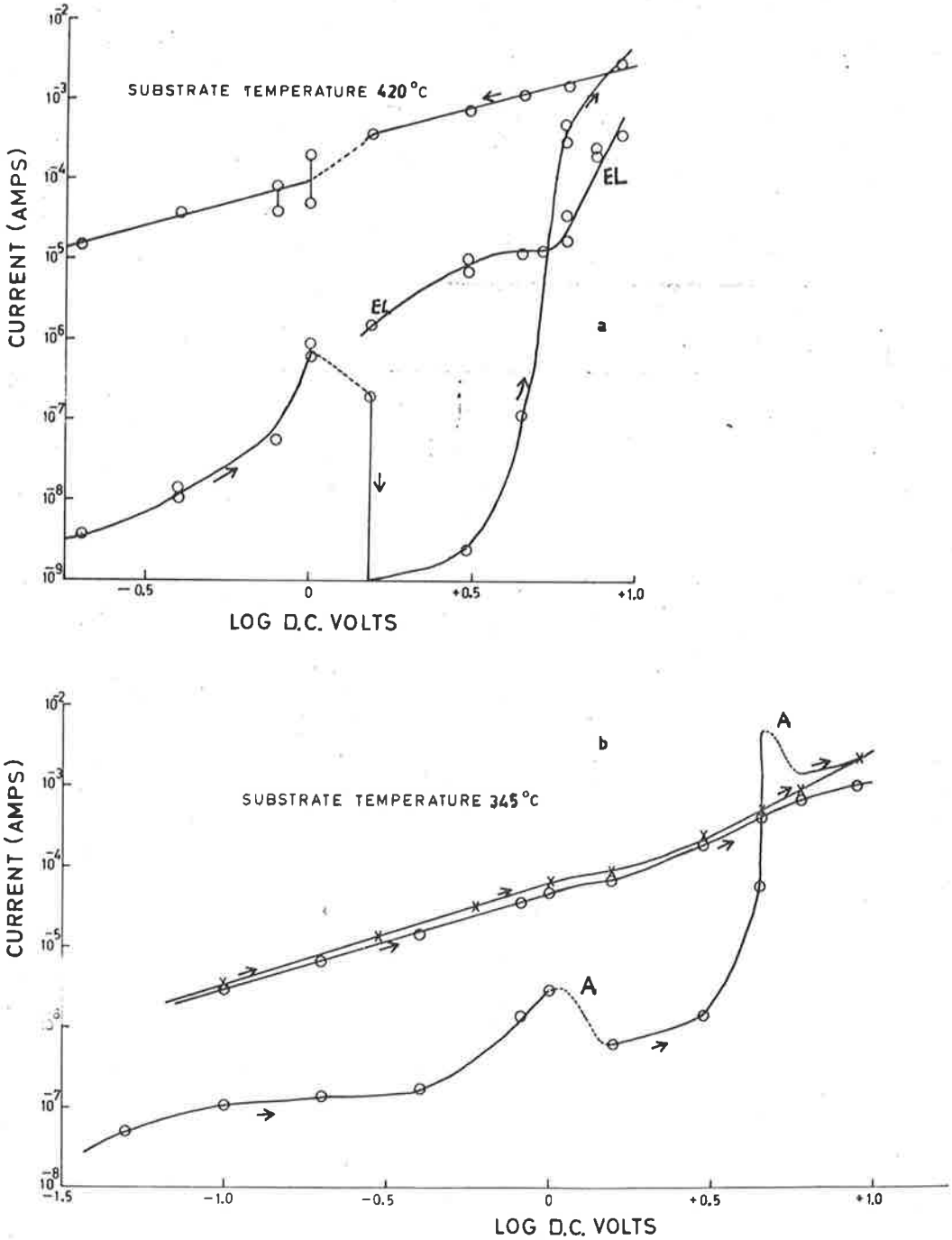


FIG. 6.5 D C CURRENT VOLTAGE CURVES FOR VARIOUS SUBSTRATE TEMPERATURES FOR A ZnS.Mn FILM. FILM THICKNESS 1300 ± 50 Å.

Meyerhofer and Ochs (1963). The effect was attributed to space charge build up in the Be O.

If the ZnS film was left (open circuit) in the dark for several hours, and a voltage was re-applied, the initial current at low voltage was smaller than the value when the film had been operating previously at that voltage. Increasing voltage resulted in increasing current until the experimental values increased along the straight line obtained earlier. Once this condition had been attained, the same lines were observed for subsequent variations as obtained previously.

The longer the film was rested, the smaller was the initial current, although the linear region was always regained by increasing the voltage sufficiently. This slow relaxation suggested a gradual emptying of traps containing electrons and also that the linear variations observed in Figures 6.4 and 6.5 were due to current flow in a film in which all traps had been filled. The current is then space charge limited. Space charge limited current is a well known form of conduction in semi-insulators. The current variation with applied voltage (D.C.) generally increases slowly at low voltage as injected electrons are trapped. The trapped charge acts to reduce the current flow and a higher voltage is needed to inject more electrons. This trend continues until all the traps are filled. The voltage at which this occurs is called the trap filled limit and for higher voltage, the current increases more rapidly (Rose 1955).

Such current flow is not a property of electroluminescent films exclusively, because very similar effects were

observed for films which did not show light emission (Figure 6.4b). However, at lower substrate temperatures (100 and 200°C) no such charge storage occurred because the current values during voltage increase and decrease were of the same magnitude. Usually, on decreasing the voltage the values fell below those observed during the increase.

Sudden decreases of current at constant values of D.C. voltage were observed (Figure 6.5b, marked A). Such effects have been observed by Boer et al (1962) in CdS films operating near dielectric breakdown and have been attributed to electrode destruction caused by localized thermal breakdown. This is a process which contributes to the forming discussed in the previous section. The voltage range used to obtain the results was purposely kept below about 20 volts to avoid any marked effects due to breakdown in the films.

Rose (1955) has observed the equation relating the space charge limited current to the applied voltage in a trap free solid. The equation is the same in the presence of shallow traps, viz

$$I = AV^2 \qquad \text{--- 6.1}$$

where A is a constant.

For a trap distribution described by a steepness factor $e^{-\frac{E}{kT_c}}$, $T_c$ a characteristic temperature greater than the lattice temperature T, this equation is modified to

$$I = BV^{(\frac{T_c}{T} + 1)} \qquad \text{--- 6.2}$$

where B is another constant.

The slope of the supposedly space charge limited current versus voltage for the 280°C substrate film is 2.0. The values decrease to 1.1 for the 420°C film. An interpretation of this behaviour is not possible because of the lack of information concerning the depth and properties of these trapping levels.

The identification of shallow levels was attempted by the thermal glow curve technique originally described by Randall and Wilkins (1945). Films were irradiated with 3650Å radiation at - 180°C in the dewar vessel described earlier, and heated at a linear rate (20°C/minute) to about + 200°C. The linear rate was obtained by programmed switching of a motor controlled heater in the dewar. However, no response was observed. Radiation in the characteristic absorption band of the manganese ion and 3300Å gave no response. Levshin and Ryzhikov (1962) have reported a decrease in the luminescent response of phosphors due to grinding (reducing particle size). The films are composed of very small crystals and this may explain the absence of luminescence (and the negative results of the glow curve experiments).

The films also showed negligible photoconductivity making the thermal stimulated current technique described by Bube (1960) of no use.

While it seemed likely that space charge conditions existed in the films discussed above, it should be pointed out that these had never been operated at voltages (A.C. or D.C.) sufficient to excite electroluminescence. The films were operated at A.C. voltages sufficient to excite electroluminescence, for about ten minutes, and the following results taken.

A portion of the D.C. current-voltage curve is shown in Figure 6.5a (marked EL). Increasing and decreasing voltage gave the same current values. If the film was left (open circuit for several hours) the low voltage current was lower indicating a decay had occurred. Increasing voltage caused the current to increase until the original curve was followed. If the film was left for a long period, low current readings were obtained which increased to the original curve at slightly higher applied voltage. Figure 6.6 shows a typical set of results (for a film evaporated from a powder). All the current values were steady (to 5%) and the curves showed no hysteresis effects in this voltage range. The current variation in the range where electroluminescence was observed was given by,

$$I = I_o \exp(\alpha V) \qquad \text{--- 6.3}$$

The general behaviour of the films, especially at low voltage (< 1 volt) indicated that space charge was accumulated in the films. Apparently, not as much was retained in a film after it had been operating at high voltage (electrode now contained microscopic holes due to forming) than if no forming had occurred. The reason for this change is not clear.

It was found in the previous section that space charge polarization, caused by electrons accumulated at the electrodes was set up during operation of a film at high A.C. voltage. The results described above suggest that there is also an accumulation of charge in the volume of the film. This will not affect the potential distribution in the film

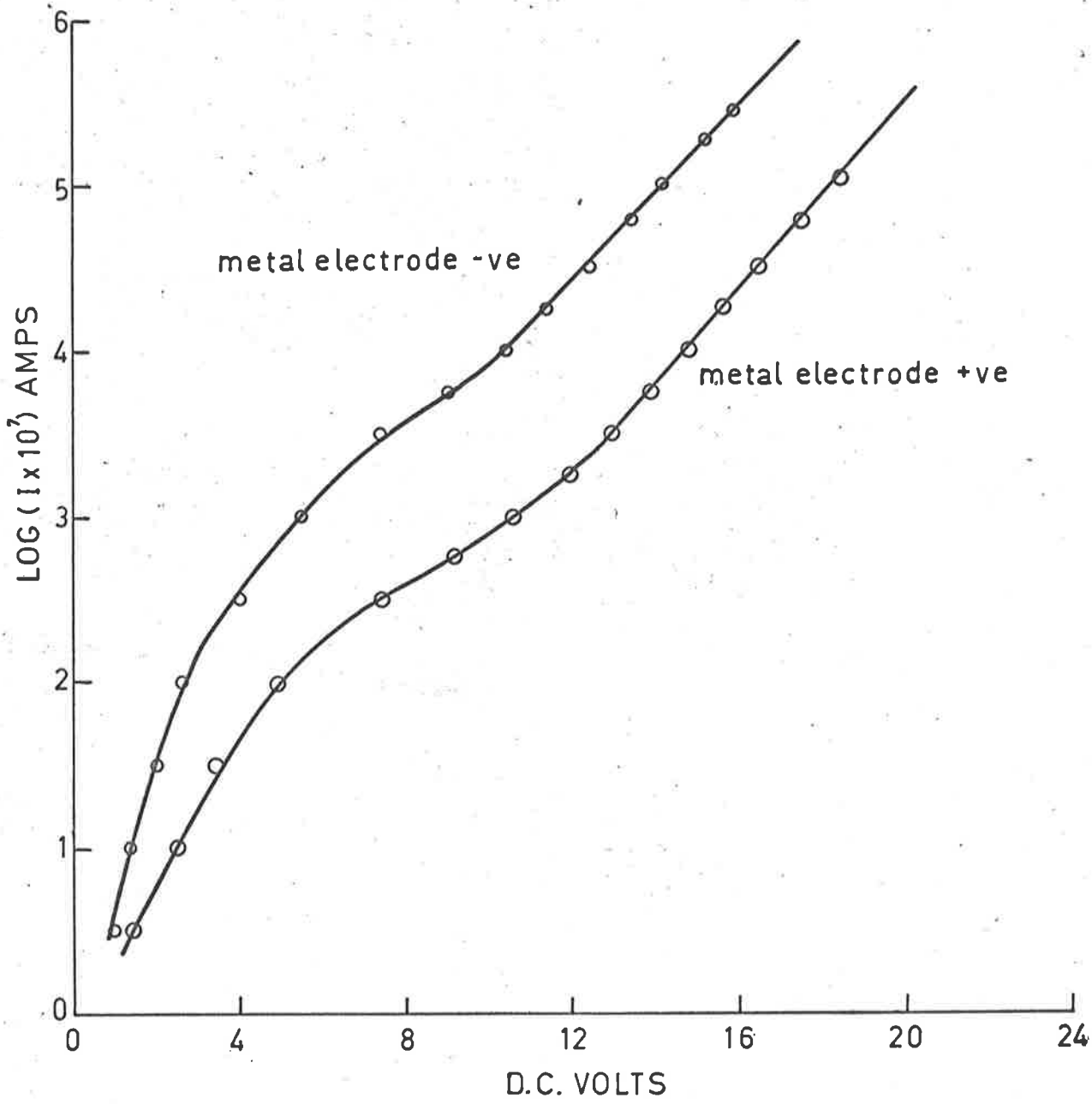


FIG. 6.6 D.C. CURRENT - VOLTAGE CURVES FOR FILM AFTER ELECTROLUMINESCENT OPERATION. EVAPORATED FROM ZnS.Mn.Zn POWDER.

to any great extent, although this potential gradient is no longer linear (Lampert 1956). This problem is discussed in the following section. If this charge is trapped uniformly in the bulk, it will diffuse out of the electrodes in a way determined by the transparency of the two electrode barriers. However, the result that the short circuit current could be observed from each electrode depending on the direction of the polarizing voltage showed that the bulk charge did not determine the direction of this short circuit current.

It is possible that the accumulation of charge in the volume of evaporated films operated with an A.C. voltage causes the initial decrease in brightness described in Chapter 6.2.

To conclude this section it should be pointed out that Rose (1955) has derived the current-voltage relation expected if the current is space charge limited and the solid contains a uniform trap distribution. This equation is

$$I = k'V \exp \alpha' V \qquad \text{--- 6.4}$$

where $k'$ and $\alpha'$ are constants.

For the case of the films used here $\alpha' V$ is large and so log I will be proportional to the voltage, V. This exponential dependence was characteristic of all films (excited by D.C. and A.C. voltages) investigated, (for example Figure 6.6). However, equation 6.3 was derived by assuming that field controlled processes, such as impact ionization were negligible. This condition is not necessarily fulfilled here, particularly because of the possibility of very high electric fields in the volume of the film.

## 6.5 Field distribution in evaporated films

The results described in this chapter have shown that the current flow in films is space charge controlled. In this case, the electric field in the film is not uniform. Rose (1955) has obtained the distribution under the assumption that the space charge is made up of a part $\rho_f$ in the conduction band and $\rho_t$ in traps, such that

$$\rho_f = A\rho_t^n$$

The field E is given by $E = \frac{n+1}{n} B\, x^{\frac{n}{n+1}}$, B a constant and x the distance from the cathode (x = 0).[1]

For n = 1 this reduced to $E \propto x^{\frac{1}{2}}$, the same result as for a trap free solid. The variation of field thus depends on the ratio of trapped to free charge, which is not readily obtainable. However, for materials with low resistance contacts, it is well known that internal field strength is appreciable (Lampert 1956). However, for an electroluminescent film with non ohmic electrodes, the finite magnitude of the internal field is not so obvious.

The determination of the fraction of the applied voltage which is dropped across the oxide layer next to the metal electrode is also difficult. It should be possible to determine this by comparing the properties of a ZnS film with an ohmic contact (or even a metallic contact with no insulator), and a ZnS film with an aluminium electrode. Because of the difficulty described in Chapter 6.1 in preparing films with metal electrodes other than aluminium, this method could not be used. It was however possible to infer the approximate

resistivity of the oxide layer by comparing the resistance of a (ZnS - aluminium) film ($R_1$) to that of a ZnS - silica-gold layer ($R_2$). The resistance of the evaporated silica layer ($R_3$) was found by depositing it separately on a conducting glass slide and evaporating a gold electrode on the surface. It was found that the value of $R_2$ was given by $R_1 + R_3$ implying that the resistance of the ZnS with an aluminium electrode was not controlled by an oxide layer. Although the conditions of such experiments were not identical, the above results were sufficiently accurate to show that there was no appreciable fraction of the applied potential across the oxide layer.

The influence of the surface barriers in determining the voltage distribution must now be considered. The tin oxide - ZnS interface will be characterized by some barrier because of the abrupt change in conductivity type. Barriers between n and $n^+$ material have been considered by Oldham and Milnes (1963). The ZnS - aluminium interface will be characterized by the usual form of semiconductor-metal barrier and will be controlled by surface states present in high concentration $10^{18-20}/cm^3$ because of the large surface area of the film. The characteristics of the emission are not changed by evaporating an aluminium electrode on the ZnS film before air is admitted to the evaporating chamber. Therefore, the surface states are not due to excessive oxidation at the surface, although it was realized that at the pressures used ($10^{-5}$torr) sufficient oxygen was present to give appreciable adsorption in the vacuum system.

Using the model of an exhaustion barrier of the

Schottky type, the width of the barrier can be calculated from the applied voltage and the ionized donor density (Henisch 1957). An average value of voltage used in the investigation was 30 volts, that is about 15 volts at each electrode if there is no voltage drop across the bulk of the film.

The results described in section 4.4 showed that, although 1% excess zinc was added to the film it was incorporated in regions of high concentration and it was supposed that this high concentration was required to compensate a high density of acceptors. Thus the donor density available to provide electrons to surface states is about $10^{19}$.

The following table shows the barrier width as a function of barrier voltage.

| Barrier voltage | Width (A) |
|---|---|
| 15 | 530 |
| 10 | 450 |
| 5 | 310 |
| 2 | 200 |

The lower voltages correspond to the case where the voltage drop over the barrier is small compared to the potential across the sulphide film.

It is clear from these figures that for films of 2000Å thickness, the barrier regions at each electrode will not interact. The presence of well defined barriers at the electrodes, as shown in Figure 6.1, therefore appeared to be

a realistic representation. However, it should be noted that even if the barrier region was wider, some accumulation could occur (Chapter 6.3).

An attempt was made to determine the potential distribution in the films by evaporation of multiple aluminium electrodes in a multilayer ZnS film. The ZnS was evaporated to form a film of thickness t. A thin aluminium electrode was then evaporated through a mask. This was continued until three aluminium probes had been formed. The film was removed and a large aluminium electrode evaporated on the surface so that the ends of the probes protruded several millimetres into the space between the tin oxide and aluminium electrode (Figure 6.7). An A.C. voltage, sufficient to excite electroluminescence was applied between the two electrodes and the voltage measured between the tin oxide and each probe with a high impedance A.C. voltmeter. Although this method is rather insensitive, it was clear that an appreciable field (not very different from the constant $\frac{V}{d}$ existed in the film, at least in regions more than several hundred angstroms from the electrodes. The experimental spread in the voltages measured from these structures, prevented an accurate determination of the shape of the potential distribution in the films.

From these considerations, although the electric field distribution is still unknown, there appears to be an appreciable electric field in the order of $10^6$ volts/cm in the bulk of ZnS films.

## 6.6 Summary

It has been shown that during operation of an

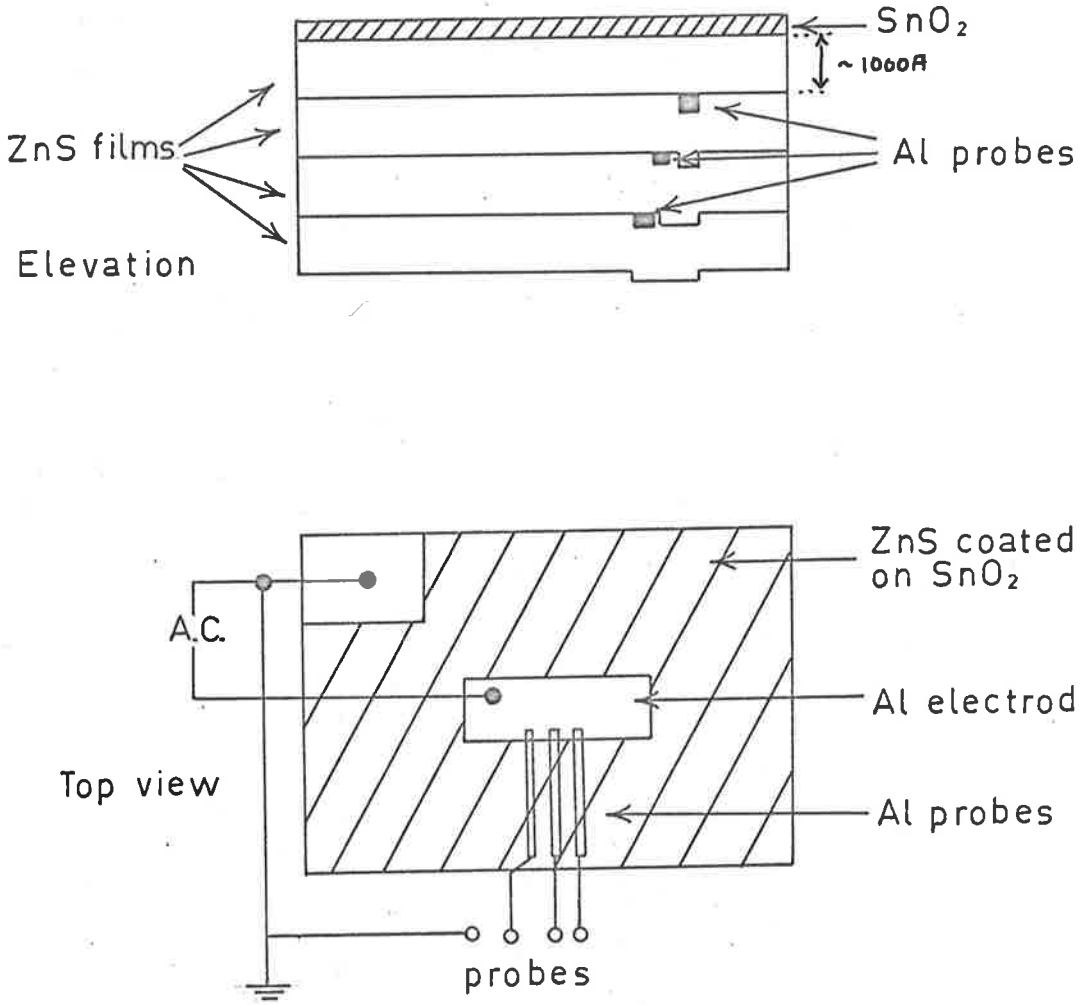


FIG 6.7 MULTIPLE FILM STRUCTURE

electroluminescent film, a number of changes occur during an initial forming period. These effects can conveniently be summarized as follows:

(a) Charge is trapped in the bulk of the film and at regions near the electrodes. These traps have very long decay times (at least minutes).

The trapping of injected electrons will be associated with a falling current, provided the transit time of the electrons is short compared to the time required for trapping. The transit time assuming a mobility of $1cm^2$/volt/sec in a field of $10^6$ volts/cm and a 1500Å film is $1.5\ 10^{-11}$ seconds which would be << than the trapping time.

(b) It was found that during A.C. and D.C. operation of films at voltages sufficient to excite light emission, the metal electrode became covered with minute holes due to localized breakdown of the film. Before the voltage is applied the film can be thought of as a large number of ZnS crystals shunted by a number of low resistance paths. These latter are destroyed, forcing the current to flow through the sulphide and therefore exciting manganese centres. This is a permanent change in the current flow through the film (a decrease) accompanied by an increase in light intensity and can explain the effects observed in ZnSe (page 118). However, it was found that after resting the film (no voltage applied) the same effect (now much smaller) could be observed.

That is the brightness showed a small increase while the current decreased. This reversible effect may have been due to the changes in the internal field distribution which

occurred as the injected electrons were trapped. This could result in a reduction of the internal field in some regions, perhaps near the cathode, so that electron injection is not so efficient. Because of this change, the initial increase in light due to the thermal forming ((a) above) will be halted before the electrode destruction is complete. If the film is rested, the trapped charge is released, so that a high field again exists when the voltage is re-applied. Thus the thermal forming continues until the internal field is again reduced by trapping. This explanation seems more convincing than the formation of an $Al_2O_3$ layer as suggested by Goldberg and Nickerson (1962). It is difficult to see how the formation of such a layer could be reversible in the sense described above.

(c) The reduction in current and brightness observed during initial operation of the film (especially for ZnS.Mn Zn) was caused by two processes. The first was a trapping of injected charge which prevented entry of electrons unless the voltage was increased to counter the effect. The second was a localized breakdown of ZnS crystallites (which were emitting light) because of excessive fields at thin spots in the film, and at other inhomogeneities.

The first effect is well known in materials which show space charge limited conduction (Smith 1955). The result of decreasing current will be a decreasing field resulting in a decreasing brightness. The second effect causes a reduction in the area of the metal electrode and a corresponding decrease in brightness. It is generally found that the decrease in brightness, in any given circumstance is always

more than expected on a simple correction of the emission for the decrease in electrode area. This shows that both mechanisms are important. Even for a film which had been stabilized by the procedure described earlier, some decrease in the current and the average brightness was always observed when a voltage was re-applied after a period of rest. This implied that the trapped electrons had been released during this period. However, the magnitude of this decrease was never as large as during the first application of a voltage. Thus this trapped charge was held very strongly.

## 7. NATURE OF EMISSION FROM ELECTROLUMINESCENT FILMS

It is of particular importance in experimental investigations of complex effects such as electroluminescence, to pay great attention to the reproducibility of results. This is not easy, as evidenced by the previously reported experimental results which are often contradictory.

It is this author's experience that reproducibility is even more difficult to obtain with evaporated films than with phosphor powders and larger single crystals. The scatter in experimental values was reduced by the technique of evaporating films from large crystals. However, it was necessary to perform a number of separate evaporations to ensure that a particular result was representative of a given condition in the film. The experimental scatter of such results for a given set of conditions in a film was 2-5%. Because of such precautions, the results described in the following chapters (as well as previously) were considered to give a true indication of the electroluminescent process in evaporated films.

### 7.1 Spectrum of the emitted radiation

#### (a) A.C. voltage excitation

The emission excited by a sinusoidal A.C. voltage consisted of two light pulses per cycle of the applied voltage. The peaks of these light pulses were approximately in phase with the voltage maxima, and for most films, the two brightness pulses were of unequal intensity.

The wavelengths of the observed radiation from various

evaporated films is given in the following table. A discussion of each is given in the text.

| Film | Emission | Film | Emission |
|---|---|---|---|
| ZnS.Zn | None | ZnSe.Zn | None |
| ZnS.Zn Mn(.01%) | 5860Å | ZnSe.Zn Mn(.01%) | 5860Å |
| | v. small 5650Å | | large 5650Å |
| ZnS.Zn Mn | 5860Å | ZnSe.Zn Mn(.1%) | 5860Å only |
| (1μthick) | broad band 5500 - 4000Å | ZnSe.Mn (1%) | 5860Å only |

For all films, the characteristic manganese emission, centred at 5860Å was observed. Films prepared from ZnSe.Mn (1%) crystals showed only this band. However, films evaporated from ZnSe.Mn (0.01) Zn (1.0%) showed a strong emission component at 5650Å in addition to that at 5860Å (Figure 7.1). If the manganese concentration was increased, the intensity of the green band decreased until at about 0.1% manganese, it was not detectable. A small component of emission at 5650Å was observed from films evaporated from ZnS.Mn (0.01%) crystals. These films were 1000-2000Å in thickness.

The observation of the same wavelength emission (5650Å) from both ZnS and ZnSe, suggested that the electronic transition responsible for this emission, occurred between a ground state and an excited state of an ion, rather than between the ground state of the ion and the conduction band of the host lattice. In this latter case a shift in the wavelength would be observed because of the different band gaps of ZnS (3.7ev) and ZnSe (2.6ev).

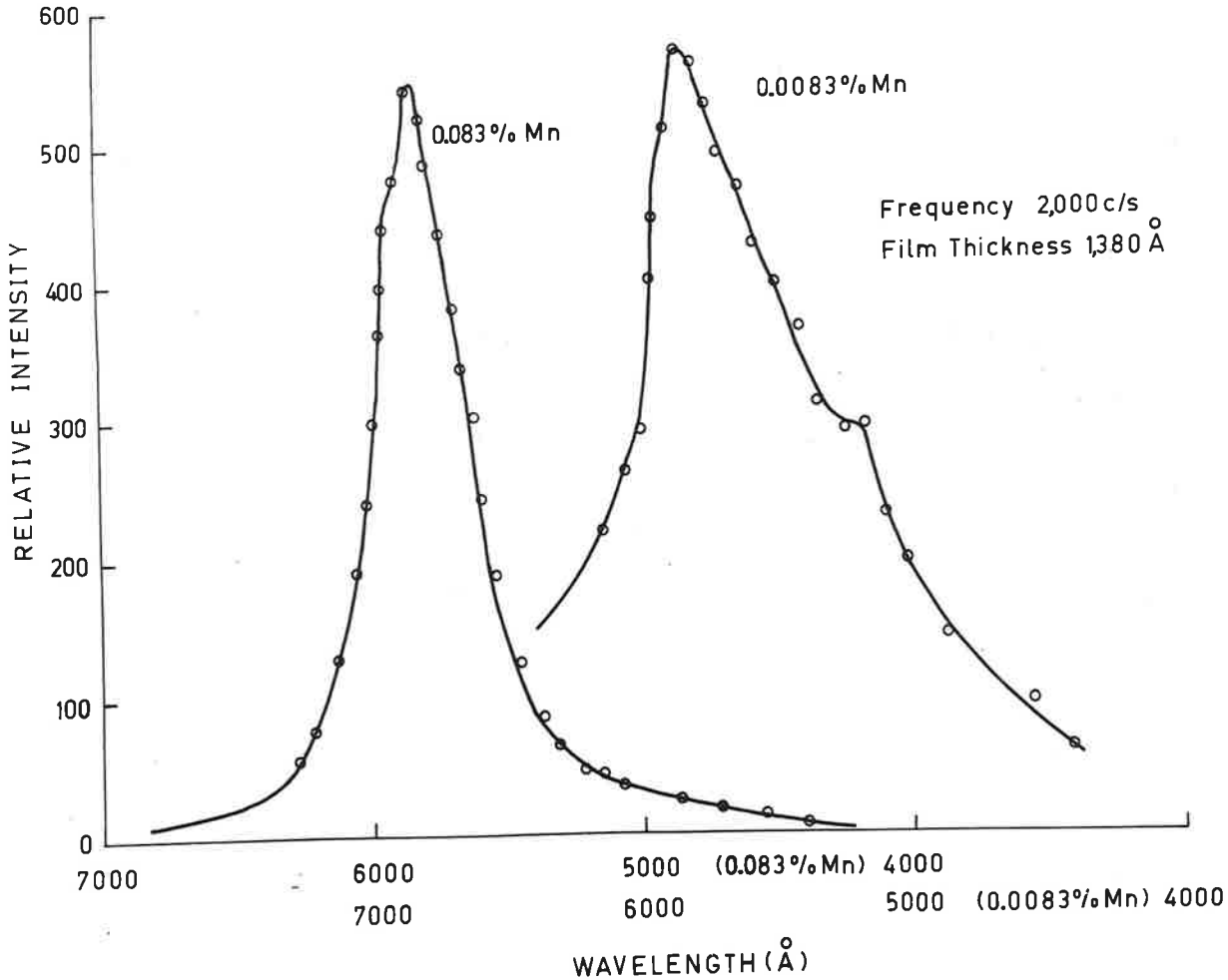


FIG.7.1 SPECTRA OF ZnSe:Mn EVAPORATED FILMS

The wavelength of the emission observed from the $Mn^{++}$ ion has been found to depend on the nearest neighbour configuration around the ion. For example, in $Zn_2SiO_4$, the manganese emission is centred at 5200Å (Curie 1960). It is therefore possible that the 5650Å emission observed here is a result of $Mn^{++}$ ions with different nearest neighbours. This explanation is not consistent with the reduction of the green emission as the manganese concentration increases. Because no green emission is observed if no excess zinc is present, this component apparently results from transitions involving some defect centre caused by the excess zinc ion. Excess zinc gives rise to two electrons localized at a sulphur vacancy. One electron is easily removed (ionization energy 0.3ev) while the second is involved in the luminescent transition giving green luminescence (wavelength not accurately known), (Kröger 1955). The evidence presented here indicates that this transition is a localized one, not involving the ionization of the electron.

There are two experimental results which require this assumption of a zinc luminescent centre to be modified. These are (a) that no electroluminescence occurs in films evaporated from ZnS (Zn) and ZnSe.Zn crystals and (b) the component of radiation at 5650Å is much stronger in ZnSe films than ZnS films.

Result (a) implies that the centre responsible for green emission must be zinc together with manganese and not zinc alone. Result (b) could imply that ZnS.Mn Zn films contained less zinc than ZnSe.Mn, Zn films (manganese concentration fixed). The addition of zinc metal to ZnS.Mn crystals

during growth did not however change the spectrum of the light emitted from the films. It therefore seems that either the energy available for excitation is greater in ZnSe films than ZnS films, or the excitation of 'yellow' manganese centres by transfer of energy from 'green' centres is more efficient in ZnS and in ZnSe. It is not possible to decide between these two mechanisms from the available evidence.

It is however certain that some energy transfer process occurs in ZnSe because of the changing spectral composition with increasing manganese concentration. Such processes are well known where two luminescent centres are present (Chapter 1.1).

A change in the spectrum of the electroluminescent emission from ZnS.Mn films was observed as the film thickness increased. Figure 7.2 shows the spectrum from a thin (1000Å) and thick (10,000Å) ZnS.Mn film. A broad band with no visible peaks was observed between 5000 and 4000Å. The intensity of this emission increased with increasing film thickness to about 5% of the manganese peak for films about one micron in thickness. The observation of this short wavelength component of the emission from thick films showed that other levels as well as those due to manganese ions were present. These levels, which are involved in luminescent transitions, must be distributed in energy to account for the broad emission band. It is difficult to see why these levels are not a part of a thin film. It must therefore be assumed that they are present, but are not excited. The presence of such levels on thin films has been confirmed by experiments with an insulating layer under the metal electrode (see chapter 8.5).

The presence of such levels, which are most probably distributed in the energy band gap and can therefore be ionized, introduces the possibility of delayed recombination. This process, as suggested by a number of authors (for example Zalm 1956) involves an ionization of luminescent centres followed by a sweeping away of electrons from the vicinity of these centres by the applied field. At the zeros of the applied voltage these electrons diffuse back to the ionized centres and a burst of light emission occurs.

This is usually observed when the luminescent centre in a phosphor is ionized (e.g. copper). For the manganese activator, the transition is localized in the manganese ion (Piper and Williams 1958) and this effect does not occur. No emission, which can be definitely attributed to this delayed recombination mechanism in ZnS.Mn films was observed. This problem is considered later (Chapter 8.3).

No radiation of energy equivalent to the band gap (3.7ev) was observed from ZnS.Mn films. Figure 7.1 shows that emission from ZnSe.Mn Zn films was observed between 4000 and 5000Å. The absorption edge in ZnSe.Mn, Zn films was not sharply defined, as shown by an absorption versus wavelength plot taken from a Unicam spectrophotometer, using a ZnSe.Mn Zn film. The 50% transmission point (defining a nominal absorption edge) was at 4500Å. At 4000Å the transmission was 40%. The 4000Å emission may therefore be the result of band to band transitions. However, the main emission bands (at 5860 and 5650Å) were considered to be of lower energy than would be expected if direct band to band transitions were important.

(b) D.C. voltage excitation

Thin films (1000Å) could be excited by a D.C. voltage, but the spectrum of the emitted radiation contained a broad range of wavelengths in addition to the radiation from the manganese ion. This was breakdown radiation and the electrode was slowly destroyed. However, for thicker films the spectrum was identical to that observed for A.C. excitation.

A variable filter was used to investigate the spectrum of the radiation excited on each polarity of a low frequency (0.1c/s) voltage. The spectral content was identical suggesting that the same centres were emitting light irrespective of the polarity of the applied voltage.

## 7.2 Absolute light intensity produced by the electroluminescent effect in ZnS

As shown in Figure 2.9, Chapter 2.5, the measured current in the anode circuit of the photomultiplier used to detect the electroluminescence, was proportional to the intensity of the illumination on the cathode surface. Therefore to describe changes in electroluminescent brightness B, it was sufficient to use the anode photocurrent, I. All graphs in this thesis labelled log B were obtained in this way. While this is sufficient for all purposes of investigation of the changes in the light emission, it is of interest to know the absolute brightness of the films which show this emission.

The transmission curve of a 6000Å interferance filter was obtained by recording the spectrum of a tungsten lamp (a) without the filter and (b) with the filter over the

entrance slit of a monochromator. A tungsten lamp, operating at a colour temperature of 2800°K was then used to illuminate this filter over the same area as usually used (calibrated by National Standards Laboratory, Sydney) for the electrode of an electroluminescent film. The filter was in the same position as that used for the electroluminescent films, directly over the photocathode of the 1P21.

From the black body radiation curves for a temperature of 2800°K, the transmission of the filter and the geometry of the system, the energy incident on the photocathode, producing an anode current I ($10^{-8}$ amps) was obtained. This anode current was used to define the threshold for light emission. The energy falling on the photocathode was 1.5 $10^{-15}$ watts. To simplify the conversion of this energy to luminous flux, it was assumed that 1 watt of radiation from the lamp was equivalent to 650 lumens through the range 5000-6000Å. This meant that the luminous flux falling on the detector was 1.5 $10^{-15}$ x 650 lumens, giving rise to a brightness of 1.0 $10^{-11}$ lamberts. The accuracy of this figure was about 20%. The brightness of the electroluminescent films used here, was therefore about the same as for films prepared by other techniques, for example by Harper (1962).

## 7.3 Properties of electroluminescent ZnS films prepared by different techniques

### 7.3.1 Voltage dependence of average brightness

During the development of a preparational technique to obtain reproducible evaporated films, a number of results concerned mainly with the variation of brightness with

voltage were recorded.

(a) Films evaporated from ZnS and metallic manganese

Films prepared by evaporation of ZnS and metallic manganese in the same boat were particularly susceptible to destruction of the electrode by arcing (see Chapter 6.2). These films were usually < 1000Å in thickness and at the voltages used to excite light emission (20-40 volts) the electric field in the films was $2 - 4.10^6$ volts/cm. This is close to the range of field strength where dielectric breakdown is observed (Whitehead 1956). The large excess of manganese present during these preparations may have resulted in deposition of sufficient manganese in the films to bring about excessive localized breakdown.

It was found that the average brightness (B) was related to the applied voltage V by an equation of the form

$$B = B_0 \exp\left(-\frac{b}{\frac{1}{V^2}}\right) \qquad \text{--- 7.1}$$

where $B_o$, b are constants.

Figure 7.3 (curves a and b) show the fit of the experimental points to this equation. It was of interest to compare the measurements from a film with an undamaged electrode to those taken after some electrode deterioration had occurred. Although the voltage at which light was first detected was greater for the film with the damaged electrode, equation 7.1 still described the results.

At least the shape of the brightness-voltage curve was not altered by this localized breakdown effect. This suggested that even although films were given a stabilization

process (causing electrode damage) as described in Chapter 6.2, the equation describing the variation of the average brightness was unaltered.

The slope of the voltage-brightness plot was found to be greater for the inferior electrode. It was thought that this change of slope was caused by the increased field strength used to obtain experimental values from the film with the damaged electrode. This higher field may cause excitation of previously inactive crystallites at a change in the mechanism of light production. Some change in the emission was also suggested by some results which showed two linear regions with a well defined discontinuity (Figure 7.4). The graphs have been displaced along the voltage axis to show the discontinuity clearly. Films showing this effect were not intentionally different from any other films, and the change in slope was independent of whether the brightness values were taken during the voltage increase or when the voltage decreased.

The discontinuity occurred at 33 volts (50c/s) and 35 volts (500c/s). This difference in voltage was quantitatively explained by the decrease in film impedance with frequency. At constant external voltage, the change was sufficient to modify the ratio of the voltage drop over the ZnS film to the voltage drop over the tin oxide electrode. Therefore, an increase of external voltage was required to maintain a constant voltage over the ZnS film (see discussion later in this section, page 155.

(b) Films evaporated from activated powders

Films evaporated from ZnS.Mn powders (with excess

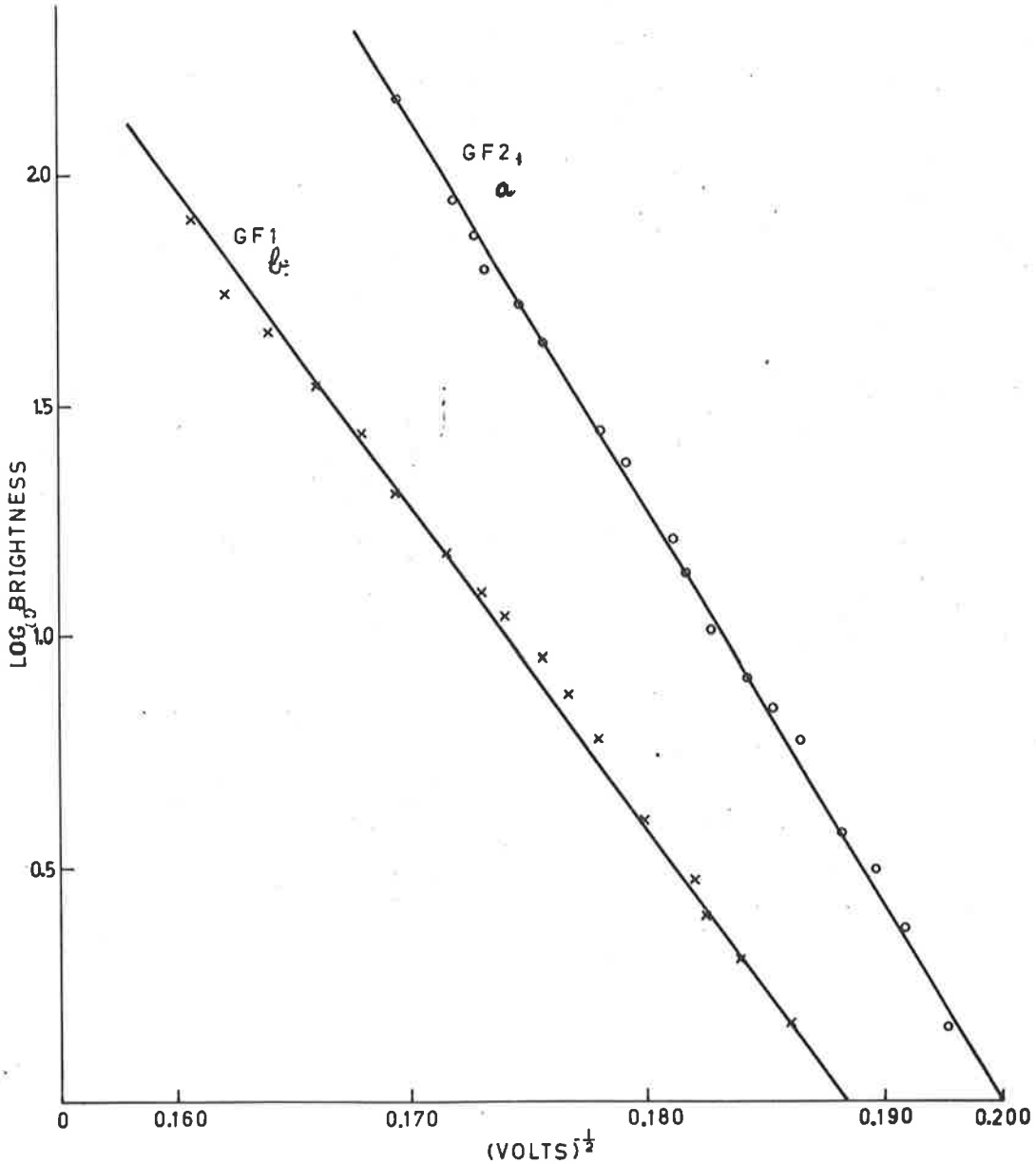


FIG. 7.3 BRIGHTNESS VARIATION WITH APPLIED VOLTAGE FOR A ZnS.Mn FILM.

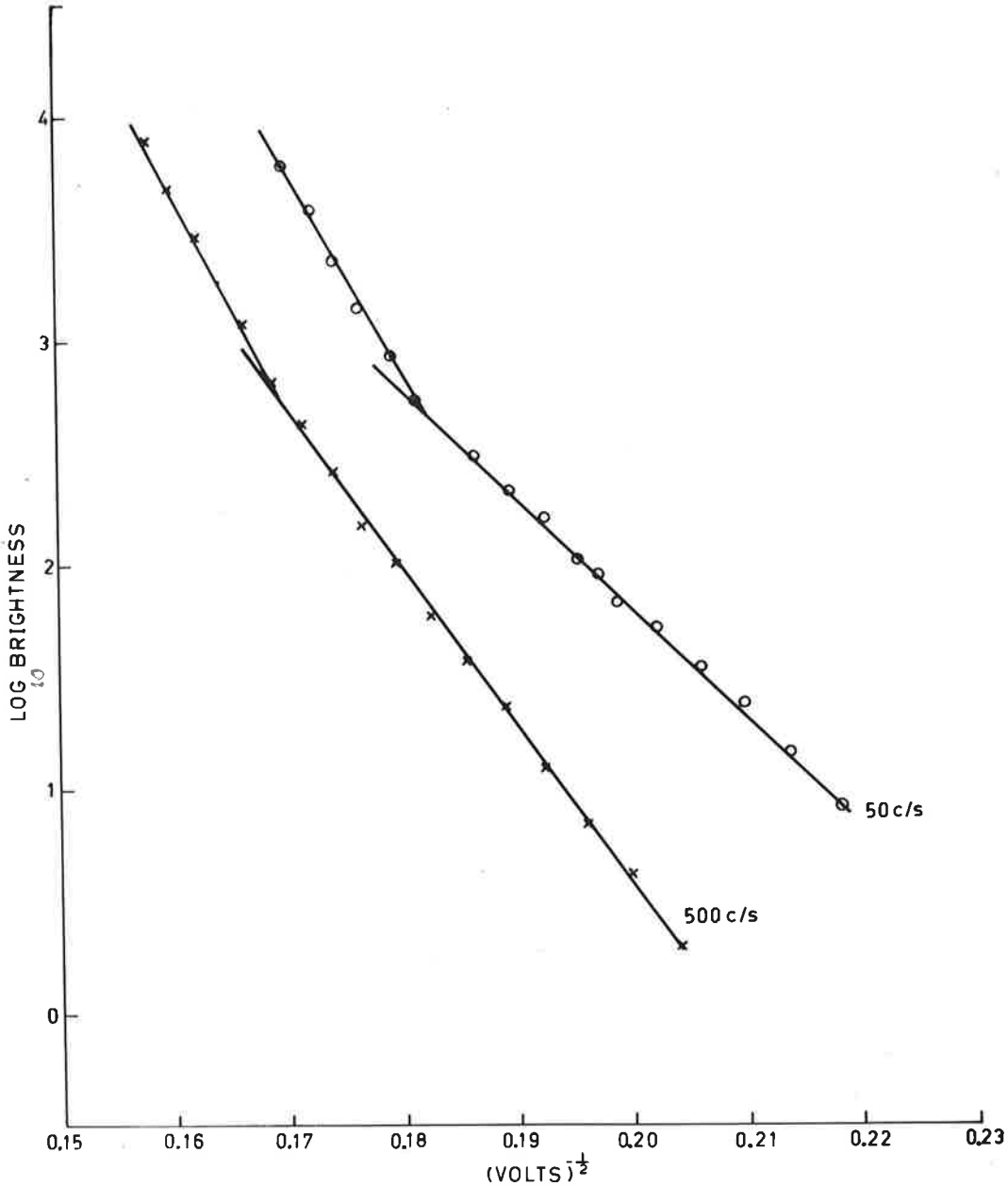


FIG. 7.4 BRIGHTNESS VARIATION WITH APPLIED VOLTAGE FOR A ZnS.Mn FILM.

zinc) showed also that the variation of brightness was given by equation 7.1. For thicker films (impossible to obtain by the above method) equation 7.1 did not describe the brightness variation correctly. An equation of the following form appeared to be adequate,

$$B = B_o \left(\frac{V}{V_o}\right)^n \qquad \text{--- 7.2}$$

where n is a constant.

For a number of films, the slope of the log B versus log V curves was between 6.5 and 7. Equation 7.2 is the same variation as observed for films in this thickness range (about 1 micron) by Halsted and Koller (1954).

The behaviour of films of intermediate thickness will be described separately (Chapter 7.4.1).

No discontinuities such as reported above were ever observed in the experimental results taken from films evaporated from electroluminescent powders.

For comparison with these films, several measurements were made of the brightness variation of the original ZnS.Mn powder. A small amount of powder was mixed with polyvinyl acetate (P.V.A.), and the mixture was sprayed (or painted) onto a conducting glass slide. An aluminium electrode was evaporated onto the top of the composite film after it had dried. The thickness was about $10^{-3}$cms and the particle size about $10^{-3}$cms (Chapter 5.1 ). No precautions were taken to isolate the phosphor grains from the electrodes. In fact they would have almost certainly settled on the conducting glass during the drying process.

The variation of brightness was also described (over 6 orders of magnitude) by equation 7.1. The slope was frequency dependent, increasing with frequency. This contrasted with the increase of brightness with voltage for films evaporated from this powder, which was independent of frequency between 50 and 5000c/s.

Since powders prepared by the method described earlier (Chapter 4.2b) were luminescent when irradiated with 3650Å light, it was possible to compare the electroluminescent and photoluminescent spectra. The spectra showed the same peak at 5860Å, but the electroluminescent spectrum was broadened with respect to the photoluminescent spectrum. Such a comparison of spectra for films was not possible because no photoluminescence was observed.

It was found that many curves of brightness against voltage (and some current-voltage curves) showed a periodic deviation of the experimental points about the best straight line which could be drawn through the points (Figure 7.3 curve GF1). These deviations were too regular and too large in magnitude to be due to experimental error. This effect has been observed before by Thornton (1961) and Vereschshagen (1962). The latter authors have attributed these deviations to the different voltage thresholds required to excite emission in different regions of large crystals. An obvious smoothing out would occur for a large number of crystallites, as for example in a film. However, it is possible to envisage a situation in which groups of the film crystallites have the same threshold voltage (e.g. for impact excitation of manganese centres). The periodic observations would then be

due to the different threshold voltage for similar groups of crystallites, perhaps with the same orientation. It is well known that electroluminescence is anisotropic at least in large crystals, (Short et al 1956).

(c) Films prepared by diffusion of manganese

Only a small number of films were prepared by diffusion. The variation of brightness with applied voltage for films of 1$\mu$ thickness showed that the brightness B was given by equation 7.2.

This variation does not agree with others obtained from films prepared by this method which showed log B approximately proportional to the applied voltage (Vlasenko and Popkov 1960). However, the films prepared by these authors were apparently sufficiently different from those used here, so that manganese luminescent emission could be observed by irradiation with 3650Å radiation. No response was observed for evaporated films prepared in this laboratory. It is therefore not surprising that the films show different electroluminescent behaviour.

There is also some doubt concerning the method used by Vlasenko and Popkov. They do not make it clear whether the pure ZnS and metallic manganese were evaporated simultaneously to give a homogeneous film or consecutively to form a ZnS film and a manganese film. It appeared from the original translation that the latter method was used, although other reviewers suggest the former.

(d) Films prepared from large crystals of ZnS.Mn

The crystals of ZnS.Mn used in the evaporation of ZnS.Mn

ZnS.Mn films showed uniform electroluminescence when excited by an alternating voltage. The electrodes on the crystal were of silver paint, and no localization of emission occurred near the electrode contact. For evaporated electrodes of other metals, no localization of the emission was observed. Similar results were observed from vapour grown crystals. (These were kindly supplied during the initial stages of this work by Dr. Indra Dev of the University of Hull, England).

The threshold for emission (5860Å radiation) was 2200 volts across a crystal 7mm in length i.e. a field strength of $3.10^3$ volts/cm. This is clearly much lower than the fields used to excite electroluminescent films. A further study of the emission from these crystals was not carried out, because a comparison of this with the light emission from films would be clearly of little value.

A more extensive study of the properties of films evaporated from crystals was made because of the improved reproducibility obtained with this preparational technique. In general these results do not disagree with those described in the chapter (7.4), following a short discussion of the frequency dependence of the emission.

### 7.3.2 Frequency dependence of brightness

At constant applied voltage, the average brightness was a function of the frequency of this voltage. Increasing frequency from 50c/s caused a monotonic decrease in the average brightness. This decrease continued up to the highest frequency considered (10,000c/s). This is shown in Figure 7.5a for a film evaporated from an activated powder.

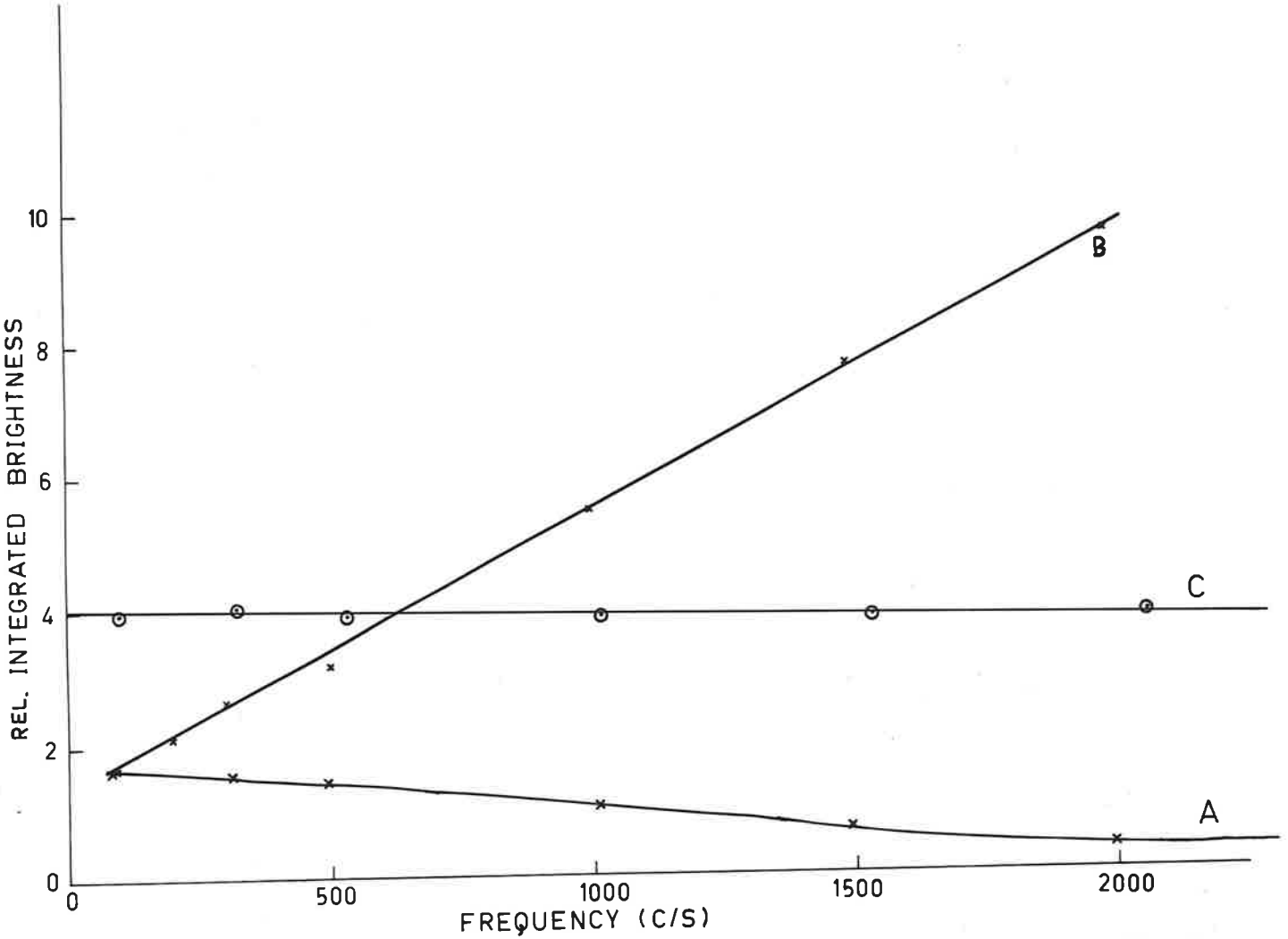


FIG. 7.5 INTEGRATED LIGHT EMISSION AS A FUNCTION OF THE FREQUENCY OF THE EXCITING A.C. VOLTAGE FOR A ZnS.Mn FILM OF THICKNESS 2,900 Å, (A & B) AND CRYSTAL FILM (C.)

Halsted and Koller (1954) have pointed out that, for thin films, the resistance of the transparent electrode may be significant. This was found to be of particular importance in determining the brightness as a function of frequency for the films used here. As the frequency increased, the film impedance decreased, while the resistance of the transparent electrode (300 ohms) was constant. This decreased the ratio of the voltage drop across the ZnS film to the voltage drop across the tin oxide electrode, so that a constant external voltage resulted in a slowly decreasing voltage drop across the ZnS film as the frequency increased.

The impedance of the films was calculated from measured values of resistance and from the capacitance obtained from the film thickness by use of the equation $C = \frac{\xi . \xi_o A}{d}$, where $\xi$ is the dielectric constant (taken as 8.0), A is the metal electrode area and d the film thickness. This value of the dielectric constant was approximately equal to the value (8.0 to 8.5) obtained from measured values of the capacity using A.C. bridge methods for a number of films. From the impedance variation with frequency, the (increasing) external voltage to maintain a constant voltage across the ZnS film was found. Although the difference in external voltage was only a few volts, this was sufficient to change the form of brightness-frequency dependence because of the strong dependence of the brightness on voltage.

A typical set of voltages is given below for a 2900Å film evaporated from a powder.

| Frequency (cycles/sec) | External voltage to give constant voltage over ZnS film |
|---|---|
| 90 | 22.4 volts |
| 200 | 22.7 |
| 300 | 22.8 |
| 500 | 23.1 |
| 1000 | 23.6 |
| 2000 | 25.6 |

Application of this procedure gave a linear increase of brightness with frequency (Figure 7.5, curve b). Above 2000c/s, the brightness increased more slowly with frequency.

The relative intensities of the two brightness pulses per cycle of the applied voltage was found to depend strongly on the frequency of excitation for films evaporated from activated powders. In general, films less than about 2500Å thick showed unequal pulses, the maximum occurring for the metal electrode positive at low frequencies (50c/s). For thicker films the maximum emission was observed for the metal electrode negative at 50c/s. As the frequency was increased, keeping the voltage across the ZnS constant (by the above method), the intensity of the smaller peak increased while that of the larger increased much more slowly. This was observed irrespective of the polarity during which the smaller brightness pulse occurred. At about 2000c/s (for the film tabulated above) the peaks were of equal intensity. Above this frequency, the intensity of the pulses increased slowly, the main effect in this range being a broadening of the light

pulses.

The resistance of films evaporated from crystals was sufficiently high so that no change in the external applied voltage was required to maintain a constant voltage over the ZnS layer. However, the brightness showed only a very small decrease (about 2%) in the average brightness as the frequency increased to 5000c/s (Figure 7.4, curve c). In this frequency range, the ratio of the intensity of the brightness pulses was generally constant.

## 7.4 Characteristics of average brightness of films evaporated from ZnS.Mn crystals

### 7.4.1 Voltage dependence

The average brightness B of electroluminescent films evaporated from crystals was related to the applied sinusoidal voltage V by equations of the form:

For thin films $$B = B_o \exp - \frac{b}{\frac{1}{V^2}} \qquad \text{--- 7.1a}$$

For thick films $$B = B_o \left(\frac{V}{V_o}\right)^n \qquad \text{--- 7.2a}$$

where $B_o$, b, $V_o$ and n are independent of voltage but may be functions of temperature.

Similar behaviour has been observed for films evaporated by other techniques (Chapter 7.3) Figure 7.6 shows how the brightness curves are modified by increasing film thickness. The data plotted in Figure 7.6 was taken from films evaporated from activated powders. In all other respects except thickness, viz. evaporation rate, substrate

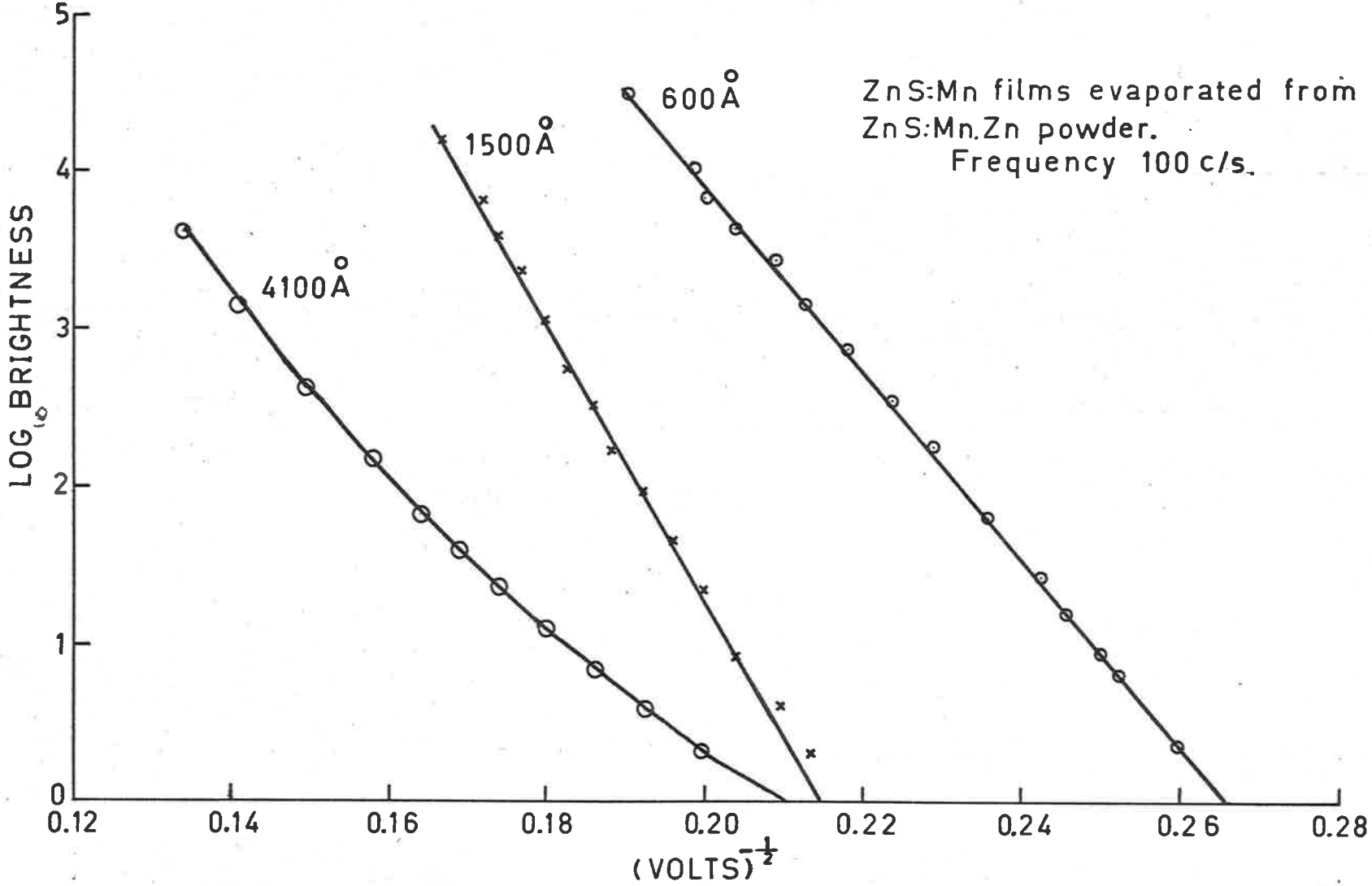


FIG. 7.6 BRIGHTNESS AS A FUNCTION OF VOLTAGE FOR VARIOUS THICKNESS FILMS

temperature and pressure during evaporation, the films were identical. As the thickness increased (e.g. 1500Å), the experimental brightness values at low voltages appeared to deviate from the linear plot of log B against $V^{-\frac{1}{2}}$ which described the results from thinner films. For films evaporated from crystals this deviation did not occur until the thickness was about 2000Å. It was clear that the results from thick films could not be described by two linear regions on a log B - $V^{-\frac{1}{2}}$ plot as observed for other films (Chapter 7.3.1).

It has been pointed out by Weizburg (1961) that many curves relating the average brightness to the applied voltage may equally well be described by two or more different equations. Figure 7.7a and 7.7b show a typical set of experimental results plotted in a number of different ways. It is clear that linearity from thin films is only obtained by plotting log B against $V^{-\frac{1}{2}}$, while for thick films only, log B against log V gives a straight line. The equations investigated were

$$\text{(a)} \quad B = B_o \exp\left(-\frac{b}{V^{\frac{1}{2}}}\right)$$

$$\text{(b)} \quad B = B_o \exp\left(V^n\right) \qquad n = \frac{1}{2}, 1$$

$$\text{(c)} \quad B = B_o V^n \exp\left(-\frac{b}{V^m}\right) \qquad n = 0\,\frac{1}{2}\,1\,2\,3 \qquad m = \frac{1}{2}, 1$$

$$\text{(d)} \quad B = B_o \exp\left(\frac{V}{V^1}\right) - 1 \qquad \text{--- 7.3}$$

While no linearity was ever observed using equation 7.1 a to c, this was not always the case for equation 7.3d. Figure 7.8 and 7.9 show the same experimental results plotted in

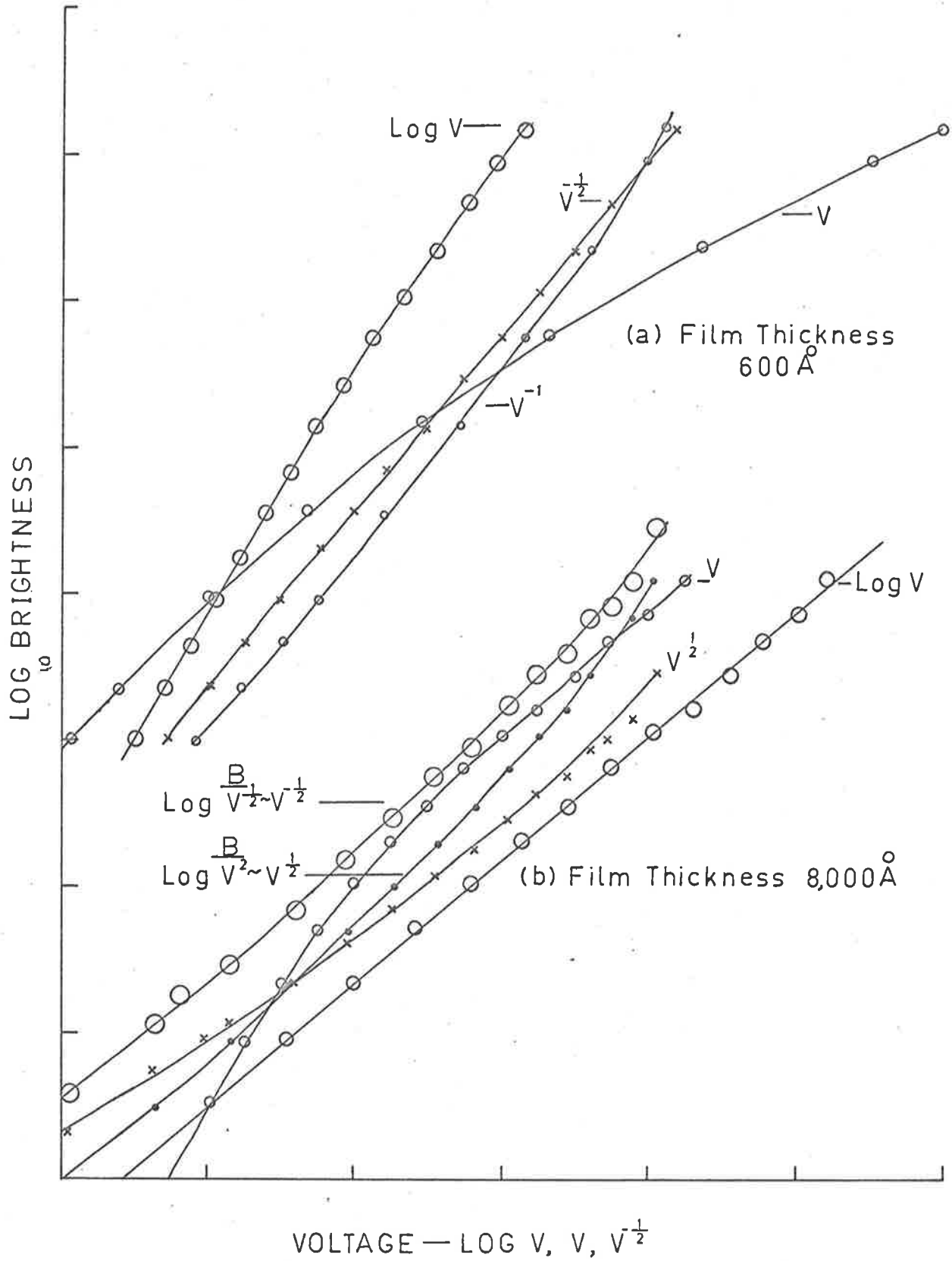


FIG. 7.7 VOLTAGE DEPENDENCE OF BRIGHTNESS FOR THIN (a), AND THICK (b), ZnS:Mn.Zn FILMS.

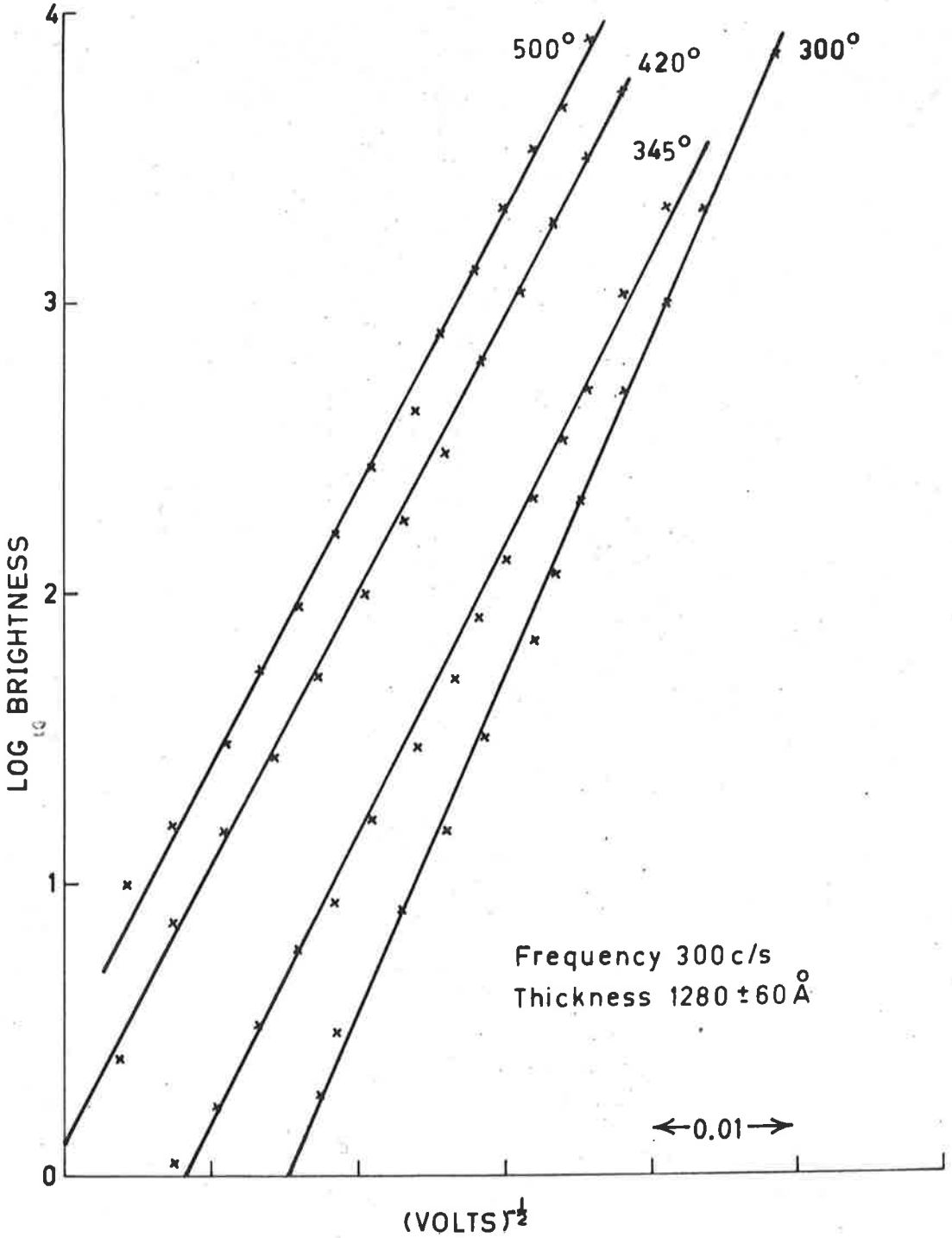


FIG. 7.8 LOGARITHM OF INTEGRATED BRIGHTNESS PLOTTED AGAINST (VOLTS)$^{\frac{1}{2}}$. SUBSTRATE TEMPERATURE AS PARAMETER.

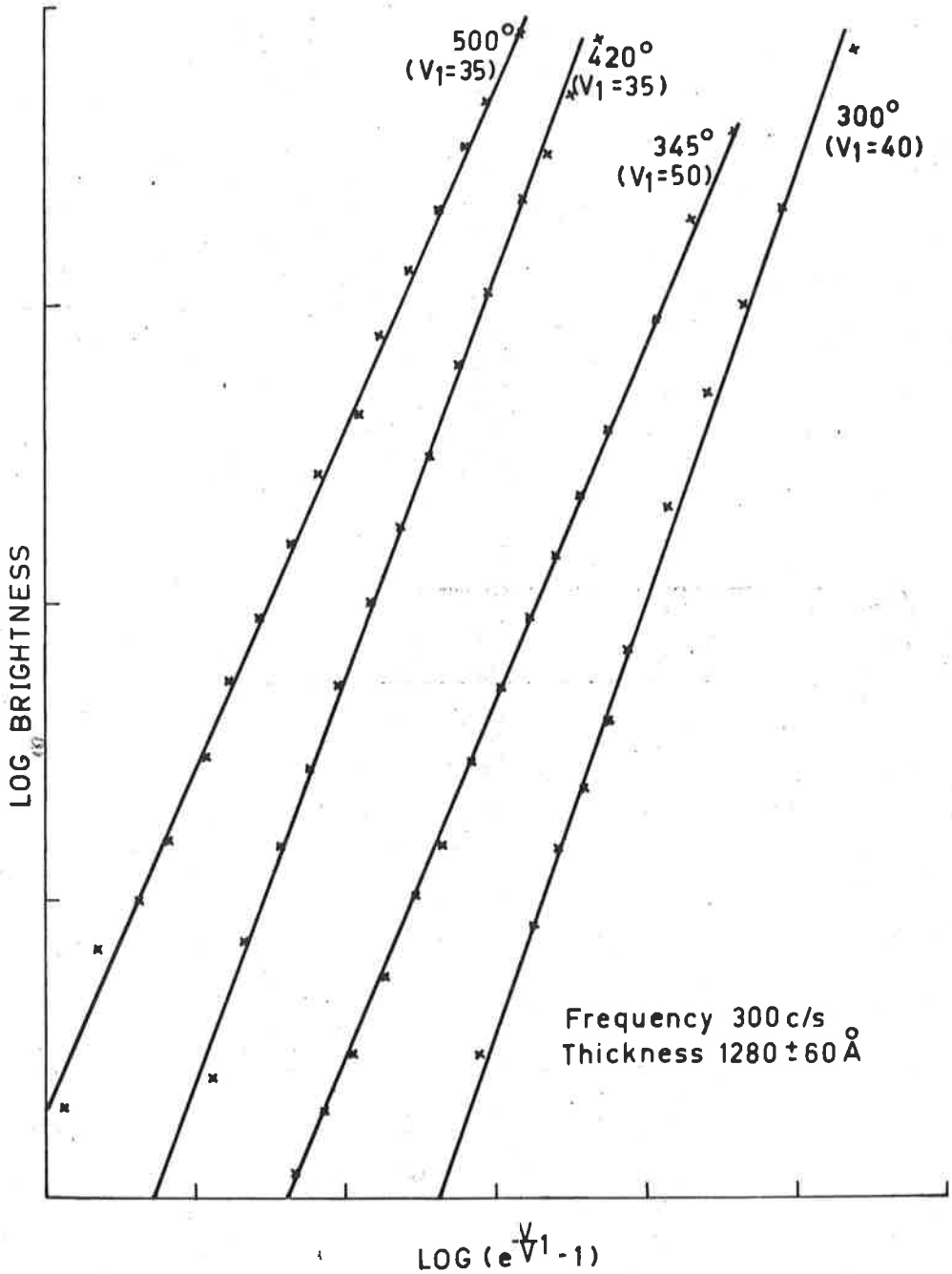


FIG. 7.9 LOGARITHM OF INTEGRATED BRIGHTNESS PLOTTED AGAINST LOG ($e^{V_1}$ - 1) FOR VARIOUS SUBSTRATE TEMPERATURES. V IS THE APPLIED A.C. VOLTAGE AND $V^1$ IS A CONSTANT.

two ways, so that linearity indicates that either 7.3a or 7.3d describes the experimental points. The value of $V^1$ (equation 7.3d) was chosen to obtain the best linearity. These values are shown on the curves but the same agreement was obtained with a variation of ± 2 volts on the values shown. For the given values of V , the ratio $\frac{V}{V'} \simeq 1$ so that equation 7.3d will give a significant difference from a simple exponential viz.

$$B = B_o \exp(\frac{V}{V'}) \qquad \text{--- 7.4}$$

This is not always the case as evidenced by the results of Korson and Kostylev (1963). They suggested that for D.C. excitation where the brightness was given by equation 7.3d, V was 13.5 volts. The applied voltage used by these authors was 170-300. Thus $\frac{V}{V'}$ is large so $\exp(\frac{V}{V'}) \gg 1$ and equation 7.3d reduces to the simple exponential, equation 7.4.

A number of experimental results were replotted according to equation 7.3d and many showed a linear relation. However, while an exception to equation 7.3a was never observed on the course of this work (for thickness less than 2000Å), several sets of experimental results could not be well described by equation 7.3d.

For example, the low frequency data from a given film agreed with 7.3d while the higher frequency values were in poor agreement with this equation. Other films showed good agreement at high frequency and poor agreement at low frequency. For thicker films, agreement with 7.3d was generally not so good as for thinner films.

Because of these exceptions, the voltage dependence of the average brightness for sinusoidal voltage excitation was more correctly given by equations 7.1 and 7.2. The importance of obtaining a large amount of experimental data from many films before deciding on the final result is clear.

The results described here do not agree with the conclusions reached by Lehmann (1960), who found that if a phosphor powder contained crystallites of one size only, the average brightness was given by equation 7.3c with $m = 1$ and $n = 0$. If the powders contained a range of crystallite sizes equation 7.3a was observed. The films used here contained crystallites of the same size (variation approximately two times) but no results were obtained which suggested 7.3a was not valid. A possible explanation of this behaviour may be found in the different size of the phosphor crystallites used here (several hundred angstroms) compared to those used by Lehmann (several microns).

The observation that two different equations are required to describe the average brightness as a function of voltage over a range of film thickness implied an appreciable change in the light emission process. It was difficult to envisage any great change in the films if only the thickness increased, since all other conditions were unchanged.

It has been reported in Chapter 7.1 that the spectrum of the emission was modified by increasing the thickness. This suggested that there may be an additional component of the emission, possibly produced by a different mechanism. If this is the case, the voltage dependence of the average brightness will be a function of two different voltage

dependent processes and appreciable changes in the functional form of the brightness dependence will occur. Figure 7.10 shows the variation of average brightness with voltage at two wavelengths viz. 5850 and 5000Å. It is clear that the yellow manganese emission (5860Å) is related to the voltage by

$$B = B_o \exp(-\frac{b}{V}) \qquad \text{--- 7.5a}$$

The 5000Å component of the emission is related to the applied voltage by an equation of the form

$$B = B_o \exp(-\frac{b'}{\frac{1}{V^2}}) \qquad \text{--- 7.5b}$$

The value of b' in this equation is much less than the values of b' obtained from thinner films.

Thus the effect of increasing film thickness is to add a component of the light whose intensity is related to the applied voltage by equation 7.5a, and also to reduce the rate of increase of the brightness component given by equations 7.1 and 7.5b.

In conclusion it should be noted that the peak brightness varied in the same way as the average brightness for films evaporated from crystals. Different behaviour was observed from films evaporated from ZnS.Mn powders and this will be discussed in Chapter 8.1.

### 7.4.2 Current dependence and efficiency of light emission

Figure 7.11 shows values of resistance and capacitance through the voltage cycle obtained by balancing an A.C. bridge at numerous points as described in Chapter 2.8. It is clear that current increases at the same position in the

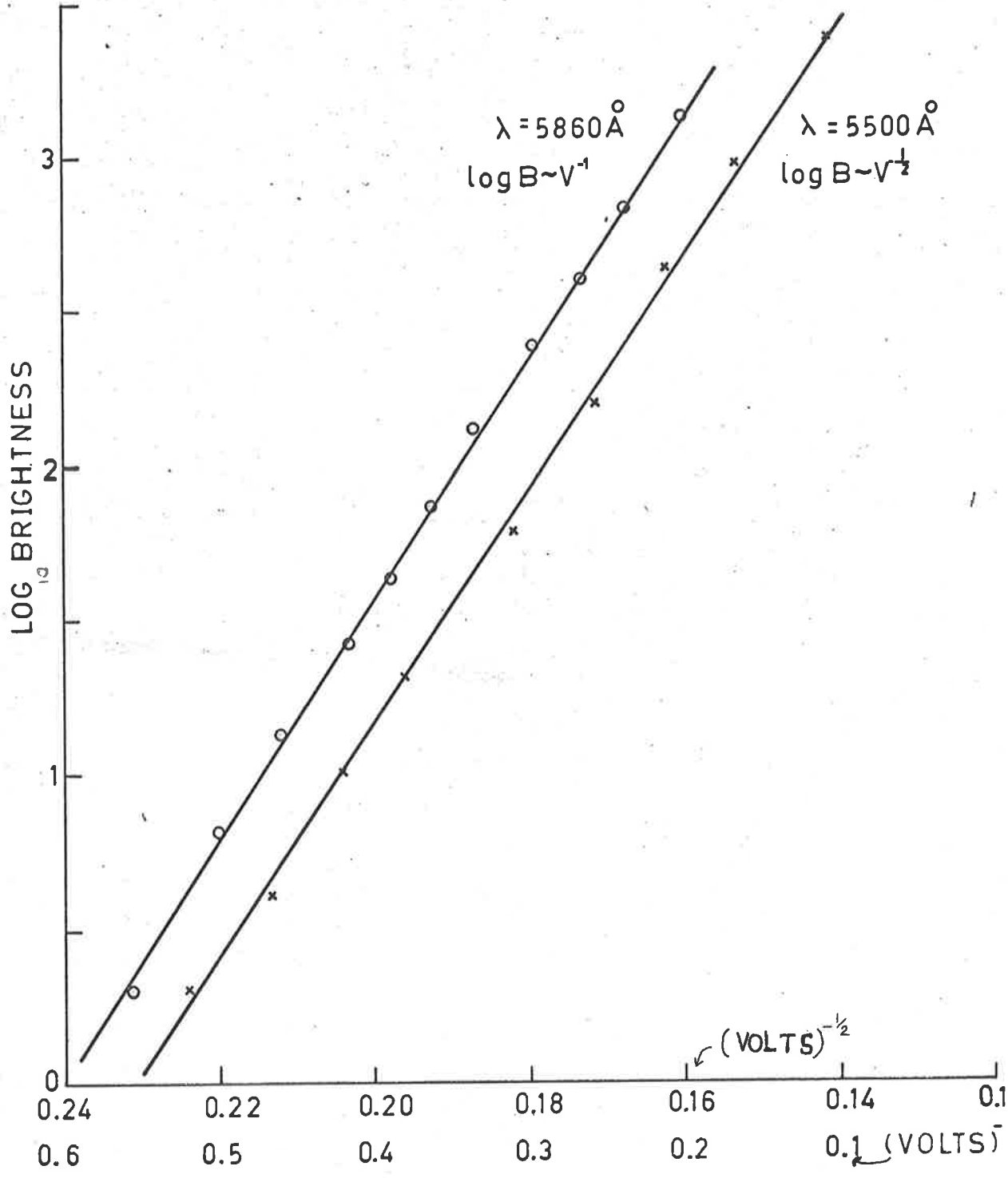


FIG. 7.10 BRIGHTNESS AS A FUNCTION OF VOLTAGE AT $\lambda = 5860\text{Å}$ AND $\lambda = 5500\text{Å}$.

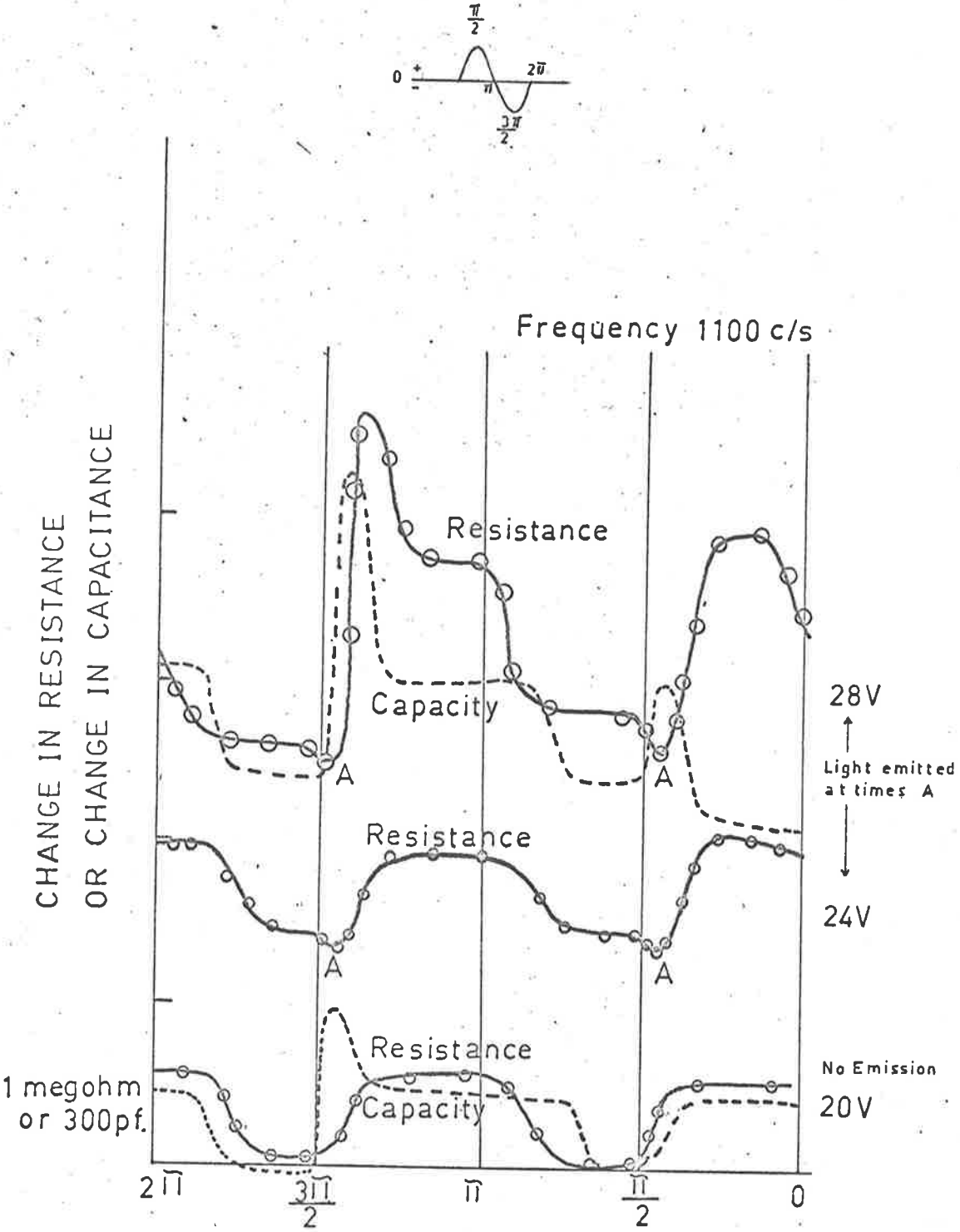


FIG. 7.11 RESISTANCE (SOLID LINES) AND CAPACITY (DASHED LINES) OBTAINED BY BALANCING AN AN A.C. BRIDGE AT THE POINTS INDICATED. THE VOLTAGE INCREASES IN POSITIVE DIRECTION FROM LEFT HAND EDGE OF THE DIAGRAM.

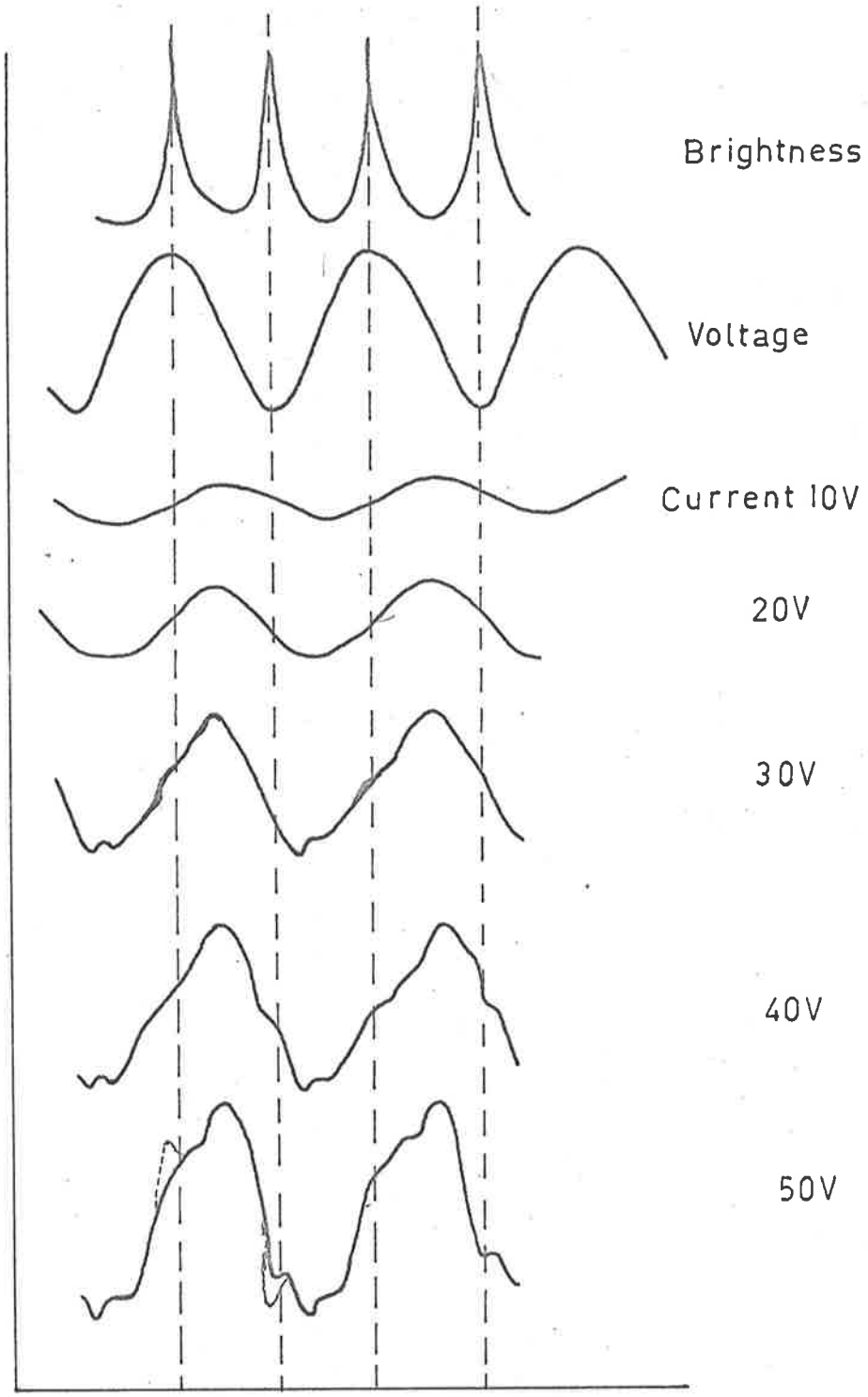


FIG. 7.12 CURRENT WAVE FORM FROM AN ELECTRO-LUMINESCENT ZnS.Mn FILM AT 500 c/s. LIGHT EMISSION DETECTABLE AT 25 VOLTS.

cycle as the brightness pulse begins. For a number of films the ratio of the intensity of these current pulses was the same as the ratio of the intensities of the brightness pulses. The accuracy involved in taking these measurements was not sufficient to obtain the amount of charge flowing through the films during these times.

Figure 7.12 shows a number of oscilloscope traces of the current waveform. A voltage proportional to the current waveform was obtained from a 10 ohm resistor in series with the electroluminescent film. Distortion occurred in the waveform predominately in positions corresponding to the two brightness peaks. If the voltage was increased so that the film was operating in the breakdown region (a noticeable fall in the intensity of the emission, these two pulses were more clearly defined, as shown by the dotted lines in the lower diagram of Figure 7.12.

The presence of distortion of the current waveform at high fields has been reported for a ZnS.Mn film by Vlasenko and Popkov (1960) and for a powder phosphor by Georgobiani et al (1963). However, no correlation between distortion and the appearance of the brightness pulses was reported.

For the films investigated here, it seemed very likely that the light pulse was caused by a pulse of electrons through the film. The presence of these pulses was confirmed by an analysis of the current waveform with a Marconi wave analyser which showed the presence of a strong, exponentially increasing 3rd harmonic component in the current.

This apparent correlation between brightness and current was also found in a number of other experimental

results. Figure 7.13 shows two examples of this. The variation of threshold voltage (i.e. the voltage at which light is just detectable) and the current at this voltage is shown for films of different thickness (7.13a and for different zinc amounts added to ZnS.Mn crystals. It is immediately clear that if a high threshold voltage is required the current is small.

The films showing the strongest emission (i.e. showing the lowest threshold voltage) were those passing large currents. Figure 7.13 suggests that the product of (V x I) may be constant i.e. the brightness proportional to the power. This was not observed.

However, it may be concluded from the trends shown in Figure 7.13, that there are two factors which affect the brightness. The observed brightness appears to be given by the product of two terms, one a function of voltage and the other a function of current. It is then clear that to maintain a given average brightness a higher voltage requires a smaller current and vice versa. If the voltage dependent term governs the rate of energy gain of the electrons, it is obvious that there must be a critical voltage below which the energy gained is insufficient to excite electroluminescence.

Figure 7.14 shows the variation of the resistive component of the A.C. current with (sinusoidal) voltage. The current was measured on the bridge described earlier (Chapter 2.8). At low voltages a rapid increase of current was observed which appeared to saturate at higher voltage. However, at the light emission threshold (12 volts in Figure

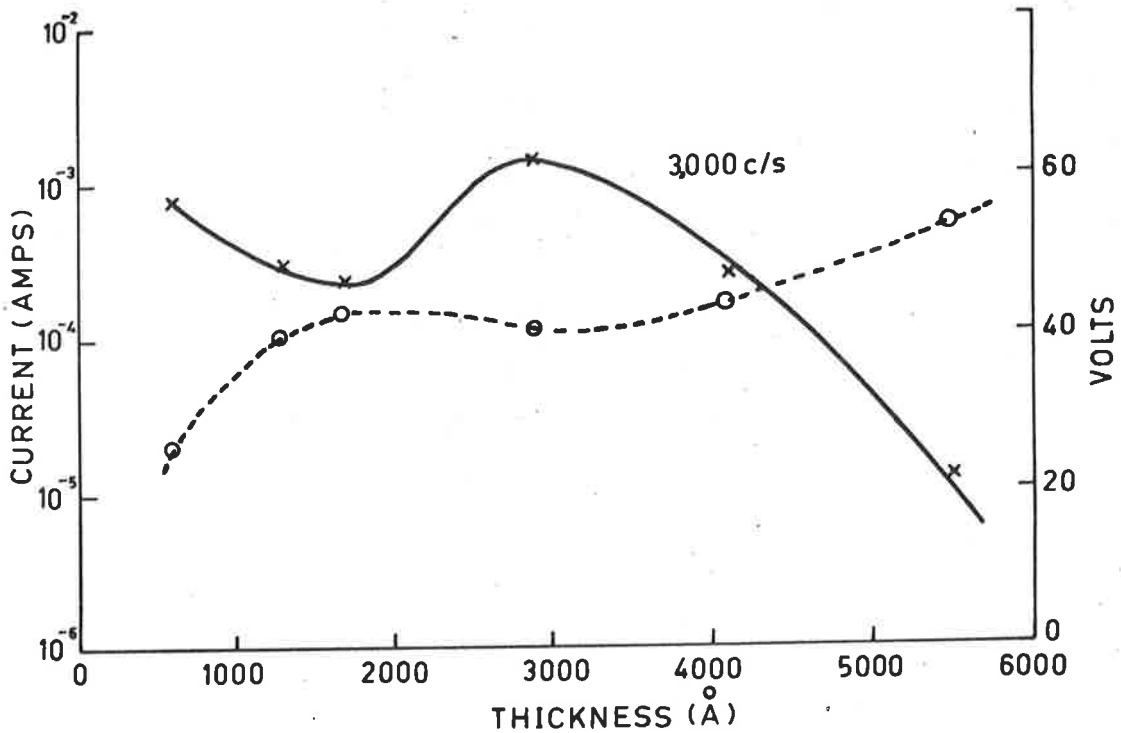


THRESHOLD CURRENT (FULL LINE) AND VOLTAGE (DASHED) AS A FUNCTION OF FILM THICKNESS.

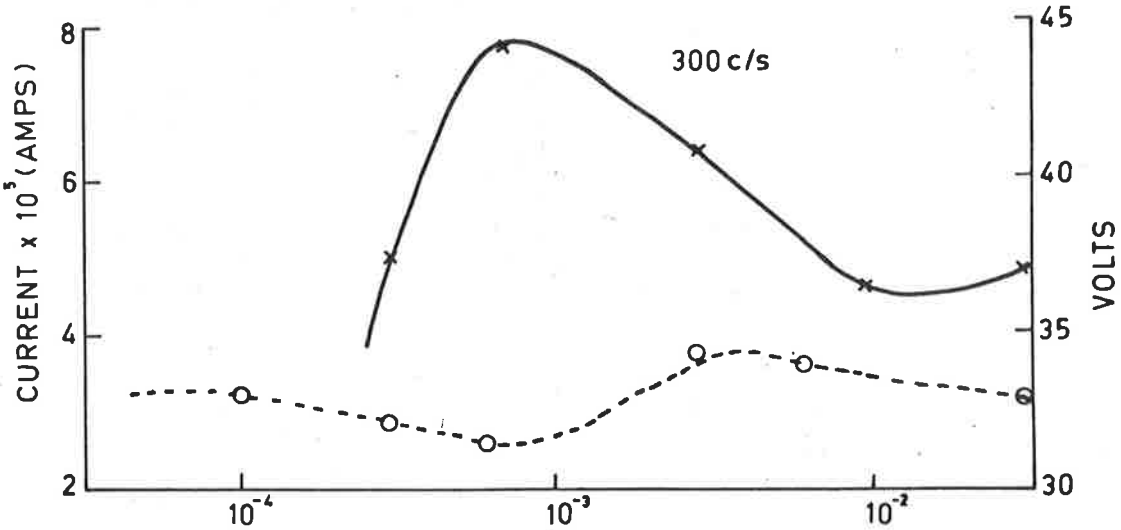


THRESHOLD CURRENT (FULL LINE) AND VOLTAGE (DASHED) AS A FUNCTION OF ZINC IN ZnS:Zn.Mn FILMS.

FIG. 7.13

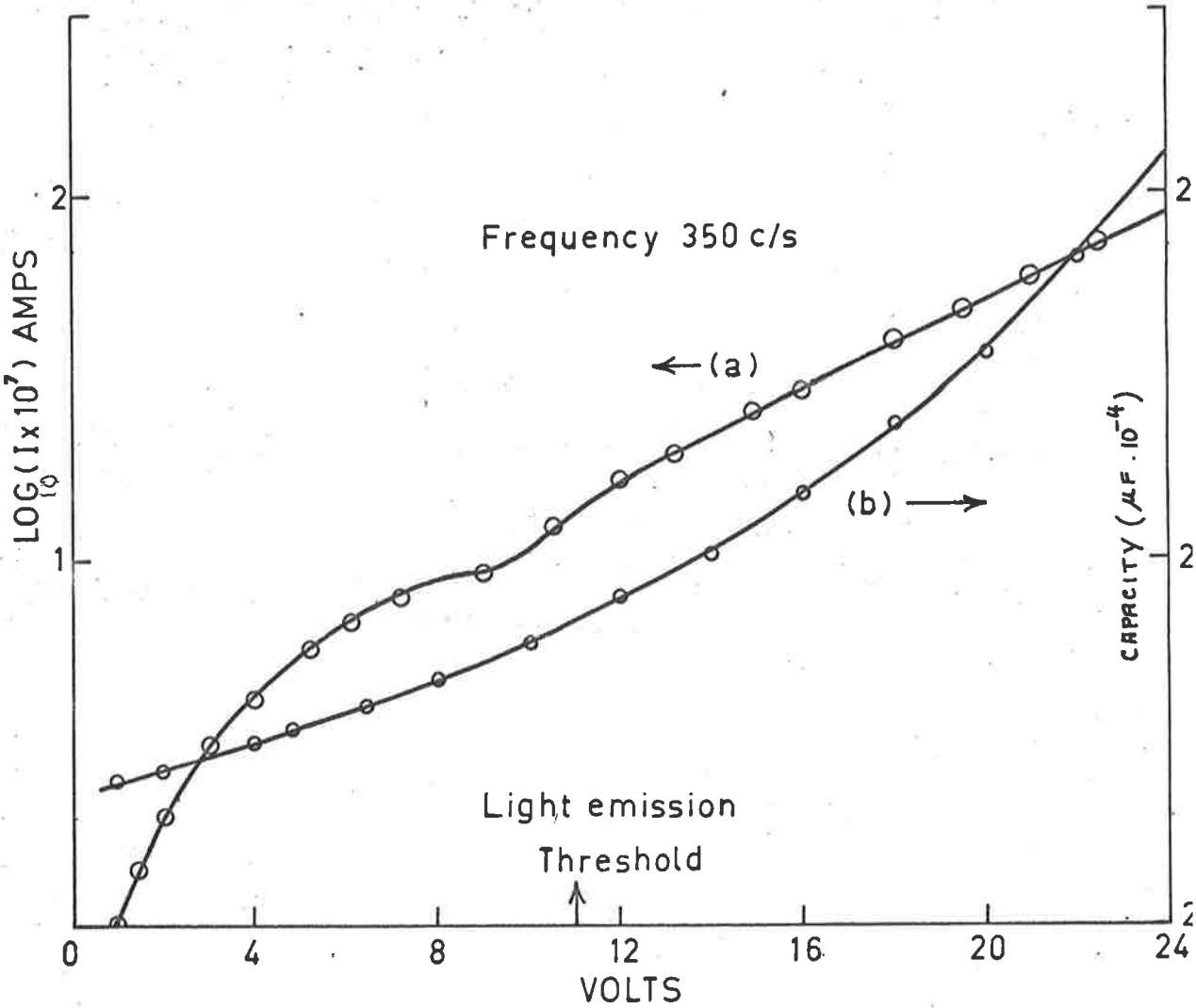


FIG. 7.14 TYPICAL VARIATION OF RESISTIVE CURRENT (a) AND CAPACITY (b) FOR A FILM EVAPORATED FROM AN ACTIVATED POWDER.

7.14), the current (I) increased exponentially, i.e.

$$I = I_o \exp \alpha V \qquad \text{--- 7.6}$$

where $I_o$ and $\alpha$ are independent of voltage but are functions of temperature.

The values of $\alpha$ in this equation (i.e. the slope of the log I against V curves) were larger for films evaporated from powders than for films evaporated from crystals. The slope also decreased as the frequency of excitation increased. This occurred from zero frequency to about 5000c/s.

It was possible that radiation from manganese centres excited by the field was sufficient to give rise to additional carriers by a photoluminescent process in the film. This was not the case because the films showed no photoconductivity when irradiated with 6000Å radiation.

Equation 7.6 was typical of many light emitting films, and it is similar to many results obtained by Thornton (1961) for ZnS.Cu, Mn, Cl films prepared by diffusion. The apparent discontinuity in the curve at the voltage where light was just detectable was observed from many films and was therefore considered as significant. Such an effect was not reported by Thornton.

As the film thickness varied there was no appreciable deviations from this exponential relation (equation 7.6).

As the voltage increased the capacitance also increased (Figure 7.14).

The variation of current with voltage observed here could be described by the diode equation over the total range of voltage considered. This equation is (cf. equation 7.3d).

$$I = I_o \left(\exp\left(\frac{V}{V_i}\right) - 1\right) \qquad \text{--- 7.7}$$

Thornton (1961) used this equation to describe his results, and interpreted it as showing that the films were composed of numerous p-n diode junctions. However, 7.4 accurately described the experimental data in the range of voltage where light emission occurred. Therefore, the diode equation (7.7) was not necessary to discuss any variation of current with voltage.

Figure 7.15 shows the rapid increase of brightness with current which was typical of all ZnS.Mn Zn and ZnS.Mn films (ZnSe films showed some differences which will be described in Chapter 9.

It is clear from Figure 7.10 that over most of the voltage range, the brightness was given by an equation of the form

$$B = \text{constant } I^n \qquad \text{--- 7.8}$$

where n varied between 5 and 6.

Note that equation 7.6 refers to a current I due to an increasing applied voltage. This equation may be compared to those observed from other electroluminescent films, where the brightness was much less sensitive to the resistive current viz. $B = \text{constant } I^2$ (Thornton 1961).

The observed dependence of the current I on the voltage did not agree with the general form of the equation relating the current due to internal field emission to the applied electric field, viz.

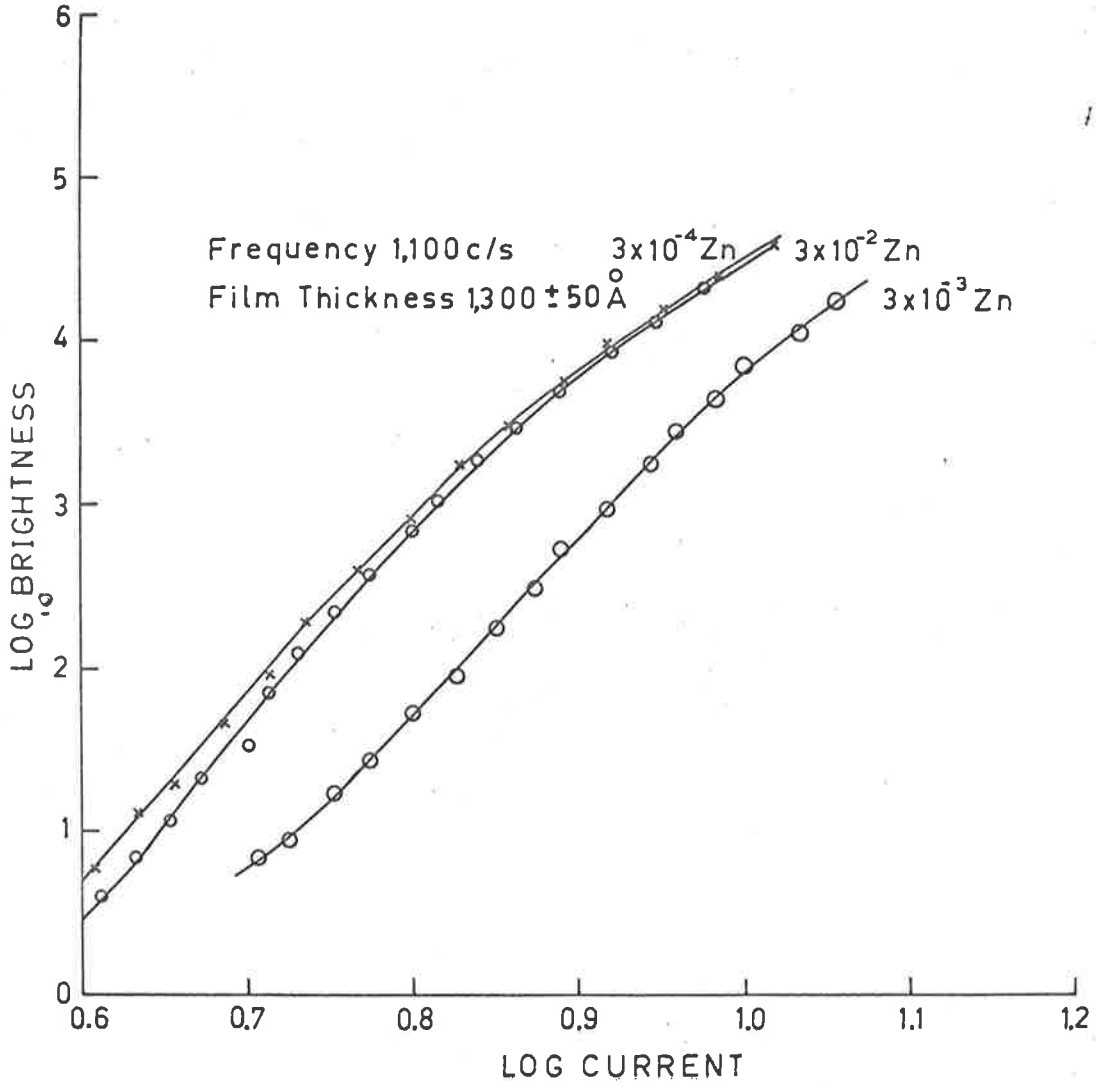


FIG. 7.15 VARIATION OF BRIGHTNESS WITH A.C. CURRENT FOR A ZnS:Zn,Mn FILM. ADDED ZINC IN CRYSTAL OF ZnS:Zn,Mn AS PARAMETER.

$$I = \text{const. } E^n \exp(-\frac{b}{E}) \qquad \text{--- 7.9}$$

for any value of the constant n.

Even for n = 0, the experimental results were not consistent with the simple exponential form of this equation. However, it should be emphasized that equations of the form of 7.9 are to be expected only if a single field emission process occurs, and the current due to this process can be measured in an external circuit. This may not be the case for the evaporated films with non ohmic electrodes. In fact, equation 7.9 could be due to a number of processes controlling the current flow in the film. *

The efficiency of the light emission process may be defined in a similar way to that suggested by Curie (1957). The average brightness may be written as the product of three field dependent terms.

$$B(E) = \beta . f_1(E) . f_2(E) . f_3(E) . \qquad \text{--- 7.10}$$

where $f_1(E)$ is an electron supply term, $f_2(E)$ is an energy gain term, $f_3(E)$ describes the excitation of the manganese centre and $\beta$ is the efficiency of light emission process in the manganese ion. $\beta$ is taken as independent of voltage.

The efficiency of the light emission process, to be called $\eta$, is then defined as

$$\eta = \frac{B(E)}{f_1(E)} = \beta f_2(E) \; f_3(E) \qquad \text{--- 7.11}$$

Figure 7.16 shows the generally observed variation of $\eta$ with applied voltage. The values of brightness (B) and

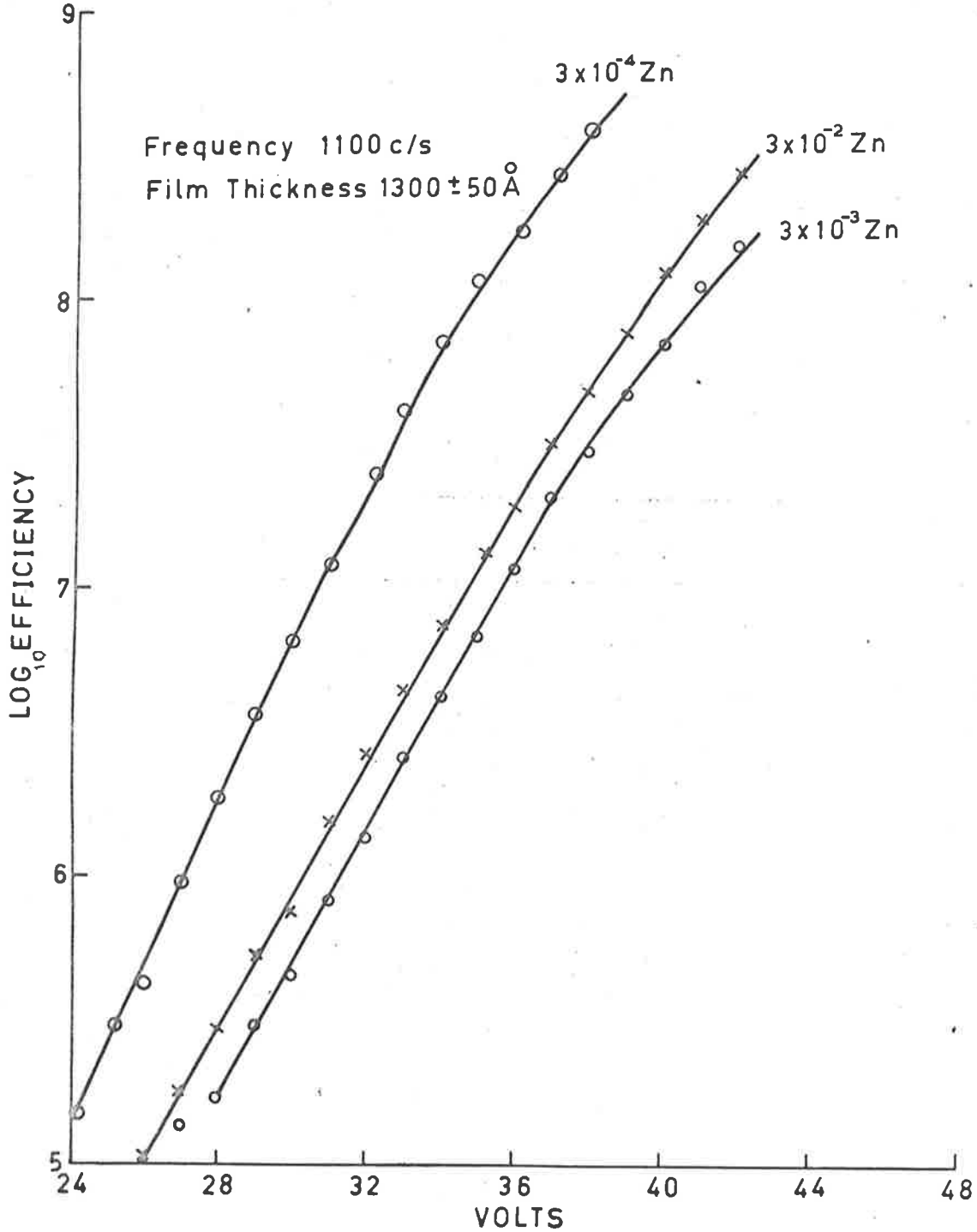


FIG. 7.16 PLOT OF EFFICIENCY AGAINST VOLTAGE FOR A ZnS:Zn.Mn FILM. ADDED ZINC IN CRYSTAL OF ZnS:Zn.Mn AS PARAMETER.

resistive current (I), (proportional to $f_1(E)$) could be measured simultaneously.

The variation of with applied voltage represents the rate of energy gain multiplied by the probability of excitation of a manganese centre, for each electron which contributes to the current. Over most of the voltage range, $\eta$ is given by

$$\eta = \eta_0 \exp \alpha V \qquad \text{--- 7.12}$$

7.4.3 Low frequency and D.C. emission

Films investigated here showed stable light emission for applied voltages of frequency less than 1c/s and at zero frequency (D.C.). For films less than about 1000Å in thickness, the spectrum of the emitted radiation contained a broad range of wavelengths between 4000 and 6000Å with a slight peak at 5680Å. This was breakdown radiation and the electrode was slowly destroyed. For thicker films, only radiation centred at 5860Å was observed but as the film thickness increased the same radiation at higher energy was observed as with A.C. voltage excitation (Figure 7.2). The spectrum from all films was identical for each polarity of D.C. or low frequency excitation.

Figure 7.17 shows the typical variation of the peak brightness with frequency for a constant A.C. voltage across ZnS.Mn films evaporated from activated powders (a) and crystals (b). For the film evaporated from the crystal, the capacitive component of the film impedance was negligible. The points above 20c/s (curve a) were corrected by the method outlined earlier (page 156).

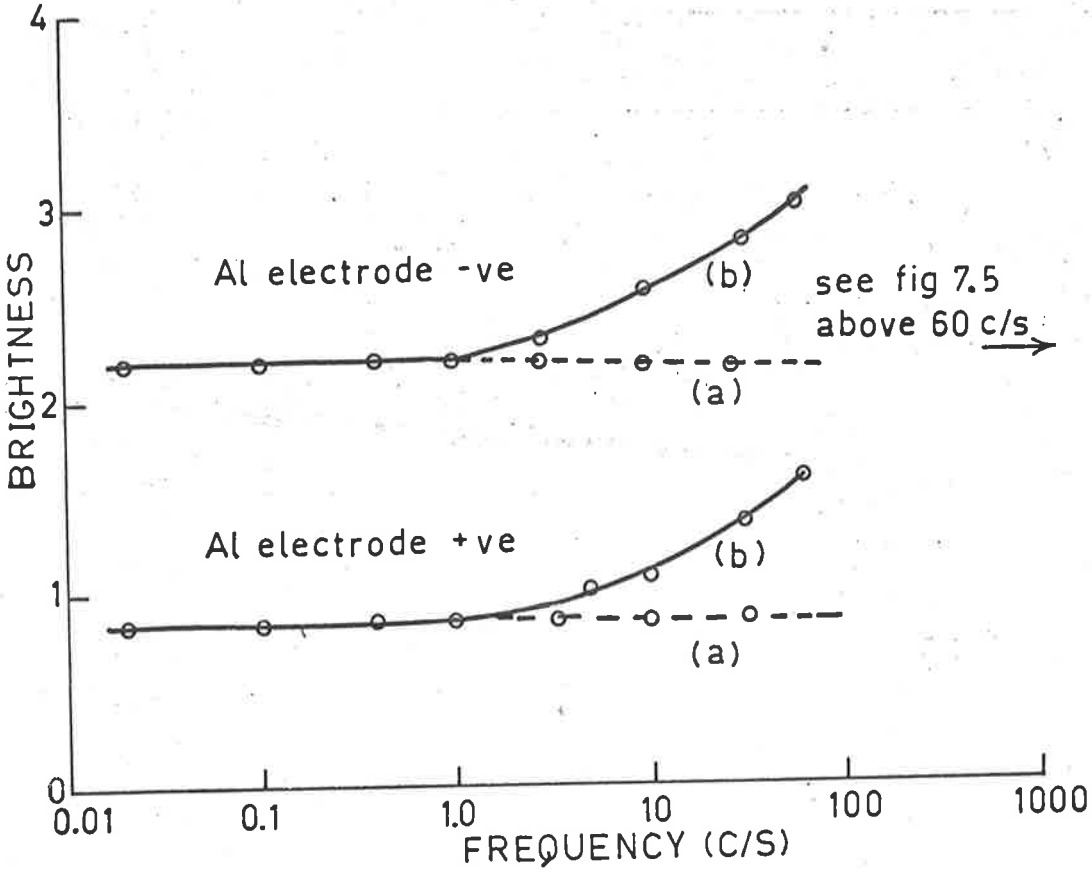


FIG. 7.17 VARIATION OF PEAK BRIGHTNESS WITH FREQUENCY FOR FILMS EVAPORATED FROM CRYSTALS (a) AND POWDERS (b).

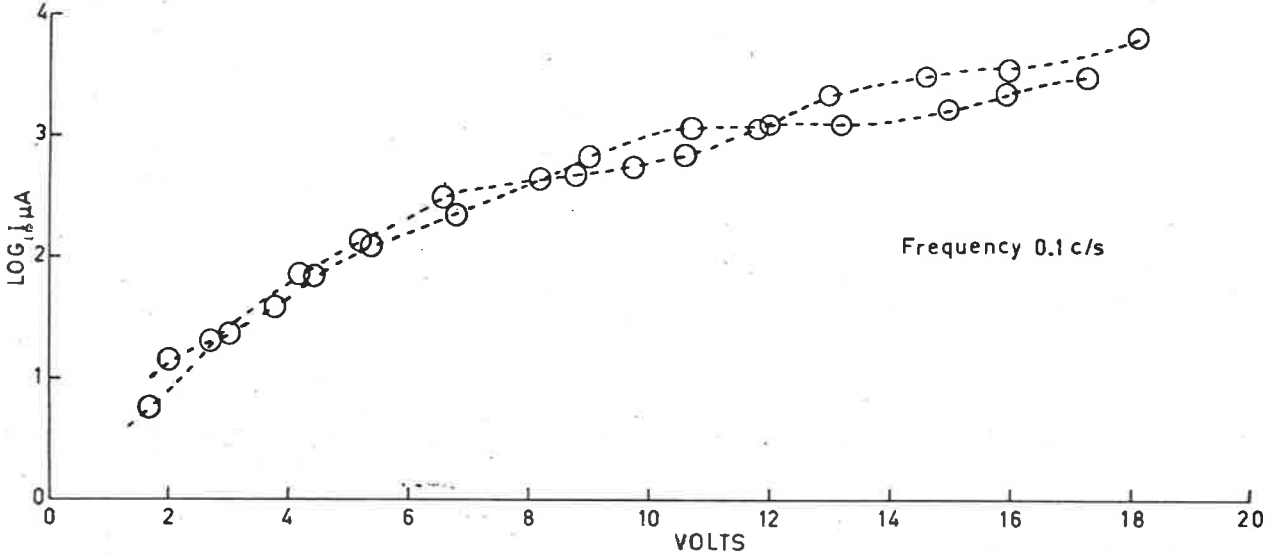


LOW FREQUENCY CURRENT AS A FUNCTION OF VOLTAGE.

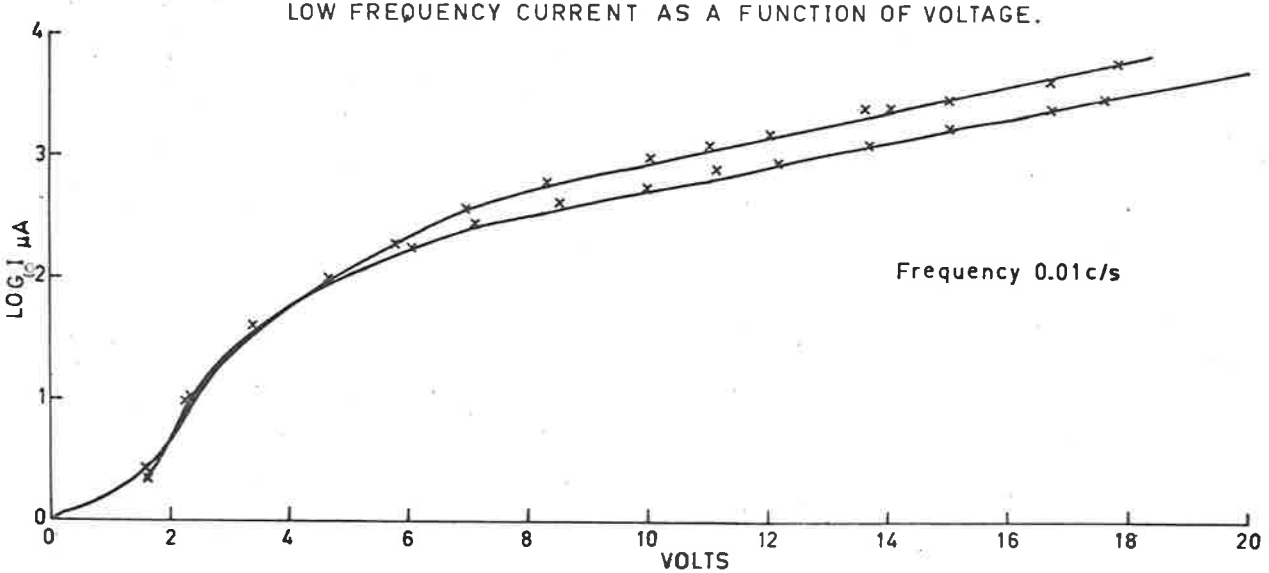


FIG. 7.18 LOW FREQUENCY CURRENT AS A FUNCTION OF VOLTAGE.

Figure 7.18 shows that the current flowing in the film at low frequency is related to the applied voltage in an identical way to that at higher frequencies viz. by equation 7.6. There is a small change in the value of $\alpha$ (in equation 7.6) with changing frequency. This is reflected in the variation of brightness with current which is given (at 0.01c/s) by

$$B = \text{const. } I^3 \qquad \text{---7.13}$$

The voltage dependence of the average brightness is unchanged from that at higher frequencies i.e. equations 7.1 or 7.2 described the brightness as a function of voltage.

Emission occurred for both polarities of an applied D.C. voltage. This is not always the case as shown by the observation of emission only for the metal electrode negative by Goldberg and Nickerson (1962). For low frequency (0.01 to 1c/s) the shape of the brightness pulses were identical to the waveform at higher frequency.

## 7.5 Properties of electroluminescent ZnS.Mn films evaporated from crystals

The results to be described in this section were obtained from films evaporated from crystals of ZnS.Mn and were generally confirmed (in less detail) for films evaporated from powders. It was found, unless stated to the contrary, that although the results showed a larger experimental scatter when powders were used, there was no significant difference between films made by either of these methods.

## 7.5.1 Zinc and manganese concentration in electroluminescent films

### (a) Zinc concentration

The presence of a large ($\simeq 1\%$) excess of zinc in the crystals used for the evaporation has been established. It is also clear that this amount is not available as a source of donor electrons since the conductivity is too small. The free carrier concentration, n, is related to the conductivity $\sigma$, by the well known equation, $\sigma = n\,e\mu$, where $\mu$ is the electron mobility (assuming carriers of one type only) and e the electron charge. The value of $\sigma$ is about $10^{-8}$ $ohm^{-1}cm^{-1}$. For such a disordered array as a film, the mobility will be much less than the value of $200cm^2/volt/sec$ obtained by Kröger (1956a) for a ZnS.Cu crystal. A value of $1cm^2/volt/sec$ may be more realistic. With these values $n \simeq 6.10^{10}/cm^3$.

The incorporated zinc must therefore be present as compensated donors or not as donors at all. This latter possibility may be caused by the local concentration of ions which was shown in Chapter 4.4. It was therefore of interest to determine whether the addition of zinc metal to crystals of ZnS.Mn grown from the melt (and already containing a zinc excess) would further increase the intensity of electroluminescence in the films.

The voltage dependence of the brightness for various zinc concentrations (added as the metal before the ZnS.Mn crystals were grown) is given in Figure 7.19. The rate of increase of brightness was the same for added zinc between 0.01 and 3.0%. The only difference between the curves was

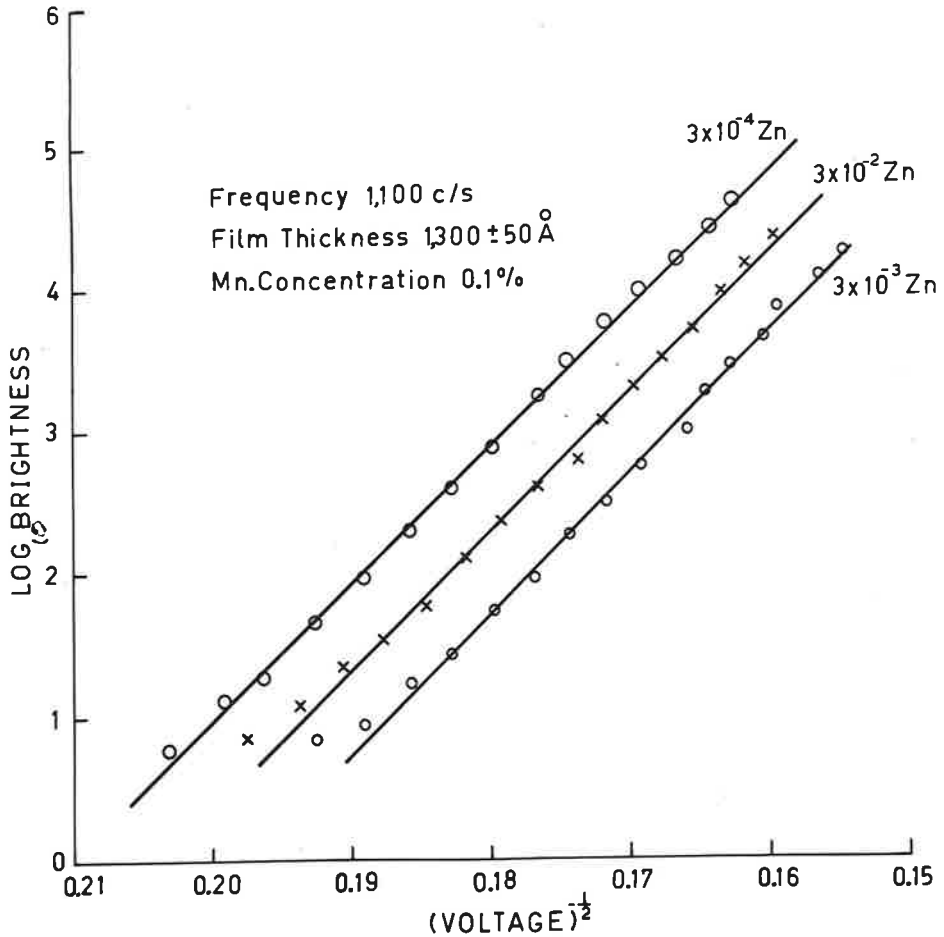


FIG. 7.19 VARIATION OF BRIGHTNESS WITH A.C. VOLTAGE FOR A ZnS:Zn.Mn FILM. ADDED ZINC IN CRYSTAL OF ZnS:Zn.Mn AS PARAMETER.

a deviation from linearity at low voltage for the highest zinc concentration.

The threshold voltage (i.e. the voltage at which light emission was just detectable) was carefully investigated for a number of films. These were deposited at a substrate temperature of 325°C and contained 0.03% manganese. The thickness of the films was 1310 ± 30Å. This uncertainty in thickness implied an uncertainty of < 1 volts in the threshold, because the threshold voltage was a function of film thickness (Chapter 7.2.2).

The threshold voltage varied as shown below (see Figure 7.20A, curve marked EL threshold).

| Added zinc gm/gm | Threshold voltage (300c/s) observed |
|---|---|
| - | 33 |
| $3.10^{-4}$ | 32.2 |
| $6.10^{-4}$ | 31.5 |
| $3.10^{-3}$ | 34.5 |
| $6.10^{-3}$ | 34 |
| $3.10^{-1}$ | 33 |

The change in threshold was small, however several films of each zinc concentration were used and averaged to give the values of threshold voltage. However,the values were never more than 0.5 volts from the mean values given in the table above. It must also be remembered that a change in potential of 1 volt in an applied voltage of 30 volts could cause the brightness to vary by a factor of about two.

The spectrum of the emitted light was unchanged by

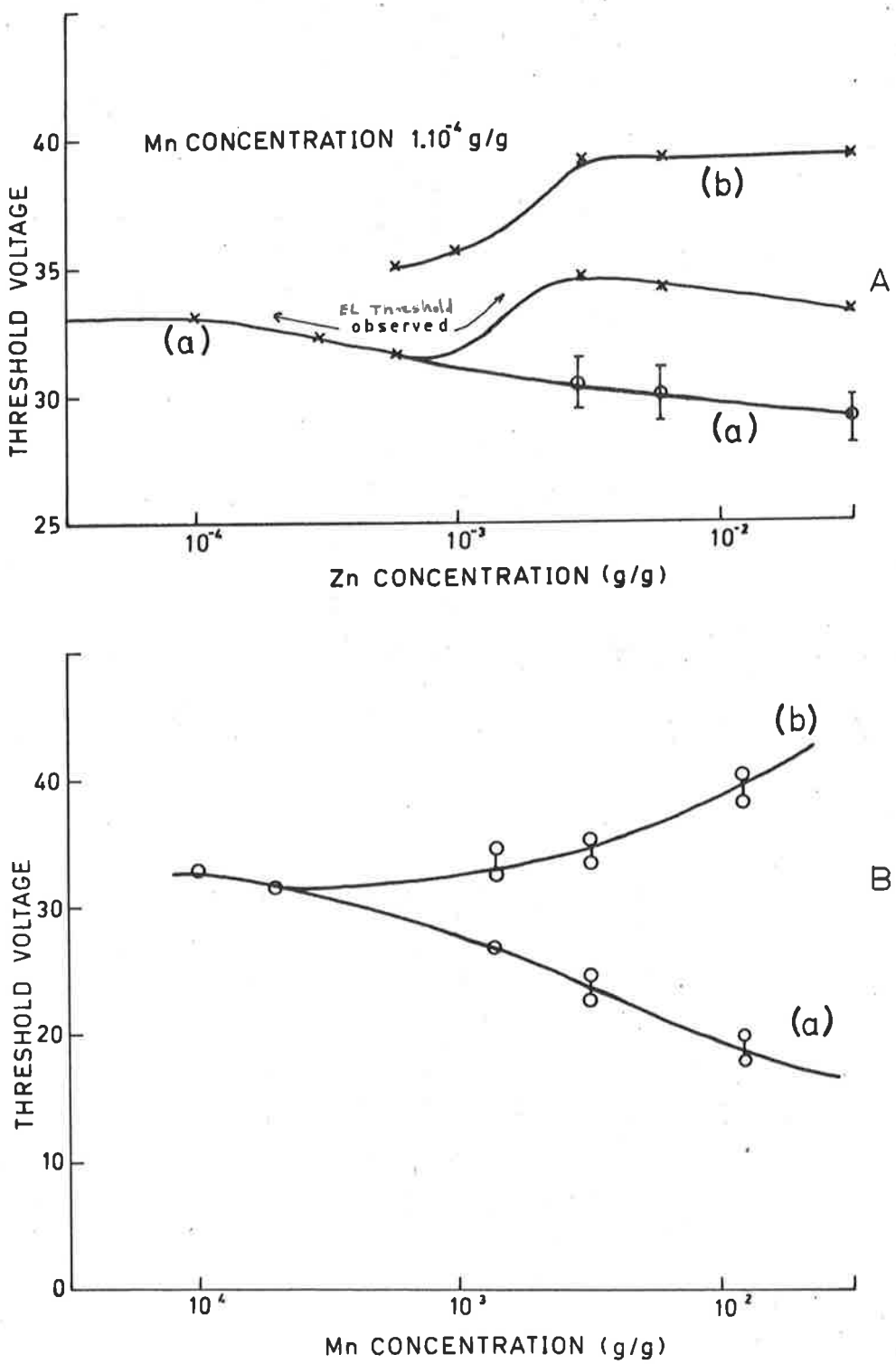


FIG. 7.20 VARIATION OF THRESHOLD VOLTAGE FOR A ZnS.Mn FILM WITH ADDED ZINC (1) AND MANGANESE (2) CONCENTRATION IN THE ORIGINAL CRYSTAL.

the addition of zinc to these films. Thus the changes in threshold voltage was not due to changes in the spectral response of the detector.

For these reasons the seemingly small changes in threshold were considered significant.

For films evaporated from crystals containing $3.10^{-3}$ gm/gm or more of added zinc, an increase in the forming process was observed. The increased electrode destruction caused the increase in threshold voltage when the concentration reached about $3.10^{-3}$gm/gm. The subsequent decrease of threshold voltage was also explained in terms of this increase in the electrode destruction.

It was assumed that the experimental relation (Figure 7.20A, marked EL) was the sum of two separate functions of increasing zinc concentration. Curve (a) represents the decrease in threshold voltage (i.e. the improvement in light emission) which should be observed if all the added zinc was incorporated and contributed to the emission process. Curve (b) shows the rate of decrease of emission (i.e. the increase in observed threshold voltage) due to the excessive electrode destruction.

An attempt was made to correct the observed curve by estimating the electrode area destroyed. This was done by counting holes in the aluminium electrode using an optical microscope. This method indicated a decrease of between 40 and 50% of the original area for films with zinc $> 10^{-3}$gm/gm. this meant that the light observed was too small by the same amount.

To convert this to a voltage the experimental brightness voltage relation must be used. However, near the threshold, this variation in brightness shows a decreased slope (Figure 7.19) which made the voltage difference corresponding to a given change of brightness uncertain. The change was between 3 and 5 volts (cf. the linear region of the brightness-voltage curves where a change of 1 volt was sufficient to change the brightness by a factor of 2). Using an average value of 4 volts to correct the observed thresholds, a more uniform decrease, with a tendency to a slight saturation was obtained (curve (a) in Figure 7.20A).

It must be remembered that this correction is only approximate because of the uncertainty in the true voltage difference used to correct the original curve. There was also strong evidence for the build up of polarization charge during the stabilization period and this would further affect the values of voltage threshold (see Chapter 6.6).

The variation of the resistive component of the A.C. current with voltage is shown in Figure 7.21 for several concentrations of zinc. The current increased exponentially with voltage with decreasing slope as the concentration increased. At high zinc concentrations the current deviated from the exponential at high applied voltage.

The variation of threshold voltage and threshold current with changing zinc concentration has already been shown and discussed (page 164) (Figure 7.13 between pages 163 and 164).

The results described in this section suggest that

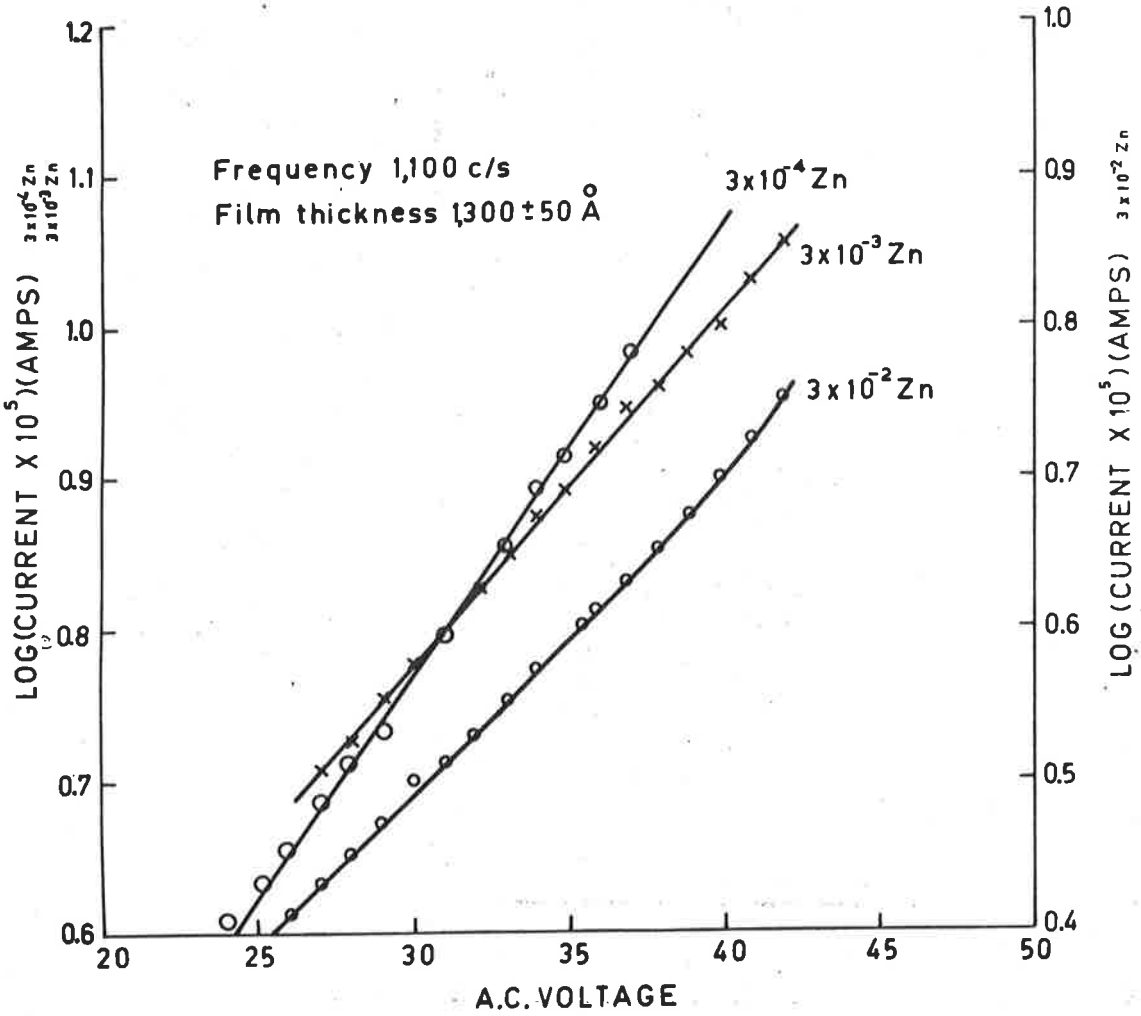


FIG 7.21 VARIATION OF A.C. CURRENT WITH A.C. VOLTAGE FOR A ZnS:Zn.Mn FILM. ADDED ZINC IN CRYSTAL OF ZnS:Zn.Mn AS PARAMETER.

more zinc may be dissolved in the ZnS crystallites than is present when a film is prepared from ZnS.Mn melt grown crystals. This is clear because of the decreasing voltage threshold at high zinc concentration (Figure 7.20A). Therefore as zinc is added to the crystals used for evaporation, the free carrier density in the films can increase (as more zinc donors are incorporated). Because a fraction of the excess zinc present in the evaporant is deposited in regions of high concentration in the films (Chapter 4.4), these deposits increase also with added zinc. At $10^{-3}$gm/gm these are present in sufficient proportions to form many more low resistance paths through the film, resulting in increased electrode destruction during the stabilization period. At higher doping levels, the amount of zinc in the crystallites increases (leading to a reduction of threshold voltage), while once the low resistance paths are formed (at $10^{-3}$gm/gm), the proportion of the electrode destroyed remains roughly constant.

From figure 7.20A it is clear that the films have been affected by as little as about $5.10^{-4}$gm/gm of added excess zinc, whereas about 1% is already present to give the electroluminescent effect. This sensitivity may be explained by assuming that most of the zinc incorporated in the crystallites gives rise to donor electrons which are localized in acceptor levels. These acceptor levels will be present in high concentration (even although a large number have been removed by sulphur re-evaporation), possibly due to surface states or other defect levels. Assuming a density about $10^{18}/cm^3$, this means that donors (excess zinc) must be

added to this concentration before they can give rise to any change in resistivity (or to the electroluminescent effect). However, once this critical value is attained, only a small increase in added zinc is necessary to cause some change. In other words the added donor concentration needs only to change from $1.10^{18}$ to $1.0001.10^{18}$ to give $10^{14}$ uncompensated donors/$cm^3$.

(b) Manganese concentration

The light emitting properties of ZnS.Mn films were also found to be a function of the manganese content. For added manganese up to about $1.10^{-3}$ gm/gm no appreciable change occurred in the light emission. However, above this concentration there was a marked increase in the amount of electrode destruction during initial operation. At $10^{-2}$ gm/gm it was nearly impossible to obtain a film which was stable enough to give any useful results. In this concentration range, the slope of the brightness-voltage curves was considerably reduced, while the linearity on the plot of log B against $V^{-\frac{1}{2}}$ was destroyed (Figure 7.22). These results showed that no improvement in the electroluminescence resulted from an increase in the density of luminescent centres. Such an improvement (in the form of an increase in slope) would occur if the shape of the brightness-voltage curve was controlled by the concentration of luminescent centres available for excitation.

A similar effect to that reported in section (a) was observed in the variation of threshold voltage with increasing manganese concentration. In Figure 7.20B, the lower points indicate thresholds for films with no stabilization,

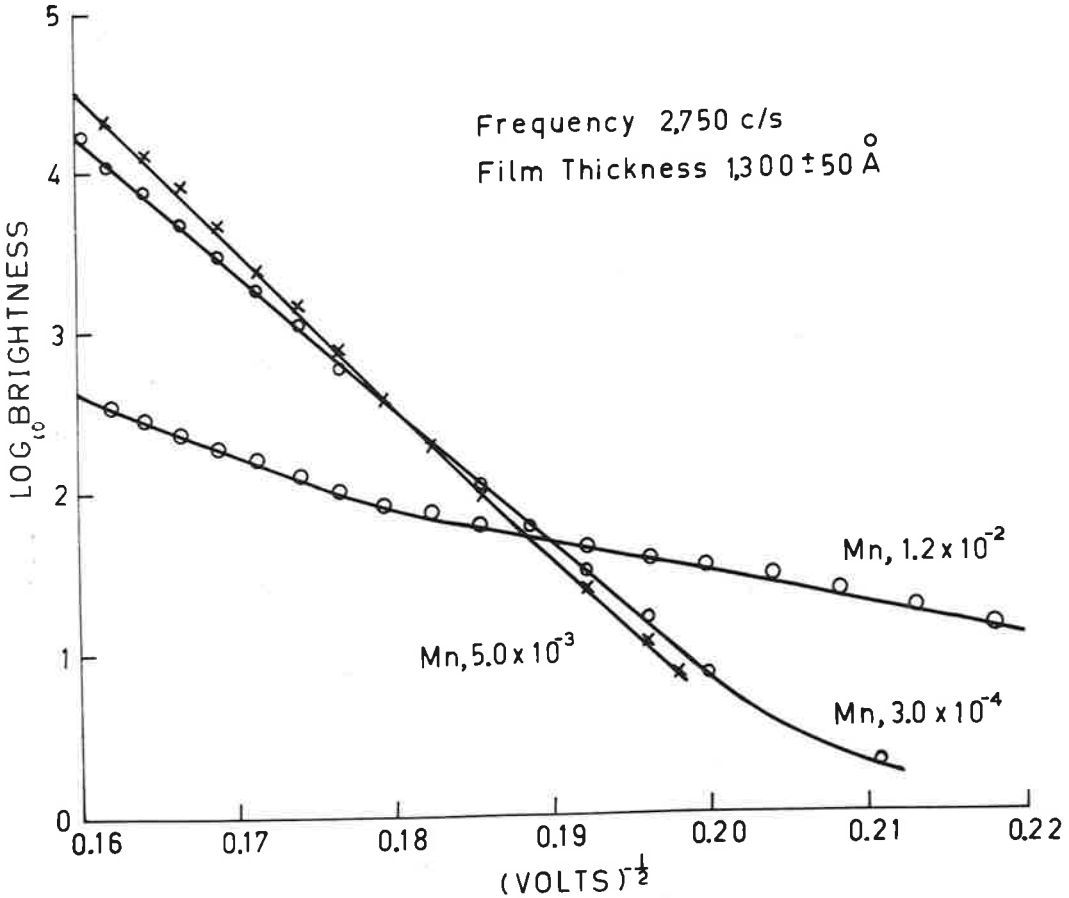


FIG. 7.22 VARIATION OF AVERAGE BRIGHTNESS WITH A.C. VOLTAGE FOR A ZnS.Mn FILM. Mn CONCENTRATION ADDED TO ZnS.Mn CRYSTAL AS SHOWN.

while after stabilization the threshold showed an increase (curve b). Therefore, the same concentration of manganese in ZnS produced more intense forming in ZnS films, than the same concentration of zinc. This may be interpreted (with caution) as showing that manganese is less soluble in ZnS than an excess of zinc.

### 7.5.2 Average brightness as a function of substrate temperature

Additional information concerning the presence of excess zinc in evaporated films was obtained by a study of light emission from films deposited on different temperature substrates.

The slope of the brightness versus $(\text{volts})^{-\frac{1}{2}}$ plot was a function of substrate temperature as shown in Figure 7.8. (This figure has already been presented in Chapter 7.1 between page 159 and 160. The graphs have been displaced along the axis to avoid confusion).

Some relevant information is shown below.

| Substrate temperature ($^{o}$C) | $\frac{\log_e B}{V^{-\frac{1}{2}}}$ | Threshold Voltage (volts) | Threshold current (amps) |
|---|---|---|---|
| 300 | 254 | 50 | $4.75\ 10^{-5}$ |
| 345 | 230 | 34 | $3.0\ 10^{-5}$ |
| 420 | 224 | 27 | $2.37\ 10^{-5}$ |
| 500 | 224 | 26 | $2.2\ 10^{-5}$ |

Figure 7.23 shows the variation of current and efficiency for two of these films with voltage. It is clear that the

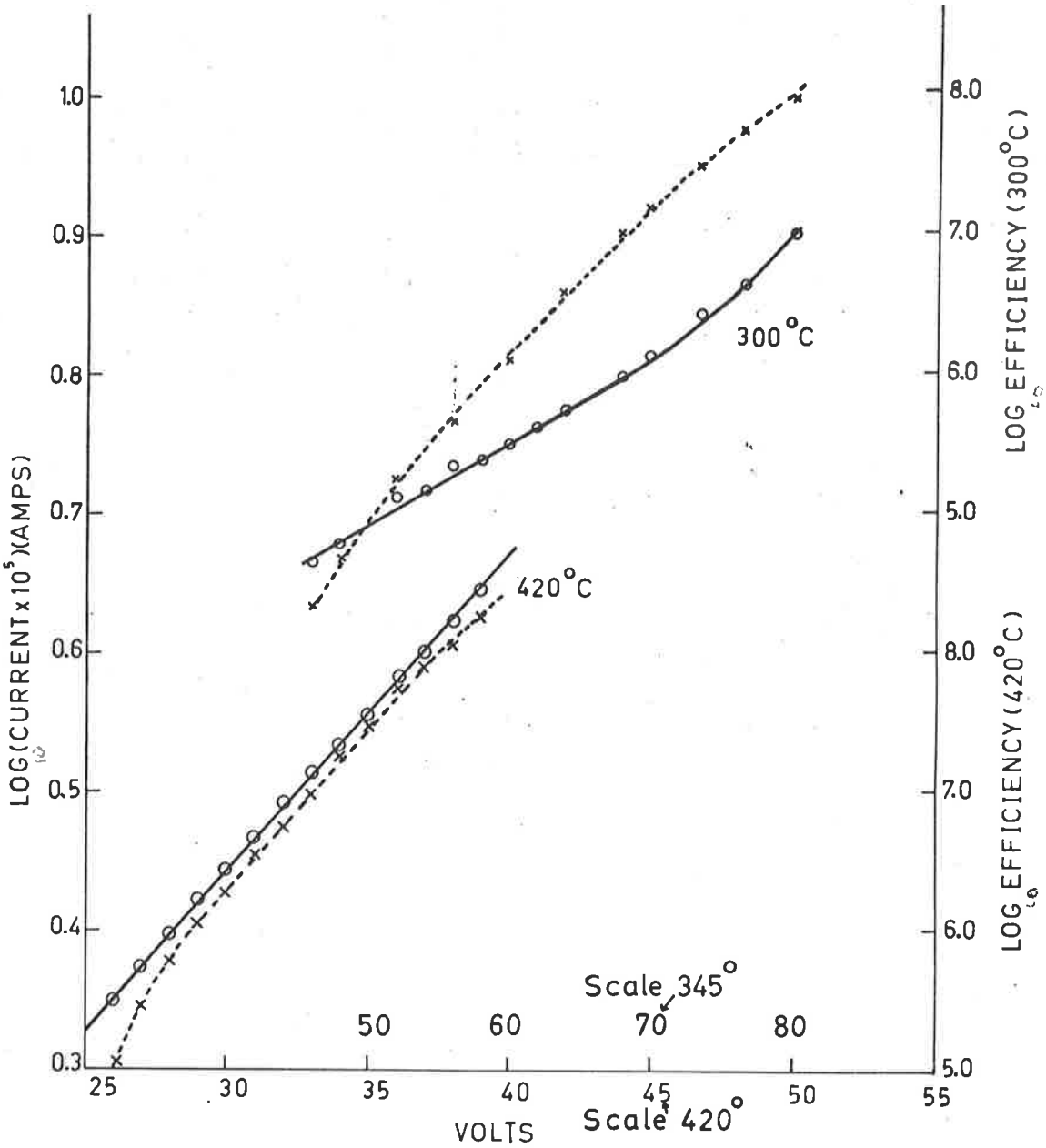


FIG. 7.23 A.C. CURRENT AGAINST VOLTAGE FOR TWO SUBSTRATE TEMPERATURES DURING EVAPORATION (FULL LINE) AND A.C. EFFICIENCY (DASHED LINE).

magnitude of the current at the threshold is not the deciding factor in determining the brightness, because the film which shows the optimum light emission effect (500°C) is the film passing the smallest current. From the general expression for brightness given earlier (page 167), it is clear that the excitation term must increase as the substrate temperature increases. This is evidently the reason for the high (50 volts) threshold for the 300°C film.

It has been shown in Chapter 5.4.1 that the crystal size increases as the substrate temperature increases above 300°C and that the crystallites tend to grow together as the temperature increases to 400-500°C. It is reasonable to assume that if light emission is due to acceleration of electrons, these changes will improve the conditions for the energy gain process and consequently a lower voltage will be required at 500° than at 300°C. It is likely that a larger current will flow through the 300°C film because of the higher voltage required to give light emission. These trends are seen in the table above.

It is observed that more intensive forming occurs for films prepared just above the critical substrate temperature. This is caused by the larger current flowing in these films.

A second process which may also affect the light emission from films deposited at different temperatures is the re-evaporation of zinc and sulphur from the substrate. For the case of ZnS crystals containing regions of excess zinc and others of excess sulphur (page 109), the amount of excess zinc increases as the substrate temperature decreases. Thus films prepared at 300°C should contain more zinc although the resistance may be higher because more excess sulphur is

is also present. This would explain the more intense forming found for these films.

The same high voltage increase of current is observed from films prepared from crystals of ZnS.Mn containing 1% added zinc and from films prepared at 300°C (cf. figures 7.21 and 7.23). This suggests that the deviations from the exponential form of the current is caused by the presence of larger than usual amounts of zinc.

It seems most likely that both of the processes discussed above contribute to the change in light emission observed as the substrate temperatures increase about 300°C.

7.5.3 Effect of oxygen pressure during film evaporation

During the evaporation of a film, oxygen from the residual air in the vacuum chamber was always present. Usually film evaporations were performed at a fixed pressure of $5.10^{-5}$ torr by using an air leak into the evaporating chamber.

The importance of this oxygen in the bell jar was investigated by making a number of films at varying pressures between $1.10^{-5}$ and $5.10^{-4}$ torr, using a controlled flow of dry air into the system. In general increasing oxygen pressure caused an improvement in the electroluminescence in so far as the voltage threshold was reduced and the A.C. current at the threshold increased. This is shown in Figures 7.24 and 7.25.

At $1.10^{-5}$ torr the voltage-brightness relation was well described by equation 7.1 while the current variation with voltage was a simple exponential of the form of equation 7.4. At higher pressures the brightness increase with voltage deviated from equation 7.1 although the high voltage

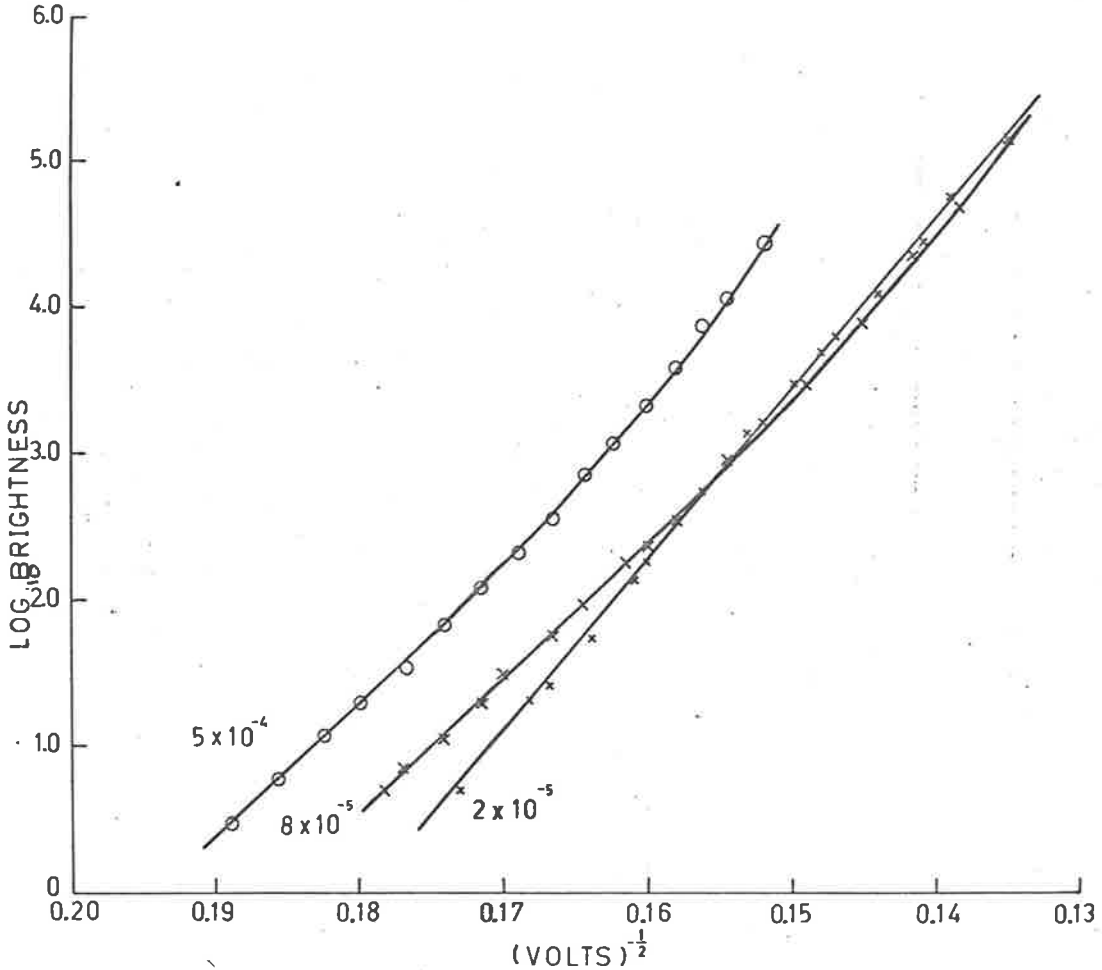


FIG. 7.24 EFFECT OF OXYGEN ON VOLTAGE — BRIGHTNESS RELATION FOR ZnS:Mn FILMS AT 1100 C/S.

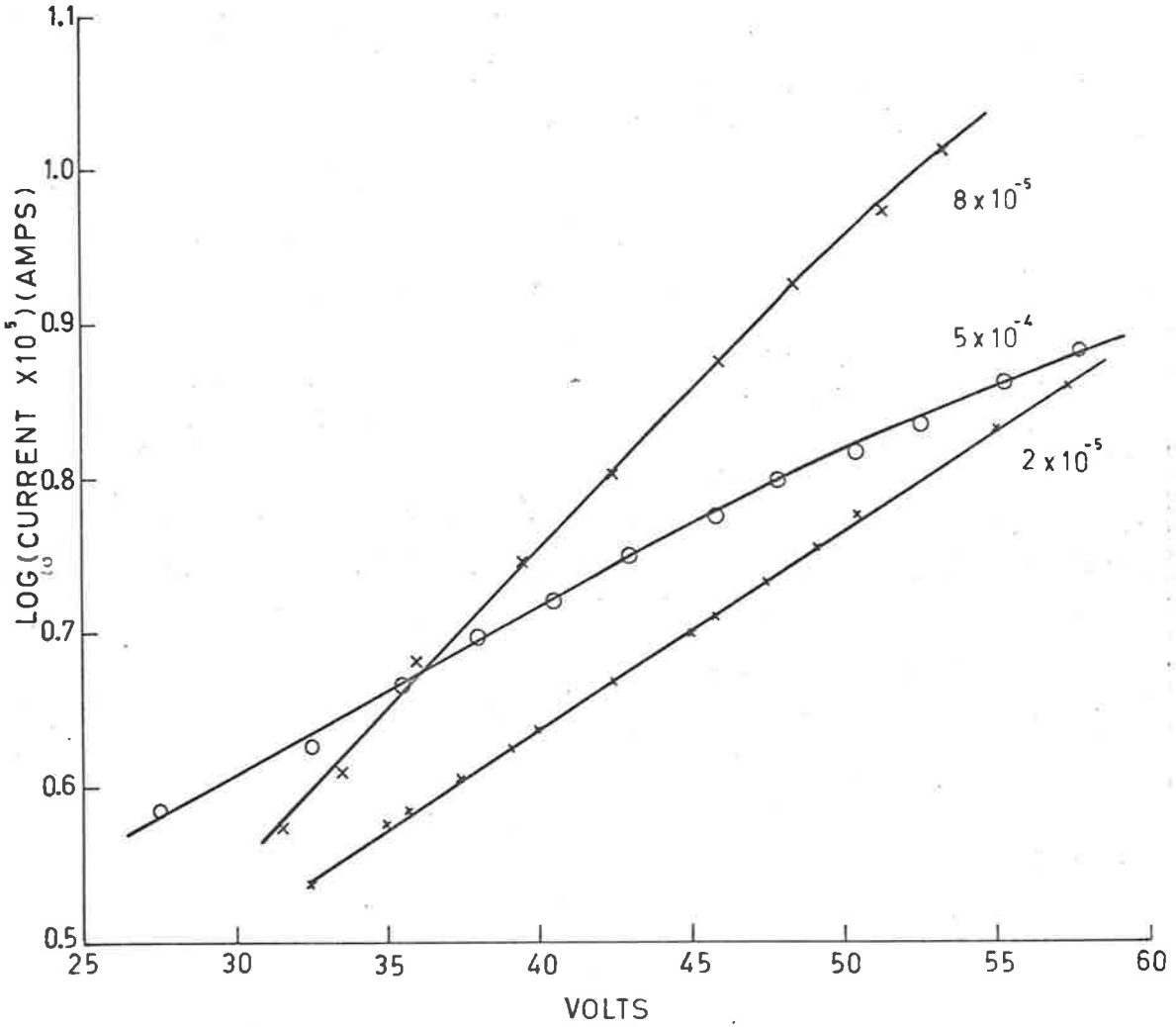


FIG. 7.25 A.C. CURRENT (1100 C/S) THROUGH ZnS:Mn FILMS AS A FUNCTION OF OXYGEN PRESSURE DURING PREPARATION.

slope was the same for all pressures.

Because excess zinc is always present in these films mainly in regions of large concentration, the formation of ZnO must be considered. The presence of ZnO was not detected by electron diffraction, but this does not preclude its presence in small quantities ($\simeq$1%). It was not possible, with the vacuum system used, to reduce the pressure sufficiently to ensure that no oxide was formed during an evaporation. However, by pumping continuously for a long period and flushing the system with oxygen free nitrogen, electroluminescent films could be prepared in a vacuum of $8.10^{-6}$ (of residual nitrogen). This suggests that ZnO is not necessary for electroluminescence in evaporated films.

However, an explanation of the results shown in Figure 7.24 and 7.25 may be found by assuming (a) increasing ZnO formation and (b) increasing incorporation of oxygen (as $O^{--}$ ions) in the ZnS lattice. It is well known that oxygen in ZnS gives rise to a complex set of traps below the conduction band edge (Hoogenstraaten 1958).

If ZnO is formed the amount of zinc deposited in regions of high concentration will be reduced. The forming process has been ascribed to this high concentration and if these regions are replaced by lower conductivity ZnO the forming (electrode destruction) will be reduced during the initial film operation. Because there is less electrode damage (quantitatively observed), the current at the threshold for light emission, increases as the oxygen content during evaporation increases. This formation of ZnO conducting paths suggests that the increased current observed will not

be effective in giving any additional light because the increased current flow is confined to ZnO. However, the threshold voltage is observed to decrease with increasing oxygen content (Figure 7.24). Thus the presence of ZnO must contribute some electrons to the ZnS crystallites, which can then excite additional manganese centres. However, above the threshold for emission, there is no correlation between the changes in the brightness-voltage and current-voltage curves.

The slope of the I-V curves showed a maximum about $5\ 10^{-5}$ torr and then decreased again as the pressure increased. The initial increase in slope was due to an increased electron supply from the ZnO phase. This increase was overshadowed by a reduction in slope due to increased trapping as the pressure increased.

The changes in the brightness at low voltage may also be explained by increased trapping of electrons at oxygen sites. This reduces the number of free electrons and hence the brightness, since the brightness has been shown to depend on the current through the film. At higher voltages these trapped electrons may be liberated by the electric field (most probably by impact ionization) which makes the number of electrons in the conduction band independent of the presence of oxygen traps. Liberation of trapped electrons at higher applied voltages has been suggested by Curie (1960) and others as a source of electrons for the electroluminescent process. If this process is important, the high voltage yield values should be independent of the oxygen pressure. This is observed in Figure 7.24.

7.5.4 Temperature dependence of emission

Considerable trouble was experienced in obtaining a contact to ZnS.Mn films which was stable throughout the temperature range - 180 to + 200°C. A number of methods of making electrical contact to the metal electrode (e.g. silver paint, aquadag) gave non reproducible curves. A more satisfactory method was to fit a hollow copper tube through the coolant container of the dewar described earlier (page and to mount the electroluminescent film (with silicone grease) with the metal electrode uppermost. It was then possible to use two pressure contacts in the form of thin copper rods held in the retaining ring around the dewar (Figure 2.10). While the form of this contact appeared to be quite stable, many measurements were still unsatisfactory. Some of the difficulties are described in the following paragraphs.

For thin films (1000-2000Å), it was not possible to obtain any useful results above about 50°C because of an increasingly rapid destruction of the metal electrode. This was the result of increased current through the films which were then assumed to be undergoing a thermally enhanced breakdown. For films about 5000Å in thickness this effect did not occur. However, even thick films showed irreversible changes in current as the temperature was increased from and decreased to 20°C. If the temperature was raised to 50° and lowered to 20° again the values of brightness (at a given voltage) and brightness were the same during the decrease as during the increase. Above this temperature the current and the brightness increased more rapidly, but on reducing the

temperature to 20° again it was found that the resistance was lower than at the beginning of the temperature cycle. For example, increasing temperature from 20° to 150° decreased the film resistance from 21.3K to 7.67K (for a thick film evaporated from a powder), but on cooling to 20° the resistance was only 13.4K.

Such changes in the film resistivity could not be induced by heating a ZnS.Mn film and then evaporated a metal electrode. It was clear that the presence of the aluminium electrode was necessary for this effect. The most probable explanation of the change was a diffusion of aluminium from the electrode into the ZnS film. The aluminium ion ($Al^{+++}$) in ZnS acts as an electron donor (Chapter 4.3). It was possible that such diffusion was enhanced by the application of the voltage which was applied just long enough to take a measurement. This irreversible fall in resistivity made any measurement above 50°C of questionable value.

Measurements below room temperature were more reproducible. Figure 7.26 curves 1, shows how the average brightness varied with temperature. The experimental points were obtained by allowing the temperature to rise from - 180°C at about 10°/minute, and switching on a constant A.C. voltage at 10° intervals. The voltage was applied for about 3 seconds at each point. The rapid increase in the emission above 50°C for both frequencies was due to the onset of diffusion. If however, the temperature was allowed to reach an equilibrium value at each point in this range, a smaller variation was found (Figure 7.26, curves 2). The same irreversible increase was observed above 50°C.

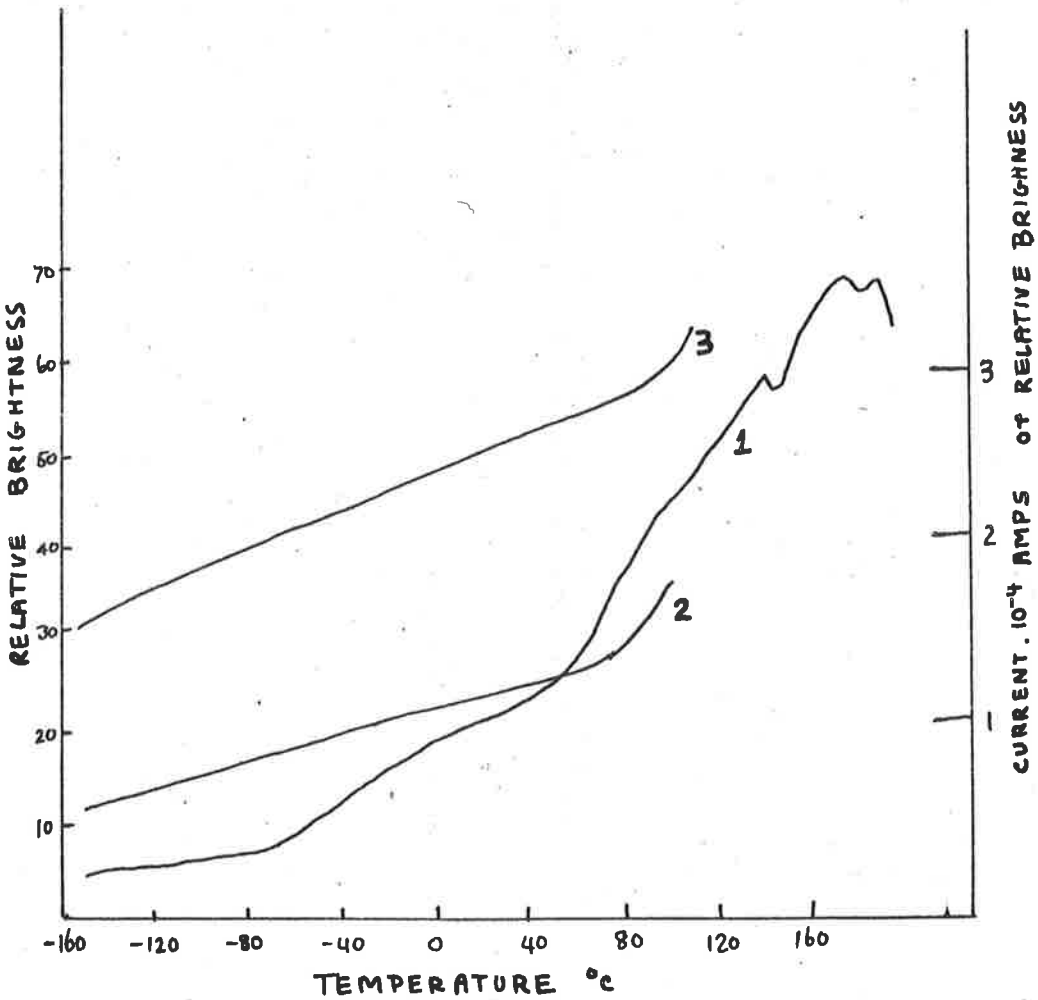


FIG 7·26 TEMPERATURE VARIATION OF BRIGHTNESS (CURVES 1 AND 2) AND OF CURRENT (CURVE 3)

Figure 7.26 curve 3, shows the variation of resistive current between - 180$^{o}$ and + 150$^{o}$C. It is clear that the brightness (B) and the current (I) are related, in fact it was found that

$$B = \text{const. } I \quad \text{(at constant voltage)} \quad \text{---7.14}$$

For such a comparison, the irreversible change in resistance above 50$^{o}$ was not relevant since even if the current increased irreversibly the brightness will still be proportional to the magnitude of the current.

Equation 7.14 should be compared to equation 7.6, which gives the average brightness as a function of current (due to increasing voltage). Equation 7.6 was

$$B = \text{const. } I^{n} \quad \text{--- 7.6a}$$

where n = 5 - 6.

The two brightness pulses per cycle of the applied A.C. voltage showed the same temperature dependence, that is the peak/peak ratio was independent of temperature.

It has been reported that the average brightness for thick films varied as the nth power of the applied voltage (Chapter 7.4). The value of n was a function of temperature. However, the equation describing the average brightness was unchanged throughout the temperature range investigated at 20$^{o}$C) was given by a similar equation at - 180$^{o}$, although the slope of the straight line on the log I - V plot was increased by 20% over this range.

7.42 <u>Resistive current as a function of temperature</u>

It is well known that the conductivity of an n-type

semiconductor increases with temperature according to an equation of the form

$$\sigma = \text{const. } \exp\left(-\frac{E}{kT}\right)$$

where E is the depth of the electron donors (in ev) supplying the electrons to the conduction band.

Therefore, a plot of log $\sigma$ against $\frac{1}{T}$ will give curves showing linear regions, whose slope is a measure of the depth of the donor level.

A small D.C. voltage was applied to the films, which were then heated from - 180°C. Because of unsteady current readings at low applied voltages (reported in Chapter 6.4), it was not possible to determine whether any linear regions were present on the log $\sigma$ versus $\frac{1}{T}$ plot. It was clear however, that the current was not changing by orders of magnitude in this temperature range. To obtain sufficiently stable readings of current through the range, the films were operated at A.C. voltages sufficient to excite a low level of light emission. Such a variation has been shown in Figure 7.26c. If the experimental points were replotted as log $\sigma$ against $\frac{1}{T}$, the conductivity showed a continuous increase as the temperature increased. This indicated no discrete donor levels. It was possible that there was a continuous distribution of levels which gave this smoothing out, but even so, the small variation of $\sigma$ with T was surprising. This was especially so since the presence of excess zinc (donors 0.3ev below the conduction band edge) is certain, and such levels should be detected in this

temperature range.

It is not clear why these levels are not detected by this method. However it is possible that the zinc donors have been emptied by impact ionization so that a change in temperature does not give rise to any additional free carriers. Harper (1962) has observed small changes in current with additional temperature which he attributed to shallow (005 - 0.03ev) donor levels. It seems certain that in the temperature range used by Harper ($> 77^{\circ}K$), such levels would be already ionized.

While all thermally controlled (or assisted) processes give rise to more rapid variations of the current than observed here, it is well known that if the current is due to tunnelling through a potential barrier, a small dependence is expected.

Chow (1963) has shown that in this case the current j can be written

$$j = j_o + \alpha T^2 \qquad \text{--- 7.15}$$

where $j_o$ and $\alpha$ are independent of temperature.

This equation has been used to describe tunnelling through a thin $Al_2O_3$ layer on an aluminium electrode. Figure 7.27 shows a plot of $(j-j_o)$ against $T^2$. It is clear that these two quantities are proportional from $-180^{\circ}$ to $-30^{\circ}C$. The values from $-30^{\circ}$ to about $+30^{\circ}C$ fall below the extrapolation of this line. Current values above $+30^{\circ}C$ were unreliable because of the diffusion effects mentioned earlier.

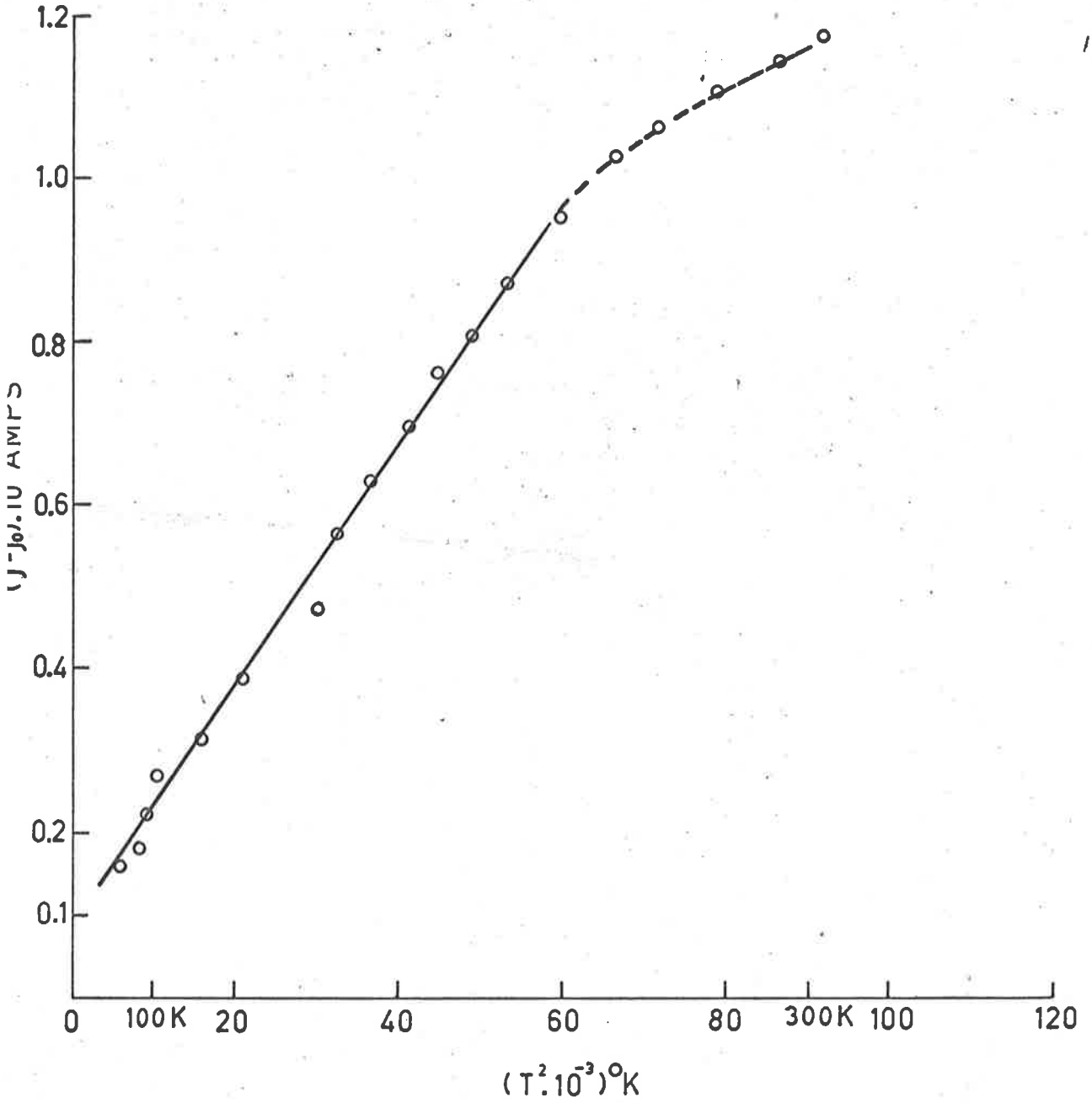


FIG. 7.27 RESISTIVE CURRENT AS A FUNCTION OF (ABSOLUTE TEMPERATURE)$^2$ FOR A ZnS.Mn.Zn FILM.

It is not certain as to the actual barrier through which electrons are tunnelling. Tunnel release of electrons from levels in the ZnS is possible. Tunnelling of electrons from the electrodes is also possible, especially as the presence of a thin $Al_2O_3$ layer has been postulated at the ZnS-aluminium interface. Equation 7.15 can be rewritten

$$\frac{j(T)-j(0)}{j(0)} = \frac{32\pi^2 m s^2 k^2}{3h^2 \bar{\Phi}} T^2 \qquad \text{--- 7.16}$$

where s is the thickness of the insulating layer, $\bar{\Phi}$ is the average height of the potential barrier and the other symbols have their conventional meaning.

Unfortunately both $\bar{\Phi}$ and s are unknown. However, an estimate of $\bar{\Phi}$ can be made by noting that if $\bar{\Phi}$ is much less than lev, thermionic emission over the barrier into the film would occur (i.e. Schottky emission) and give rise to a more rapid change in current with temperature than is observed. If $\bar{\Phi}$ = lev, the graph of Figure 7.26 is consistent with a value of 70A for s, the $Al_2O_3$ thickness. This is a reasonable value for the thickness of the oxide layer.

Such an oxide layer is however present only at the metal electrode. It is possible that such tunnelling governs the current flow in each direction. Alternatively the tunnelling transition may occur across the surface barriers of the ZnS.Mn film at each electrode.

# 8. CHARACTERISTICS OF BRIGHTNESS PULSES FROM ELECTRO-LUMINESCENT FILMS EXCITED BY AN A.C. VOLTAGE

## 8.1 Amplitude

An A.C. voltage produces electroluminescence in the form of two light pulses, approximately in phase with the voltage maxima (of a sinusoidal voltage). These pulses are in general, of unequal intensity. The value of the peak to peak ratio was found to depend appreciably on the electrical history of the film (i.e. previous voltage and frequency operation), although the average brightness did not reflect any change.

The investigation of a number of supposedly identical films was absolutely necessary to obtain any reliable information on the processes governing the brightness waveform.

It should be stated at the outset of this discussion, that films of thickness less than about 2500A showed maximum emission when the metal electrode was positive. Films of greater thickness showed maximum emission when the metal was negative (see Chapter 8.2 for a further discussion).

Figure 8.1 (a to d) shows the brightness waveform as a function of the frequency of the exciting voltage for a film evaporated from a ZnS.Mn crystal. The peak to peak ratio decreases slightly with increasing frequency. However for most films evaporated from crystals, this ratio was observed to be independent of frequency. For films evaporated from ZnS.Mn powders, this ratio changed more rapidly with frequency (Chapter 7.3.2). The effect of increasing frequency for all films, was to decrease the peak to peak ratio, irrespective of the polarity on which the maximum brightness occurred.

At high frequencies ( $\simeq$1000 c/s) the brightness waveform from some films (not all), developed an associated noise

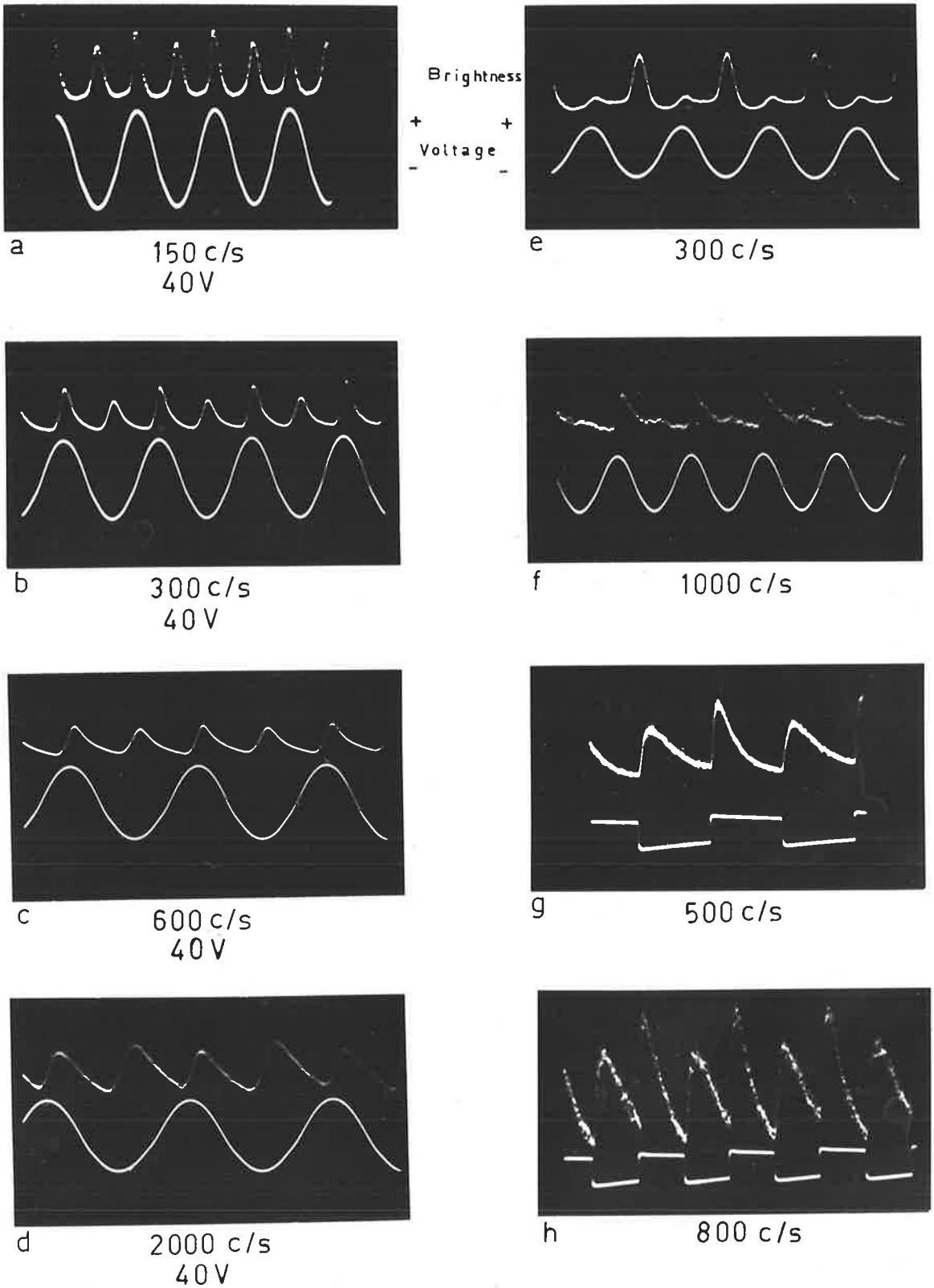


FIG 8.1 BRIGHTNESS WAVEFORMS.

level which appeared on the oscilloscope trace. This effect is seen in figure 8.1 f and h. For some films, this effect prevented any useful display of the brightness waveform.

Another effect which was commonly observed was a finite brightness level between two brightness pulses (figure 8.1 d and e). In these diagrams this level appears as the polarity of the applied voltage changes from positive to negative irrespective of the half cycle on which the maximum brightness pulse occurs. However a similar effect was often observed as the voltage changed from negative to positive. There was no apparent correlation between the appearance of this brightness level and any particular condition in the films. There are several mechanisms which can account for this effect. It is however not possible to decide which of the following processes will be the predominate one for any given film.

(a) An explanation in terms of the characteristic decay time $\tau$ of the manganese activator may be obtained. The lifetime of the excited state involved in the luminescent transition giving 5860A radiation, is 0.4 milliseconds (Curie 1960). Halsted and Koller (1954) suggest 1.4 millisecond. The decay time of the light pulses observed here was seen more clearly for A.C. square wave voltage excitation. At low frequency (100 c/s) the peaks were well separated appearing to decay to a constant level before the following half cycle. At 500 c/s the decay appeared to be just complete. At higher frequency, a finite brightness level appeared as the voltage changed from negative to positive (figure 8.1 g,h).

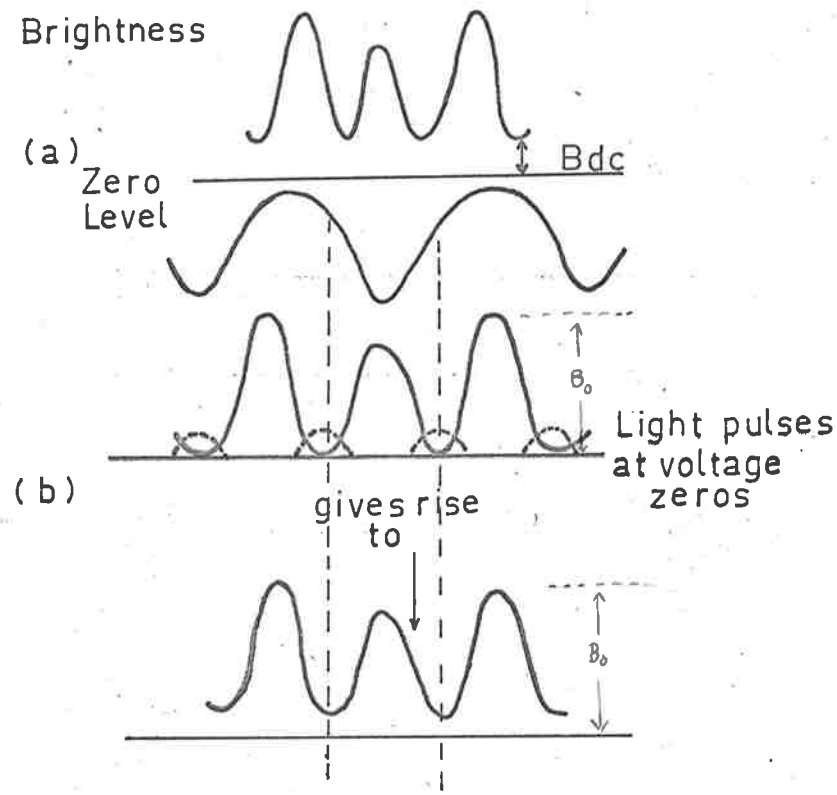


FIG. 8.2 D.C LEVEL OF EMISSION (a), FORMATION DUE TO SMALL LIGHT PULSES AT VOLTAGE ZEROS (b).

From these traces, the decay time appeared to be about .35 milliseconds.

The number of manganese centres remaining excited at time $t$ is

$$n_e(t) = n_e^o \exp(-t/\tau)$$

where $N_e^o$ is the total number of excited centres at t = 0. As the time for one half cycle of the applied voltage approaches the decay time of the activator, the decay of one light pulse is not complete before the next pulse appears. If both brightness peaks are equally intense and the decay time of each is the same, this effect will cause the appearance of a constant component of the emission on which the remaining parts of the brightness pulses are superimposed. (Figure 8.2). If however one peak is more intense than the other, ($N_e^o$ greater), a finite brightness will appear after this maximum pulse, because more centres remain excited at a given time t. This will produce a waveform as in figure 8.1 f. This mechanism predicts that this effect will occur after the most intense brightness peak irrespective of the polarity on which it occurs. This explanation is only applicable above about 500 - 800 c/s.

(b) For most films investigated here, the less intense peak appeared to be characterised by a longer decay time. This was particularly noticeable for films prepared from crystals. The effect of this is clearly seen in figure 8.1 g and h. This longer decay was a property of the less intense pulse regardless of the polarity on which the pulse occurred. Because of this longer decay, the presence of a

finite emission after the smallest light pulse will be observed.

For a given film the waveform will be determined by which of these processes is of most importance.

During the experiments with square wave voltage excitation it was observed that the brightness pulses at higher voltage appeared broader than for sinusoidal excitation. Thus the average brightness may be a function of the shape of the exciting voltage wave. Figure 8.3 shows the average brightness as a function of voltage for a sinusoidal and a square (to 1%) wave voltage. The other curves in figure 8.3 were taken from a progressively distorted square wave voltage as shown on figure 8.3. It is clear that as this distortion increases the experimental points fall away from a straight line on a log B - V plot which implies

$$\text{for a square wave, } B = B_o \exp \alpha V$$

The sinusoidal voltage gave experimental points which, if repeated, showed linearity of log B against $V^{-\frac{1}{2}}$

The current waveform for square wave voltage excitation consisted of current pulses coincident with the changes of voltage. These were of very short duration decaying to a constant D.C. value in about 10 $\mu$sec, and were clearly associated with the brightness pulses.

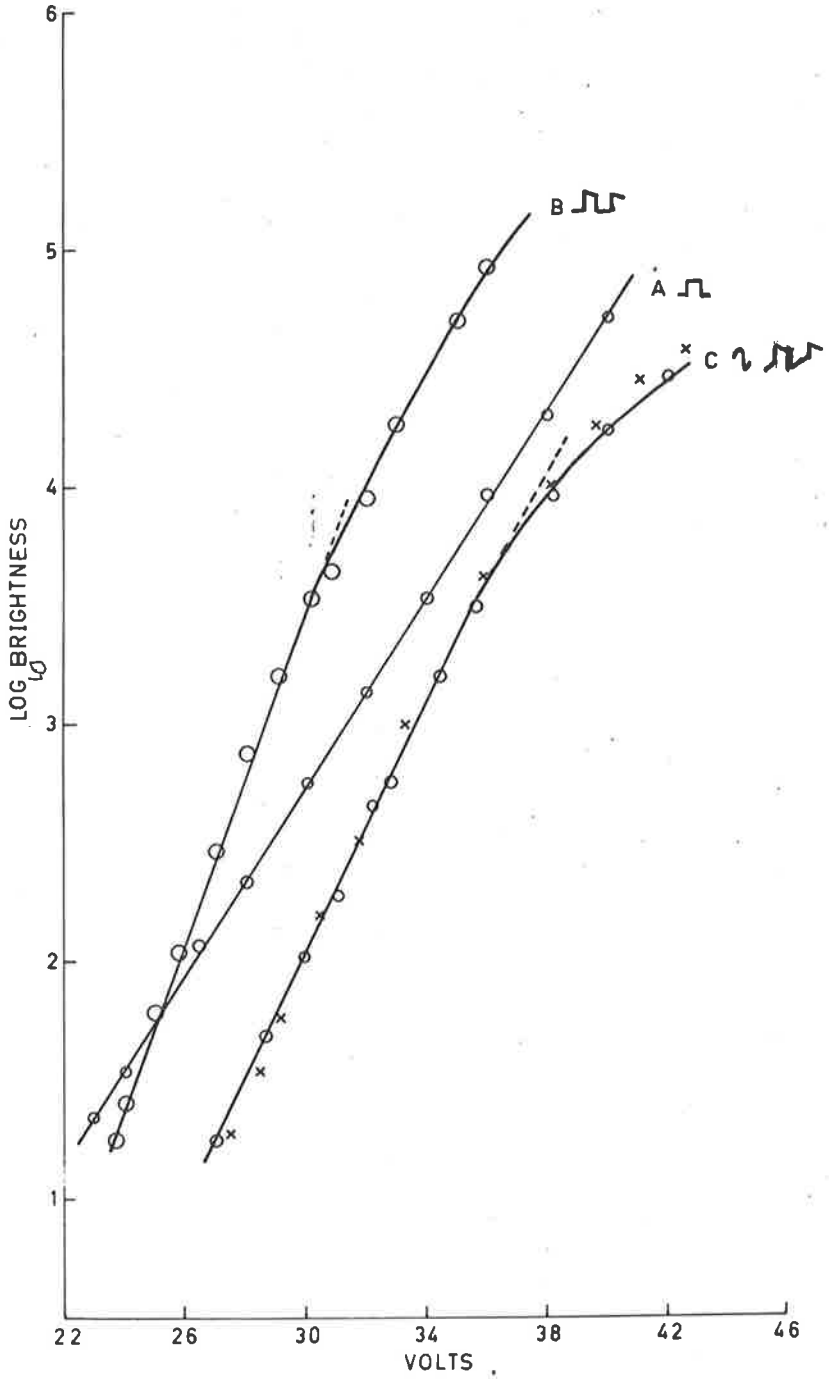


FIG. 8.3 VARIATION OF AVERAGE BRIGHTNESS WITH SQUARE WAVE VOLTAGE (A), DISTORTED (5%) SQUARE (B). CURVE (C) CONTAINS POINTS OBTAINED WITH 20% DISTORTED SQUARE o, AND SINUSOIDAL VOLTAGE ×.

## 8.2 Intensity of brightness pulses as a function of film thickness and applied voltage

It has been reported by Vlasenko and Popkov (1960) that for a particular film, each brightness pulse increases at a different rate as the applied voltage is increased. For low applied voltage they observed the maximum light pulse when the metal electrode was negative, while at high voltage the maximum appeared when the metal electrode was positive.

The voltage range over which light emission could be detected from evaporated films was usually from some voltage V, to a voltage 2V. The range was limited at high voltage by excessive localized breakdown. The reversal of the voltage polarity associated with the maximum light pulse was not observed here. Figure 8.4 shows how the two brightness pulses increase with applied voltage for a film evaporated from an activated powder (figure 8.4a) and for a film evaporated from a crystal (8.4b).

The film evaporated from the powder shows that the brightness pulse occurring when the metal electrode was positive increased more rapidly than the other as the voltage increased. No reversal in the sense mentioned above, was observed. This difference in the rate of change of the brightness pulses was increased as the frequency decreased. At 0.01 and 0.1 c/s a reversal was observed as is shown in figure 8.4(c)). It may be noted that the magnitude of the current flow through the films did not show this reversal in magnitude as the voltage increased. In fact the rate of increase of the current in this case showed no difference on

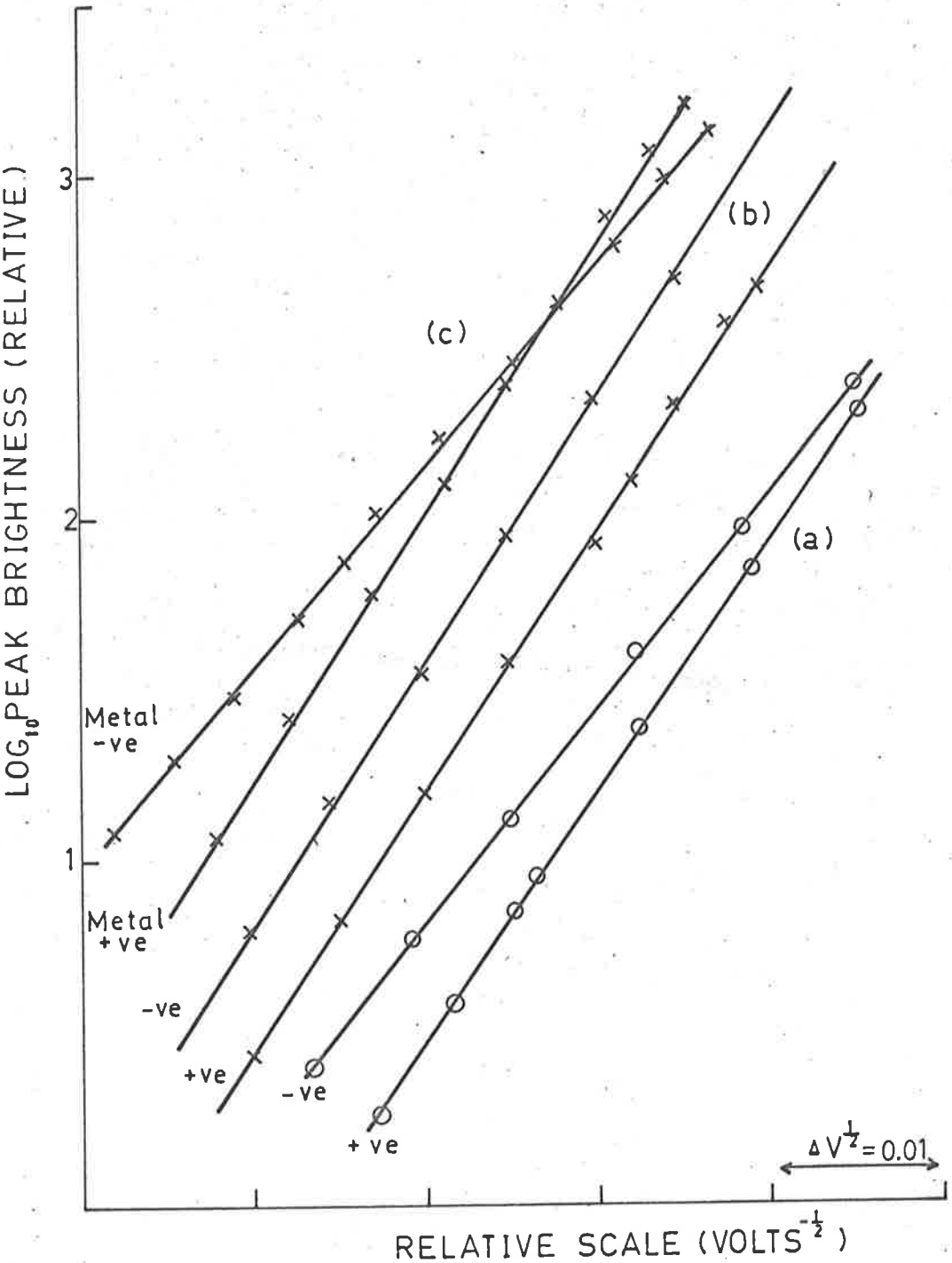


FIG. 8.4 VARIATION OF PEAK BRIGHTNESS FOR FILMS EVAPORATED FROM (a) POWDER, (b) CRYSTAL. CURVE (c) IS TAKEN WITH D.C. EXCITATION.

each polarity. This is shown in Figure 7.17. The remarks in this paragraph concern films which show maximum emission at low voltage during the half cycle when the metal electrode is negative. For films which showed maximum emission at low voltage when the metal electrode was positive, the difference in the rate of increase of each peak was small. There was however, a slightly more rapid increase of the pulse during the metal positive half cycle (i.e. the smaller pulse). For thin films evaporated from crystals of ZnS.Mn, the two peaks generally increased in the same way as the voltage increased. For some films there was a small difference as shown in Figure 8.1 a to d. For thick films, which showed the maximum intensity when the metal electrode was negative, the smaller peak increased more rapidly in a similar way to films evaporated from powders.

The range over which Vlasenko and Popkov varied the voltage applied to their films was V to 2.9V. In an attempt to increase the range of field strength available with evaporated films, films of increasing thickness were investigated. As the film thickness increased, the voltage at which light was just detectable (i.e. an average brightness level) increased as shown in the following table.

| Thickness | Threshold Voltage | $\frac{V}{d}$ volts/cm | $\frac{+ \text{ peak}}{- \text{ peak}}$ (av.) |
|---|---|---|---|
| 600 | 25 | $4.20\ 10^6$ | 3.5/1 |
| 950 | 33 | $3.55\ 10^6$ | 3/1 |
| 1700 | 40 | $2.35\ 10^6$ | 2/1 |
| 2900 | 46 | $1.13\ 10^6$ | 1/1 |
| 5500 | 57 | $1.04\ 10^6$ | 1/3 |

Column 3 shows the value of the threshold voltage divided by the film thickness. If barriers at the electrodes are important this ratio will not define the magnitude of the internal electric field. However it has been shown that for thick films (about 2000A), there is an appreciable field in the bulk. Although the presence of space charge will distort the linear potential gradient across the film, the value may not be very different from $E = {}^{V}/_{d}$. This may not be sufficiently accurate for very thin films, for example of thickness 600Å. This problem will be discussed further in Chapter 10.

It was observed for thin films where $t < 2500A$, that the maximum light pulse occurred when the metal electrode was positive. For films of greater thickness, the maximum emission occurred when the metal was negative. It was not possible to predict the peak/peak ratio from a knowledge of the film thickness since there was always some variation depending on the electrical history of the film (Chapter 8.1). However the reversal of the polarity associated with the maximum pulse was well established.

From column 2 above, a relatively low voltage gives rise to maximum emission during the metal-positive half cycle while a high voltage gives maximum emission on the opposite half cycle. It should however be noted that the smallest voltage implied the largest field strength. The results of the changing polarity for the most intense brightness pulse obtained here, agree with the observations of Vlasenko if it is assumed that the magnitude of the field strength and not

that of the applied voltage determines the value of the peak/peak ratio. In comparing results obtained from films of varying thickness with those obtained under conditions of constant thickness, any changes in the emission processes due to the changing thickness must be carefully considered. It seems likely that such thickness dependent changes do occur. For example, as evidenced by the change in the voltage dependence of the average brightness reported in Chapter 7.4.1, page 158.

It was not possible to obtain a value of the peak/peak ratio at constant voltage as the film thickness increased because of the increasing threshold voltage. It was however possible to obtain this ratio at the same voltage for two films, not very much different in thickness. In this case a common voltage V could be found which gave a low brightness from the thicker film and a high brightness from the thinner film. The peak/peak ratio could be observed then as a function solely of the film thickness. A number of films of different thickness investigated in this way, showed that the peak/peak ratio was dependent on the film thickness at constant voltage.

## 8.3 Constant component of light emission excited by an A.C. voltage

When the brightness waveform was displayed on a D.C. oscilloscope, the presence of pulses superimposed in many cases on a constant light level was observed (figure 8.2). This constant component has been noted by Georgobiani and Fok (1958) for a ZnS.Cu,Al powder phosphor. They attributed

the emission to the formation of holes in the valence band thermally released from ionized copper centres. This is a plausible explanation for luminescent centres which are ionized but is of doubtful significance if manganese centres are present.

It should be noted that if the decay of a brightness pulse is incomplete before the following pulse begins, a constant component of the emission will appear,(chapter 8.1). This effect will occur at about 800 c/s, and has been observed from films evaporated from crystals. The amplitude of this constant component increases with frequency as expected.

The constant component of emission at low frequencies was not always observed. Films deposited from ZnSe.Zn,Mn crystals and from activated ZnS powders showed no trace of this component. It was observed from some (N.B. not all) films evaporated from ZnS.Mn crystals. This shows that this constant component is not a fundamental property of electroluminescent films.

When observed, the constant component (Bd.c.) increased in the same way with voltage as the peak brightness (Bp) and the average brightness Bav as shown in figure 8.5. No change in the spectrum of the emitted radiation was observed when the constant component was present. Increasing frequency of excitation also increased the magnitude of the constant component. This effect is simply caused by the overlap of the two brightness pulses on each cycle.

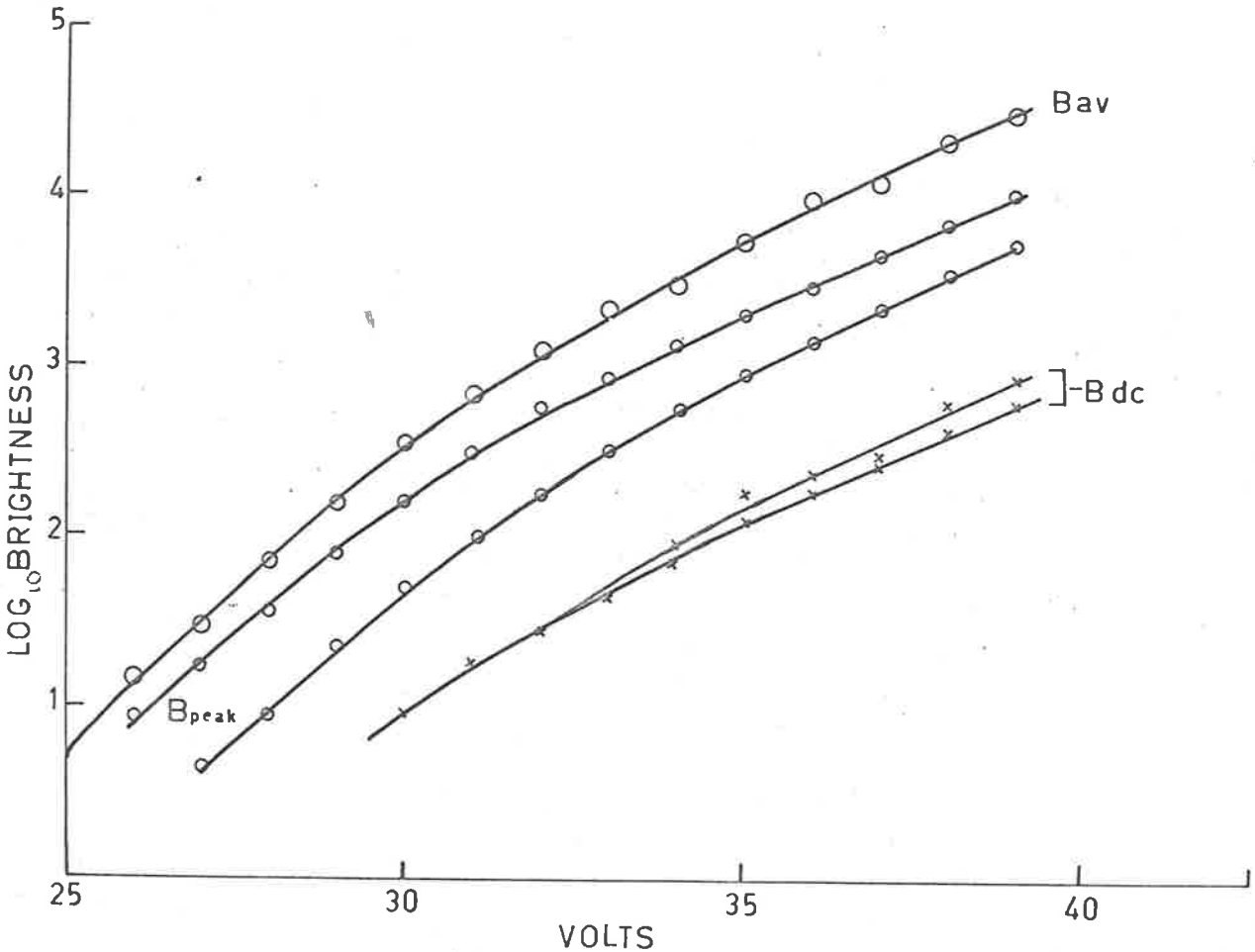


FIG 8.5 AVERAGE EMISSION (Bav), PEAK BRIGHTNESS (B peak) AND D.C. COMPONENT OF BRIGHTNESS (B dc) AS A FUNCTION OF A.C. VOLTAGE (300 c/s).

It was found that if a film was provided with a new electrode, no constant component was present. However, if the film was operated for a considerable time at high voltage so that the electrode was badly affected by destructive forming, the constant component appeared. A correlation between the destruction of the electrode by localized arcing and the constant component was also suggested by a study of films of ZnS.Mn containing added zinc. The addition of zinc to the ZnS.Mn crystals used for evaporation increased the forming in these films (Chapter 7.5.1). The magnitude of the constant component increased threefold as the zinc concentration increased from $3.10^{-4}$ to $1.10^{-2}$ gm/gm. There was however, no change in spectrum of the emitted radiation.

An explanation of the constant component should therefore be obtainable in terms of the changes brought about in the films by the destructive forming. It is possible that the localized breakdown gives rise to new levels in the band gap of the ZnS. It is known that defects may be caused by bombardment with high energy particles or x-rays (e.g. Kulp and Kelley, 1960). The breakdown of regions of the film may cause the formation of such defect levels. These levels must lie about 2ev from the conduction band edge (since the emitted spectrum is unchanged) and they must be ionizable levels so that emission can occur by delayed recombination (see page 147). This will give rise to the constant level because of presence of light about the zeros of voltage (figure 8.2b). Similar radiative recombination has been observed at dislocations in Germanium by Gippius and Vavilov (1963).

This explanation is difficult to justify. A more simple explanation is available if the width of the brightness pulses is increased by the excessive electrode destruction. The necessity for a higher voltage to produce emission after the electrode has been affected may give rise to this increase. Then the constant component is simply due to overlapping of the pulses. This model of the emission process may be reasonable in view of the many complex effects observed in the brightness waveforms.

## 8.4 Excitation by combined A.C. and D.C. voltage

If light emission is observed on each polarity of an applied voltage it is important to decide whether excitation of manganese centres occurs during each half cycle or if excitation occurs on one half cycle followed by recombination on the next half cycle. Thornton (1961a) investigated films of ZnS.Cu,CL prepared by a diffusion method and found emission only when the metal electrode was positive. He found that a D.C. bias of either polarity decreased the emission and concluded that excitation occurred during the negative half cycle while field driven recombination occurred during the positive half cycle. By decreasing either of the voltage swings the emission was reduced, so both half cycles were clearly essential to the light emission process.

A D.C. bias (from a dry cell) was used in series with the electroluminescent film to vary the zero point of the applied sinusoidal alternating voltage. The films did not show any detectable emission when the D.C. voltage was applied

without the A.C. These films showed D.C. electroluminescence, but at higher voltage than used here. If the magnitude of the D.C. bias was equal to half the peak to peak value of the A.C. voltage, the light emission waveform showed only one peak per cycle, when the D.C. and A.C. voltages were of the same polarity. For smaller D.C. voltages there was an increase in the emission when the A.C. and D.C. were of similar polarity and a decrease when they were opposed.

The amplitude of the peak to peak voltage required to maintain a constant <u>average</u> brightness level, is shown below. The values given refer to two average brightness levels $B_1$ and $B_2$ which are two orders of magnitude apart.

The results were obtained from a film which gave maximum light emission when the metal electrode was negative.

Low average brightness $B_1$

| D.C. volts | P/P A.C. volts | Maximum positive voltage | Maximum negative voltage |
|---|---|---|---|
| 0 | 8.0 | 4.0 | 4.0 |
| 2 | 8.25 | 6.1 | 2.15 |
| 4 | 7.5 | 7.75 | - |
| 6 | 9.0 | 10.5 | - |

High average brightness $B_2$

| D.C. volts | P/P A.C. volts | Maximum positive voltage | Maximum negative voltage | peak + / peak - |
|---|---|---|---|---|
| 0 | 12.0 | 6.0 | 6.0 | 1/2.3 |
| 2 | 12.0 | 8.0 | 4.0 | 1/2 |
| 4 | 11.5 | 9.75 | 1.75 | 2/1 |
| 6 | 10.5 | 11.25 | - | positive only |

A change of 0.5 volts is significant because such a change gave a variation in the brightness of about 20%.

A D.C. voltage of approximately 3.0 was required to equalize the peaks and at D.C. levels greater than this, the positive peak predominated. This is clearly a result of the increasing positive excursion of the A.C. voltage.

If the D.C. voltage was applied so that the metal electrode was negative (to the D.C.), the peak/peak ratio increased from 2.3:1 until no emission could be observed during the metal-positive half cycle (now the zero of the unidirectional alternating voltage).

The same results were obtained if films were used which showed a maximum of light emission when the metal electrode was negative, viz. an enhancement when the A.C. and D.C. voltages were in the same direction.

Further evidence of excitation followed by prompt recombination was obtained by using a clipped sinusoidal voltage excitation as used by Thornton, (1961). A reduction in the emission intensity on the half cycle which was clipped was observed, while the brightness peak on the other half cycle was unchanged.

The observations of strong emission produced by a unidirectional voltage of either polarity proves that excitation and recombination are rapid. This is to be expected if the manganese ion is involved in the emission process because after excitation, the emission process is controlled only by the decay time of the excited state of the $Mn^{++}$ ion involved in the luminescent transition. This observation

may explain why phosphors containing manganese show strong electroluminescence when excited by D.C. voltages. This has been reported by a number of authors, for example Goldberg and Nickerson (1963). Once a manganese ion has been excited recombination must follow in about one millisecond. The centre is then available for re-excitation. For a centre which can be ionized (e.g. copper) the ionized electrons are swept away from the centres so that no rapid recombination can occur. If the applied voltage is of constant direction all the excited electrons become localized at the anode. This may reduce the net internal field if the electrodes are blocking. No emission would be observed from such a system.

## 8.5 Nature of the electrode contact to electroluminescent films

### 8.5.1 Effects of insulating silica layers

It has been shown in Chapter 6.1 that an aluminium electrode or a metal with a silica layer forms a necessary component of an evaporated film if electroluminescence is to be observed. The dependence of the light emission on the nature of the electrode was further investigated by modifying the electrode contact to the ZnS film. The results in this section describe some changes in the peak brightness caused by artificial barrier layers. Only two brightness pulses per cycle of the exciting voltage were observed (for triangular, square, or sinusoidal voltages). This contrasts with the more complex waveform obtained from ZnS.Cu Cl films by Harper (1962) using triangular voltages.

Figure 8.6 shows the peak brightness - voltage relation for a thin (500Å) ZnS.Mn film with increasing thickness of silica under the aluminium electrode. The main brightness peak occurred for the metal positive if no silica was present, and the peaks increased at the same rate with increasing voltage. However the presence of the artificial barrier layer markedly increased the metal negative peak relative to the positive, also increasing the voltage at which light emission occurred. The peaks increased at the same rate at low voltage, but at higher excitation levels the metal negative peak showed decreased slope so that the peak/peak ratio decreased. A reversal at an observable light level, occurred for thicker silica films together with a further decrease in slope.

As the silica thickness increased the voltage drop across the ZnS layer decreased. The threshold voltage (to obtain a given average brightness) is shown in the following table together with the resistive component of the film impedance. The capacitance was such that this component of the impedance could be neglected in determining the voltage across the ZnS and the $SiO_2$ layers. The values of resistance which were obtained by balancing the bridge of the voltage zero balance point (chapter 2.8) implied that the resistance for ZnS alone was 300 K ohms while the resistance of the ZnS with 700A of silica was greater than 20 megohms. For ZnS with 1160A of silica the resistance was 2.7 megohms. This anomolous behaviour was not observed if the values of resistance were obtained by balancing the A.C. bridge at the

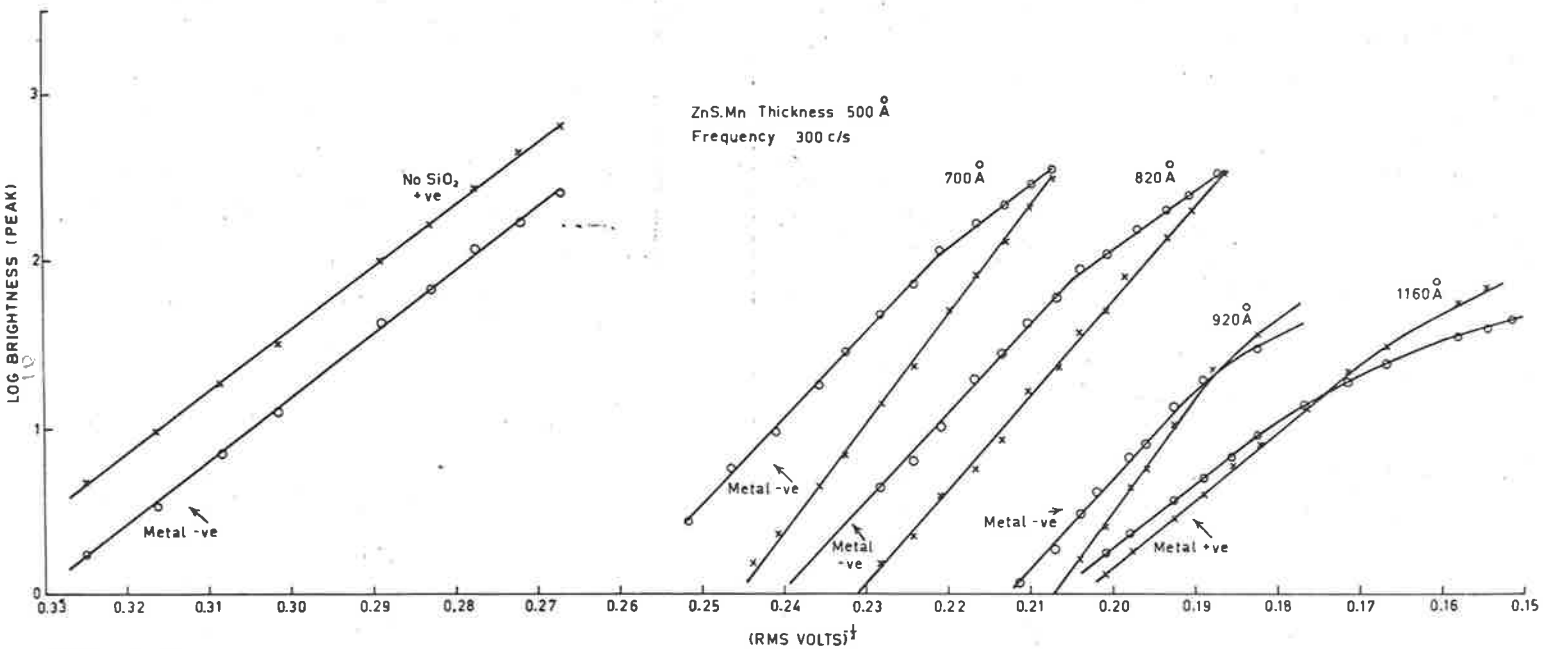


FIG. 8.6 PEAK BRIGHTNESS - VOLTAGE RELATION FOR INCREASING $SiO_2$ THICKNESS BETWEEN ALUMINIUM AND ZnS.Mn.

two points coincident with the two brightness pulses. The values of resistance at these two points were different on each half cycle. For the films studied this variation was, at the most, 25%. The values below represent an average which is sufficient to demonstrate the trend of the results. Some change appeared in the spectrum of the emitted radiation when silica layers were present between the aluminium electrode and the ZnS. The spectrum was the same for all thicknesses of silica. The voltage threshold for the ZnS.Mn film (9.5 volts) given below has been obtained from the measured value by correcting the measured value for the changing spectral response of the detector. The spectral change of the emitted light is discussed in chapter 8.5.1.

| Silica thickness (A) | Threshold volts R.M.S. | Resistance (AC) of composite film | Volts over ZnS | Field in $S_1O_2$ layer V/cm. |
|---|---|---|---|---|
| Zero | 9.5 | 200K | 9.5 | - |
| 200 | 10 | 250K | 8.0 | $1.0\ 10^6$ |
| 700 | 16.5 | 500 | 6.6 | $1.40\ 10^6$ |
| 820 | 19.0 | 630 | 6.0 | $1.60\ 10^6$ |
| 1000 | 23.4 | 800 | 6.0 | $1.75\ 10^6$ |
| 1160 | 26.5 | 1100 | 5.5 | $1.80\ 10^6$ |

It is clear that as the silica layer is increased in thickness, the voltage across the ZnS.Mn layer required to maintain a constant average brightness decreases. Therefore the presence of the barrier layer must give rise to an increase in light from the sulphide film.

Figure 8.6 shows that 700A of silica causes the maximum brightness pulse to occur when the metal electrode is negative, that is, the reverse half cycle to when no silica was present. This indicates that the modification to the electrode (by the silica) did not result in hole injection into the bulk film, but rather in a change in the electron injection through the electrode. It is assumed that the function of an electrode barrier (whether due to $Al_2O_3$ or silica) is to inject electrons into the film with energies greater than thermal energy. This will occur only when the metal electrode is the cathode. The decreasing slope of the brightness - voltage curves with increasing silica thickness was thought to be due to a voltage dependent energy loss in the silica layer. This decrease would also explain the decrease in intensity of the emission peak when the metal electrode was negative (figure 8.6).

For ZnS films with 200 and 700A of silica a component of the emission excited at higher voltage was observed in the wavelength range between 4000 and 5000A. This agrees with the proposed injection of higher energy electrons which could then excite deeper levels (see chapter 8.5.2).

The effect of similar thickness layers between the conducting glass electrode and the ZnS film (500A) was not so marked as for layers beneath the metal electrode. Increasing silica thickness reduced the peak to peak ratio slightly (10%) and caused a reduction (threefold) in the slope of the brightness - voltage curves for both brightness peaks.

It has been shown (chapter 8.4) that excitation of luminescent centres can occur on each half cycle of an applied A.C. voltage. Also each peak showed the same voltage dependence, (figure 8.5), although for films evaporated from powders the slope of their increase was different for each peak. Thus the mechanism of light production on each half cycle must be similar. Electron injection across the insulator can only account for the brightness pulse when the metal electrode is negative. This suggests that some barrier exists at the conducting glass electrode to account for the brightness peak when the aluminium is negative. Some authors consider that the conducting glass electrode forms a low resistance contact to ZnS, because of the low resistance observed when other metals are used in place of aluminium. It has been shown in chapter 6.1 that such an observation does not conclusively prove that the tin oxide gives a low resistance contact. In the presence of surface states a barrier will exist at the conducting glass - ZnS interface. In fact n-$n^+$ junctions (Oldham and Milnes 1963), provide a good degree of rectification.

It may be reasonable to suppose that electrons injected from the conducting glass electrode may have energy greater than thermal energy, that is with energy sufficient to pass the electrode barrier. The small effect of silica layers on this electrode shows that the injecting properties are not improved by artificial layers. In fact energy loss in these layers can account for the small decrease in the peak corresponding to injection from the conducting glass (viz

metal positive). The relative excitation occurring from injection at the two electrodes is discussed in chapter 10.

The results described above were taken from a thin (500A) ZnS film which showed the most intense brightness pulse when the metal electrode was positive. It was of interest to see if similar effects occurred for films which gave maximum emission on the metal negative half cycle. This required films of thickness greater than about 2500A, (chapter 8.2). Silica layers of similar thickness to those used above gave rise to no noticeable change in the peak to peak ratio. If layers were provided of comparable thickness to the ZnS film, it was found that this ratio decreased slightly (20%) when the layer was on the conducting glass and increased by about the same amount when it was under the metal electrode. No reversal of the peak emission was obtained by using silica on the transparent electrode (cf. reversal observed above with silica under the metal electrode). This was interpreted as showing that for a thick film, the peak intensity is not so sensitive to the electron supply from the electrodes. In this case the bulk of the ZnS film appeared to play a more important role than in thinner films.

### 8.5.2 Transparent cadmium oxide electrodes and other multiple film structures

Studer and Cusano (1955) have reported the properties of ZnS.Mn films prepared by a chemical reaction and deposited on transparent conducting titanium dioxide. This is the only report of electroluminescence not using a tin oxide electrode, (except for large crystals).

Transparent CdO films were prepared by cathodic sputtering (chapter 3.2). A number of ZnS.Mn films were deposited simultaneously on CdO and $SnO_2$ coated glass and the light emission from each film was measured as a function of voltage. The variation of average brightness with voltage was independent of the nature of transparent electrode. The peak to peak ratio was also independent of the electrode used.

The Fermi level in the sulphide is fixed at the same position as the Fermi level in the transparent electrode. The energy difference between the Fermi level and the conduction band edge in the CdO or $SnO_2$ will be approximately the same. Therefore the details of the energy band diagram at the interface will be relatively unchanged if CdO is used instead of $SnO_2$. There may be small changes in the electron supply across the interface. However a much more dramatic change should occur at the Valence band edge, since the band gap Eg of ZnS is 3.7ev while Eg for CdO is 2.5ev (Lakshmanan 1963) and Eg for $SnO_2$ is 4.2ev (Bube 1960). If the emission process was dependent on hole injection from the electrode, the change of the electrode material would certainly be reflected in the observed light intensity. As there are no such changes the light emission is not solely a minority carrier phenomenon.

ZnTe is a good hole emitter into materials such as ZnS and ZnSe as discussed by Fischer (1961). Films of ZnTe were evaporated, using two boats in the vacuum system, to form films between the $SnO_2$ and the ZnS, and between the ZnS and the aluminium electrode. The ZnTe crystals were

grown in the apparatus described in chapter 4. For either of the above structures the observed brightness was changed very little by the presence of these films. A slightly higher threshold voltage was required because of high resistance ZnTe films. Thus the conclusion of negligible minority carrier effects is confirmed.

There are obvious advantages in constructing a perfectly symmetric film structure. This is possible with CdO electrodes because an electrode can be deposited on the ZnS film without raising its temperature more than about 30°C. However ZnS between two CdO electrodes showed no light emission although the voltage applied was greater than the threshold for emission from the ZnS film. The film resistivity was low. This negative result shows that if a barrier exists at the ZnS - transparent electrode, it is not sufficient to give light emission without an additional barrier layer at the other electrode. If silica layers were introduced at each CdO - ZnS interface (still a symmetric film structure), light was observed. The waveform of the light emitted from this structure showed two nearly identical brightness pulses. This suggests that a symmetric structure emits an identical brightness pulse on each half cycle. However because of the sensitivity of the peak to peak ratio to small changes in the electrical history of the films (chapter 8.1), this conclusion must not be considered as proved conclusively.

A feature of all multiple layer films was the presence of a low conductivity layer if electroluminescence was to be observed.

It was reported earlier that a film evaporated from a ZnS melt grown crystal was not electroluminescent (chapter 7, page 143). The presence of as little as 0.01% of manganese was sufficient to produce strong emission. A layer of this pure ZnS (with excess zinc) was ideally suited for experiments with multiple layer films because the properties of the ZnS films were identical to those of the ZnS.Mn film, except that the former showed no light emission.

An important problem in electroluminescent systems is the location of the emission region, whether at the electrodes or throughout the interelectrode space, (see chapter 1 for a review). If light emission from films occurs only in a thin region next to the electrodes the deposition of films of pure ZnS either side of a ZnS.Mn film should prevent excitation of manganese centres. In such a system the material directly in contact with the electrodes is not electroluminescent. The evaporations were carried out consecutively without admitting air to the evaporating chamber. Such a structure showed light emission in the form of two brightness pulses per cycle of the applied voltage. The emission from a ZnS.Mn film with (a) ZnS between the conducting glass and the ZnS.Mn and (b) ZnS under the metal electrode, was compared. The spectrum of the emitted light from (a) was the same as for the ZnS.Mn film with no other layers. However the spectrum from (b) showed a shorter wavelength component, similar to that observed from thick ZnS films (figure 7.2). The intensity between 4000 and 5000A was about 5% of the intensity of the manganese

peak (5860Å). The value of threshold voltage was corrected for the changing response of the detector for structure (b) and was found to be 75 volts. The threshold for structure (a) was 82 volts and for the ZnS.Mn film itself it was 75 volts. For thin ZnS.Mn films with pure ZnS under the metal rapid destruction of the metal electrode occurred at high voltages. Thicker films were less affected.

The results of these experiments proved that light was not emitted solely from the regions near the electrodes. The power threshold for the film with a ZnS layer under the metal electrode indicated that more light was being emitted from the ZnS.Mn film than if no pure ZnS layer were present. This would occur if electrons were able to gain energy in crossing the pure ZnS layer which was available to excite more centres in the ZnS.Mn film. This would account for the similarity in the spectrum of the radiation observed from these structures and from ZnS.Mn films with silica layers under the metal electrode (page 202).

The observation of shorter wavelength emission from thin ZnS.Mn films with artificial layers under the electrodes, shows that luminescent centres are available which are not excited when a ZnS.Mn is operated in the conventional way. This should be compared to the results described in chapter 7, page 144, which showed that this short wavelength emission could be observed from thick films but not for thinner films. The results described here prove that these levels are present in films of all thickness, but are apparently not excited in films less than about 2000A thick. The problem of the energy of the electrons entering the ZnS.Mn film will be considered in chapter 10.

# 9 Properties of electroluminescent films of other II-VI compounds

## 9.1 ZnSe.Mn,Zn and ZnSe.Mn films

ZnSe.Mn,Zn and ZnSe.Mn films were used to provide important information concerning the problem of the critical substratetemperature required for the evaporation of electroluminescent films (see chapter 4). It was reported in chapter 4.4 that electroluminescent films could be prepared with no excess zinc, provided the amount of manganese in the crystals used for evaporation was about 1%. The properties of these films were very similar, except for their spectra, to those evaporated from ZnSe.Mn,Zn crystals. This is an important result, because it shows that centres which are not ionized, only excited, are sufficient to produce electroluminescence in these evaporated films.

A number of measurements were taken from films of ZnSe.Zn,Mn and these will be briefly reported. By the complete evaporation of doped crystals of ZnSe and ZnS, it was assumed that a given impurity content could be transferred to films of ZnSe and ZnS although the evaporating temperatures of each were slightly different. Therefore a comparison between films of ZnS and ZnSe should be valid. It must be noted however that such a comparison must be carefully considered because of the many differences which exist between ZnS and ZnSe, for example the energy band gap (page 144).

Figure 9.1 shows the brightness - voltage curves for several ZnSe.Zn,Mn films with increasing manganese content

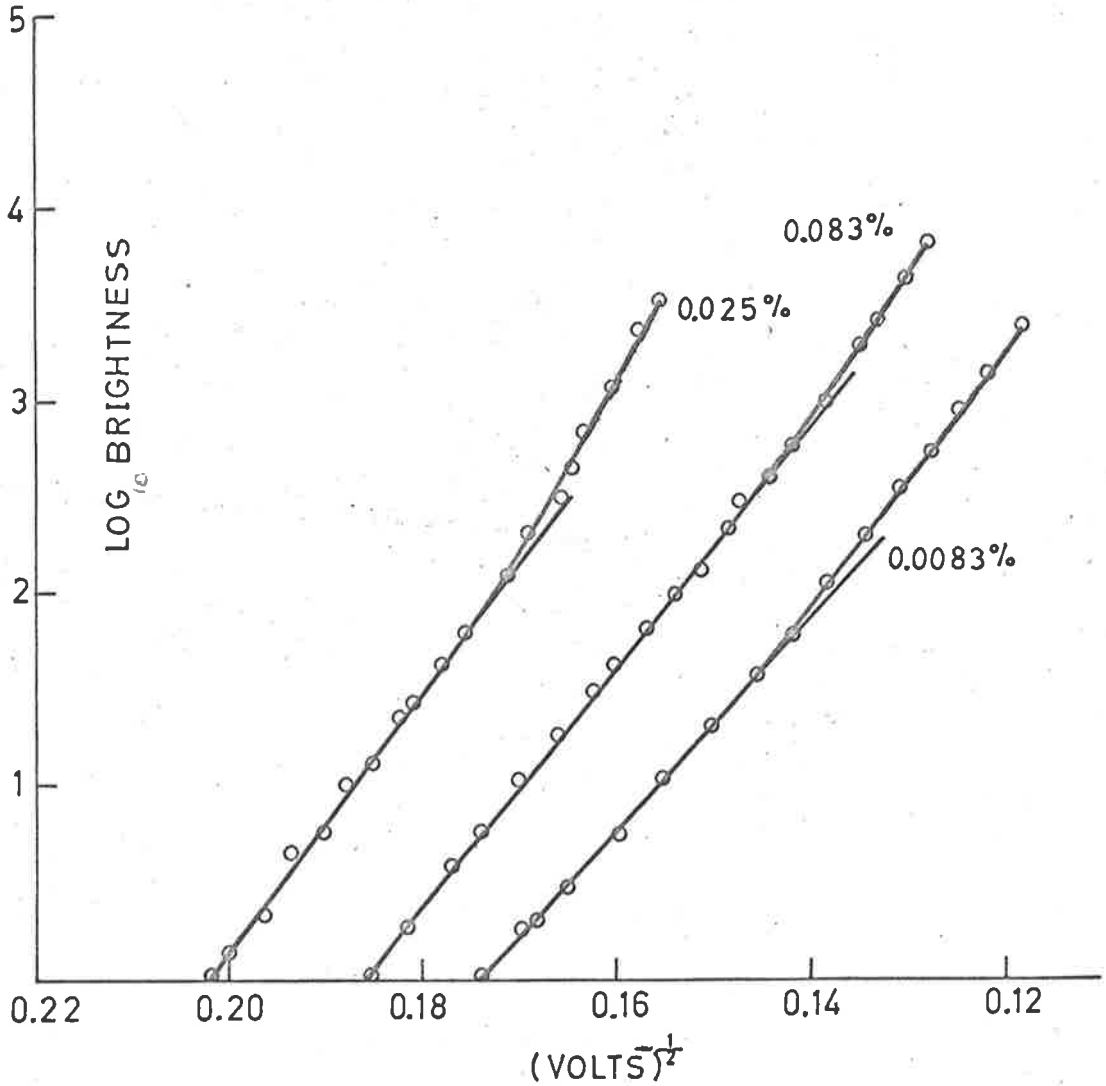


FIG. 9.1 A.C VOLTAGE DEPENDENCE OF BRIGHTNESS FOR ZnSe.Mn FILMS.

as parameter. The curves show two linear regions, similar to some reported earlier for ZnS.Mn films (chapter 7.3).

The voltage threshold (an indication of the brightness) decreased as the activator concentration increased from 0.008 to 0.25%. This behaviour should be compared to the effect of increasing manganese concentration in ZnS.Mn films, where a rapid increase in forming occurred at about 0.1% (page 175). This increase in forming was observed at about 0.8% Mn for ZnSe.Mn,Zn films. If $Mn^{++}$ ions are incorporated in interstitial positions, this apparent increase in solubility of the ions in ZnSe, may be due to the increase in lattice spacing (5.41Å for ZnS and 5.46Å for ZnSe). However the change in lattice spacing seems rather too small to convincingly describe this effect.

As observed for ZnS.Mn films, there was a correlation between the threshold current and the threshold voltage (see page 164). This is shown in the following table. It is also apparent that the slopes of both linear regions of the brightness - voltage curves increased with manganese concentration. This suggests that the rate of increase of brightness with voltage is limited by the number of luminescent centres available at low concentrations. The rate of increase of brightness (i.e. the slope of these curves) is reduced in the same range of manganese concentration in ZnS.Mn films (page 175). Therefore it appears that the conditions for excitation of centres are more favorable in ZnSe.Zn,Mn films.

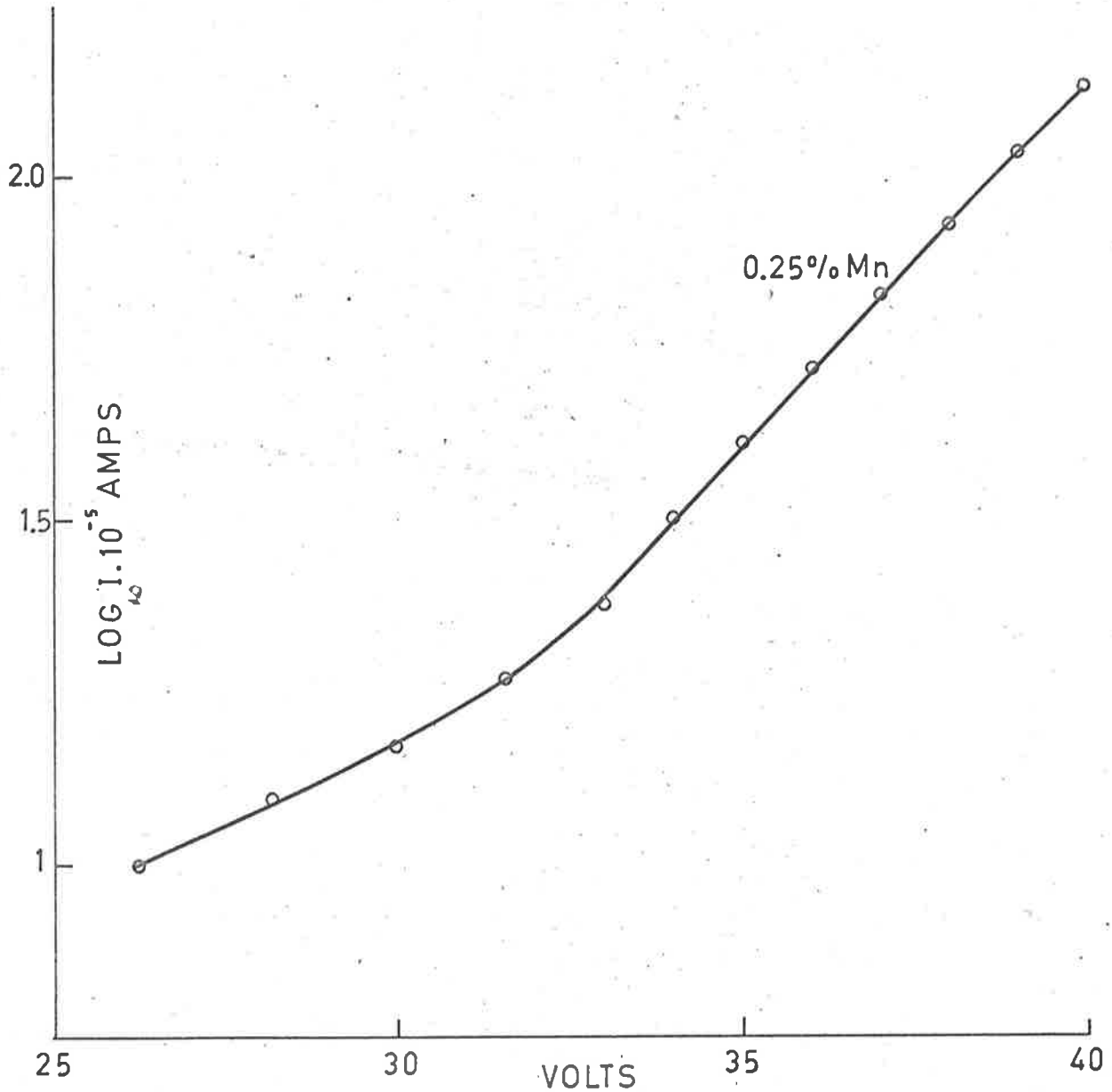


FIG. 9.2 TYPICAL INCREASE IN CURRENT WITH VOLTAGE FOR ZnSe. Mn. Zn.

| Manganese Concentration, % | High Voltage Slope | Low Voltage Slope | Voltage Threshold (volts) | Current Threshold (amps) |
|---|---|---|---|---|
| .0083 | 149.5 | 127.5 | 33 | $7.3\ 10^{-5}$ |
| .025 | 160 | 136 | 33 | $7.5\ 10^{-5}$ |
| .083 | 168 | 144 | 29 | $8.8\ 10^{-5}$ |
| .25 | 209 | 153 | 24.5 | $10.0\ 10^{-5}$ |
| .83 | 235 | 162 | 24.5 | $11.0\ 10^{-5}$ |

The results in this table show that the resistive component of the A.C. current at the threshold is of approximately the same magnitude as for comparable ZnS.Mn films. However the rate of increase of the current was much more rapid for ZnSe.Mn,Zn. Over the useful light emission range the current increased by a factor of about 30 (compared to about 3 for ZnS.Mn films). Although the current increase was more rapid a corresponding increase in the rate of change of brightness with voltage was not observed. In fact the slope of the brightness - voltage curves was not so great as for sulphide films. Discontinuities in the current curves occurred at the same voltage as those observed in the brightness curves (figure 9.2). The increased current through the films gave a brightness variation with current (due to an increasing voltage) of the form

$$B = \text{const. } I^n$$

where $n = 5\text{-}6$ at low voltage

$n = 2.5$ at high voltage.

It is clear that most of the electrons which contribute to the current do not excite manganese centres. Because the impurities in the films are similar, the reason for this increase appears to be in a change in the rate of supply of electrons from the electrodes. This is likely because of the large change in band gap from ZnS (3.7ev) to ZnSe (2.6ev).

The waveforms of the emitted light were similar to those from ZnS.Mn films. The two brightness pulses occurred over a shorter time than in ZnS.Mn films and this resulted in well separated pulses at all frequencies (up to 10 kc/s). Even at these frequencies the brightness waves were not associated with any troublesome noise level (cf ZnS.Mn, page187 ). However, some asymmetry, in the sense defined in chapter 8.1, was observed following the main brightness peak. It was observed that for ZnSe.Zn,Mn films about 1500A thick, the maximum light pulse occurred during the half cycle when the metal electrode was negative (cf ZnS.Mn where for films of this thickness the maximum occurred during the opposite polarity). Thicker films of ZnSe (and ZnS) showed maximum emission when the metal electrode was negative.

## 9.2 CdS.Mn and ZnTe.Mn films

To extend the range of materials from which electroluminescence was observed, a number of films of ZnTe and CdS were made. A 1% excess of zinc was added to ZnTe.Mn crystals but the resulting films were high resistance and not electroluminescent. ZnTe is a p-type semiconductor and this explains why the excess zinc (a donor) does not lead to a decrease in resistance. It should be possible to dope the

films with excess sulphur, for example, or other acceptors to produce the light emission effect. This may require a similar investigation of the properties of these materials to that reported in this thesis for an n-type material.

CdS is an n-type material which may be easily evaporated. CdS.Mn powder was evaporated, but the film resistance was < 500 ohms. This was true for a range of substrate temperatures and for several different evaporating techniques. It is probable that the films contain a high concentration of excess cadmium (donors) due to dissociation of CdS in the evaporating boat. It is clear that the problem involved here is to increase the film resistivity.

## 9.3 Summary

In general the results obtained from ZnSe films were similar to those obtained from ZnS films. The most important difference appeared to be the more rapid increase of resistive current with voltage. This implied a decreasing efficiency, relative to ZnS.Mn films, because the increased current did not give rise to a corresponding increase in brightness. It must however, be pointed out that a complete comparison between ZnSe and ZnS electroluminescent films would require a more extensive study of ZnSe films than has been reported here.

## 10. DISCUSSION OF THE ELECTROLUMINESCENT PROCESS IN EVAPORATED FILMS

Electroluminescence is a high field effect in films of ZnS and ZnSe. The range of voltage over which useful measurements can be made is small and limited at higher voltage by breakdown of the films. It is realized that there may be more than one satisfactory explanation for many of the results described in the previous three chapters. A model of the emission process in the presence of an electric field will be discussed in the following sections. This model supposes that light is due to acceleration of electrons to sufficient energies so that excitation of manganese centres can occur. In so far as these ideas were originally suggested by Piper and Williams (1955, 1958) the model proposed here is similar to that proposed by those authors.

The fundamental problem facing an interpretation of any results is the electric field distribution between the electrodes. This magnitude of the field clearly determines the probability of all field controlled energy gain processes, while the field distribution determines the location of the light emission region.

It has been shown that light emission is produced in the bulk of the film by the multiple layer films (page 207). Therefore, the model proposed is one in which there are contributions to the light from the regions adjacent to each electrode and from the volume of the film i.e. relatively far from the electrodes. Of course if the potential gradient across the film is linear, these three regions are

indistinguishable.

## 10.1 Low conductivity layers

Light is emitted from films on both cycles of an A.C. voltage and for both polarities of a D.C. voltage. The spectrum of the radiation is independent of polarity and the intensity of the brightness pulses is comparable on each polarity. Thus any model of the light emission process must predict comparable effects during each polarity of the applied voltage.

It is certain that an aluminium electrode stabilizes the films, most likely by preventing diffusion of the metal. While this appears to be a necessary condition, there are other well known effects which may occur because of the presence of such layers. For example, the production of hot electrons in Al-$Al_2O_3$-Al structures has been reported by Collins Davies ($19_{64}$ ). It is possible that such injection of high energy electrons into the ZnS can occur when the aluminium electrode is negative. Such injection may effect the electroluminescence process as can be shown by the following reasoning. Seitz (1949) has investigated electron processes in the presence of high fields in polar and non polar materials. One difference between them is that it is difficult to accelerate electrons to energies much greater than thermal polar materials because of a peak in the collision frequency at low energies. If an electron escapes this thermal barrier it remains outside during its subsequent history, as do any secondaries it may produce. Thus the injection of electrons with energy >> kT initiate a departure from equilibrium

which is sufficient to excite manganese centres, whereas if no injection occurred there would be very few electrons capable of excitation.

While such a process may well affect the intensity of the brightness pulse when the metal electrode is negative, it is clear that if such injection is necessary for electroluminescence, light would only occur during this polarity. It must therefore be concluded that the oxide layer associated with the aluminium electrode is primarily a stabilizing device allowing an electric field to be maintained across the film. Artificial barrier layers of silica thus allow operation of films with metal electrodes other than aluminium.

## 10.2 Field Configurations

Because of the apparent complexity of many of the results described in the previous chapters, an attempt will be made to formulate a model to account for the principal findings. These were the following:-

(a) For films thinner than about 1500Å, the brightness varies with voltage according to

$$B = B_o \exp\left(-\frac{b}{V^{\frac{1}{2}}}\right) \qquad \text{--- 10.1.}$$

The emitted radiation is centred about 5860A. The maximum brightness pulse occurs when the metal is positive, and increasing the voltage results in a relatively small decrease in the peak to peak ratio.

(b) For thicker films the emitted radiation has two spectral components.

The brightness measured at 5860Å is given by

$$B = B_o \exp\left(\frac{b'}{V}\right) \qquad \text{--- 10.2}$$

while the brightness at 5000A is given by

$$B = B_o \exp\left(\frac{b''}{V^2}\right) \qquad \text{--- 10.3}$$

For films 1 micron in thickness the intensity of the short wavelength component is 1/20 of the manganese emission peak. The maximum brightness pulse now occurs when the metal electrode is negative (for both wavelengths). Increasing voltage causes more rapid increase of the smaller (metal positive) brightness pulse.

It is considered that excitation of manganese centres occurs by impact excitation. Field ionization is unlikely because no emission occurs for a manganese doped film with no excess zinc.

The probability of impact excitation in a field E is given by

$$p \propto \exp\left(-\frac{b}{E}\right) \qquad \text{--- 10.4}$$

$$p \propto \exp\left(-\frac{b'}{E^2}\right) \qquad \text{--- 10.5}$$

Equation 10.4 is valid at pre-breakdown field strengths if acceleration of statistical electrons is important. If <u>all</u> conduction electrons are accelerated, equation 10.5 is valid. Because of the small free electron density in ZnS.Mn films, equation 10.1 is expected to give the probability of impact excitation.

The width of exhaustion barriers at the electrodes may be about 500Å (chapter 6.5). Thus for a thin film (1500 - 1000Å), most of the volume will be a region where the electric field is proportional to (voltage) $^{1}/_{2}$. If acceleration of electrons and excitation of centres occurs in reverse biased barriers, the probability of excitation should be proportional to exp $(-\frac{b}{V^{\frac{1}{2}}})$. The brightness B is given by the product of the number of electrons x probability of excitation,

$$\text{i.e} \quad B = K \exp \propto V. \quad \exp - \frac{b}{V^{\frac{1}{2}}}$$

where K is a constant.

For current flow in ZnS films $\propto V << \frac{b}{V^{\frac{1}{2}}}$ so that the brightness should be given by

$$B = B_o \exp (-\frac{b}{V^{\frac{1}{2}}}) \qquad \text{--- 10.3a.}$$

This is observed experimentally for thin films. Deviations from equation 10.3a occur if the films are thicker than about 1200A when evaporated from powders, and 1800Å when evaporated from crystals. Clearly the barrier is wider for the higher resistance crystal-films, as expected for exhaustion barriers (Henisch 1957).

It is observed for thin films that the maximum brightness pulse occurs when the metal electrode is positive. This observation may be interpreted in two ways. The barrier field may be greater at the conducting glass electrode giving higher energy electrons. Alternatively, the barrier at this electrode is not as effective as the barrier at the metal electrode but it allows more electrons into the ZnS.Mn film.

Results described later in this section suggest that the metal electrode barrier produces higher energy electrons. As the applied voltage is increased, the importance of the difference in the barrier field at each electrode relative to the applied potential, decreases. Thus the peak to peak ratio will decrease. This should be a small change because for thin films the surface barriers are particularly important.

As the thickness of the film increases, the two exhaustion regions are separated by an increasing bulk region where the electric field may be more nearly proportional to the applied voltage. The current flow through the film is now limited by the bulk resistance. If the emission from the volume of the film is more important than the barrier contribution, the brightness will be given by

$$B = B_o \exp\left(-\frac{b}{V}\right) \qquad \text{--- 10.2a.}$$

This equation describes the experimental brightness variation for 5860A emission (figure 7.10). For thick films it is observed that the maximum brightness occurs when the metal is negative. It has been shown in Chapter 6.3 that charge accumulates preferentially near the metal electrode. This will change the potential distribution on the region near the metal electrode as shown in figure 10.1. For thick films bulk trapping may also occur so that the potential will also be affected in the bulk predominately near the metal electrode. The net effect is to increase the bulk field when the aluminium is negative and reduce this field when the aluminium is positive. Therefore if the

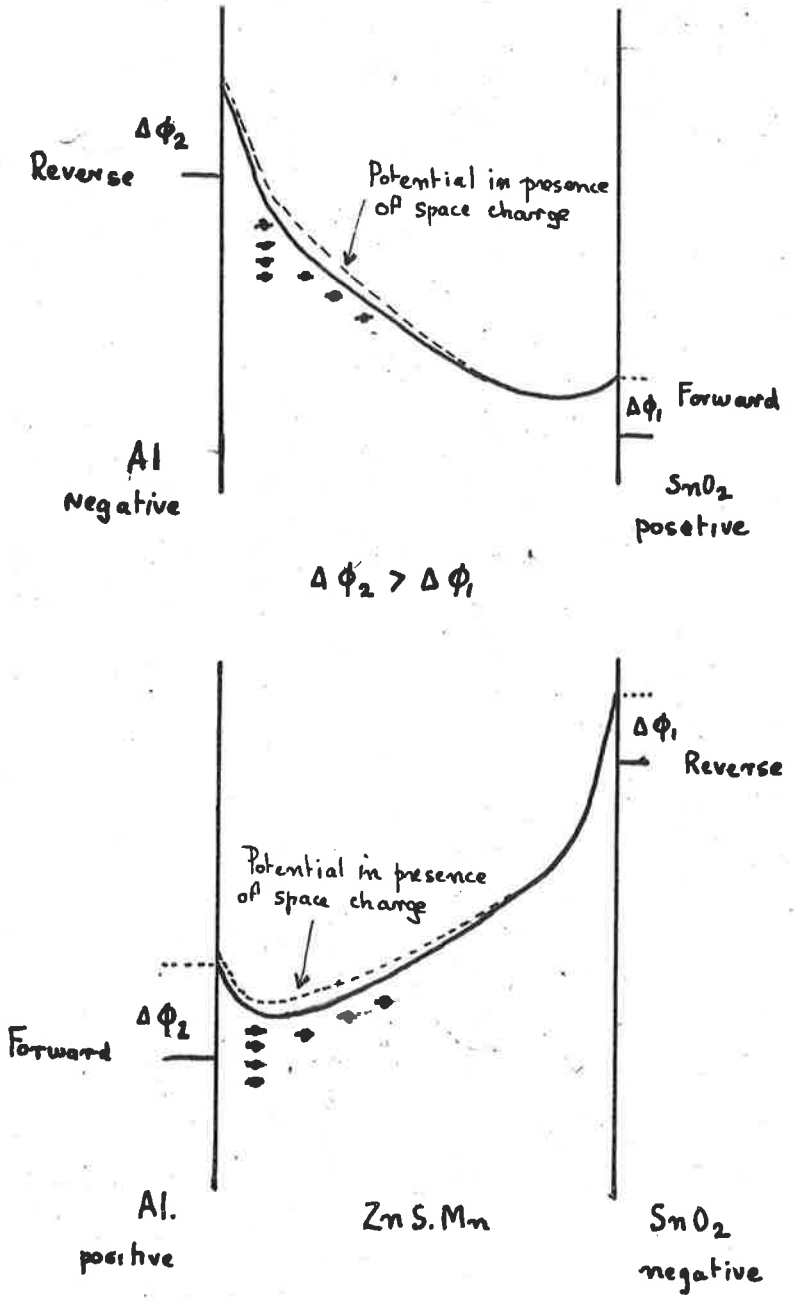


FIG 10.1 POTENTIAL DISTRIBUTION IN THICK FILMS IN THE PRESENCE OF TRAPPED CHARGE.

electrode contribution is small and electrons are accelerated in the bulk, a larger brightness pulse will occur when the metal is negative. Increasing voltage tends to make this polarization field effect smaller with respect to the applied potential, so the peaks will tend to equalize. As the voltage increases, the presence of emission from the electrode regions (that is a maximum when the metal is positive) may even give rise to a reversal of the polarity associated with the largest brightness pulse.

It is observed that for thick films, there is a component of the emission between 4000 and 5000Å. This intensity of this emission is proportional to exp $(- V^{-\frac{1}{2}})$ as given by equation 10.3. This suggests that this component may originate near the electrode area. Since the spectrum is the same for each polarity of the applied voltage, such centres are excited at each electrode.

It appears that both types of centres are present in films of all thickness but they are only excited in thick films. This suggests that the energy gain process is more efficient, i.e. a higher field exists in thick films. However it is also possible that these deeper centres have a different excitation probability relative to the manganese centres. The luminescent centre formed from a sulphur vacancy which has localized one electron (due to excess zinc) has a single negative charge and may be less efficiently excited by impact. If the film thickness is increased, the probability of excitation will increase relative to the probability of manganese excitation. However it is clear

that there is insufficient knowledge of the field distribution to profitably continue this explanation.

This short wavelength emission is also observed if a pure ZnS film is deposited between the metal electrode and the ZnS.Mn. However if the same 'pure' ZnS film is evaporated onto the conducting glass electrode there is no spectral change. It is likely that this pure ZnS contains these deeper luminescent centres (supposed due to excess zinc). These levels may result in some way from the manganese incorporation because no emission between 4000 and 5000 occurs in a ZnS (zinc doped) film. Therefore if this 'pure' ZnS is placed under the metal electrode, the barrier field exists in this region. Since only these deep centres are present some excitation of these centres occurs. This explains the observed increase in the metal-negative brightness pulse. It should be noted that the combined thickness of the ZnS and ZnS.Mn films is less than the thickness of a single ZnS.Mn film which shows the same amount of short wavelength emission.

Because no short wavelength emission is observed in thin films, it is clear that if both types of centre are present, the manganese is preferentially excited. The observation that no excitation of deeper centres occurs if the pure ZnS is on the conducting glass electrode shows that the field in this barrier is not sufficient to excite these deeper centres. This indicates that the most effective barrier field exists at the aluminium electrode. This may be due to either work function differences or to electron

injection from the $Al_2O_3$ layer at the metal electrode. Thus the only effect of the pure ZnS on the conducting glass is to confine the barrier field to a region where no excitation occurs. This explains the observed decrease of the brightness peak when the conducting glass is negative.

These experiments show that efficient excitation of centres occurs at distance of at least 1000Å from the electrodes.

A short wavelength component of the emission is also observed if a thin silica layer is deposited beneath the metal electrode. This layer must modify the barrier profiles considerably in this region. However electrons should be accelerated in the insulator and injected into the ZnS.Mn film with higher energy than is possible with the $Al_2O_3$ layer at the metal electrode. Thus deeper centres may be excited. This explains the observed increase of the metal-negative brightness pulse when these silica layers are present. A similar effect should occur if the silica is deposited at the conducting glass electrode. However no short wavelength emission is observed and there is even a small decrease in the brightness when this electrode is negative. Therefore the silica is not acting as an accelerating region. It is well known that silica films are very susceptible to pinhole formation through the film (Vergara et al 1963). When the ZnS.Mn is deposited on the silica film (on the conducting glass) it fills these holes,so forming a large number of paths of ZnS.Mn through the film. These paths carry most of the current, and so no efficient acceleration in the silica

is possible. A decrease in the conducting glass negative brightness may result if this distorts the barrier profile in the ZnS.Mn. If the silica is evaporated on the top surface of the ZnS.Mn film this effect does not occur, since the $Al_2O_3$ fills the holes.

## 10.3 Current flow in films

For a constant A.C. voltage, the current through the film should determine the brightness because of changes in the number of electrons available for acceleration. This is observed in the temperature variation of brightness where approximately $B \propto I$ at constant voltage. If however the current is increased by increasing the voltage, there will be rapid changes in the brightness because of the exponential variation of the acceleration term. The observations that the average brightness B is proportional to $I^6$ to $I^3$, reflects this strong dependence. The importance of both current and voltage in determining the light intensity has been shown in figure 7.13.

These results suggest that minority carrier injection is not important because of the strong dependence of the brightness on the current. It seems clear that the applied voltage does not simply act to bias any injecting type junction.

The necessity for excess zinc in the films is evidently to increase the number of electrons available in the film for acceleration. It is not possible to decide definitely if these donor electrons are released by impact ionization, although the discontinuity in the current-voltage curves

suggests that some field release of electrons is occurring. The observation that no electroluminescence is produced if the resistivity of the film is high indicates the importance of the bulk effect in these films. It is clear that manganese excitation is not caused directly by the electric field as no light emission is observed unless the resistivity is intentionally reduced. The measured conductivity of films shows that the free carrier concentration is about $10^{n}$ electrons / c.c.

Since most of the donor electrons compensate acceptors (chapter 4.4), the density of levels contributing electrons to the conduction band will be much less than the number of excess zinc ions incorporated. It is surprising that the presence of these donor levels is not indicated by the variation of conductivity. From a plot of log $\sigma$ against $\frac{1}{T}$, the slope should show the donor depth. These appears to be two possible explanations for the small, continuous variation of current observed.

(a) The current is controlled by tunnelling through barriers at each electrode. The $Al_2O_3$ layer may control the flow in both directions as discussed in chapter 7.5.4.

(b) Bube (page 72, Bube 1960), has shown that if the Fermi level is in the midst of a uniform distribution of levels, the free carrier concentration is relatively independent of temperature. Because most donors are compensated, the Fermi level will be several tenths of an electron volt below these donor levels (assumed to be about 0.3ev). Therefore if there is a distribution of electron traps in

this energy range, $\sigma$ will be approximately independent of temperature. It is of interest to note the theoretical equation describing space charge limited current flow in a system containing a uniform trap distribution (page 135 ). This is

$$I = K \exp \alpha V \qquad \text{--- 10.6.}$$

This form of current dependence is observed for evaporated films. It is however not possible to differentiate further between these mechanisms because of the lack of knowledge of levels in the band gap of ZnS.Mn. The presence of non ohmic contacts on a ZnS.Mn film suggests that the agreement between equation 10.6 and experiment is perhaps fortuitous. This is because equation 10.6 refers to space charge limited current in a solid with ohmic contacts.

In a recent paper, Russ (1963) demonstrated that surface conduction in large ZnS crystals can influence the current voltage curve. Since it has been shown in chapter 4.4 that evaporated electroluminescent films contain regions of high concentration of zinc (manganese), it is possible that conduction is controlled by crystallite surfaces. Because of the destruction of these low resistance paths by forming, the effects of such conduction is minimized. However while it is clear that current must flow through ZnS crystallites to give light emission, the current-voltage curves may be affected by surface effects.

## 10.4 Conclusion

Reviewing this work, it is evident that there are many parts requiring further experimental study in order to answer many of the questions which have arisen. Only when the results of such studies are available will a complete explanation of the light emission process be possible. Because of this, the theories advanced in the previous pages must be regarded as tentative at present.

In particular, the following matters might well be further investigated.

The evaporation of the II - VI compounds clearly needs more detailed investigation to determine the evaporation products which appear on the substrate surface. The techniques of mass spectrometry should be useful in this respect. The importance of re-evaporation from a substrate above 20°C is also largely unknown for these materials. A study of the accommodation coefficient for each element of a compound evaporated separately should give valuable information on the importance of these processes.

Some attempt was made to determine the electric field distribution in these films by the multiple film technique. As the field distribution is of fundamental importance, a further development of this method may lead to a more reliable interpretation of effects which are sensitive to the magnitude of the field.

## BIBLIOGRAPHY


Addamiano,A., 1963, Private communication.

Addamiano,A. and Aven,M., 1960, J.App.Phys., 31, 36.

Aven,M. and Cusano,D.A., 1964, J.App.Phys., 35, 606.

Aven,M. and Parodi,J.A., 1960, J.Phys.Chem.Solids, 13, 56.

Ballentyne,D.W.G., 1960, J.Electrochem.Soc., 107, 807.

Baum,F.J. and Darnell,F.J., 1962, J.Electrochem.Soc., 109, 165.

Boer,K.W., Dziesiaty,J., Kummel,U. and Misselwitz,W., 1962, Phys.Status Solidi, 2, 48.

Boer,K.W. and Kummel,U., 1952, Z.Phys.Chem., 200, 193.

Bullough,R., Newman,R.C., Wakefield,J. and Willis,J.B., 1960, Proceedings of the International Conference on Semiconductors, Prague 1960, P.811.

Bube,R.H., 1960, Photoconductivity of Solids (Wiley).

Bube,R.H., 1962, J.App.Phys. 33, 1733.

Baba,H., 1963, J.Electrochem.Soc., 110, 79.

Cardon,F., 1963, Phys.Stat.Solidi, 3, 339.

Cavenett,B.C., 1964, Proc.Phys.Soc., B84, 1.

Chow,C.K., 1963, J.App.Phys., 34, 2918.

Chuenkov,V.A., 1960, Soviet Physics, Solid State 1, 1601.

Chynoweth,A.G., 1960, Progress in Semiconductors (Heywood), Vol.4, P.97.

Chynoweth,A.G., 1960, J.App.Phys., 31, 1161, 1960.

Collins,R.E. and Davies,L.W., 1964, Solid State Electronics, 7, 445

Cosslett,V.E., 1951, Practical Electron Microscopy (Butterworths).

Curie,D., 1952, J.Phys.Radium, 13, 317, 1952.

Curie,D., 1957, Progress in semiconductors, Vol.2., P.251.

Curie,D., 1960, Luminescence in crystals (translated by Garlick,G.F.J., 1963).

Curie,D., 1964, Comptes Rendus, 258, 1694.

Cusano,D.A., 1955, Phys.Rev., 98, 547.

Czyzack,S.J., 1962, J.App.Phys., 33, 180.

Danforth,W.E., 1963, J.App.Phys., 33, 1972.

Davey,J.E., Tiernan,R.J., Pankey,T. and Montgomery,M.D., (1963), Solid State Electron 6, 205.

Davies,D.A., 1960, J.Sci.Instrum., 37, 15.

Destriau,G., 1936, J.Chem.Phys., 33, 587.

Dexter,D.L., 1953, J.Chem.Phys., 21, 836.

Diemer,G., 1954, Philips Res. Reports, 9, 109.

Diemer,G., 1955, Brit.J.App.Phys., 54, 47.

Feldman,C. and O'Hara,M., 1957, J.Opt.Soc.Amor, 47, 300, 1957.

Fischer,A.G., 1961, Solid State Electron, 2, 232.

Frankl,D.R., 1956, Phys.Rev., 100, 105.

Franz,W., 1952, Ann.Phys., 11, 17.

Frerichs,R., 1947, Phys.Rev., 72, 549.

Frohlich,H., 1937, Proc.Roy.Soc., A160, 230, 1937.

Frohlich,H. and Paranjape,B.V., 1956, Proc.Phys.Soc., B69, 21.

Garlick,G.F.J., Cunliffe,A. and Jones,M.N., 1962, Proc.Phys. Soc., 79, 223.

Georgobiani,A.N., 1961, Optics & Spectros, 11, 231.

Georgobiani,A.N., and Fok,M.V., 1958, Opt. i Spectr., 5, 167.

Georgobiani,A.N., and Fok,M.V., 1961, Optics & Spectros 9, 407; 10, 95.

Georgobiani,A.N., Yu L'vova,E., and Fok,M.V., 1963, Optics & Spectros, 15, 142.

Gilles,J.M., and Von Cakenberghe,J., 1958, Nature 182, 862.

Gillson,J.L., and Darnell,F.J., 1962, Phys.Rev., 125, 149.

Gippius,H.A. and Vavilov,V.S., 1963, Soviet Physics, Solid State, 4, 1777.

Glang,R., Kren,J.G., and Patrick,W.J., 1963, J.Electrochem. Soc., 110, 407.

Goffaux,R., 1956, J.Phys. Radium, 17, 763.

Goldberg,P. and Nickerson,J.W., 1963, J.App.Phys., 34, 1601.

Goldfinger,P. and Jeunehomme,M., 1959, Advances in Mass Spectrometry (Pergamon), P.539.

Gomer,R., 1953, Rev.Sci.Inst., 24, 993.

Goodman,A.M., 1963, J.App.Phys., 34, 329.

Greene,L.C., Reynolds,D.C., Czyzack,S.J. and Baker,W.M., 1958, J.Chem.Phys., 29, 1375.

Gunn,J.B., 1956, Proc.Phys.Soc., B69, 781.

Hacskaylo,M. and Feldman,C., 1962, J.App.Phys. 33, 3042.

Hahn,D. and Seeman,F.W., 1957, Z.Phys., 149, 486.

Halsted,R.E. and Keller,L.R., 1954, Phys.Rev., 93, 349.

Harper,W.J., 1962, J.Electrochem Soc., 109, 103.

Henisch,H.K., 1957, Rectifying Semiconductor contacts (Oxford).

Henisch,H.K., 1962, Electroluminescence (Pergamon).

Henisch,H.K. and Marathe,B.P., 1960, Proc.Phys.Soc., 76, 782.

Henry,N.F.M., Lipson,H. and Wooster,W.A., 1953, Interpretation of X-ray diffraction photographs (Macmillan).

Honig,R., 1957, R.C.A. Rev., 18, 195.

Holland,L., 1960, Vacuum Deposition of thin films (Wiley).

Hoogenstraaten,W., 1958, Philips Res. Reports, 13, 515.

Jaklevic, R.C., Donald, D.K., Lamb, J. and Vassel, W.C., 1963, App.Phys. Letters, 2, 7.

Kallman, H. and Rosenberg, B. 1955, Phys. Rev. 87, 1596.

Klick, C.C., 1955, Brit.J.App.Phys., Supp. 4, S74.

Koller, L., 1960, J.Electrochem Soc., 107, 973.

Koysun, V.M. and Kostylev, S.A., 1963, Optics and Spectros 15, 488.

Kovtonyuk, N.F., 1963, Optics and Spectros, 15, 140.

Kroger, F.A., 1955, Brit.J.App.Phys., Supp. 4, 558.

Kroger, F.A., 1956a, Physica, 22, 637.

Kulp, B.A. and Kelley, R.H., 1960, J.App.Phys., 31, 1057.

Lampert, M., 1956, Phys.Rev., 103, 1648.

Laksmanan, T.K., 1963, J.Electrochem Soc., 110, 548.

Langmuir, I., 1961, Collected works of I. Langmuir (Pergamon), Vol. 9.

Lawrance, R., 1965, to be published.

Lehmann, W., 1960, J.Electrochem Soc., 107, 20.

Lehovic, K., 1949, J.App.Phys., 20, 123.

Lossev, O.W., 1923, Telegr.i.Telef., 18, 61.

Lovshin, V.L. and Ryzhikov, B.D., 1962, Optics and Spectros, 12, 219.

Macdonald, R., 1958, J.Chem.Phys., 29, 1346.

Marshall, R. and Franks, J., 1964, Brit.J.App.Phys., 15, 63.

McCoy, D.G., 1965, to be published.

Mead, C.A., 1962, Phys.Rev., 128, 2088.

Melamed, N.T., 1958, J.Phys.Chem., Solids, 7, 146.

Meyerhofer, D. and Ochs, S.A., 1963, J.App.Phys., 34, 2535.

Morrison, A.D. and Lachonmeyer, R.R., 1963, Rev.Sci.Inst., 34, 106.

Murbach, H.P. and Wilman, H., 1953, Proc.Phys.Soc., B66, 905.

Morgan, T.N., 1957, Bull.Amer.Phys.Soc. II, 2, 265.

Morgan, T.N., 1958, Bull.Amer.Phys.Soc., 3, 13.

Nagy, E., 1956, J.Phys.Radium, 17, 773.

Oldham and Milnes, 1963, Solid State electronics, 6, 121.

Osiko, V.V., 1962, Optics & Spectros, 12, 345.

Peters, J., Singer, T., Brophy, V.A. and Birman, J.L., 1963, J.App.Phys., 34, 2210.

Piper, W.W., 1952, J.Chem.Phys., 20, 1343.

Piper, W.W. and Williams, F.E., 1952, Phys.Rev., 87, 151.

Piper, W.W. and Williams, F.E., 1955, Brit.J.App.Phys., Supp. 4, S39.

Piper, W.W. and Williams, F.E., 1958, Solid State Physics (Seitz and Turnbull), Vol. 6, P. 95.

Prener, J.S. and Williams, F.E., 1956, Phys.Rev., 101, 1427.

Preston, J.S., 1950, Proc.Roy.Soc., A202, 449.

Randall, J.T. and Wilkins, M.H.F., 1945, Proc.Roy.Soc. A184, 347-89.

Rose, A., 1955, Phys.Rev., 97, 1538.

Rose, F.W.G., 1957, J.Electron. and Control, 3, 396.

Schneider, E.E. and England, T.S., 1951, Physica 17, 221.

Seitz, F., 1949, Phys.Rev., 76, 1376.

Semilitov, S.A., 1962, Soviet Physics, Solid State, 4, 909.

Shockley, W., 1949, Electrons and Holes in Semiconductors.

Short, M.A., Steward, E.G., Tomlinson, T.B., 1956, Nature 177, 240.

Smit, N.W. and Kroger, F.A., 1949, J.Opt.Soc.Amer., 39, 661.

Smith, R.W., 1955, Phys.Rev., 97, 1525.

Sohm, J.C., 1961, J.Phys.Chem. Solids, 18, 181.

Stratton, R., 1957, Proc.Roy.Soc., A242, 355.

Stratton, R., 1961, Progress in Dielectrics, Vol.3, p.233, (Ed. Birks and Hart).

Studer, F.J. and Cusano, D.A., 1955, J.Opt.Soc.Am., 45, 493.

Swanson, H.K. and Fuyat, R.K., 1953, Standard X-ray powder diffraction patterns, N.B.S. Circular, 539, Vol.2.

Thomson, G.P. and Cochrane, W., 1939, Theory and Practice of Electron Diffraction (Macmillan).

Thornton, W.A., 1956, Phys.Rev., 102, 38.

Thornton, W.A., 1959, J.App.Phys., 30, 123.

Thornton, W.A., 1961, J.Electrochem. Soc., 108, 636.

Thornton, W.A., 1961a, Phys.Rev., 123, 1583.

Thornton, W.A., 1962, J.App.Phys., 33, 3045.

Thornton, W.A., 1963, J.Electrochem. Soc., 110, 370.

Tolansky, S., 1960, Surface Microphotography (Longmans).

Vereshchagin, I.K., 1962, Optics and Spectros, 12, 424.

Vergara, W.C., Greenhouse, H.M. and Nicholas, N.C., 1963, Rev.Sci.Instrum., 34, 520.

Vlasenko, N.A. and Popkov, I.A., 1960, Optics and Spectras, 8, 39.

Von Hippel, A., 1935, Ergdn.exakt.Naturw., 14, 79.

Whitehead,S., Dielectric breakdown of solids (Oxford) 1951.

Weizburg, J., 1961, Acta Phys.Hungar, 13, 61.

Weslowski, J., 1961, Acta Phys. (Pol.), 20, 303.

Whelan, M.J. and Hirsh, P.B., 1957, Phil.Mag., 2, 1121.

Williams, R., 1961, 1955, Phys.Rev., 123, 1645 and J.Phys. Chem. Solids, 22, 129.

Williams, R., 1962, Phys.Rev., 125, 850.

Wolff, P.A., 1954, Phys.Rev., 95, 1415.

Salm, P., 1956, Philips Res.Reports, 11, 353.

Zener, C., 1934, Proc.Roy.Soc., A145, 523.